Yu-jie Liu
Jing Xue
Chang-ming Huang
Chun-bao Li
Editors

Advanced Application of Arthroscopy

A Practical Guide with Illustrative Cases

Springer

Advanced Application of Arthroscopy

Yu-jie Liu • Jing Xue
Chang-ming Huang • Chun-bao Li
Editors

Advanced Application of Arthroscopy

A Practical Guide with Illustrative Cases

Springer

Editors
Yu-jie Liu
Department of Orthopedics
Chinese PLA General Hospital
Beijing
China

Jing Xue
Department of Orthopedics
Air Force Medical Center
Beijing
China

Chang-ming Huang
Department of Orthopedics
The 73 Group Army Hospital
Xiamen
China

Chun-bao Li
Department of Orthopedics
Chinese PLA General Hospital
Beijing
China

ISBN 978-981-15-4683-9 ISBN 978-981-15-4684-6 (eBook)
https://doi.org/10.1007/978-981-15-4684-6

This Springer imprint is published by the registered company Springer Nature Singapore Pte Ltd.
The registered company address is: 152 Beach Road, #21-01/04 Gateway East, Singapore 189721, Singapore

Foreword

Dear Reader,

Over the past several decades, the clinical applications for arthroscopy have expanded greatly. This can be attributed, in large part, to the innovative and insightful work of Professor Liu and colleagues.

I have known Professor Liu for many years and have closely followed his productive career. His works have expanded our understanding of arthroscopy techniques and the broader utility of this important surgical tool. And he has helped to pilot the use of arthroscopy into the twenty-first century for both intra-articular and extra-articular musculoskeletal pathologies.

This text promises to be an excellent reference for the ever-expanding applications of arthroscopic techniques. With detailed procedures and beautiful, clear illustrations, this important work is the new handbook for the advanced applications of arthroscopy. I would like to thank Professor Yujie Liu and colleagues for putting this text together and now translating it into English, making it more accessible to the next generation of surgical innovators. Thank you, my friends, for your wonderful, important work.

Yours truly,

Freddie H. Fu
Department of Orthopaedic Surgery
University of Pittsburgh School of Medicine
Pittsburgh, PA, USA

Department of Athletics
University of Pittsburgh School of Medicine
Pittsburgh, PA, USA

Preface

Micro-invasive arthroscopy has brought revolutionary progress to the development of sports medicine. Many new technologies and new surgical methods have sprung up quickly.

As we all know, arthroscopic technology is used for the diagnosis and treatment of intra-articular diseases. Can extra-articular diseases be treated by arthroscopy? It is well known that the bottleneck restricting the application of arthroscopy outside the joint is that there is no natural cavity outside the joint for arthroscopic operation. Through years of intensive research and trials, inspired by tunneling engineering technology, we artificially created an arthroscopic working cavity in the diseased area. The arthroscopic procedure can now be performed just like inside of the joint. This innovative concept breaks the traditional concept that arthroscopy technology cannot be applied outside joints.

Since 2000, the authors have successively designed and carried out innovative subjects of extra-articular application of arthroscopy techniques such as arthroscopic gluteal muscle contracture release, sternocleidomastoid muscle release treatment for torticollis, metacarpus contracture release, carpal tunnel incision release, steel plate screw removal, hallux valgus orthopedics, arthroscopic curettage of benign bone tumors, Achilles tendon rupture suture, radiofrequency ablation of tendons, and tennis elbow. These innovative techniques have attracted a lot of attention in academia at home and abroad.

A series of arthroscopic minimally invasive techniques for the treatment of intra-articular fractures has also been launched: the design and development of arthroscopic neckwear-knot-loop-ligature fixation technique for tibial intercondylar fractures with ACL injury and arthroscopic suture anchor fixation for ACL attachment point injuries. We also designed percutaneous reduction by leverage under arthroscopic monitor in the treatment of intra-articular fractures, such as avulsion fractures of the humerus head, comminuted fracture of the scapula, and radial head fracture. These surgical methods provide innovative ideas for the treatment of intra-articular fractures.

Moreover, we have independently developed a series of brand-new allogeneic cortical bone suture anchor for more than ten years, which has been used to treat intra-articular osteochondral injury, intra- and extra-articular fractures, repair rotator cuff and Bankart injuries, and fixation and reconstruction of knee cruciate ligament injuries. The follow-up results are encouraging.

Some of the above techniques may still have disadvantages, but if they have some value for updating concepts and promoting independent innovation for doctors, and reducing pain and medical costs for patients, it is worth to be shared with you. After thoughtful thinking, through careful planning, we use a simple and easy-to-understand atlas method for the writing of the manuscript, which not only introduces innovative ideas but also introduces technical methods with pictures and texts. I hope this book could be helpful for the reader.

Here I sincerely appreciate all my colleagues who have worked very hard for this book, and many thanks to my family for their understanding, support, and care for me, so that this book can be presented to the readers.

Beijing, China — Yu-jie Liu
Beijing, China — Jing Xue
Xiamen, China — Chang-ming Huang
Beijing, China — Chun-bao Li

Acknowledgments

We are very grateful to Professor Lei Zhang and Dr. Yan Li from the Department of Joint Surgery and Sports Medicine, Wangjing Hospital, China Academy of Chinese Medical Sciences. Lei Zhang is a good friend of mine, and he introduced Dr. Yan Li to us. Dr. Yan Li helped us to draw more than 20 beautiful illustrations for this book.

Yu-jie Liu

Contents

Part III Innovative Technology for Repair and Reconstruction of Joint Injuries

About the Editors and Contributors

About the Editors

Yu-jie Liu is the chief of Arthroscopy and Sports Medicine Center at Chinese PLA General Hospital, and professor of Orthopedic Surgery at Medical School of Chinese PLA, part-time. He is a clinical professor of Arthroscopy and Sports Medicine at the Chinese PLA General Hospital for the past 40 years. He has had a long-standing interest in sports medicine and pioneered arthroscopy in China.

As an excellent doctor, Dr. Liu enjoys special government allowances and special military allowances of the State Council of China. He is an expert of the Central Health Commission of China, expert of the Health Commission of the Central Military Commission of China, and expert of the State General Administration of Sports for the Olympic Games. He is the image ambassador of the 2019 World Military Games and awarded the second national Bethune-style good doctor.

In academics, Dr. Liu is Chairman of Medical Science and Technology Committee of the Chinese PLA Orthopaedics Arthroscopy and Sports Medicine branch, former Deputy Chairman of the Chinese Medical Association Sports Medical Branch and the leader of the Shoulder and Elbow Surgery Group, Deputy Leader of the Arthroscopy Group of the Chinese Medical Association, Standing Committee Member, Deputy Chairman of the Sports Medicine Branch, Deputy Chairman of the SICOT China Sports Medicine Branch, Deputy Chairman of the Physical Disability Committee of the Rehabilitation Society of the Ministry of Civil Affairs, and Member of ISAKOS.

For his research, he has received the Second Prize of National Science and Technology Progress Award of China in 2007, First Prize of Chinese PLA Science and Technology in 2006, Third Prize of Beijing Science and Technology in 2014, and many other prizes.

As a Professor, Dr. Liu had trained 62 masters, doctoral, and postdoctoral students. He has authored more than 342 peer-reviewed articles and 16 books.

Jing Xue, MD, Ph.D., is the chief surgeon of the arthroscopy and sports medicine team of the Orthopaedics Department at the Air Force Medical Center of Chinese PLA. After completing his undergraduate education in clinical medicine at the Fourth Military Medical University, he learned from Professor Yu-jie Liu and Academician Shi-bi Lu in Medical School of Chinese PLA and successively obtained a doctorate in orthopedics in 2010.

Dr. Xue is engaged in arthroscopy and sports medicine for more than 10 years. He is good at the treatment of joint injuries and degenerative diseases, and he has accumulated rich clinical experience. Dr. Xue is enthusiastic about public welfare and has participated in the Han Hong Love Charity Foundation to support medical activities in poor areas for many years.

He is a member of the Youth Committee of Medical Science and Technology Committee of the Chinese PLA Orthopaedics and Youth Committee of sports medical branch of Beijing Medical Association. He has won 2 third prizes of Chinese PLA Science and Technology and has authored more than 30 peer-reviewed articles and 12 books.

Chang-ming Huang is the director of joint minimally invasive surgery at 73 Group Army Hospital of Chinese PLA; he is also a clinical professor of Xiamen University and Nanchang University.

Because of his medical achievements, he serves as a committee member of the Chinese Medical Association Sports Medical Branch upper limb movement traumatology, Vice-Chairman of the Medical Science and Technology Committee of the Chinese PLA Orthopaedics Arthroscopy and Sports Medicine branch, member of Chinese Handicapped Physical Disability Committee of the Rehabilitation Society, and member of Chinese Medical Doctor Association orthopedic branch.

He is an editorial board member of the *Chinese Journal of Shoulder and Elbow* (Electronic Edition) and the *Journal of Cervicodynia and Lumbodynia*. He is also a standing editorial board member of the *Chinese Journal of Bone and Joint Injury* and *Orthopedic Journal of China*.

For his numerous research papers related to arthroscopy, he has gained National Utility Model Patent eight times, the Third Prize of Fujian Province Scientific and Technological Achievements in 2011, and the Third Prize of Chinese PLA Scientific and Technological Achievements in 2007.

Dr. Huang is active in imparting arthroscopy knowledge, which provides a strong impetus to the development of Fujian Province and Chinese PLA arthroscopy, and has gained a lot of respect from many scholars.

Chun-bao Li, MD, Ph.D., is deputy chief physician, associate professor, and master tutor of Sport Medicine Center of orthopedics department of PLA general hospital (301 hospital) of China. He has achieved the joint MD & Ph.D. Degree from Harvard Medical School and the Military Medical School of PLA. After being awarded a Sports Medicine and Orthopedics Fellowship in the PLA General Hospital, he has visited several internationally renowned orthopedics and sports medicine centers in the USA, like the Hospital for special surgery (the first visitor of Sports Medicine Observership Program, HSS-China Exchange Education Program), Massachusetts General Hospital, Mayo Clinic, UPMC, the Steadman Clinic, Nashville Sports Medicine Center, and others, and has established good relationship with Dr. Bryan Kelly, Marc Philippon, Thomas Byrd, Michael Millis, and others.

His specialties are the diagnosis of hip and knee joint sports injury and arthroscopy surgery. His research interests include novel surgical technique of arthroscopy surgery and the clinical, biology, and biomechanics study of the hip and knee joints.

He is the Funding Member and secretary of the Society for Hip Arthroscopy, Deputy Chairman of Youth Committee of sports medical branch of Chinese Medical Association, and Deputy Chairman of Youth Committee of sports medical branch of Beijing Medical Association.

Contributors

Shao-hua Ding Department of Orthopedics, Medical Center of Ningbo, Lihuili Hospital, Ningbo, China

Chang-ming Huang Department of Orthopedics, The 73 Group Army Hospital, Chenggong Hospital Affiliated to Xiamen University, Xiamen, China

Chun-bao Li Department of Orthopedics, Chinese PLA General Hospital, Beijing, China

Hai-peng Li Department of Orthopedics, The 7th Medical Center of Chinese PLA General Hospital, Beijing, China

Yu-jie Liu Department of Orthopedics, Chinese PLA General Hospital, Beijing, China

Ming Lu The Fourth Comprehensive Service and Support Center of the PLA Beijing Administration of Veterans Service Affairs Department, Beijing, China

Wei Qi Department of Orthopedics, Chinese PLA General Hospital, Beijing, China

Feng Qu Department of Orthopedics, Beijing Tongren Hospital, Capital Medical University, Beijing, China

Jing Xue Department of Orthopedics, Air Force Medical Center, Beijing, China

Part I

Application of Arthroscopy Technology Outside Joints

1 Endoscopic Release of Congenital Muscular Torticollis with Radiofrequency Under Local Anesthesia

Yu-jie Liu and Jing Xue

1.1 Introduction

Congenital muscular torticollis (CMT) is due to contracture of the sternocleidomastoid muscle which may cause activity limitations of the neck, tilt of the head, craniofacial asymmetry, and deformity of the skull. The cause of CMT is not very clear. Some people think that it may be related to abnormal intrauterine fetal sternocleidomastoid myofascial compartment syndrome, and some people think that it is related to local bleeding and muscle degeneration of sternocleidomastoid muscle caused by forceps during delivery.

1.2 Clinical Features

Although CMT is more common in preschool children (Fig. 1.1), because of neglect in childhood, adult patients are also common clinically (Fig. 1.2). With unilateral sternocleidomastoid muscle contracture, the face deformed due to long-term deviation of the head and neck to one side (Fig. 1.3); the distance between the corners of the mouth and the lateral corners of the eyes is not equal (Fig. 1.4). As the age increases, bilateral zygomatic asymmetry can occur, and facial deformities become more obvious (Fig. 1.5).

1.3 Clinical Classification

According to the site of sternocleidomastoid muscle contracture, it is divided into clavicle head contracture type (Fig. 1.6), sternal head contracture type (Fig. 1.7), and sternoclavicular head contracture type (Fig. 1.8).

Fig. 1.1 A preschool child with congenital muscular torticollis (CMT) of right side

1.4 Radiographic Appearances

Due to sternocleidomastoid muscle contracture and stretch, cervical scoliosis may occur (Fig. 1.9). X-ray examination may show a stretch osteophyte at the site that the sternocleidomastoid muscle is attached to the clavicle (Fig. 1.10).

Y.-j. Liu (✉)
Department of Orthopedics, Chinese PLA General Hospital, Beijing, China

J. Xue
Department of Orthopedics, Air Force Medical Center, Beijing, China

Y.-j. Liu et al. (eds.), *Advanced Application of Arthroscopy*, https://doi.org/10.1007/978-981-15-4684-6_1

Fig. 1.2 A young female adult with CMT of right side

Fig. 1.3 Long-term head and neck deflection to one side causes facial deformation

Fig. 1.4 The distance between the corners of the mouth and the lateral corners of the eyes is not equal

Fig. 1.5 As the age increases, bilateral zygomatic asymmetry can occur, and facial deformities become more obvious

Fig. 1.6 Clavicle head contracture type of CMT

Fig. 1.7 Sternal head contracture type of CMT

Fig. 1.8 Sternoclavicular head contracture type of CMT

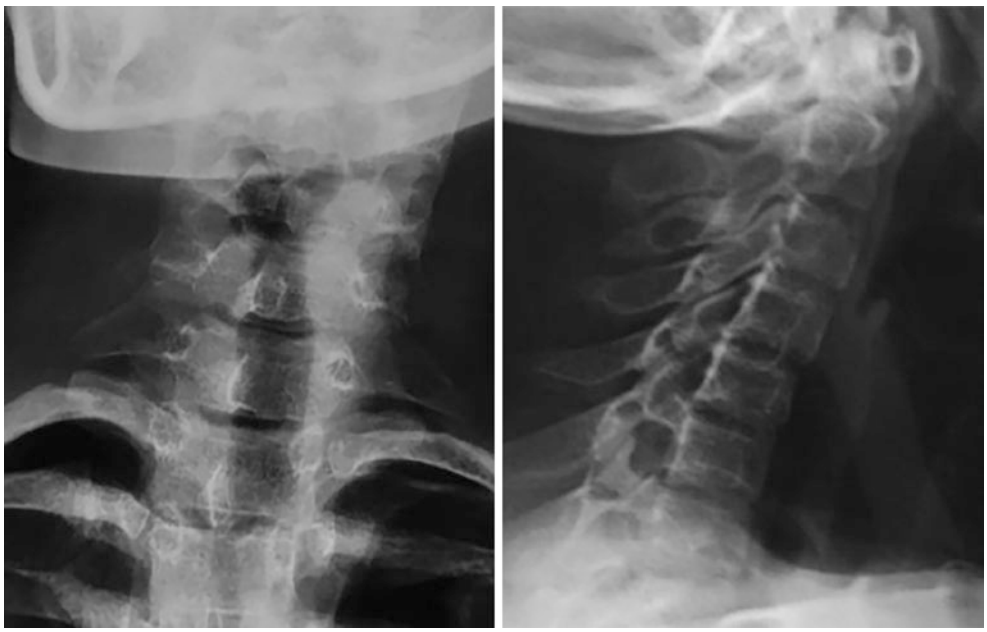

Fig. 1.9 X-ray examination shows mild cervical scoliosis

Fig. 1.10 X-ray examination shows a stretch osteophyte at the site that the sternocleidomastoid muscle is attached to the clavicle

1.5 Treatment Options

Generally, CMT are treatment with open surgery, by cut off the sternocleidomastoid muscle at the attachments of the clavicle or mastoid process. In some cases, the sternocleidomastoid muscle is completely resected, and patients need to be fixed with plaster after surgery. The surgical trauma is large, and cord-like scars are left on the neck, which affects the appearance (Fig. 1.11).

We present our experience of arthroscopic tight fibrous band release with radiofrequency under local anesthesia [1].

1.6 Preoperative Preparation

All patients are positioned in a supine position with extension of the neck and rotation of the head toward the unaffected side. Surface landmarks of sternocleidomastoid muscle, clavicle, neurovascular structures, and arthroscopic portals are identified by careful palpation and marked using a surgical marker (Fig. 1.12). Two portals are typically used, including the anterolateral working portals and the anteromedial portal which accommodates the arthroscopy. The anteromedial portal is placed at 3 cm inferior and 1.5 cm medial to the sternoclavicular joint of the affected side, and the working portal is placed at 3 cm inferior to the midpoint of the clavicle (Fig. 1.12).

Routine sterile preparation and drape are then performed. Local infiltrating anesthesia of the portal sites and the surgical region is performed with 20 ml 2% lidocaine and 0.2 ml 0.1% epinephrine, which is diluted with 40 ml saline water (Fig. 1.13).

1.7 Arthroscopic Operative Technique

A 2–3-mm transverse incision is made just over the marking portals. The subcutaneous tissue is blunt-dissected from underlying structures with a periosteal elevator to create a working space (Fig. 1.14). The mean size of the working space was 5 × 5 cm. After a 30° 4-mm arthroscopy and a

Fig. 1.11 A young female patient, scar left in neck after open torticollis surgery (arrow)

radiofrequency probe (ArthroCare Atlas System with TriStar 50 ArthroWand; ArthroCare Corporation, Sunnyvale, CA) are introduced to the working space, clean up the fibrous tissue affecting the range of vision (Fig. 1.15). Patients are asked to hyperextend and rotate the head to tense muscles, and then the clavicular and sternal heads of the sternocleidomastoid muscle are identified (Fig. 1.16).

With the radiofrequency probe, gradually transect the contracture band from superior to inferior in the insertion regions (Fig. 1.17). As the contracture band is resected, the muscle fibers retract proximally (Fig. 1.18). Then, patients are requested to laterally bend and rotate the neck toward the contralateral side to evaluate the degree of release and not to leave a residue of contracture.

During arthroscopic-assisted release, care should be taken not to resect too deep and thus stay clear of the neurovascular structures. Any bleeding point should be coagulated using radiofrequency energy to maintain a clear vision and prevent a hematoma formation after the operation.

Due to the perfusion pressure, the neck region may be swelling because of water infiltration (Fig. 1.19). The swelling will subside within 24 hours after surgery.

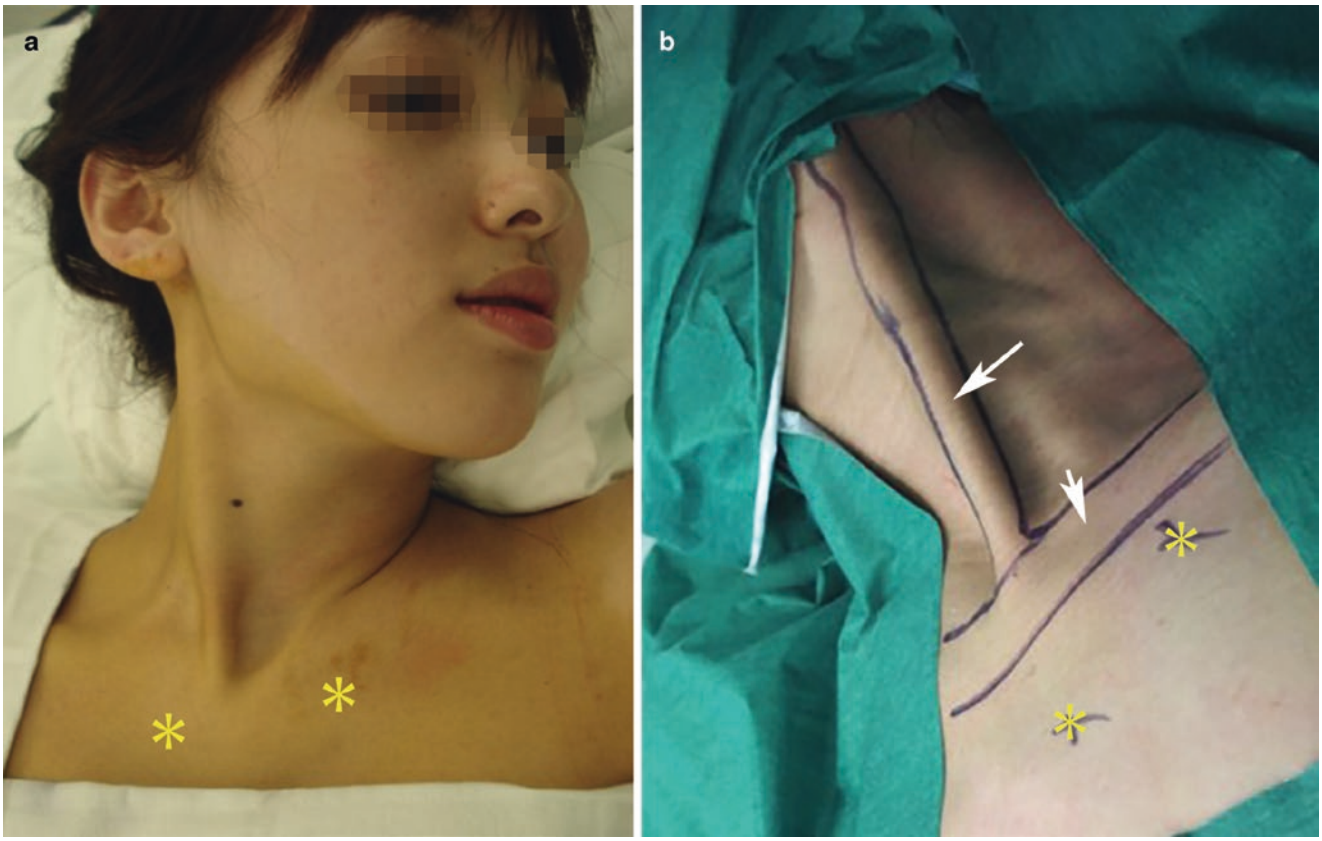

Fig. 1.12 (**b**) Mark the sternocleidomastoid muscle contracture (arrow), clavicle (short arrow), and (**a** and **b**) surgical approaches (∗)

Fig. 1.13 Local infiltrating anesthesia of the portal sites and the surgical region

Fig. 1.14 The subcutaneous tissue is blunt-dissected from underlying structures with a periosteal elevator to create a working space

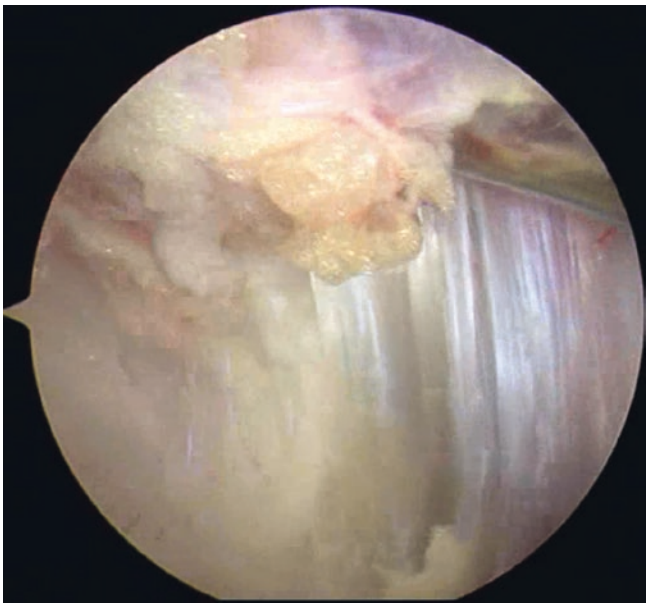

Fig. 1.15 Clean up the fibrous tissue affecting the range of vision to create a working space and reveal sternocleidomastoid muscle contracture

1.8 Postoperative Treatment

Gentle ROM exercises and strengthening exercises were initiated from the first postoperative day and continued for 4–6 weeks after surgery. No brace was needed postoperatively. Facial deformities gradually returned to normal after surgery (Fig. 1.20).

1.9 Critical Points

1. The surgeon must be familiar with the local anatomy of the neck. The external jugular vein around the sternocleidomastoid muscle is obliquely crossed, and in the deep layer, there is the common carotid artery, internal jugular vein and its branches, and the vagus nerve. The upper half of the sternocleidomastoid muscle has branches of the cervical plexus and parasympathetic sympathetic trunks, the lower part of the sacral nerve, the left chest tube, and the supraclavicular nerve at the lower 1/3 of the posterior

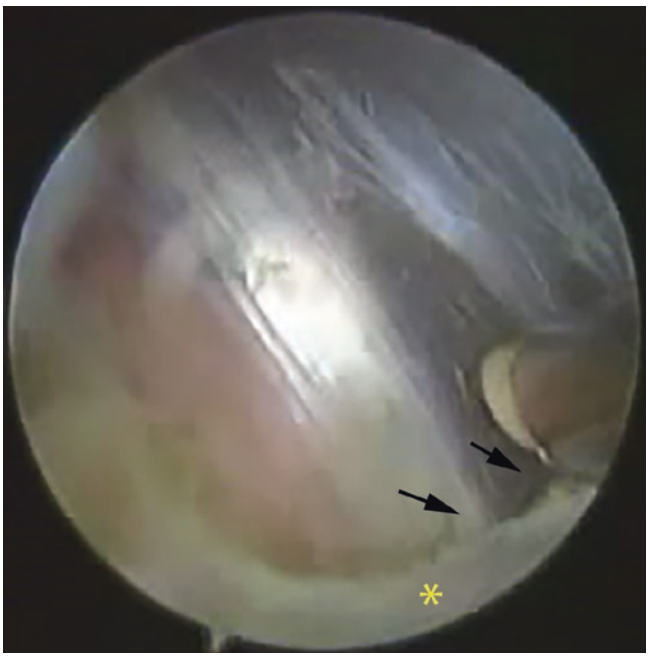

Fig. 1.16 The sternocleidomastoid muscle (arrow) is attached on the clavicle (∗)

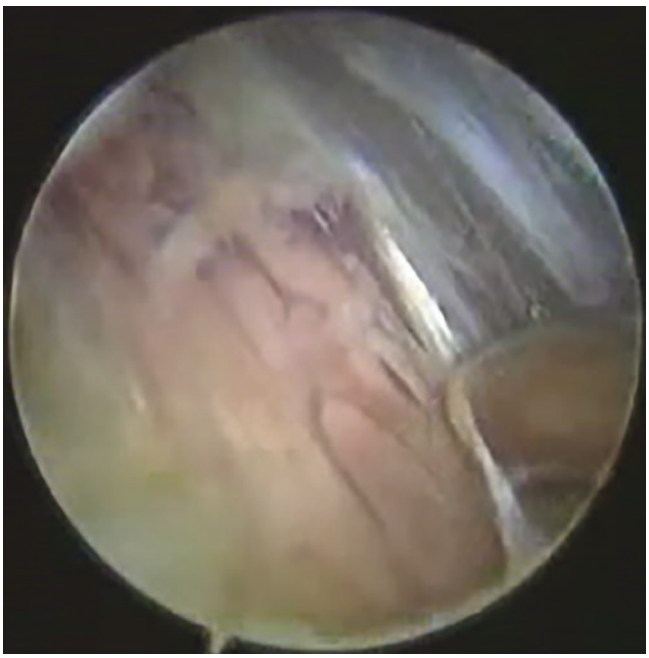

Fig. 1.17 With the radiofrequency probe, gradually transect from superior to inferior in the insertion regions

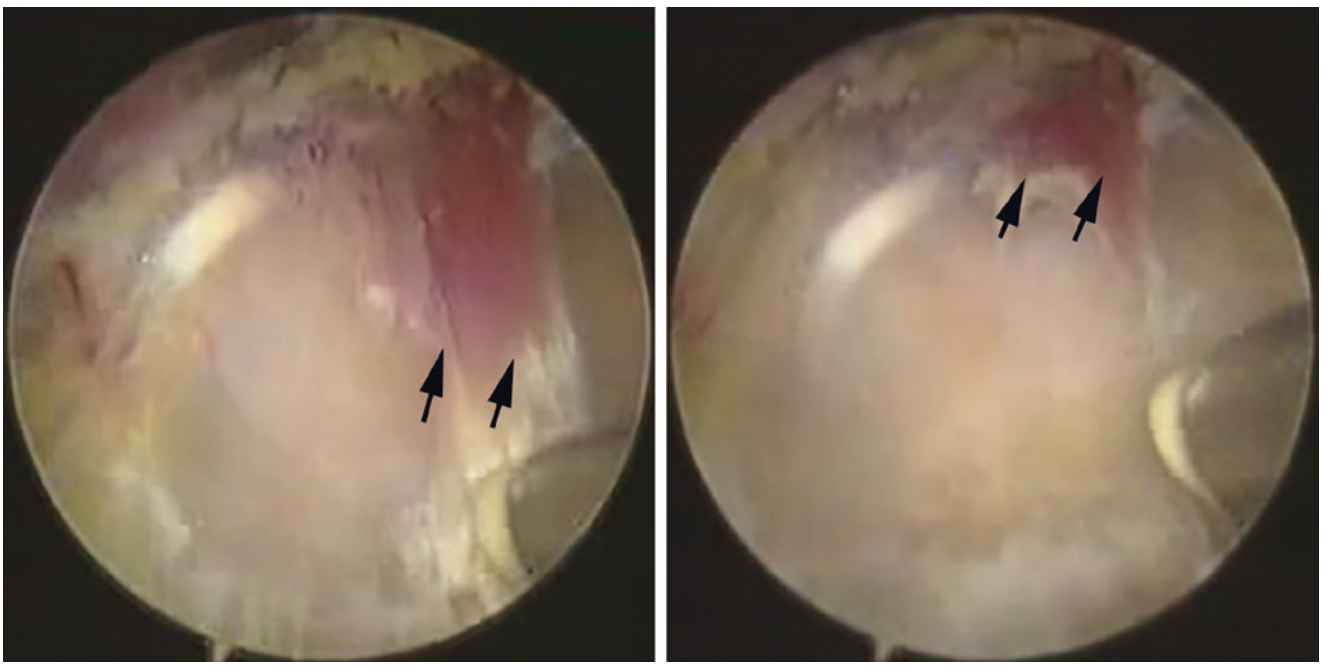

Fig. 1.18 As the contracture band is resected, the muscle fibers retract proximally

margin. The deep side is adjacent to the dorsal scapular nerve, transverse carotid artery, and anterior oblique muscle. The brachial plexus nerve root runs through the interstitial space, and the carotid sheath is in deep layer.

2. On the deep side of the sternocleidomastoid muscle, there are accessory nerves and the greater auricular nerve. 63% of the auricular nerves travel at the intersection of the upper 1/4 and lower 3/4 of the anterior margin of the sternocleidomastoid muscle and the upper and middle 1/3 of the posterior margin. The line of intersection is the line connecting the tip of the mastoid at 4 cm and 5 cm at the posterior edge of the muscle. The deep side has accessory

Fig. 1.19 Due to the perfusion pressure, the neck region may be swelling because of water infiltration

Fig. 1.20 7 years after operation. (**b**) The facial deformity is completely corrected (**a** is before surgery)

nerves, and its travel is basically consistent with this connection, accounting for 80%. Injuries should be avoided during surgery.

3. In order to avoid injure the important blood vessels and nerves of the neck, the local anatomy should be clearly marked before surgery. When transecting the contracture band, the radiofrequency probe should be near the surface of clavicle and sternum. Do not away from the clavicle and sternum into the deep tissue of the supraclavicular socket! So as not to injure important structures of the neck.
4. It is very important to choose a surgical indication before surgery. This surgery is only suitable for congenital muscular torticollis. The spastic torticollis caused by the central nervous system and structural torticollis caused by cervical hemivertebral deformities are not surgical indications.
5. It is not recommended to use a pressure pump for perfusion. Adjust the flow of perfusion fluid during the operation to avoid too much pressure, which will cause more fluid infiltrate into the loose tissue of the neck and affect breathing.

Reference

1. Wang JL, Qi W, Liu YJ. Endoscopic release of congenital muscular torticollis with radiofrequency in teenagers. J Orthop Surg Res. 2018;13(1):100. https://doi.org/10.1186/s13018-018-0801-6.

2 Arthroscopic Acromioclavicular Arthroplasty for Acromioclavicular Impingement

Yu-jie Liu and Chang-ming Huang

2.1 Introduction

Acromioclavicular joint is composed of acromion and articular surface of distal clavicle (Fig. 2.1). Acromioclavicular disease accounts for 31% of shoulder pain [1–3]. Acromioclavicular arthritis is increasing as aging society is coming. Distal clavicle excision (DCE) should be considered if conservative treatment is invalid. Distal clavicle excision (DCE) is often performed open operation. Arthroscopic DCE may have advantages in term of reducing postoperative pain and a short rehabilitation period. This surgical operation is an effective, safe, and less trauma treatment.

2.2 Clinical Features

Push-ups can bring out acromioclavicular joint pain (Fig. 2.2). When the affected limb rests on the healthy shoulder joint and raises the elbow joint upward, it may induce acute pain of acromioclavicular joint (Fig. 2.3). Acromioclavicular joint touches the obvious pain and pain disappeared after lidocaine injection (Figs. 2.4 and 2.5). These characteristics are helpful for the diagnosis of acromioclavicular arthritis [4, 5].

2.2.1 Imageology

X-ray showed that the acromioclavicular joint space was narrow, with irregular destruction or hyperplasia (Fig. 2.6). MRI showed that the acromioclavicular space was irregular mixed

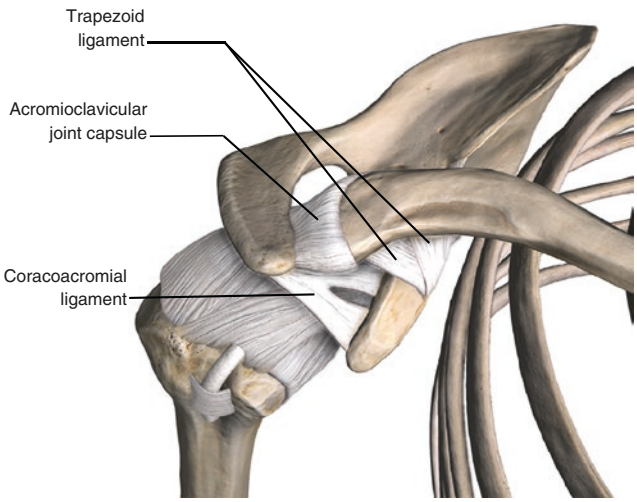

Fig. 2.1 Anatomy of acromioclavicular joint

Fig. 2.2 Push-ups can bring out acromioclavicular joint pain

Y.-j. Liu (✉)
Department of Orthopedics, Chinese PLA General Hospital, Beijing, China

C.-m. Huang
Department of Orthopedics, The 73 Group Army Hospital, Chenggong Hospital Affiliated to Xiamen University, Xiamen, China

Y.-j. Liu et al. (eds.), *Advanced Application of Arthroscopy*, https://doi.org/10.1007/978-981-15-4684-6_2

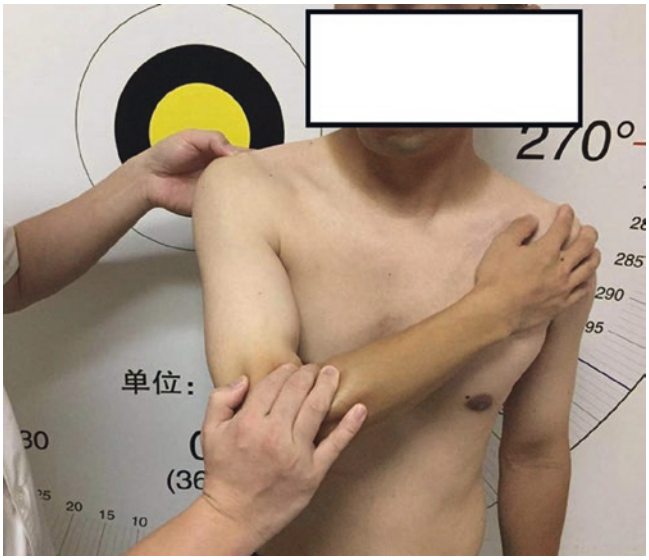

Fig. 2.3 Shoulder abduction and lifting induced pain

Fig. 2.4 Local tenderness of acromioclavicular joint

Fig. 2.5 Pain disappears after anesthesia

Fig. 2.6 X-ray showed that the acromioclavicular joint space was narrow, with irregular destruction or hyperplasia

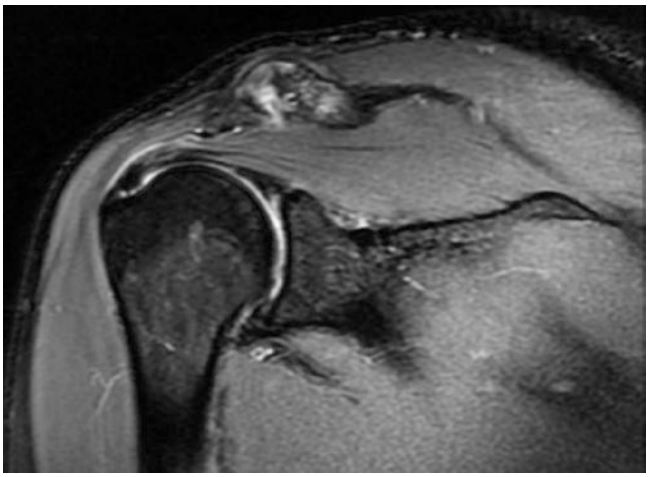

Fig. 2.7 MRI show that the acromioclavicular space signal abnormal phenomena

signal and high signal (Fig. 2.7) and irregular and hyperplasia of articular cartilage (Fig. 2.8) [6–8].

2.3 Operative Technique

Lie face upward with a cushion under patient's head, dorsal elevated position, turn head to the healthy side, and lean back slightly (Fig. 2.9). Mark acromioclavicular joint, acromion, clavicle and coracoid process preoperatively (Fig. 2.10). Conventional surgery area disinfection, shop sterile surgical towels single, Lidocaine anesthesia of acromioclavicular joint (Fig. 2.11). It is important to locate the space of acromioclavicular joint before operation; the needle can be inserted into it (Fig. 2.12).

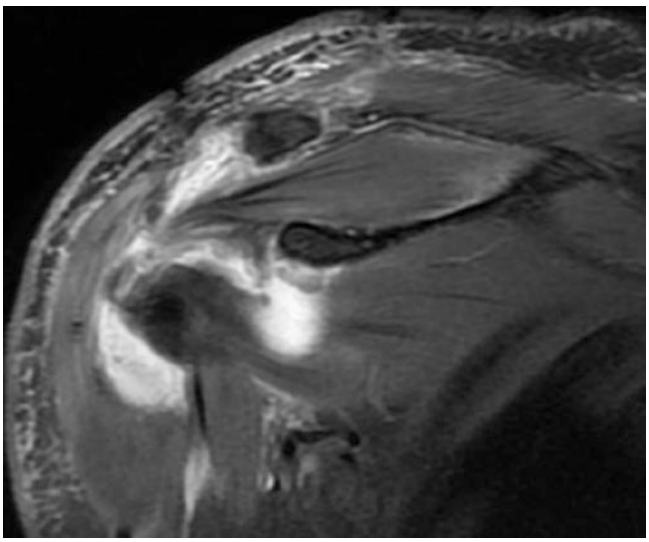

Fig. 2.8 MRI showed that the acromioclavicular space was irregular and hyperplasia of articular cartilage

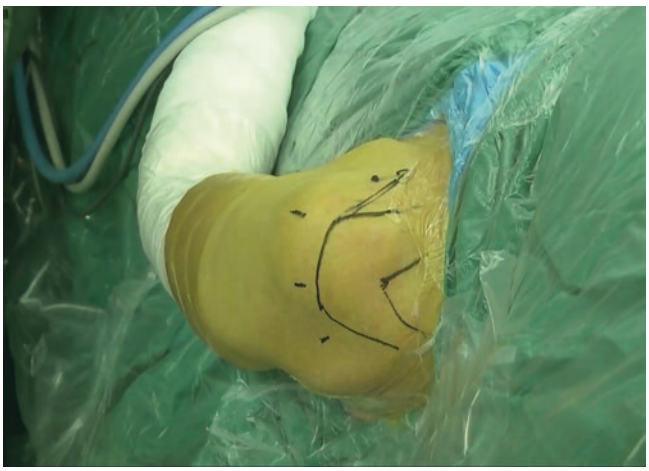

Fig. 2.9 Lie face upward with a cushion under your head, dorsal elevated position

Puncture into acromioclavicular joint with a puncture cone after skin incision. Then, insert arthroscopy and motorized shaver (Fig. 2.13) found that cartilage disappeared and coarseness articular surface in the space of acromioclavicular joint (Fig. 2.14). Using shaver or radiofrequency probe to clean up the proliferative soft tissue in joint. (Fig. 2.15) grinding drill for acromioclavicular arthroplasty, remove the hyperplastic osteophytes by grinding from the outside to the inside (Fig. 2.16), the distal clavicle was resected about 4–5 mm, medial margin of acromion was resected about 3–4 mm. After grinding, the shoulder Joint space was about 6–8 mm (Fig. 2.17). In abduction, lifting, and rotation of shoulder joint during operation, check

Fig. 2.10 Mark acromioclavicular joint, acromion, clavicle, and coracoid process in preoperative

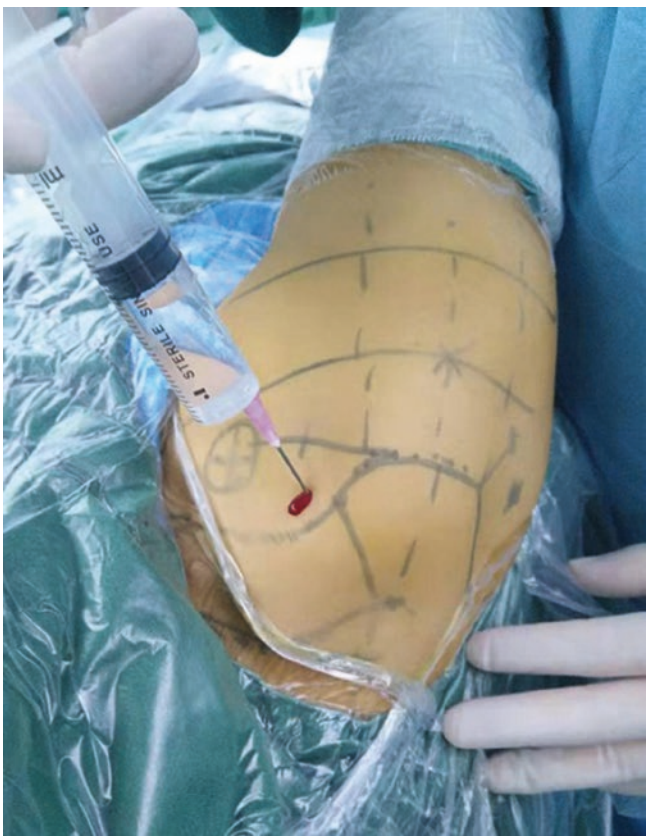

Fig. 2.11 Lidocaine anesthesia of acromioclavicular joint

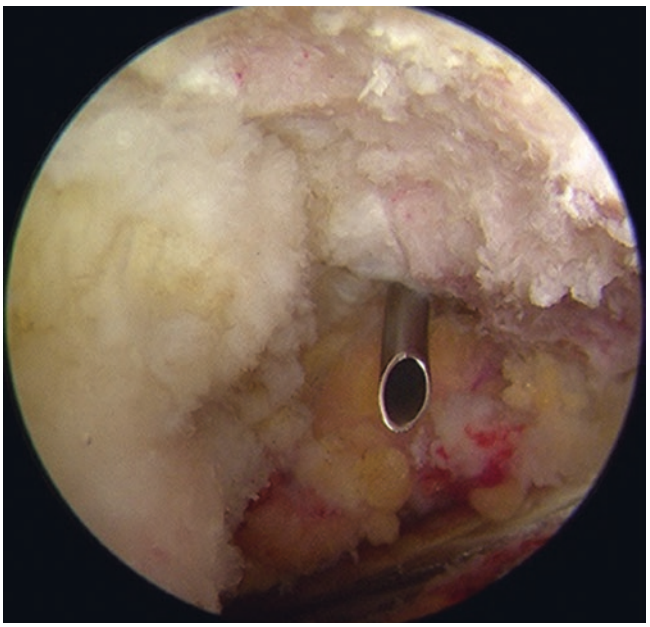

Fig. 2.12 Needle insert into acromioclavicular joint

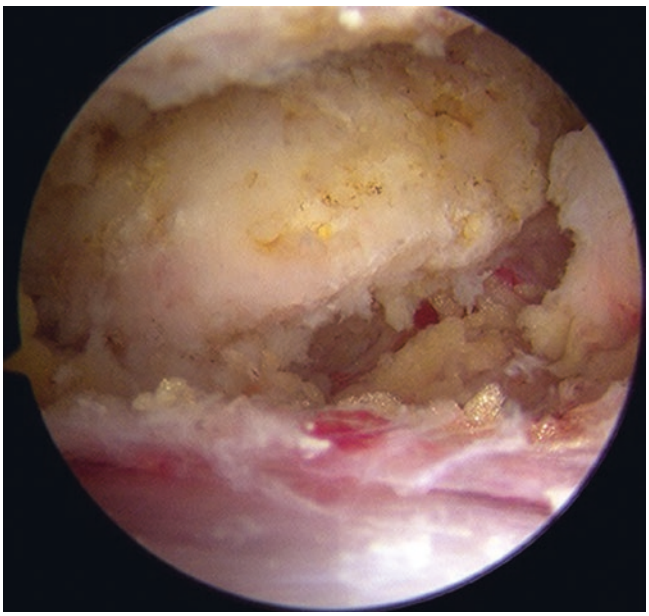

Fig. 2.14 Found that the cartilage of the acromioclavicular joint was damaged and the articular surface was rough

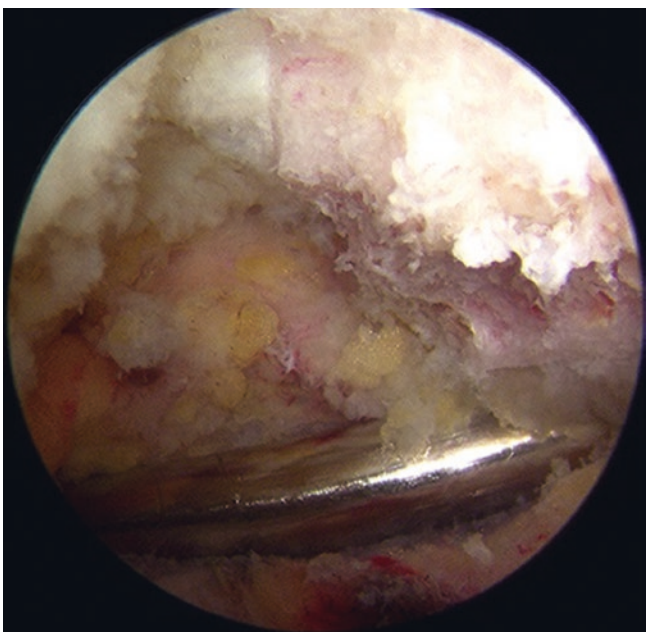

Fig. 2.13 The puncture cone and planer were respectively placed into the acromioclavicular joint

Fig. 2.15 Planing and radiofrequency scalpel clean up the fibrous tissue of acromioclavicular joint

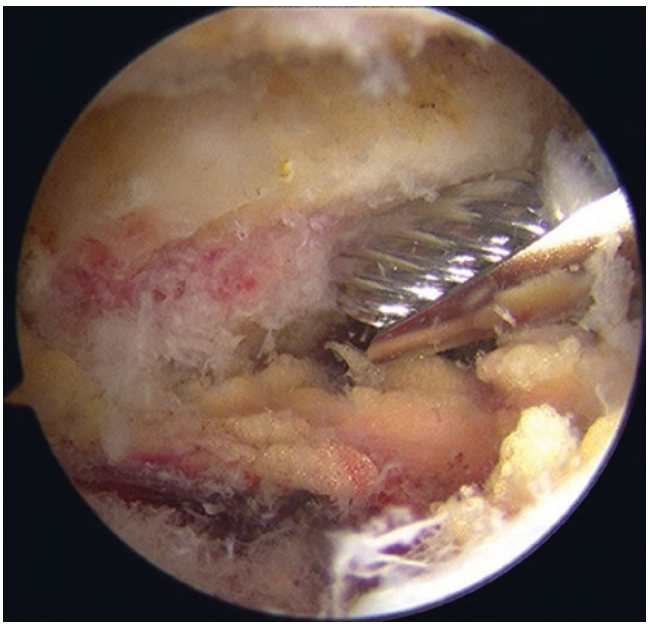

Fig. 2.16 Remove the osteophyte and perform acromioclavicular arthroplasty

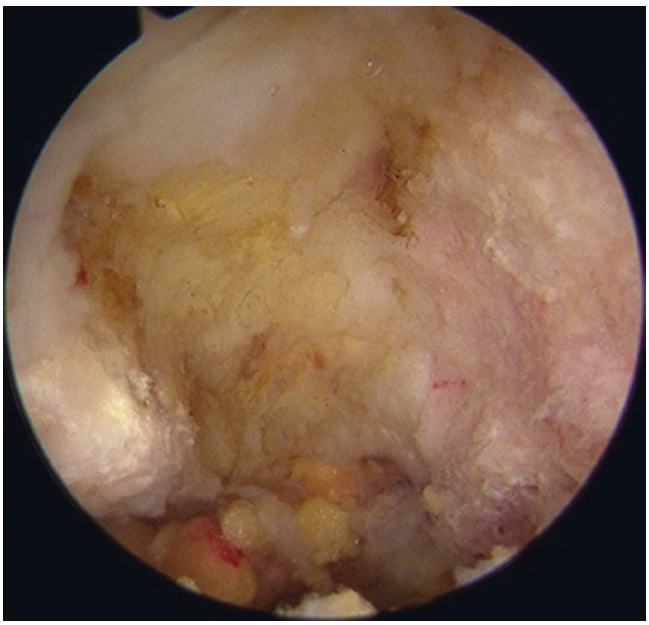

Fig. 2.18 Ligament and capsule tissue preserved after acromioclavicular arthroplasty

Fig. 2.17 The gap of acromioclavicular joint after forming is 6–8 mm

the acromioclavicular joint for impact. To ensure the stability of acromioclavicular arthroplasty paid attention to remain the acromioclavicular capsule tissue (Fig. 2.18), protect the ligaments and joints of acromioclavicular joint at the upper and superoposterior avoid affecting stability after resection [9, 10].

2.4 Postoperative Treatment

Bag suspension brake 1 week postoperation, guide patients to perform shoulder joint function exercises, pain significantly reduced or disappeared, and function is restored after 5–6 week.

With the development of shoulder arthroscopy, arthroscopic acromioclavicular arthroplasty has become an alternative to open surgery. And helps in early recovery of motor function after the operation. However, this technique requires a high level of precision and careful screening of patients before operation, which is the key to success.

2.5 Critical Points

1. The impingement sign of acromioclavicular joint may be accompanied by rotator cuff injury, biceps tendon disease, slap injury, and other shoulder diseases. Preoperative diagnosis and comprehensive treatment should be further defined.
2. Insufficient or excessive osteotomy of acromioclavicular joint will affect the postoperative effect, and the gap between acromioclavicular joint will be kept 6–8 mm.

3. Iatrogenic acromioclavicular instability will be caused after the removal of acromioclavicular joint capsule and acromioclavicular ligament.

References

1. Richards CA, Prevost AT, Speed CA, Hazleman BL. Diagnosis and relation to general health of shoulder disorders presenting to primary care. Rheumatology. 2005;44(6):800–5.
2. Chen MR, Huang JI, Victoroff BN, Cooperman DR. Fracture of the clavicle does not affect arthritis of the ipsilateral acromioclavicular joint compared with the contralateral side: an osteological study. J Bone Joint Surg Br. 2010;92(1):164–8.
3. Colegate-Stone T, Allom R, Singh R, Elias DA, Standring S, Sinha J. Classification of the morphology of the acromioclavicular joint using cadaveric and radiological analysis. J Bone Joint Surg Br. 2010;92(5):743–6.
4. Neer CS II. Impingement lesions. Clin Orthop Relat Res. 1983;173:70–7.
5. Bigliani LU, Ticker JB, Flatow EL, Soslowsky LJ, Mow VC. The relationship of acromial architecture to rotator cuff disease. Clin Sports Med. 1991;10(40):823–38.
6. Mall NA, Foley E, Chalmers PN, Cole BJ, Romeo AA, Bach BR Jr. Degenerative joint disease of the acromioclavicular joint: a review. Am J Sport Med. 2013;41(11):2684–92.
7. Strauss EJ, Barker JU, McGill K, Verma NN. The evaluation and management of failed distal clavicle excision. Sports Med Arthrosc. 2010;18(3):213–9.
8. Stine IA, Vangsness CT. Analysis of the capsule and ligament insertions about the acromioclavicular joint: a cadaveric study. Arthroscopy. 2009;25(9):968–74.
9. Pandhi NG, Esquivel AO, Hanna JD, Lemos DW, Staron JS, Lemos SE. The biomechanical stability of distal clavicle excision versus symmetric acromioclavicular joint resection. Am J Sports Med. 2013;41(2):291–5.
10. Apivatgaroon A. Arthroscopic distal clavicle and medial border of acromion resection for symptomatic Acromioclavicular joint osteoarthritis. Arthrosc Tech. 2017;6(1):e25–9.

Radiofrequency Microdebridement Under Arthroscopy for Tennis Elbow (Lateral Epicondylitis)

3

Yu-jie Liu and Jing Xue

3.1 Introduction

Tennis elbow or lateral postoperative treatment is named after tennis players for they are prone to this disease. Golfers, plumbers, painters, gardeners, bricklayers, civil carpentry and housewives are also prone to tennis elbow.

In the past, for patients whose conservative treatment was failed and work and daily life were seriously affected, open operative surgery with incisional tendon dissection was performed on the humeral epicondyle extensor tendon. Since 2002, we have used open surgery to expose the attachment of extensor carpi radialis brevis (ECRB) muscle at lateral epicondyle. The treatment with bipolar radiofrequency ablation under direct vision (Fig. 3.1) has received good results. However, for a 2 mm diameter radiofrequency treatment, the open surgery is too traumatic and does not meet the principles of minimally invasive principle [1]. In 2004, the author designed a minimally invasive surgery for the treatment of tennis elbow with radiofrequency microdebridement under local anesthesia with arthroscopic monitoring and achieved good results [2, 3]. This method is suitable for patients who recurrent after 3 months of regular conservative treatment.

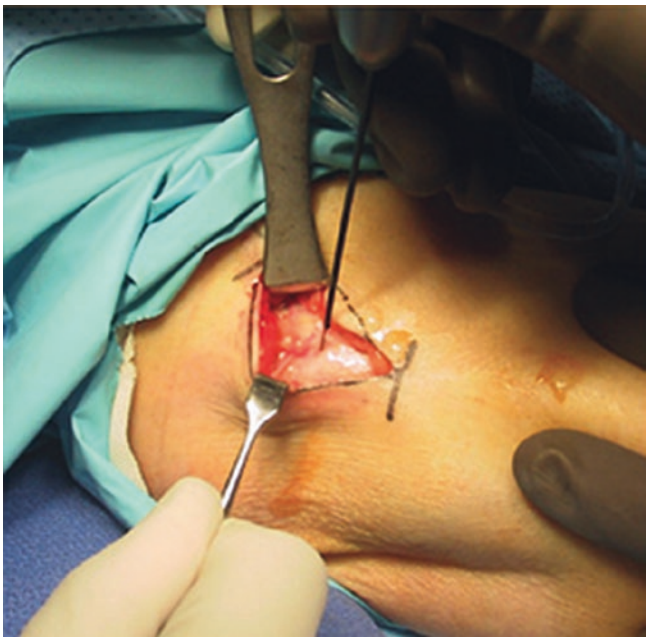

Fig. 3.1 Bipolar radiofrequency ablation under open surgery

3.2 Clinical Features

Recent studies show that tennis elbow is often due to overuse injury secondary to eccentric overload of the common extensor tendon at the origin of the extensor carpi radialis brevis (ECRB) tendon [4]. The lateral epicondyle is the attachment of the forearm common extensor tendon (Fig. 3.2). Due to repeated excessive traction, microscopic tears, hemorrhagic

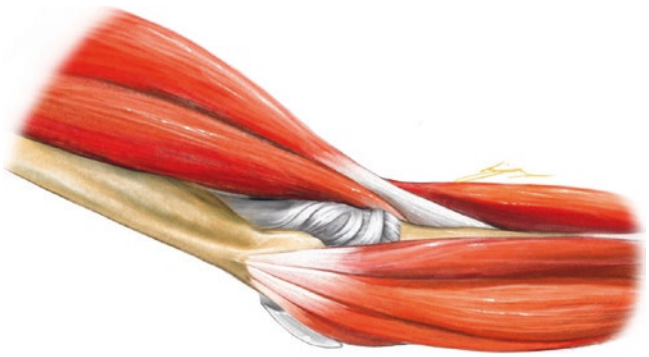

Fig. 3.2 The lateral epicondyle is the attachment of the forearm common extensor tendon

Y.-j. Liu (✉)
Department of Orthopedics, Chinese PLA General Hospital, Beijing, China

J. Xue
Department of Orthopedics, Air Force Medical Center, Beijing, China

Y.-j. Liu et al. (eds.), *Advanced Application of Arthroscopy*, https://doi.org/10.1007/978-981-15-4684-6_3

Fig. 3.3 Positive tenderness at outside of the elbow (lateral epicondyle)

edema, and scar adhesion formed in the tendon where it attaches to the lateral epicondyle. The local healing was poor after the injury, which leads to inflammation and pain. Pain is produced by any activity which places stress on the tendon, such as gripping or lifting. Daily life and work of serious patients were affected.

The pain is located on the outside of the elbow. This area is tender to the touch (Fig. 3.3). With activity, the pain usually starts at the elbow and may travel down the forearm to the hand. Occasionally, any motion of the elbow can be painful. Mill's sign (+), the grip strength of the affected side, is reduced.

3.3 Preoperative Preparation

Use of a marker to mark the tenderness of the lateral epicondyle and the surgical approach preoperatively. Local infiltration anesthesia with 10ml of 0.5% lidocaine around the external epicondyle (Fig. 3.4).

3.4 Operative Technique

At a distance of 3 cm from the external tender point of the humerus, the skin was cut 3 mm, and a periosteal stripper was inserted between the subcutaneous tissue and the attachment of the extensor tendon to make cavity of 15 × 15 mm^2 as working space (Fig. 3.5). After the working cavity is created, the arthroscope is placed into the cavity (Fig. 3.6). Under arthroscopic monitoring, the coblation wand (Topaz EZ microdebrider coblation wand, Smith & Nephew) was inserted vertically into the upper and lower pain points of the humerus, deep into the deep side of the ECRB muscle and subperiosteal.

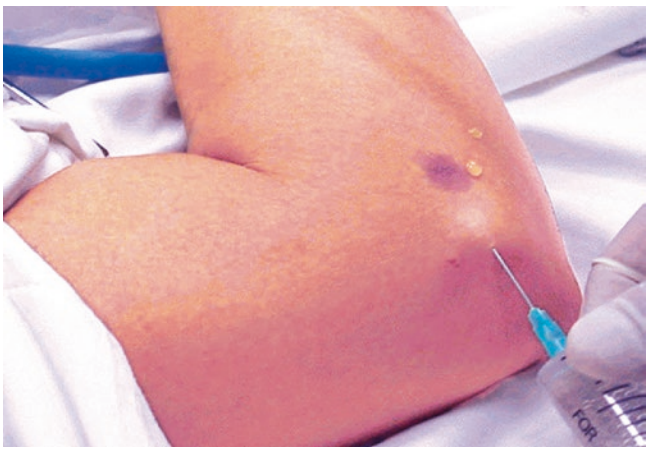

Fig. 3.4 Local infiltration anesthesia with 10ml of 0.5% lidocaine around the external epicondyle

Fig. 3.5 A periosteal stripper was inserted between the subcutaneous tissue and the attachment of the extensor tendon to make cavity of 15 × 15 mm^2 as working space

Then, radiofrequency microdebridement was performed. Set an ablation point every 3 mm, and the treatment area is mesh-like after radiofrequency ablation (Fig. 3.7). There is no need to suture the skin incision after surgery.

3.5 Postoperative Treatment

Avoid strenuous wrist movements and lifting heavy objects within 6 weeks after surgery to facilitate postoperative recovery. Grip strength test can be used as a reference for evaluation before and after treatment (Fig. 3.8).

With arthroscopic radiofrequency microdebridement for tennis elbow, we minimized trauma and avoided interference of the tissue around the tendon. The result showed no postoperative scar adhesion.

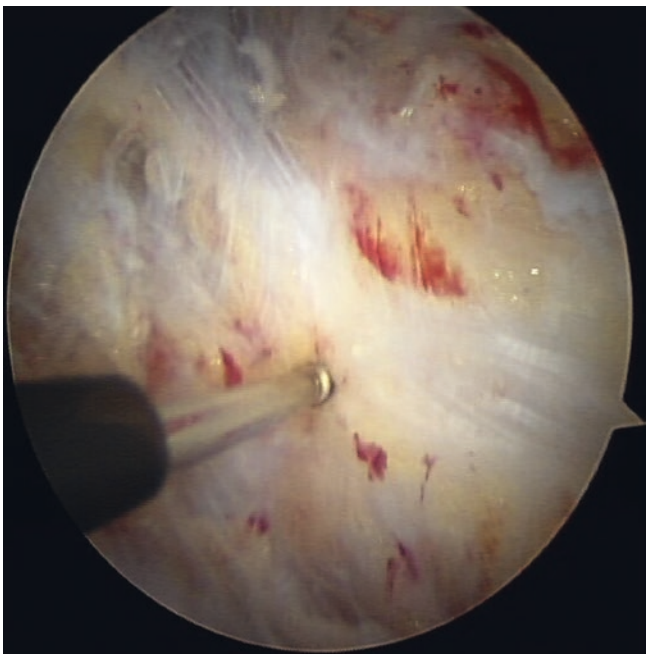

Fig. 3.6 Place the arthroscope and the coblation wand (Topaz EZ microdebrider coblation wand, Smith & Nephew) into the working cavity

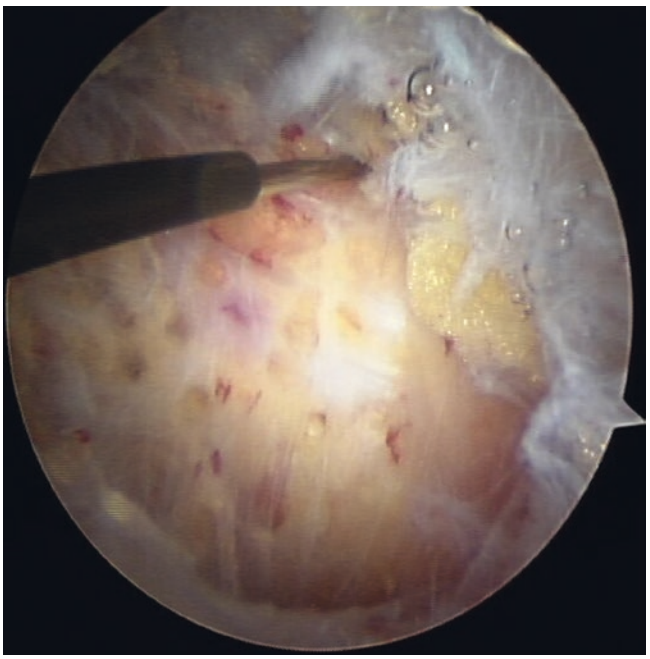

Fig. 3.7 Set an ablation point every 3 mm, and the treatment area is mesh-like after radiofrequency ablation under arthroscopy

Fig. 3.8 Grip strength test can be used as a reference for evaluation before and after treatment

References

1. Tasto JP, Richmond JM, Cummings JR, Hardesty R, Amiel D. Radiofrequency microtenotomy for elbow epicondylitis: mid-term results. Am J Orthop (Belle Mead NJ). 2016;45(1):29–33.
2. Yu-Jie L, Xu C, Mi Z, Zhong-Li L, Zhi-Gang W, Yan W, et al. Radiofrequency treatment of tennis elbow in 8 cases of arthroscopic surveillance (in Chinese). Chin J Sports Med. 2004;06:654–6.
3. Xue-Zhen S, Hong-Liang L, Qi G, Xi L, Wei Q, Feng Q, et al. Efficacy of arthroscopic guided radio frequency thermoablation for refractory lateral epicondylitis (in Chinese). Chin J Mult Organ Dis Elderly. 2016;15(05):326–9.
4. Buchanan BK, Varacallo M. Tennis elbow (lateral epicondylitis). Treasure Island (FL): StatPearls; 2019.

4 Arthroscopic Transverse Carpal Ligament Release for Carpal Tunnel Syndrome

Yu-jie Liu and Jing Xue

4.1 Introduction

The carpal tunnel is a semiannular tunnel surrounded by the carpal and transverse ligament of volar wrist. The carpal tunnel contains median nerve, flexor digitorum, superficial tendon, and flexor hallucis longus (Fig. 4.1).

Because these boundaries are very rigid, the carpal tunnel has little capacity to increase in size. Carpal tunnel syndrome occurs when the tunnel becomes narrowed or when tissues surrounding the flexor tendons swell, which lead to increased pressure and compression of the median nerve. Because the nerve tissue is very sensitive to ischemia and hypoxia, the axon can undergo demyelination. Clinical manifestations of numbness and motor dysfunction in the median nerve innervation. Cervical spondylosis should be excluded before diagnosis of this disease.

The traditional treatment of carpal tunnel syndrome is by open surgery; the incision is about 10 cm long (Fig. 4.2a). There is a risk of injury to the palmar nerve and palmar archery during surgery. Postoperative scar formation affects the sensation of palm (Fig. 4.2b). Under local anesthesia, and with small surgical incision, the author used arthroscopic transverse ligament release to treat this disease. It resulted minimize trauma and quick recovery. This technique was first described by Dr. James C.Y. Chow at 1989 [1]; we modified the procedure and introduced it into China [2].

Y.-j. Liu (✉)
Department of Orthopedics, Chinese PLA General Hospital, Beijing, China

J. Xue
Department of Orthopedics, Air Force Medical Center, Beijing, China

4.2 Clinical Features

Numbness, tingling, burning, and pain—primarily in the radial three fingers, weakness and clumsiness in the hand such as thumb-to-palm dysfunction (Fig. 4.3), and intrinsic muscle atrophy.

4.3 Portal Placement

The surgical portals should be clearly marked before surgery.

The volar portal: the patient is supine, the limb is abducted, the palm is flat, and the thumb is abducted 90°. A parallel line is drawn along the ulnar side of the first web of thumb to the ulnar side of the palm. Then a perpendicular is drawn from the radius side of ring finger. Ulnar and proximal move 1 mm from the intersection of the two lines as the distal volar portal (Fig. 4.4).

The wrist portal: 15 mm proximal and 15 mm lateral to the bean bone, that is, the intersection of the proximal transverse wrist crease and the ulnar side of palmaris longus (Fig. 4.4).

Routinely disinfection, laying sterile towels. Local infiltration anesthesia in the surgical incision and carpal tunnel. No tourniquets are needed.

4.4 Surgical Technique

4.4.1 Establish Surgical Access

Use a sharp knife to cut the skin 4 mm at the proximal wrist portal, separating the subcutaneous tissue (Fig. 4.5). During the whole procedure, the wrist joint should be kept hyperextended so that the nerves and tendons in the carpal tunnel can be tightly attached to the back side of the carpal tunnel to protect them from injured. Then a blunt tip trocar is inserted under transverse carpal ligament. The trocar is

Y.-j. Liu et al. (eds.), *Advanced Application of Arthroscopy*, https://doi.org/10.1007/978-981-15-4684-6_4

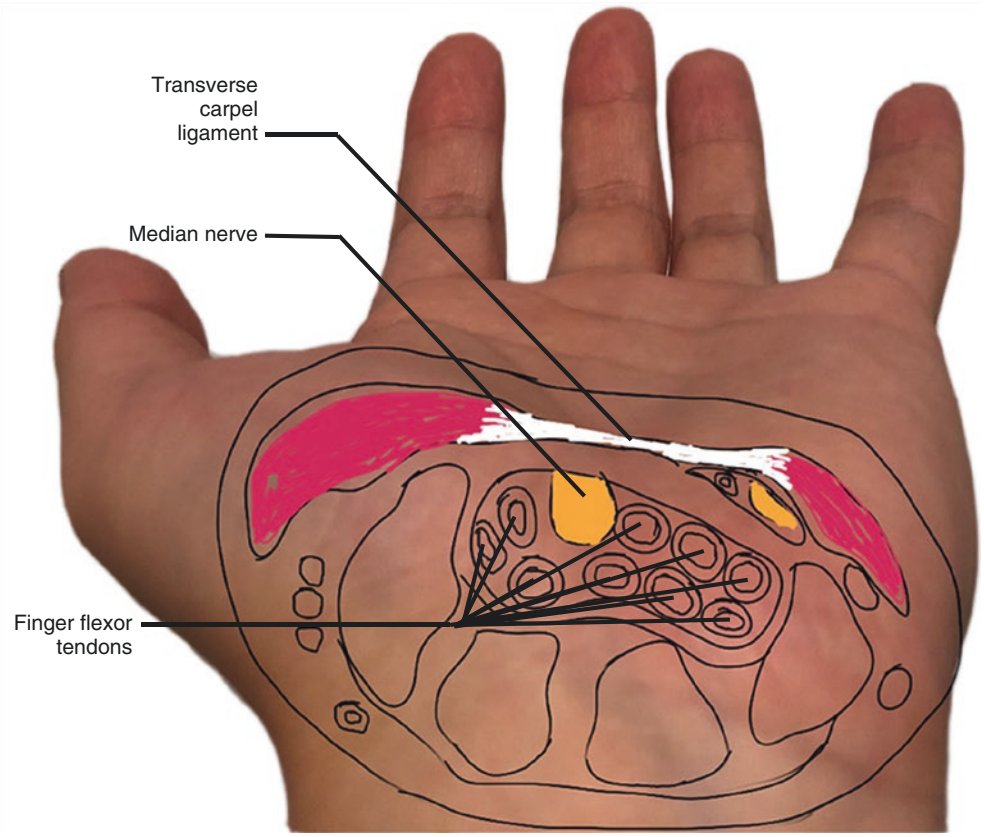

Fig. 4.1 Carpal tunnel and its contents

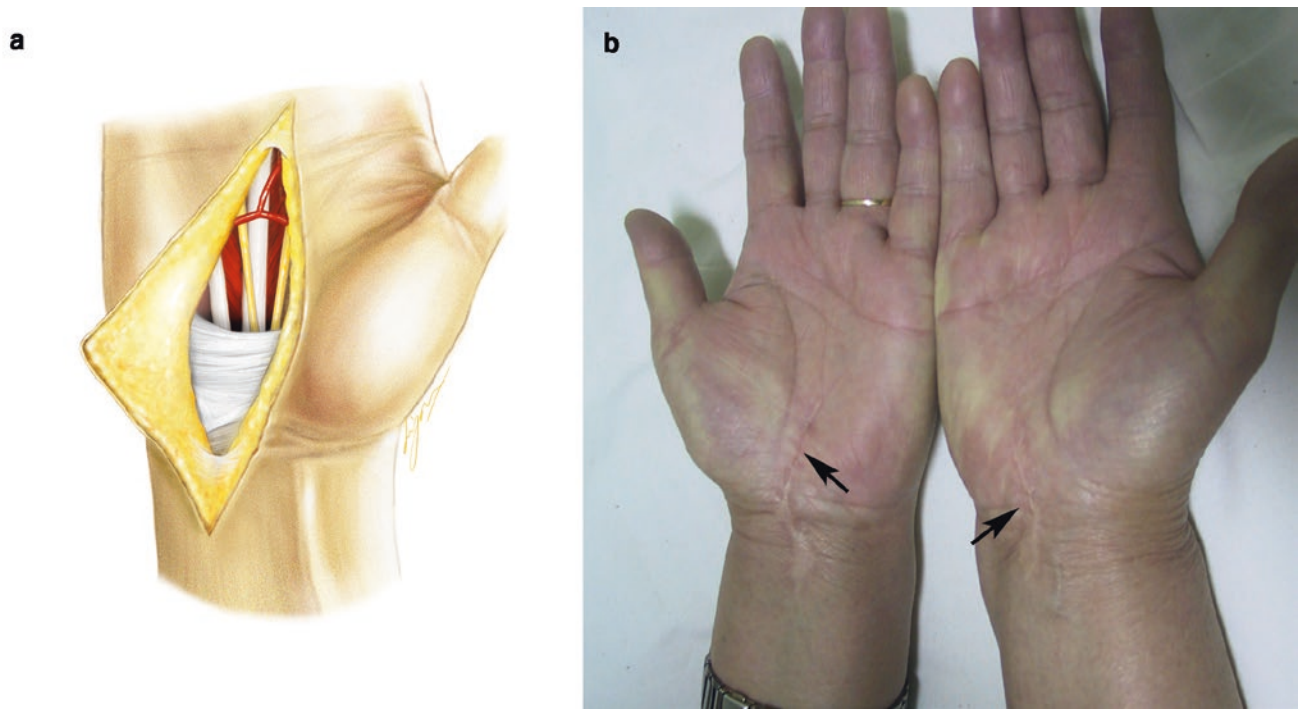

Fig. 4.2 Surgical incision (**a**) and scars (**b**) of open surgery of carpal tunnel syndrome

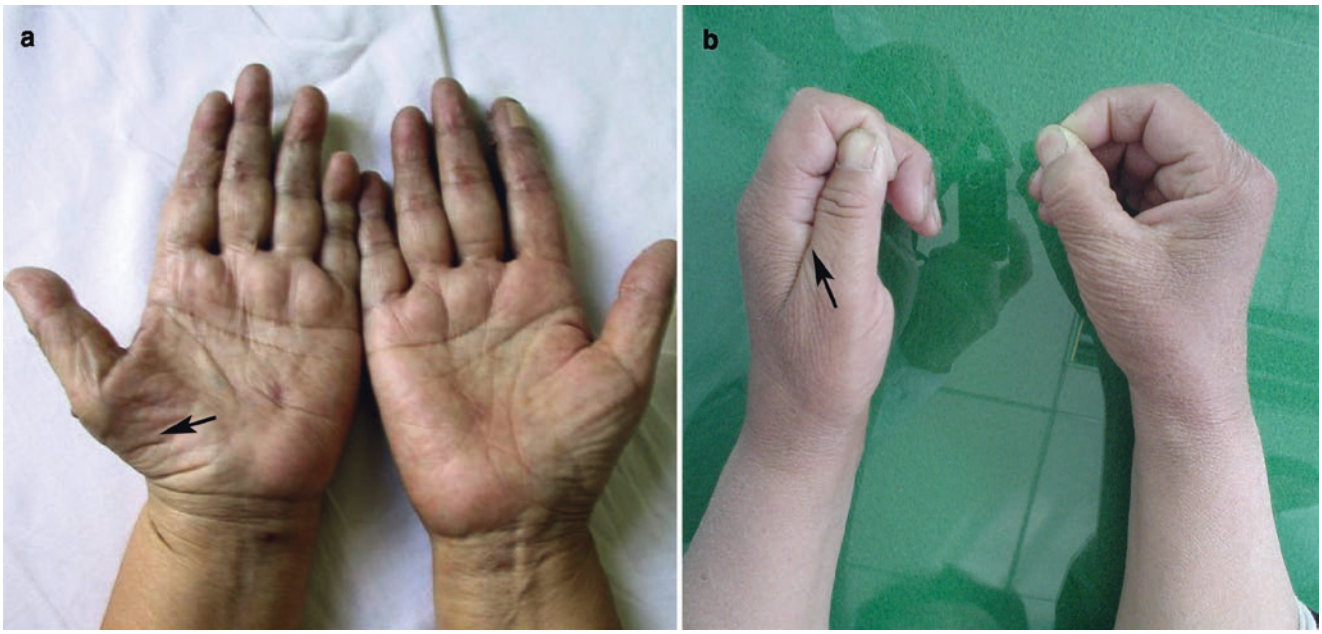

Fig. 4.3 Intrinsic muscle atrophy (**a**); thumb-to-palm dysfunction (**b**)

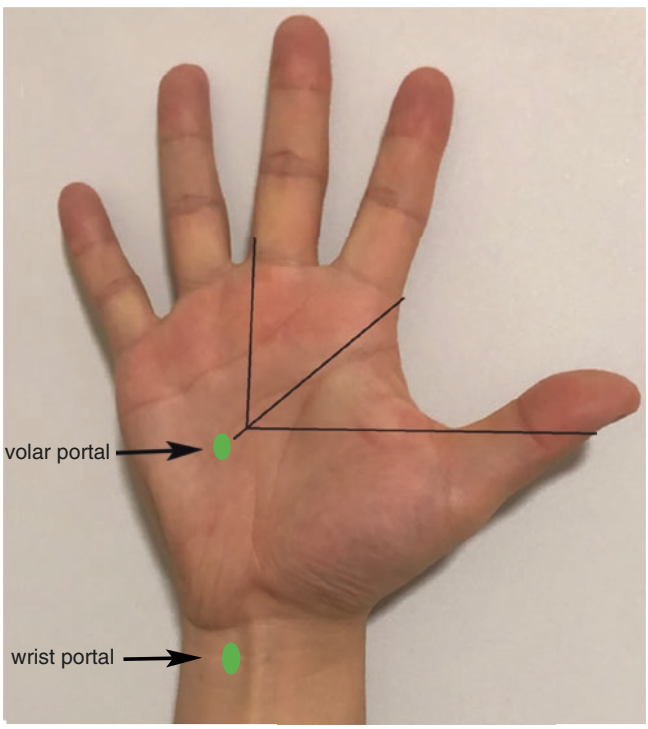

Fig. 4.4 Placement of volar portal and wrist portal

placed strictly against the wall of the carpal tunnel and then advanced toward the volar portal, reaching the subcutaneous tissue, and a second 4 mm skin incision is made so that the trocar can penetrate out (Fig. 4.6). Then a special arthroscopy sheath is inserted from distal to proximal. The groove of the sheath is turned toward the transverse carpal tunnel (Fig. 4.7). Place the arthroscope from the distal end of the cannula for observation (Fig.4.8). Carefully probe and make sure the entire carpal ligament is under vision and no other tissue is caught between the trocar and the carpal ligament.

4.4.2 Arthroscopic Transverse Carpal Ligament Release

Thickened wrist transverse ligament is milky white under the view of arthroscopy (Fig. 4.9). A hook knife is inserted from proximal portal to upward cut the carpal ligament, and the carpal ligament fibers are released until it is completely released (Fig. 4.10). The releasement can also be done by a retrograde knife (Fig. 4.11). As the transverse ligament is cut, fat tissue protrudes into the cannula (Fig. 4.12).

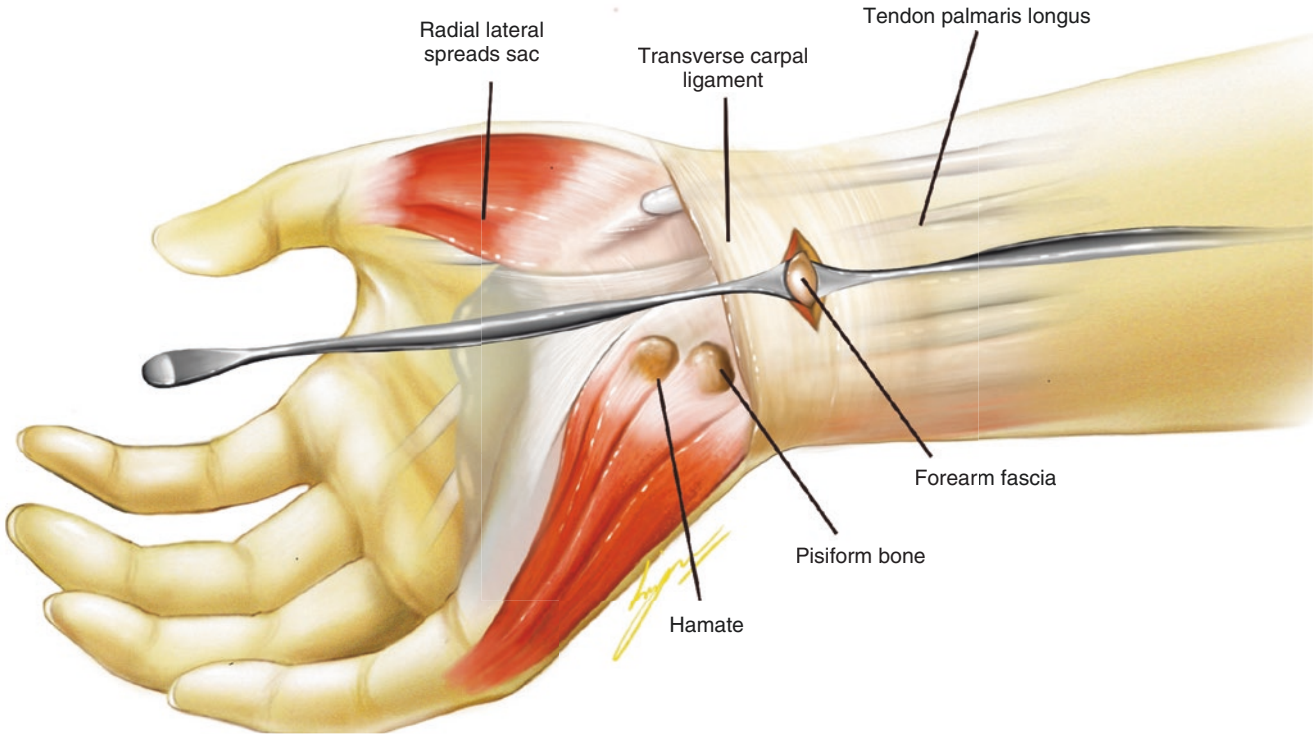

Fig. 4.5 Use a sharp knife to cut the skin 4 mm at the proximal wrist portal, separating the subcutaneous tissue

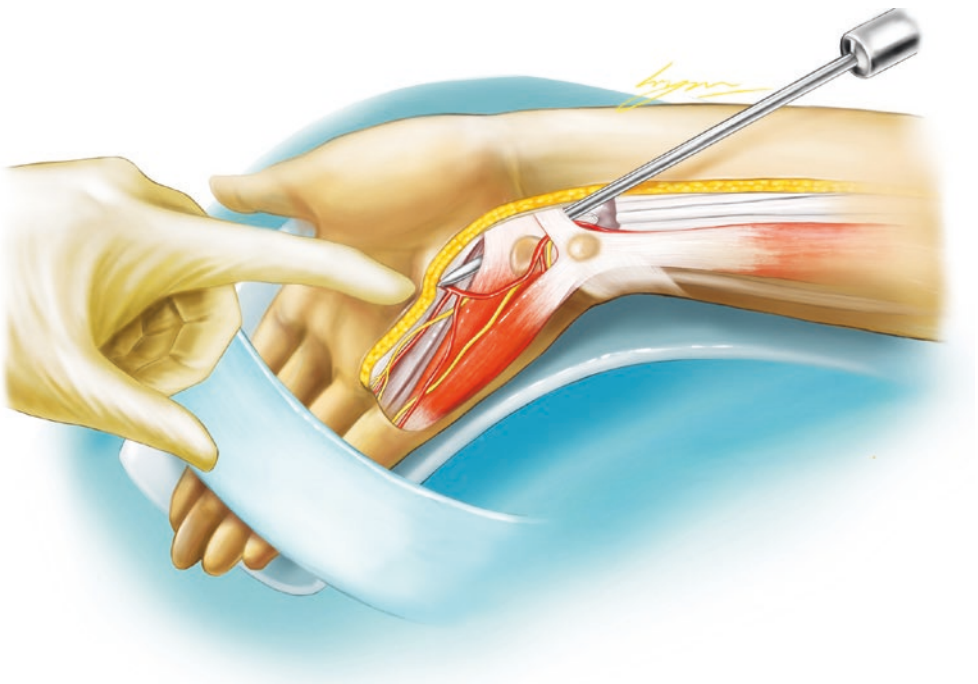

Fig. 4.6 The trocar is placed strictly against the wall of the carpal tunneland then advanced toward the volar portal, reaching the subcutaneous tissue, and a second 4 mm skin incision is made so that the trocar can penetrate out

Use the probe to explore the incision of the transverse ligament (Fig. 4.12). If there is no abnormality, pull out the sheath; the incision is no need of suture. Pressure bandaging with gauze and the cold bag is used to stop bleeding after operation.

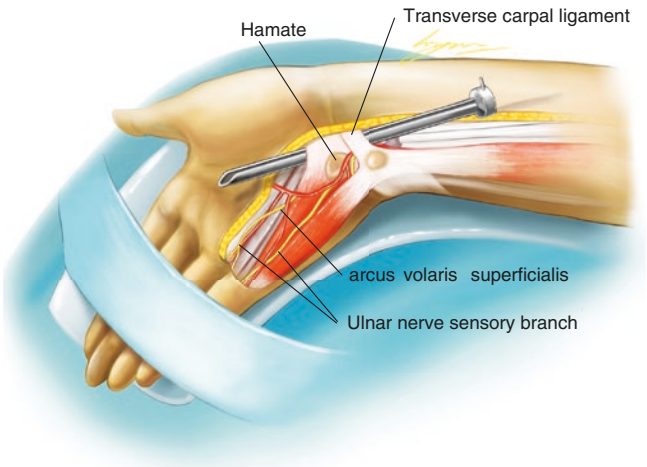

Fig. 4.7 The groove of the sheath is turned toward the transverse carpal tunnel

4.4.3 Postoperative Treatment

Patients should be encouraged to perform gripping activities after surgery to prevent adhesions.

Arthroscopic "two-portal" technique is an effective surgical procedure for transverse carpal ligament release with minimal incision (Fig. 4.13), less tissue trauma, and shorter operation time. The effect is satisfying (Fig. 4.14).

4.5 Critical Points

1. Carpal tunnel syndrome should be differentiated from cervical spondylosis. The disease is characterized by a loss of sensory area in the distal median nerve branch below the wrist joint, and a positive Tinel's sign on the volar side of the wrist. Cervical MRI or limb electromyography should be performed if necessary.
2. Strict selection of surgical indications, if there is median nerve recurrent branch entrapment syndrome (RMNES), and there is serious muscle atrophy of thenar, muscle strength 0–1, EMG shows denervation potential, and it is difficult to restore postoperatively.

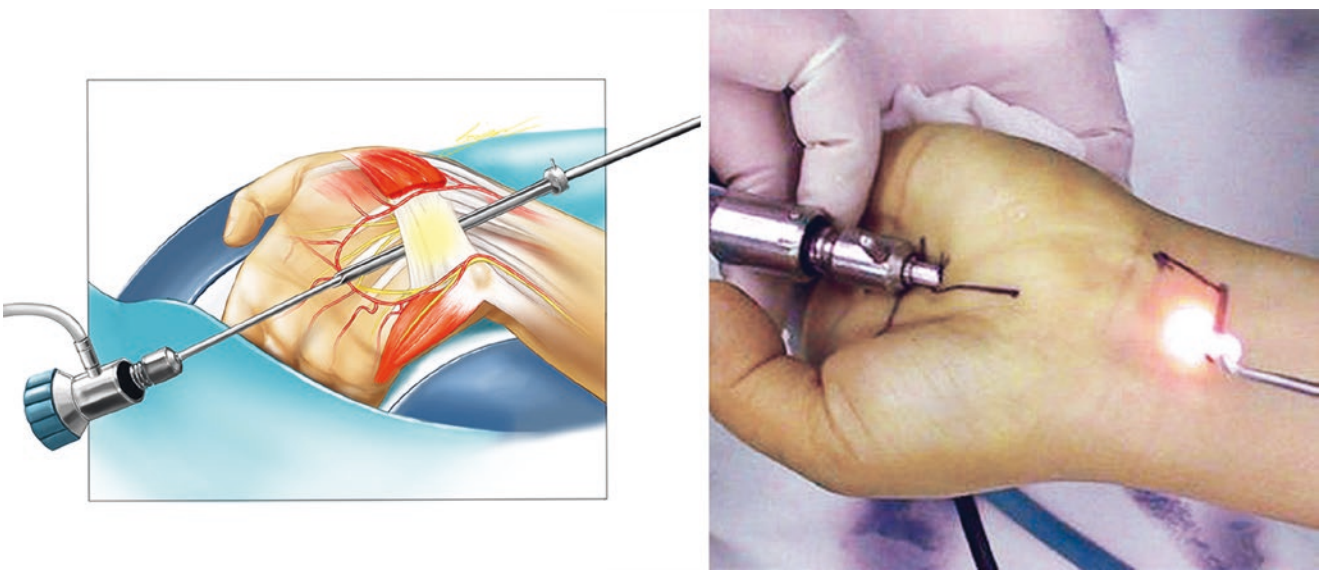

Fig. 4.8 Place the arthroscope from the distal end of the cannula for observation

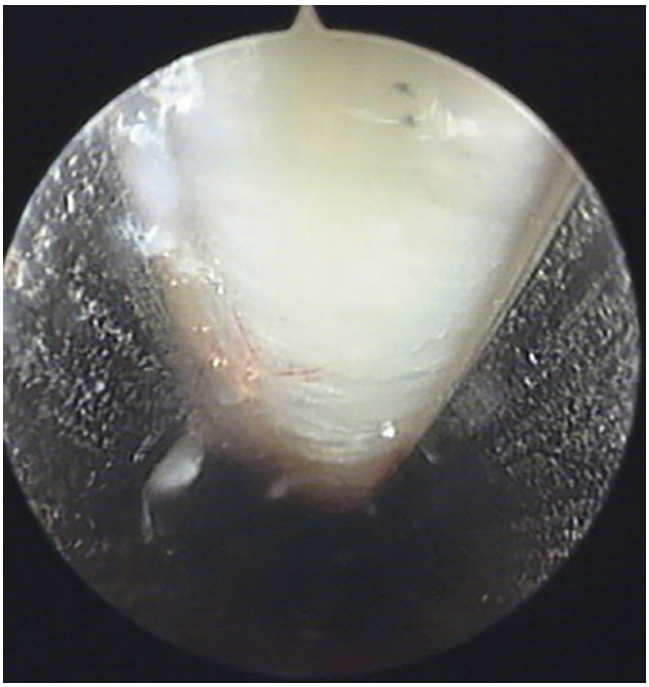

Fig. 4.9 Thickened wrist transverse ligament is milky white under the view of arthroscopy

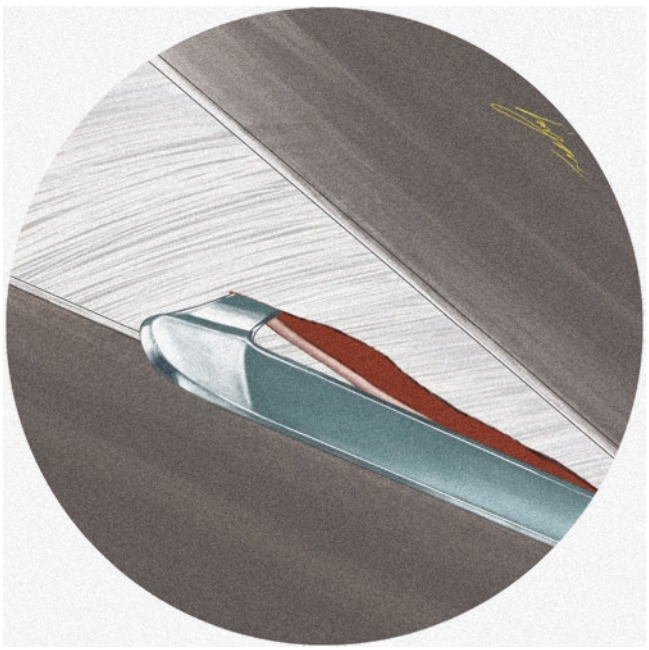

Fig. 4.11 The releasement can also be done by a retrograde knife

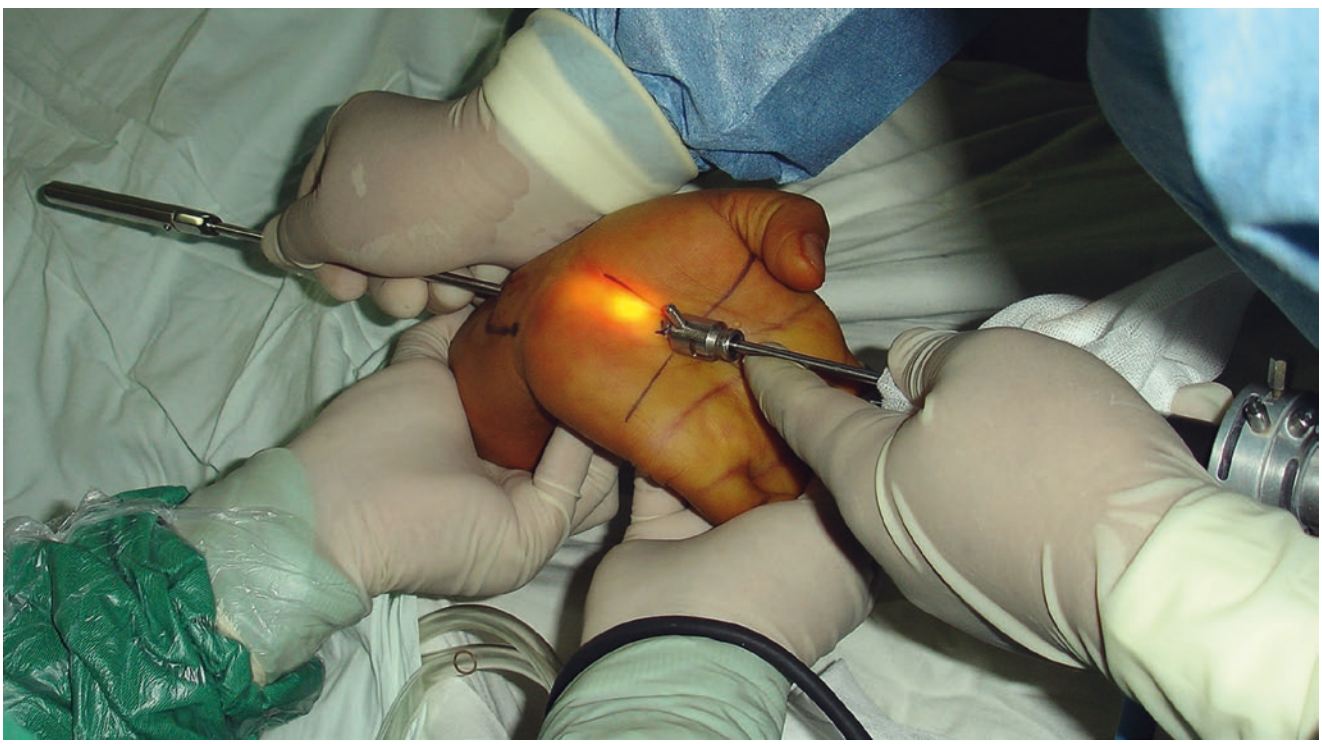

Fig. 4.10 A hook knife is inserted from proximal portal to upward cut the carpal ligament, and the carpal ligament fibers are released until it is completely released

Fig. 4.12 As the transverse ligament is cut, fat tissue protrudes into the cannula

Fig. 4.13 Small surgical scar after arthroscopic transverse carpal ligament release

Fig. 4.14 The patient was satisfied with result of the operation

3. If the carpal tunnel syndrome is caused by the angular deformity of a Colles' fracture. The deformity should be corrected first, for it is difficult to solve the compression only by release the transverse carpal ligament.
4. During the operation, the wrist joint should be kept hyperextended so that the nerves and tendons in the carpal tunnel can be tightly attached to the back side of the carpal tunnel to protect them from injured.
5. Do not move the hook knife out of the sheath, taking care not to damage the superficial palmar venous arch.

References

1. Chow JC. Endoscopic release of the carpal ligament: a new technique for carpal tunnel syndrome. Arthroscopy. 1989;5(1):19–24. https://doi.org/10.1016/0749-8063(89)90085-6.
2. 刘玉杰，陈继营，王志刚，李众利，张文涛，王岩, et al. 关节镜镜视下行腕横韧带切开术. 中华手外科杂志. 2002(03):30–1.

Arthroscopic Palmar Membrane Release for Dupuytren's Disease

5

Yu-jie Liu and Jing Xue

5.1 Introduction

The main function of the palmar aponeurosis is to increase grip of the hand. The central portion of palmar aponeurosis occupies the middle of the palm, triangular in shape (Fig. 5.1). Dupuytren's contracture or Dupuytren's disease (DD) is a progressive condition that causes the fibrous tissue of the palmar fascia to shorten and thicken. The ring finger and little finger are the fingers most commonly affected. The middle finger may be affected in advanced cases, but the index finger and the thumb are nearly always spared [1]. The disease is common in men older than 40 years; in persons of Northern European descent; and in persons who smoke, use alcohol, or have diabetes [2]. A review and meta-analysis results support the hypothesis of an association between high levels of work exposure (manual work and vibration exposure) and Dupuytren's contracture in certain cases [3].

5.2 Clinical Features

The patient typically presents with a loss of range of motion of the hand and palpable cords in the palm extending into the affected digits. If presenting early in onset, they may only notice the palpable cord. The tabletop test (Hueston) is performed by having the patient attempt to place the palm flat on the exam table. If there is any flexion contracture deformity, the patient will be unable to straighten the fingers, resulting in a positive test [4].

Disease progression is classified using a grading system (Fig. 5.2). Grade 1 disease presents as a thickened nodule and a band in the palmar aponeurosis; this band may progress to skin tethering, puckering, or pitting. Grade 2 presents as a peritendinous band, and extension of the affected finger is limited. Grade 3 presents as flexion contracture [2].

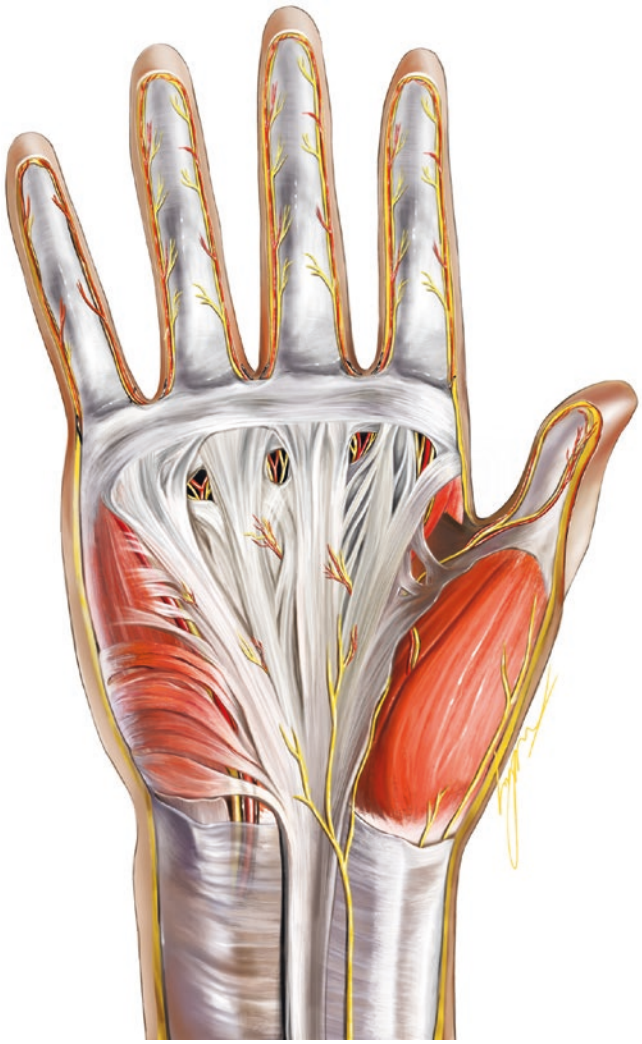

Fig. 5.1 Anatomy of the palmar fascia

Grade 1 disease initially can be managed expectantly, but injecting the nodule with a steroid can be helpful [2]. Surgery

Y.-j. Liu (✉)
Department of Orthopedics, Chinese PLA General Hospital, Beijing, China

J. Xue
Department of Orthopedics, Air Force Medical Center, Beijing, China

Y.-j. Liu et al. (eds.), *Advanced Application of Arthroscopy*, https://doi.org/10.1007/978-981-15-4684-6_5

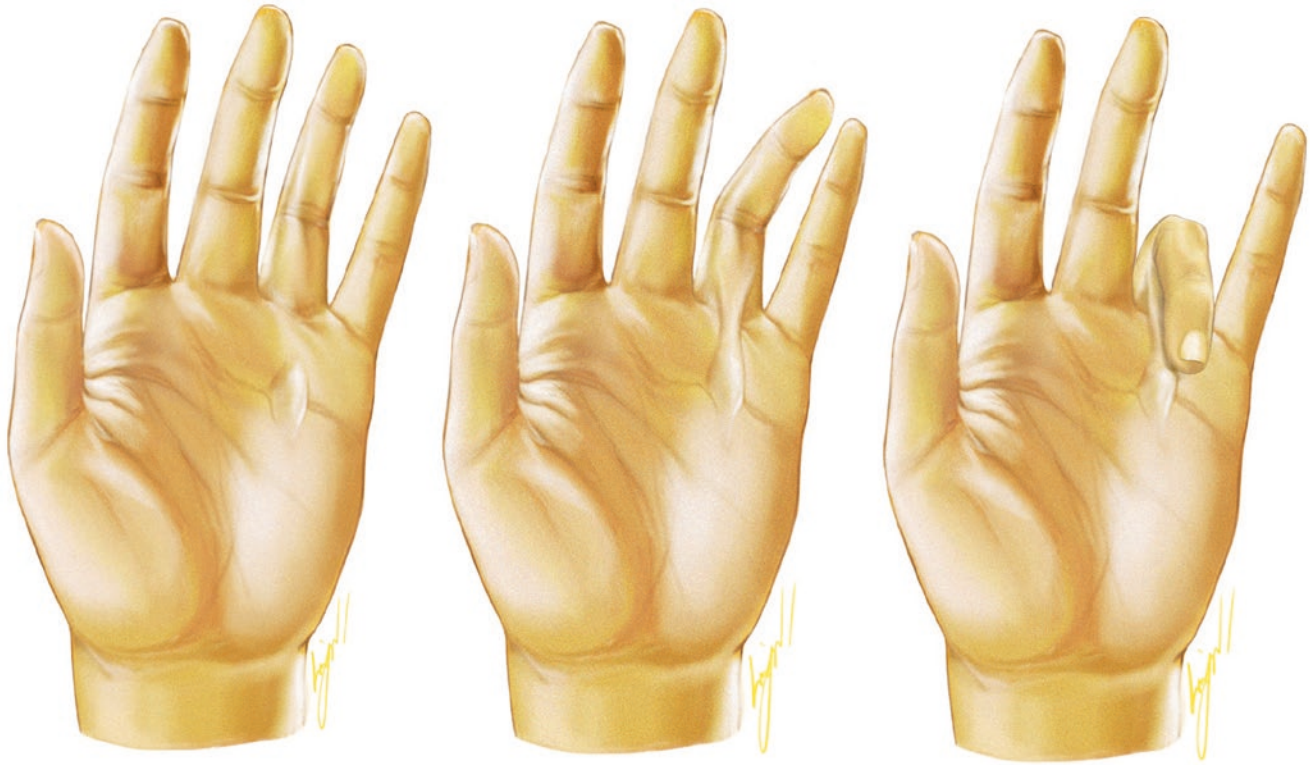

Fig. 5.2 Grades of Dupuytren's disease

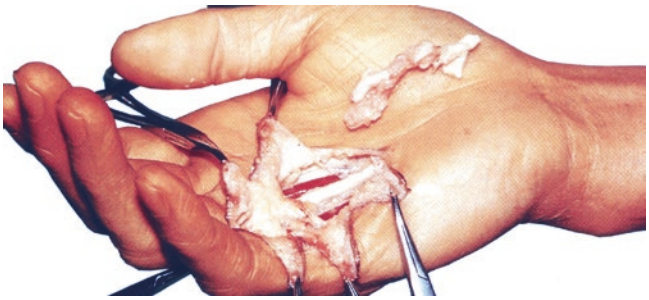

Fig. 5.3 Open surgery is routinely used to perform partial palmar fasciectomy to relieve contractures of the metacarpophalangeal and interphalangeal joints

is recommended if function is impaired, contracture is progressing, or severe deformity is disabling. Accepted indications for surgical intervention include metacarpophalangeal joint contracture of 30° and any degree of proximal interphalangeal joint contracture [5].

Open surgery is routinely used to perform partial palmar fasciectomy (Fig. 5.3) to relieve contractures of the metacarpophalangeal and interphalangeal joints. The author used arthroscopy for the treatment of metatarsal contractures with palm fasciolysis, which is a minimally invasive operation, which is beneficial to early functional exercises and has achieved good results.

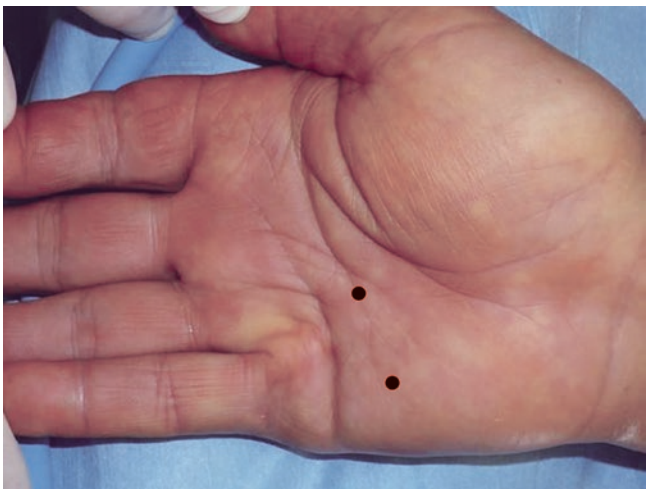

Fig. 5.4 Before operation, arthroscopic portals are marked

5.3 Preoperative Preparation

The surgery is performed under brachial plexus block anesthesia and upper arm tourniquet. Before operation, the fascia contracture bands and arthroscopic portals are marked (Fig. 5.4). The patient is supine, with upper limb abduction and routine disinfection of the surgical field.

5.4 Operative Technique

In order to obtain a clear surgical view field, physiological saline containing epinephrine was injected into the subcutaneous tissue of the contracture zone of the palmar membrane (Fig. 5.5).

Next to the contracture band of the palm, make two 2–3 mm incisions for arthroscopic portal (Fig. 5.6) and instrument portal. Insert a stripper to make a working cavity between the contracture band and the subcutaneous tissue. Then, arthroscopy sheath (Fig. 5.7) with a wide-angle 2.7 mm 30° arthroscope is placed from one portal. A shaver is placed from another portal to clear scar tissue (Fig. 5.8) and reveal the palmar aponeurotic contracture band (Fig. 5.9).

Fig. 5.5 In order to obtain a clear surgical view field, physiological saline containing epinephrine was injected into the subcutaneous tissue of the contracture zone of the palmar membrane

Fig. 5.6 Next to the contracture band of the palm, make a 2–3 mm incision for arthroscopic portal

Fig. 5.7 Insert arthroscopy sheath to establish a view portal

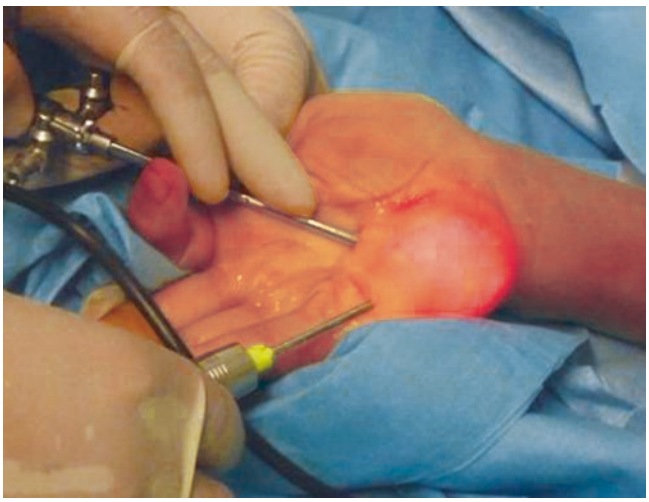

Fig. 5.8 A shaver is placed from another portal to clear scar tissue

Then, use radiofrequency blade to release the palmar aponeurotic contracture band. Attention should be paid to protecting the vascular, nerves, inner hand muscles (Fig. 5.10), and flexor tendons (Fig. 5.11) during the operation. When the release is close to the carpal tunnel, be careful not to injure the median nerve interstitial branch and ulnar nerve (Fig. 5.12). Completely stops bleeding and drainage is placed in the wound after surgery. The palm area is compressed with gauze rolls to stop bleeding, eliminate dead space, and prevent hematoma formation.

5.5 Postoperative Treatment

Remove drainage 12–24 h after surgery. Patients are encouraged to stretch fingers and practice grasping after surgery to prevent tendon adhesions.

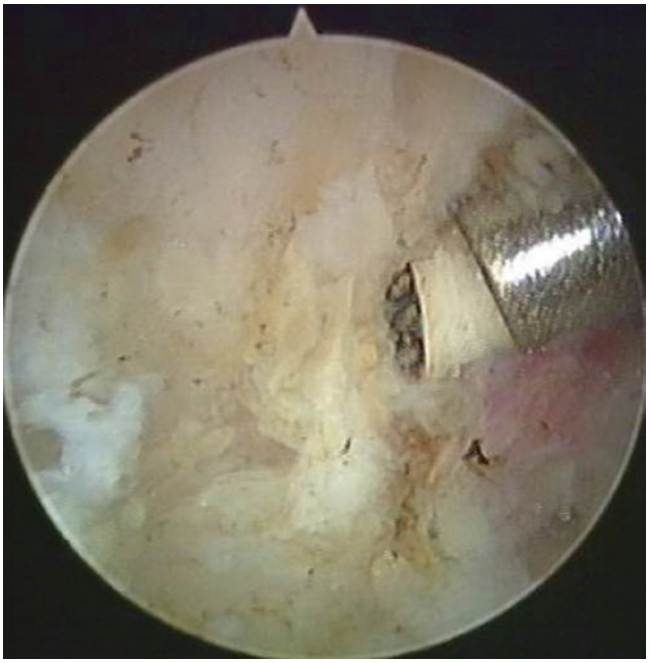

Fig. 5.9 Revealing the palmar aponeurotic contracture band

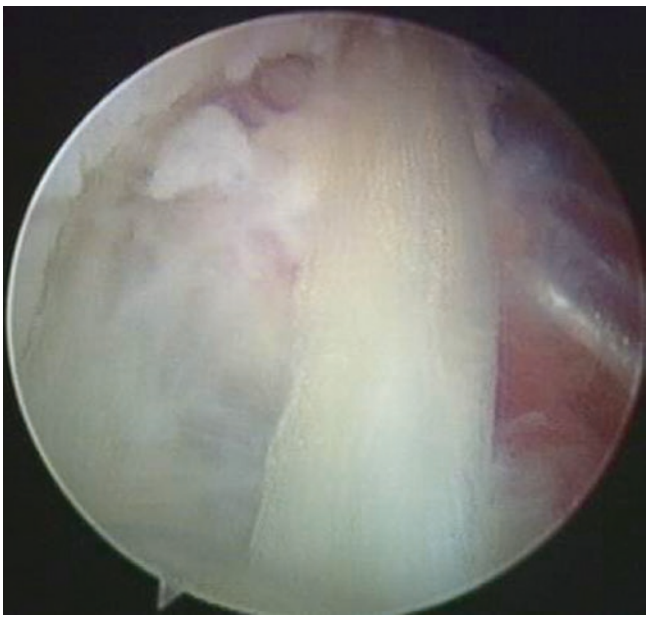

Fig. 5.11 Flexor tendons, viewed under arthroscopy

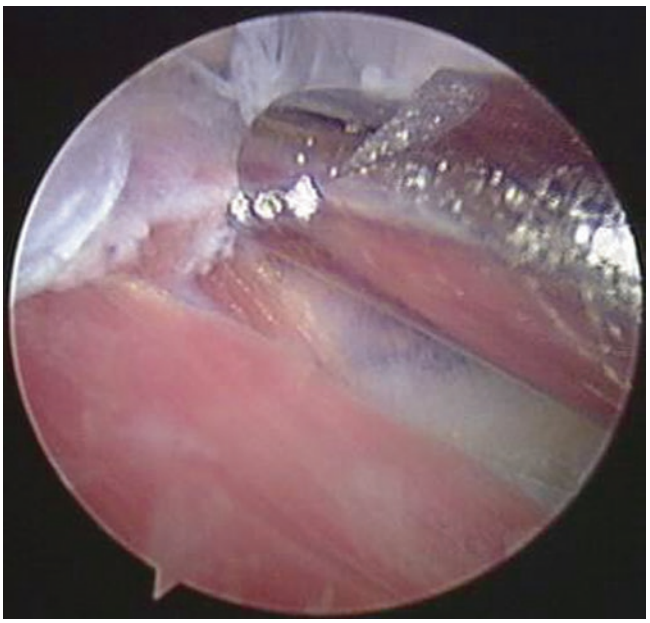

Fig. 5.10 Attention should be paid to protecting the vascular, nerves, inner hand muscles

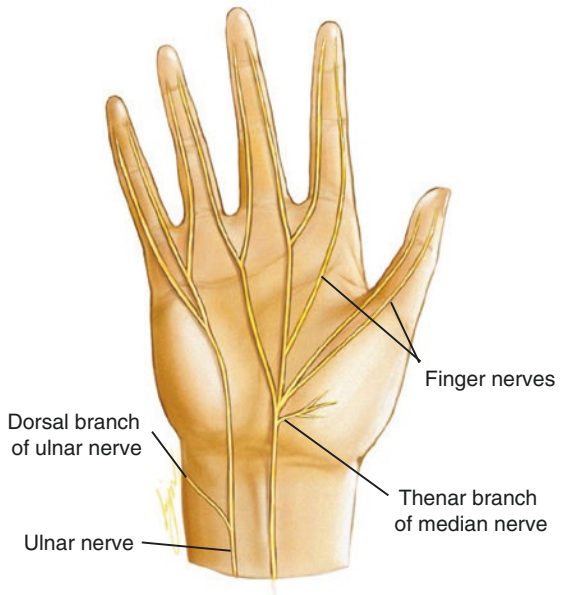

Fig. 5.12 Anatomical diagram of the median nerve interstitial branch and ulnar nerve

5.6 Critical Points

- Attention should be paid to protecting the vascular, nerves, inner hand muscles (Fig. 5.10), and flexor tendons (Fig. 5.11) during the operation.
- When the release is close to the carpal tunnel, be careful not to injure the median nerve interstitial branch and ulnar nerve (Fig. 5.12).

References

1. Tastos JP, Richmond JM, Cummings JR, Hardesty R, Amiel D. Radiofrequency Microtenotomy for elbow Epicondylitis: mid-term results. Am J Orthop (Belle Mead NJ). 2016;45(1):29–33.
2. Yu-Jie L, Xu C, Mi Z, Zhong-Li L, Zhi-Gang W, Yan W, et al. Radiofrequency treatment of tennis elbow in 8 cases of arthroscopic surveillance (in Chinese). Chinese Journal of Sports Medicine. 2004;06:654–6.
3. Xue-Zhen S, Hong-Liang L, Qi G, Xi L, Wei Q, Feng Q, et al. Efficacy of arthroscopic guided radio frequency thermoablation for refractory lateral epicondylitis (in Chinese). Chinese Journal of Multiple Organ Diseases in the Elderly. 2016;15(05):326–9.
4. Buchanan BK, Varacallo M. Tennis elbow (lateral Epicondylitis). Treasure Island (FL): Stat Pearls; 2019.
5. Townley WA, Baker R, Sheppard N, Grobbelaar AO. Dupuytren's contracture unfolded. BMJ. 2006;332(7538):397–400.

Arthroscopic Release of the Deltoid Contracture

6

Yu-jie Liu and Jing Xue

6.1 Introduction

The deltoid is comprised of three distinct portions (anterior or clavicular, middle or acromial, and posterior or spinal) and acts mainly as an abductor of the shoulder and stabilizer of the humeral head. Though deltoid contracture is uncommon in developed countries, it is much more common in developing countries, often is associated with intramuscular injection in deltoid [1, 2]. Congenital fibrosis and trauma also are causes of deltoid contracture [3].

6.2 Clinical Features

Typical clinical manifestations of deltoid contracture are a palpable fibrous cord within the deltoid muscle, abduction and extension contracture of the shoulder (Fig. 6.1), skin dimpling overlying the fibrous bands (Fig. 6.2), and winged scapula (Fig. 6.3).

The surgery was indicated in patients with abduction deformity of more than 30 degrees at the shoulder [1]. However, the approach has not been well defined. A large transverse or longitudinal skin incision is made to release the band and has the disadvantages of keloid formation, intramuscular hematoma, wound dehiscence, and prohibition of immediate postoperative rehabilitation [1]. In 2003, we designed and performed arthroscopic release of deltoid contracture which caused by repeated intramuscular injection and achieved good results.

Fig. 6.1 This young male patient with deltoid contracture of right shoulder showed a palpable fibrous cord (arrow) within the deltoid muscle and limited shoulder adduction

Y.-j. Liu (✉)
Department of Orthopedics, Chinese PLA General Hospital, Beijing, China

J. Xue
Department of Orthopedics, Air Force Medical Center, Beijing, China

Y.-j. Liu et al. (eds.), *Advanced Application of Arthroscopy*, https://doi.org/10.1007/978-981-15-4684-6_6

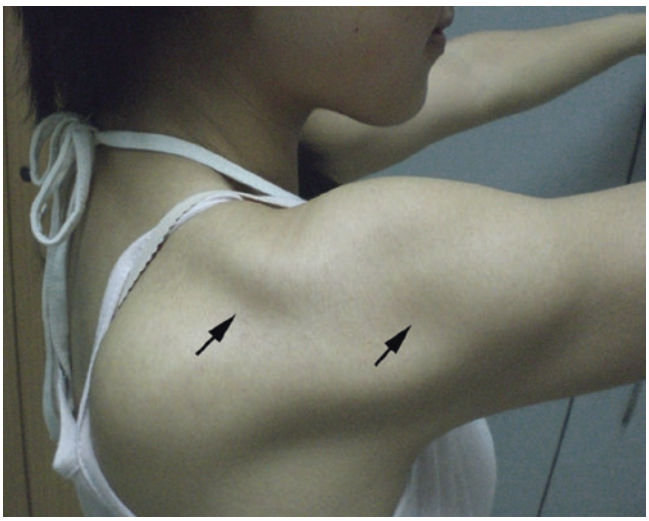

Fig. 6.2 This young female patient showed contracture sulcus in the deltoid muscle area (arrows) that had received repeated intramuscular injection

6.3 Preoperative Preparation

Mark the osteo-anatomical landmarks of the shoulder joint and deltoid muscle contracture bands before operation. With general anesthesia, the patient is positioned in supine with a towel beneath the back, and the upper extremity is draped so that it is freely accessible (Fig. 6.4).

6.4 Operative Technique

Between the subcutaneous tissue and the contracture zone of deltoid muscle, 40–50 ml of normal saline containing epinephrine is injected before operation to achieve the purpose of stopping bleeding and maintaining clear vision during operation. Two 4 mm skin incisions are made at 2 cm anterior inferior and 2 cm posterior inferior of the acromion as arthroscopy and instrument portals (Fig. 6.5). Then, insert a

Fig. 6.3 This young female patient showed winged scapula while shoulder joint put down from upper to lower (arrows)

Fig. 6.4 With general anesthesia, the patient is positioned in supine with a towel beneath the back, and the upper extremity is draped so that it is freely accessible

Fig. 6.5 Two 4 mm skin incisions are made at 2 cm anterior inferior and 2 cm posterior inferior of the acromion as arthroscopy and instrument portals

stripper bluntly separates the surface of the deltoid muscle contracture zone to create a working cavity (Fig. 6.6). The arthroscope is inserted through one portal, and a shaver is inserted through the other. Under arthroscopic surveillance, the fatty tissue on the surface of the contracture band is cleared to reveal the contracture band (Fig. 6.7). Then, release the deltoid contracture band with radiofrequency along the edge of the acromion (Fig. 6.8).

During the operation, pay attention to find out the position, depth, and range of deltoid muscle contracture zone, and pay attention to protect the normal deltoid muscle fiber. While releasing, massage and check the passive ROM of the shoulder joint. With the contraction band released, the passive ROM of the shoulder joint should return to normal, and the affected upper limb could be close to the chest wall.

The ROM of shoulder joint returned to normal after surgery (Fig. 6.9).

Fig. 6.6 Insert a stripper bluntly separates the surface of the deltoid muscle contracture zone to create a working cavity

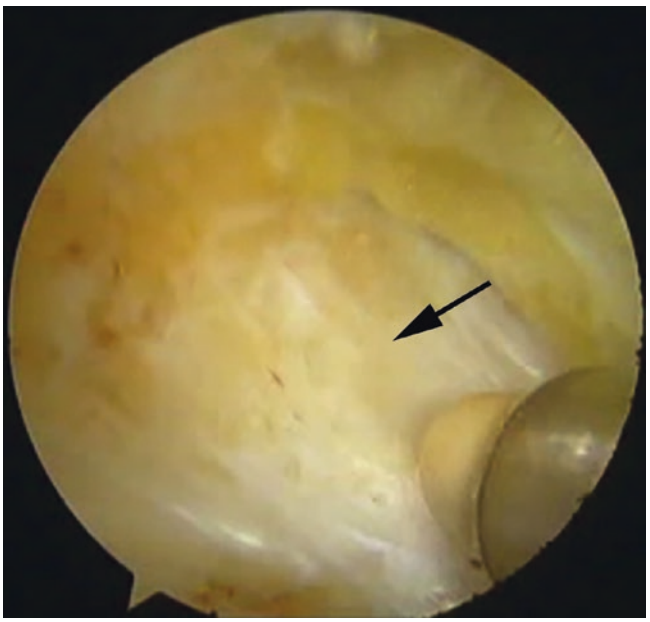

Fig. 6.7 Under arthroscopic surveillance, the fatty tissue on the surface of the contracture band is cleared to reveal the contracture band

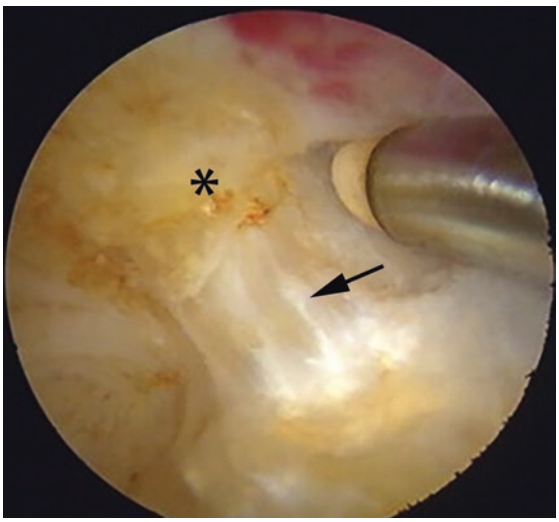

Fig. 6.8 Release the deltoid contracture band (arrow) with radiofrequency along the edge of the acromion (*)

Fig. 6.9 The ROM of shoulder joint returned to normal after surgery

Fig. 6.9 (continued)

References

1. Banerji D, De C, Pal AK, Das SK, Ghosh S, Dharmadevan S. Deltoid contracture: a study of nineteen cases. Indian J Orthop. 2008;42(2):188–91. https://doi.org/10.4103/0019-5413.40256.
2. Wang HJ, Yan H, Cui GQ, Ao YF. Arthroscopic release of the deltoid contracture. Chin Med J. 2010;123(22):3243–6.
3. Moser T, Lecours J, Michaud J, Bureau NJ, Guillin R, Cardinal E. The deltoid, a forgotten muscle of the shoulder. Skelet Radiol. 2013;42(10):1361–75. https://doi.org/10.1007/s00256-013-1667-7.

7 Arthroscopic Gluteal Muscle Contracture Release with Radiofrequency Energy

Yu-jie Liu and Jing Xue

7.1 Introduction

Gluteal muscle contractures (GMC) usually are associated with repeated intramuscular injection into the buttocks. Adolescent patients with a history of mixed injections of penicillin and benzyl alcohol in the 1980–1990s were more common in China. In 2011, we have reported an incidence of 0.7% in adolescents in recruit enlistment.

7.2 Clinical Features

Repeated intramuscular injections of the buttocks cause adhesions between the subcutaneous tissue and the muscle fascia, which are manifested as localized skin dimpling (Fig. 7.1). Adduction of the hip in the lateral position shows grooves in the hip (Fig. 7.2). The patient showed a gait with the toes pointing outward (Fig. 7.3).

Due to the restriction of the gluteal muscle and sacroiliac tibial contracture band, patients are unable to put their back near the back of the chair when sitting down (Fig. 7.4). Patients are unable to bring their knees together when they lay down sideways with knees flexed (Fig. 7.5) or when they squat (Fig. 7.6). One may also palpate fibrotic band movement over greater trochanter with snapping sound while patients squatting. The Ober's sign is positive (Fig. 7.7). There is always difficulty in overlapped the legs while siting (Fig. 7.8).

Clinical characteristics of GMC can be summarized as incorrect standing (Fig. 7.9) and sitting posture (Fig. 7.10), indecent squatting position (Fig. 7.11), discomfort lying position (Fig. 7.12), poor body shape, and abnormal gait.

7.3 Clinical Classification

According to clinical characteristics and intraoperative situation, we classified GMC into four types: cable strip, fan-shaped, mixed, and iliotibial band contracture. The classification of gluteal muscle contracture is beneficial for choose surgical strategy and improves curative effect [1].

- **Fan-shaped type:** Due to the wide range of injections, the gluteal muscle contracture scar tissue is mainly involved in the upper and outer quadrants of the gluteal muscle. In severe cases, the gluteal muscle scar tissue is fibrotic as hard as a plate. Surgical exploration revealed that the contracture band involved the gluteal muscle and the broad fascia tensalis muscle, and it was fan-shaped in the upper and inner quadrants of the gluteal muscle (Fig. 7.13).
- **Strip-shaped type:** The gluteal muscle contracture band forms a strip-like depression between the iliac crest and the greater trochanter (Fig. 7.14). During the flexion of the hip joint, the contracture band slides on the greater trochanter with snapping. The contracture band involves the full thick of outer and upper quadrants of gluteus maximus, sometimes deep down into the sacrum.
- **Mixed type or so-called sandwich type:** The contracture bands are distributed at different depths of the gluteus maximus, latissimus fasciae, and gluteus medius muscles. The contracture bands are layered and mixed like sandwiches between muscle tissues (Fig. 7.15).
- Iliotibial band (ITB) contracture: Contractures are mainly distributed in the broad fascia tensalis muscles and causing tension of the ITB. When the hip joint moves, the contracture band slides on the greater trochanter. The patient shows positive Ober's sign, and hip adduction is limited. Arthroscopy showed that the ITB is thickened and tense (Fig. 7.16). After the contracture band is cut off, the snaps disappeared, and the hip joint is normal in motion.

Y.-j. Liu (✉)
Department of Orthopedics, Chinese PLA General Hospital, Beijing, China

J. Xue
Department of Orthopedics, Air Force Medical Center, Beijing, China

Y.-j. Liu et al. (eds.), *Advanced Application of Arthroscopy*, https://doi.org/10.1007/978-981-15-4684-6_7

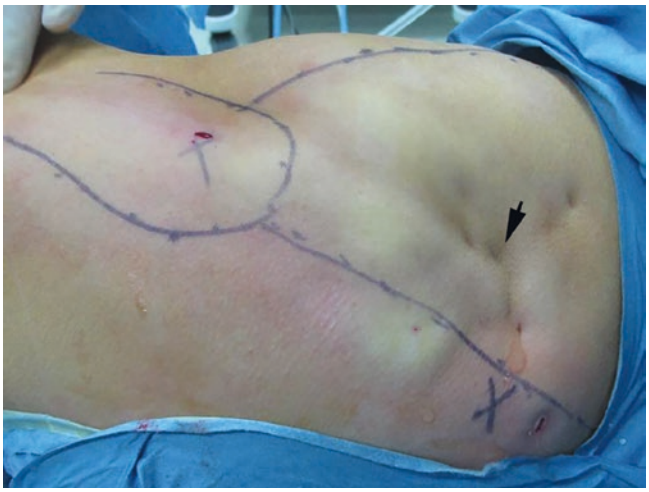

Fig. 7.1 A patient showed localized skin dimpling at buttocks because of repeated intramuscular injections in childhood

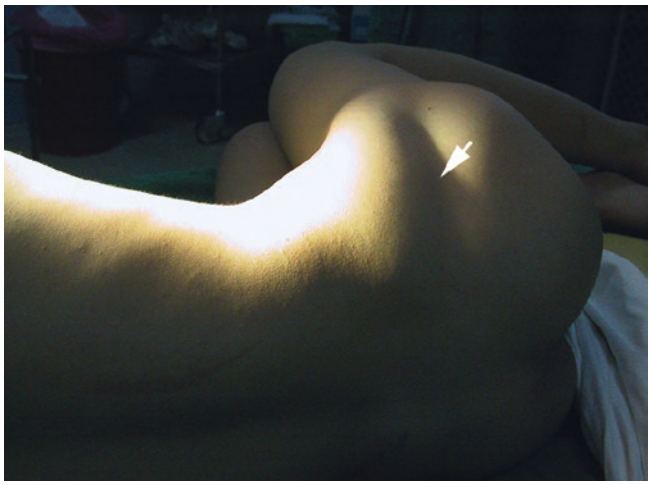

Fig. 7.2 Adduction of the hip in the lateral position shows grooves in the hip

7.4 Preoperative Preparation

Since we first published arthroscopic gluteal muscle contracture release with radiofrequency energy in 2009 [2], we have improved surgical techniques [3, 4].

Under general anesthesia or spinal anesthesia, position the patient in a lateral position. Place the affected lower limb in the tensest position of hip (Fig. 7.17). Before surgery, outline the greater trochanter, anterior and posterior borders of the contracted gluteal muscle, and the sciatic nerve (Fig. 7.18). We used a two-portal technique to perform the

Fig. 7.3 The patient showed a gait with the toes pointing outwards

operation, which are placed 5 cm anterior inferior and posterior inferior to the greater trochanter (Fig. 7.18). After sterilization, a saline solution containing epinephrine (Fig. 7.19) was injected between the gluteal muscle contracture zone and the subcutaneous fascia to achieve hemostasis during the operation.

7.5 Operative Technique

Two portals were made below the great trochanter as arthroscopy and instrument approaches, respectively. By inserting a periosteal elevator from one portal, we enlarged the potential space between the gluteal muscle group and the subcutaneous fat using blunt dissection. Then insert arthroscope and motorized shaver, respectively, to debride and remove fatty tissue overlying the contracture bands of the gluteal muscle group to make an arthroscopic working space (Fig. 7.20). A radiofrequency device then was introduced through one portal and obliquely sectioned the contracture bands of ITB from anterior to posterior (Fig. 7.21). Then upward, longitudinally loosen the gluteal muscle contraction band attached to the posterolateral ITB behind the great trochanter, the path of the releasing is "L" shaped (Fig. 7.22). If the ROM of hip joint is still limited and the contracture band is still tight,

Fig. 7.4 Due to the restriction of the gluteal muscle and sacroiliac tibial contracture band, this patient is unable to put his back near the back of the chair when sitting down

Fig. 7.5 This patient is unable to bring his knees together when he lay down sideways with knees flexed

then continue release the contraction band above the great trochanter from posterior to anterior. This makes the overall release path like a letter of "C" (Fig. 7.23). The trochanteric bursitis will be exposed after the posterior contracture bands have been released (Fig. 7.24). After the release, the hip joint is moved in different directions until the hip joint gets full ROM without snapping and has a negative Ober's sign. Pay attention to the scope and depth of releasement. Don't cut off the muscle; otherwise it will easily bleed during operation and affect muscle strength and function post-operation. Special attention should be paid to the anatomical position of the sciatic nerve and superior gluteal nerve to prevent injury during operation.

Fig. 7.6 The patient is crouched with the lower limbs separated in a frog-leg position

Fig. 7.7 This patient shows a positive Ober's sign

Fig. 7.8 This patient is difficulty in overlapped the legs while siting

Fig. 7.9 Incorrect standing posture

Fig. 7.10 Incorrect sitting posture

7.6 Postoperative Treatment

Since the arthroscopic incision for surgical approach is only 4–5 mm (Fig. 7.25), it may no need to be sutured, and without drainage set. Residual fluid and blood will leak out within 24–48 hours after surgery. Pay attention to changing the dressing and keep it dry. After the operation, the patient is alternately positioned on both sides to compress the hemostasis. Exercising the gluteal muscles with lateral lower leg abduction (Fig. 7.26), patient can practice squatting down (Fig. 7.27) and cross leg exercises after the recovery of anesthesia (Fig. 7.28).

Fig. 7.11 Indecent squatting position

Fig. 7.12 Discomfort lying position

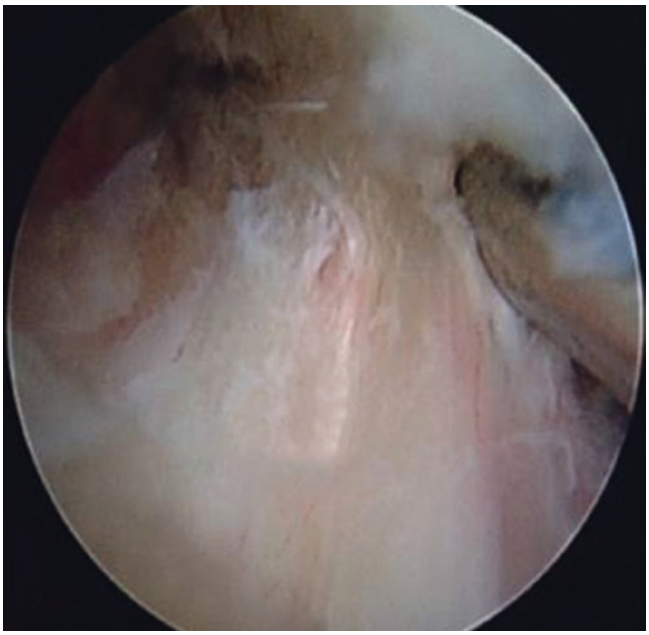

Fig. 7.13 (Use figure provided separately) Cable strip type of GMC

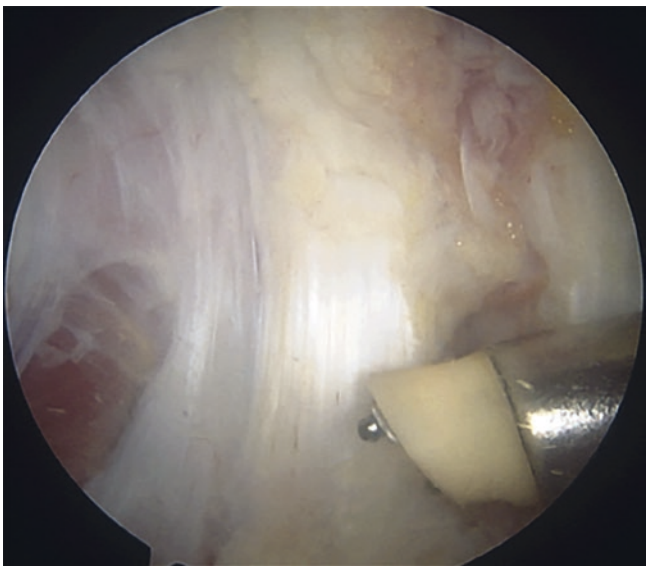

Fig. 7.14 A strip-shaped contracture band extends along the ridge to the greater trochanter

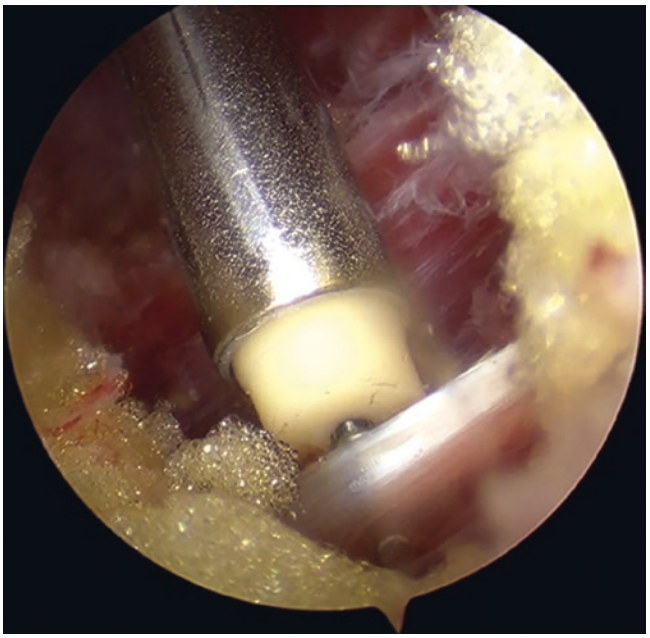

Fig. 7.15 Mixed type or so-called sandwich type of GMC

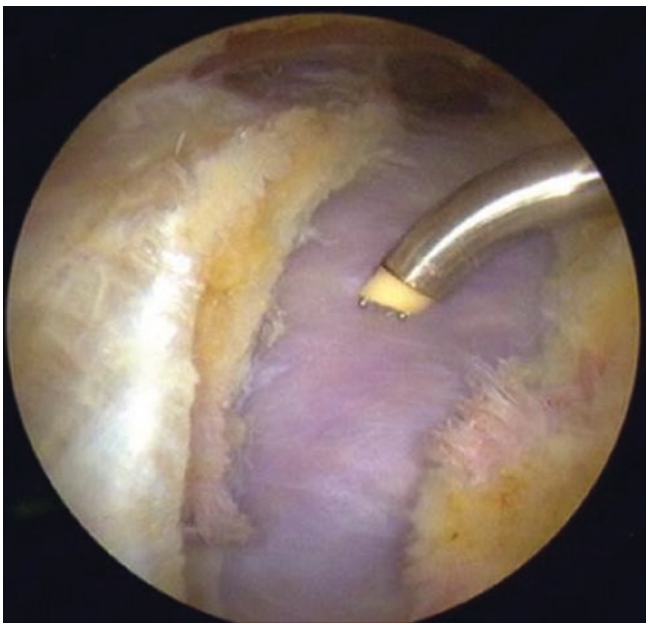

Fig. 7.16 Arthroscopy showing thickened and tense tibiofibular contracture band is cut off by radiofrequency head

Fig. 7.17 Place the affected lower limb in the tensest position of hip

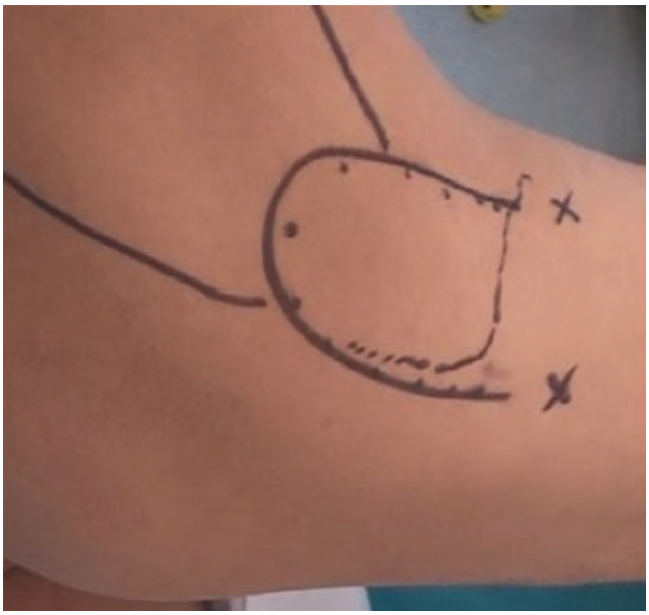

Fig. 7.18 Before surgery, outline the greater trochanter, anterior and posterior borders of the contracted gluteal muscle, and the sciatic nerve. We used a two-portal technique to perform the operation, which are placed 5 cm anterior inferior and posterior inferior to the greater trochanter (x mark)

Fig. 7.19 Epinephrine-containing saline was injected between the gluteal muscle contracture zone and the subcutaneous fascia to achieve the purpose of hemostasis during the operation

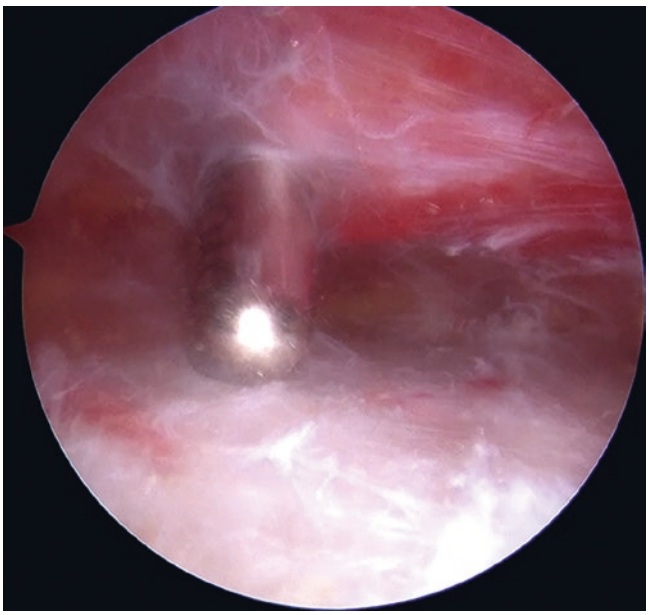

Fig. 7.20 Insert arthroscope and motorized shaver, respectively, to debride and remove fatty tissue overlying the contracture bands of the gluteal muscle group to make an arthroscopic working space

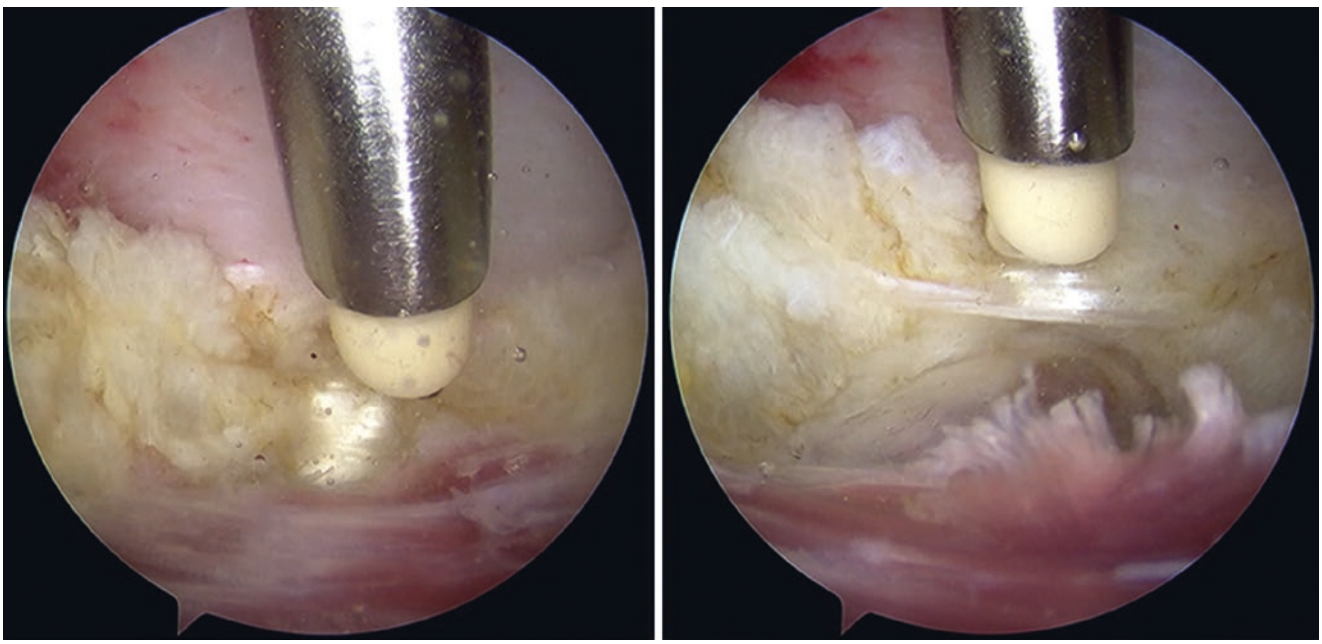

Fig. 7.21 A radiofrequency device then was introduced through one portal and obliquely sectioned the contracture bands of ITB from anterior to posterior

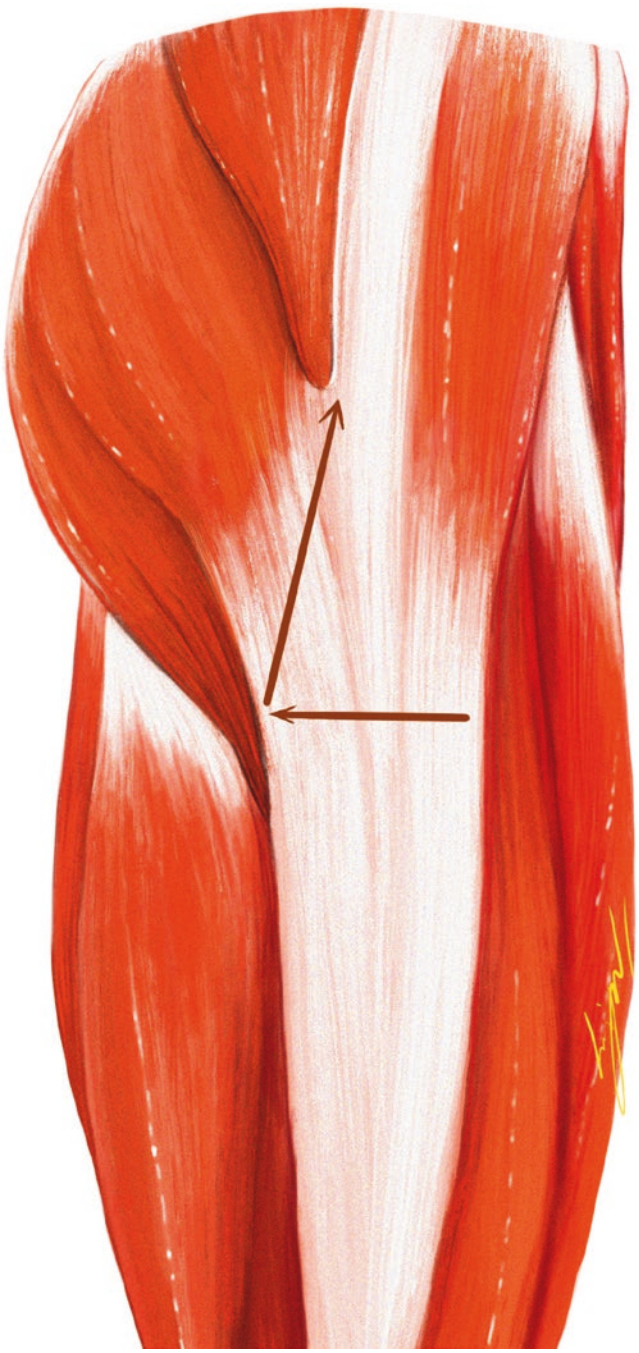

Fig. 7.22 The path of the releasing is "L" shaped (arrow)

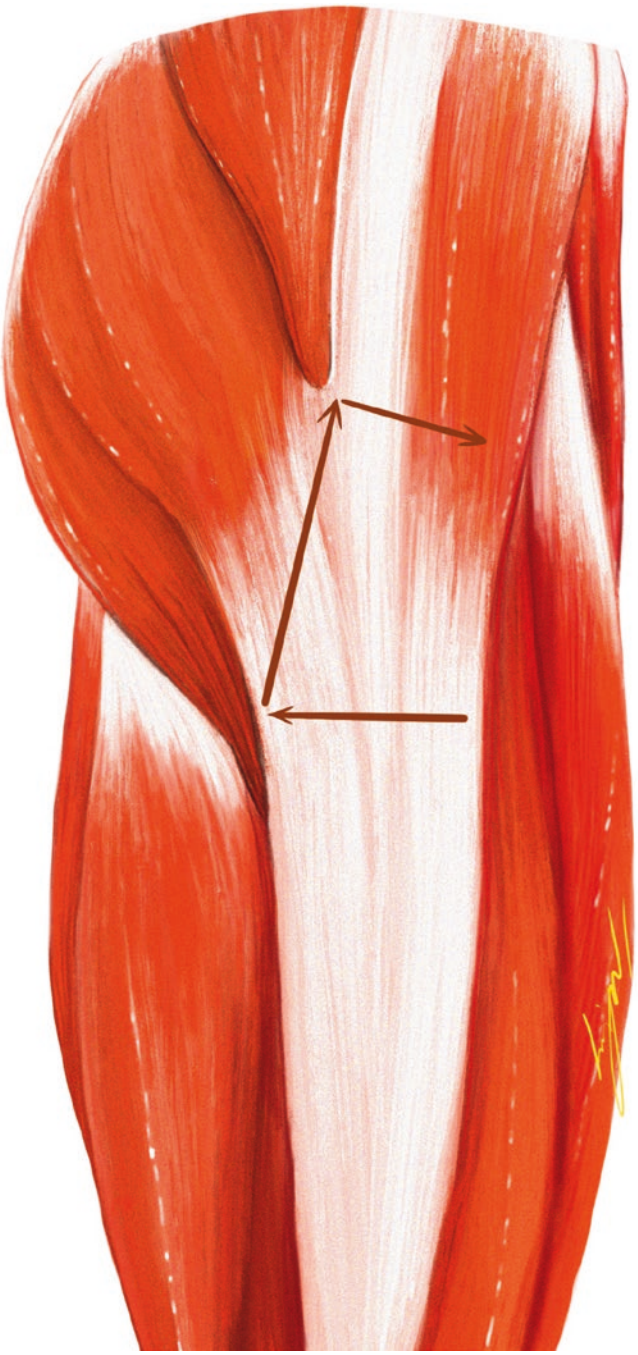

Fig. 7.23 If the ROM of hip joint is still limited and the contracture band is still tight, then continue release the contraction band above the great trochanter from posterior to anterior. This makes the overall release path like a letter of "C"

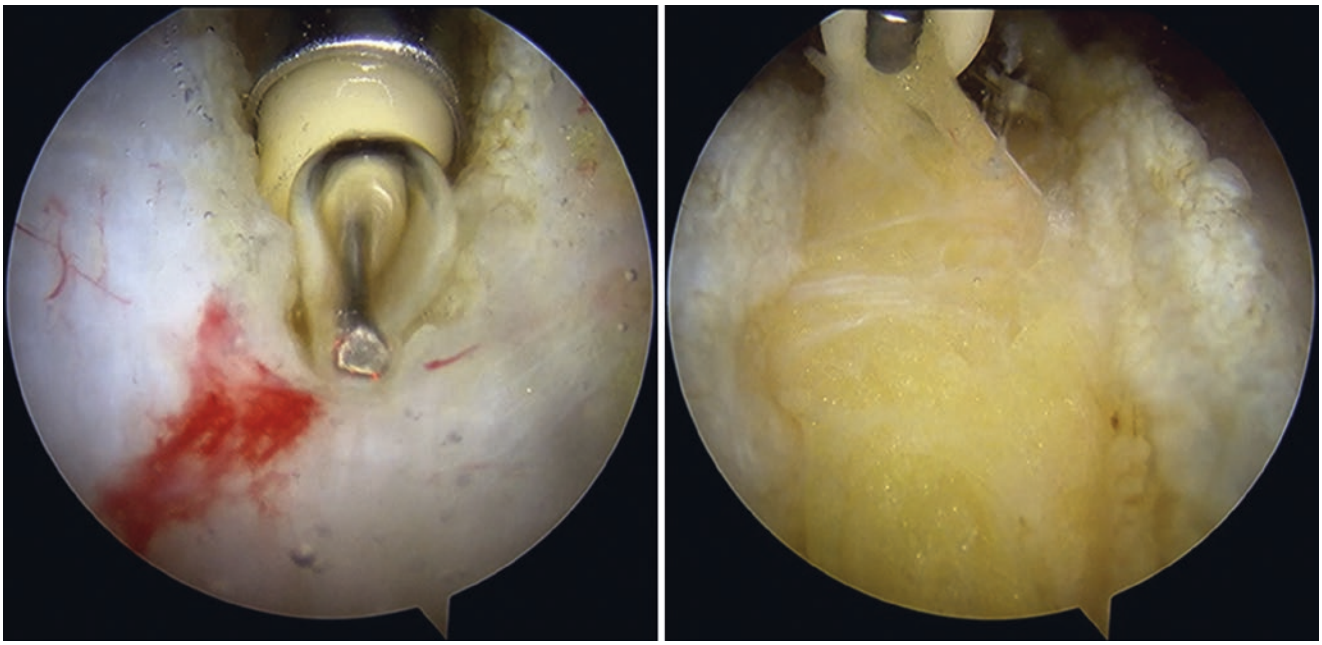

Fig. 7.24 The trochanteric bursitis will be exposed after the posterior contracture bands have been released

Fig. 7.25 Compared to open surgery incision (**a**), the arthroscopic incision for surgical approach is only 4 to 5 mm (**b**), it may no need to be sutured, and without drainage set

Fig. 7.26 Exercising the gluteal muscles with lateral lower leg abduction

Fig. 7.27 (Use figure provided separately) Patient can practice squatting down after the recovery of anesthesia

Fig. 7.28 (Use figure provided separately) Patient can practice cross leg exercises after the recovery of anesthesia

References

1. Liu YJ, Wang ZG, Wang JL, Li SY, Li HF, Qu F, et al. Clinical classification of gluteal muscle contracture under arthroscopy. Zhongguo Gu Shang. 2013;26(6):468–70.
2. Liu YJ, Wang Y, Xue J, Lui PP, Chan KM. Arthroscopic gluteal muscle contracture release with radiofrequency energy. Clin Orthop Relat Res. 2009;467(3):799–804. https://doi.org/10.1007/s11999-008-0595-7.
3. 唐翔宇， 李春宝， 刘玉杰， 申学振， 常晗， 鹿鸣, et al. 关节镜下大转子周围组织松解术治疗臀肌挛缩症. 中国骨与关节杂志. 2017;6(09):661–4.
4. 唐翔宇, 刘玉杰， 李春宝， 齐玮， 曲峰， 李海峰, et al. 臀肌挛缩症功能量化评分表的信效度检验. 中国矫形外科杂志. 2017;25(04):336–9.

Removal of Popliteal Cyst Under Endoscopy

8

Yu-jie Liu and Hai-peng Li

8.1 Introduction

The pathogenesis of popliteal cyst (Baker's cyst) is related to meniscus injury, knee osteoarthritis, and synovitis. The cyst is common connected with the joint cavity, and it can be touched at the popliteal fossa. When the synovial fluid exudates more in the knee joint, it can flow into the popliteal cyst through the passage. The cyst can shrink when patient lies on prone position. Large cysts may affect the movement of the knee joint, and sometimes it even compress the blood vessels or nerves behind the knee, causing local swelling pain, numbness of the foot, or other neurological symptoms. The traditional treatment of popliteal cyst is open surgery. Because of the abundant blood vessels and nerves in popliteal area, and the location of the cyst is deep and difficult to expose, the incision is always long, and the trauma is large. The scar after surgery not only affects the beauty but also affects the function of knee joint. The recurrence rate of popliteal cyst after resection is high (Fig. 8.1). The author removed the popliteal cyst under endoscopy with local anesthesia and received good results.

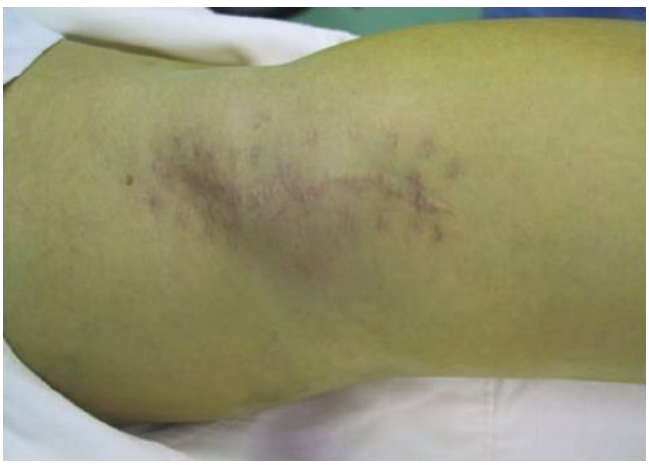

Fig. 8.1 Recurrence of popliteal cyst after resection

8.2 Imaging Evaluation

Arthrography (Fig. 8.2) and ultrasonography (Fig. 8.3) show that the popliteal cyst is located in the deep of popliteal fossa. MRI (Fig. 8.4) shows the meniscus lesion and the damage of cartilage (Fig. 8.5). These examinations show the relationship between the popliteal cyst and the surrounding anatomical structure from different ways, which is important for making the treatment plan.

Fig. 8.2 Evaluation of popliteal cyst with arthrography

Y.-j. Liu (✉)
Department of Orthopedics, Chinese PLA General Hospital, Beijing, China

H.-p. Li
Department of Orthopedics, The 7th Medical Center of Chinese PLA General Hospital, Beijing, China

Y.-j. Liu et al. (eds.), *Advanced Application of Arthroscopy*, https://doi.org/10.1007/978-981-15-4684-6_8

Fig. 8.3 Evaluation of popliteal cyst with ultrasonography

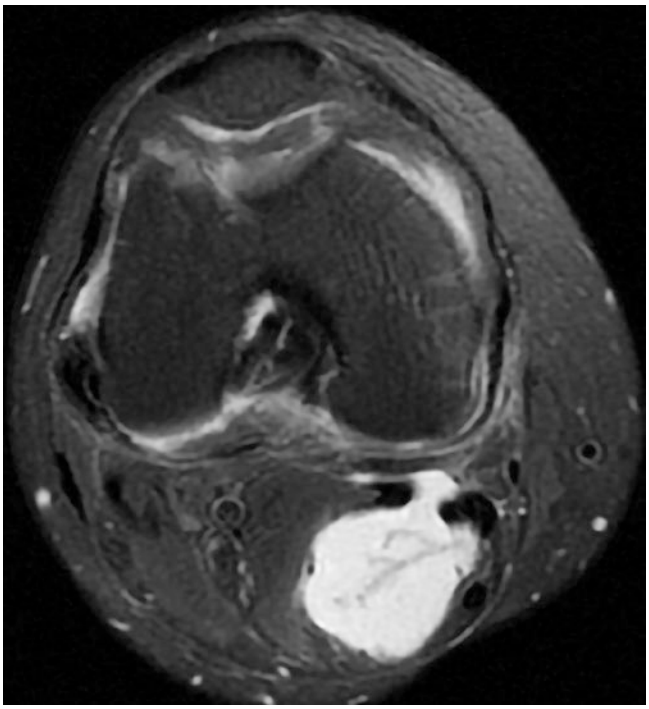

Fig. 8.4 MRI shows the popliteal cyst is connected with the knee joint cavity

8.3 Preoperative Preparation

Surgery was conducted in patients with prone position under local anesthesia. The contour of popliteal cyst, the posterior tibial vessels and nerves, and the portals were marked (Fig. 8.6). Local anesthesia was performed with 2% lidocaine 20 ml + 1% ropivacaine 10 ml + 0.9% saline 30 ml + 0.1% adrenaline 6 drops. Local infiltration anesthesia were performed at the portals and intra-articular.

Fig. 8.5 MRI shows the meniscus lesion and the damage of cartilage

Fig. 8.6 Mark the popliteal cyst, posterior tibial vessels and nerves, and the portals

8.4 Operative Technique

8.4.1 Making the Working Cavity for Endoscopy

Portal of endoscopic view and portal of instruments were performed at the distal end of popliteal cyst (Fig. 8.7). Cut the skin for 3 mm, insert the puncture between the subcutaneous tissue and the cyst for blunt separation, and make the working cavity of endoscopic operation (Fig. 8.8). The other portal is made for the surgical instruments. The removal of popliteal cyst can be divided into two ways: intracapsular and extracapsular.

Fig. 8.7 Make portals for endoscopy and instruments

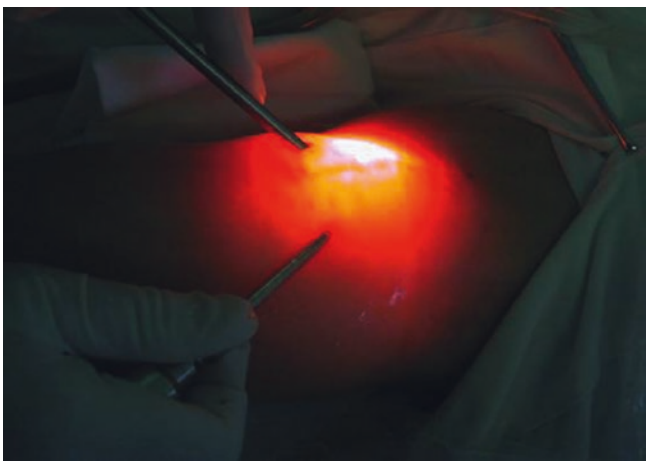

Fig. 8.8 Making the working cavity between the subcutaneous tissue and the cyst for endoscopy

8.4.2 Extracapsular Exfoliation

Endoscopy was inserted into the working cavity. Blunt dissection was performed between the cyst wall and the surrounding soft tissue under endoscopy (Fig. 8.9). The cyst is completely separated from the surrounding tissue until the pedicle of the cyst is connected with the posterior joint capsule channel. After puncturing the cystic wall tissue, there is viscous jelly like cystic fluid flowing out (Fig. 8.10). After

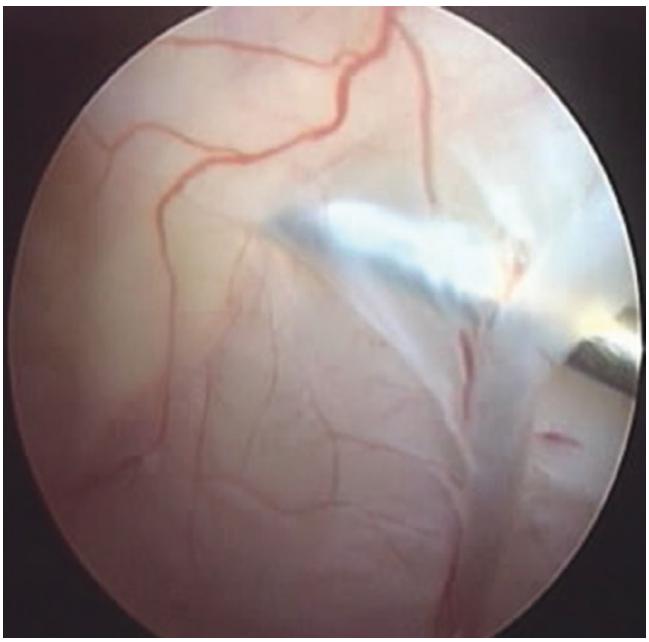

Fig. 8.9 Blunt dissection was performed between the cyst wall and the surrounding soft tissue under endoscopy

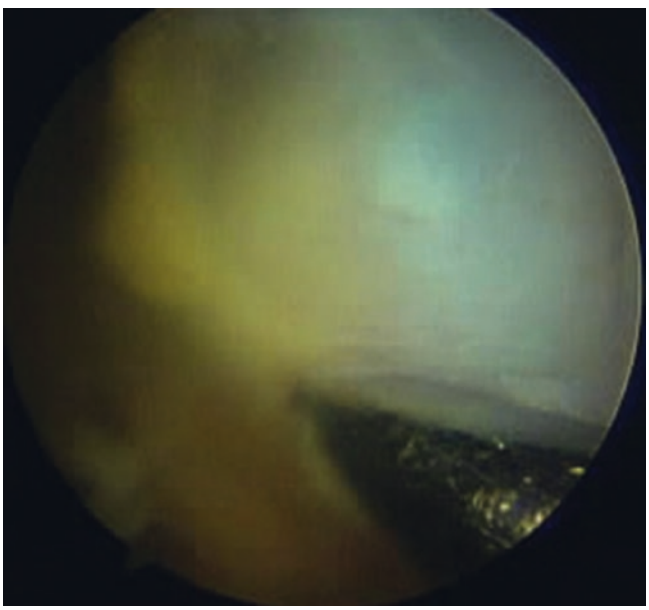

Fig. 8.10 There is viscous jelly like cystic fluid in the popliteal cyst

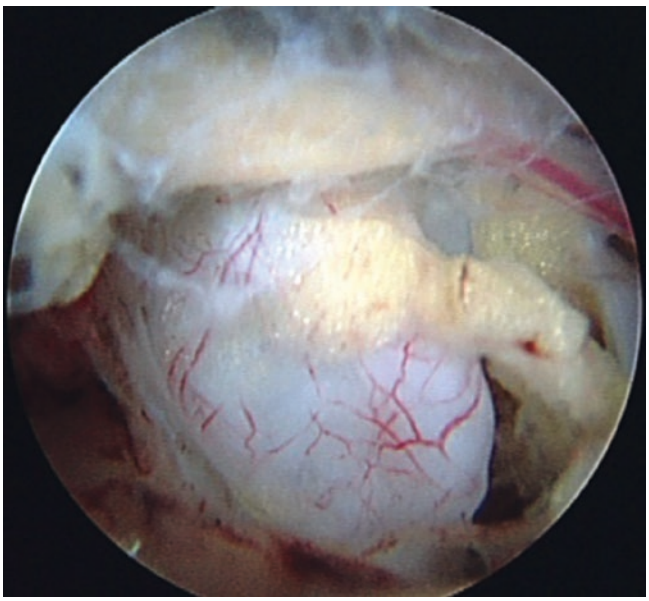

Fig. 8.11 The cystic wall tissue is left after emptying the cystic fluid

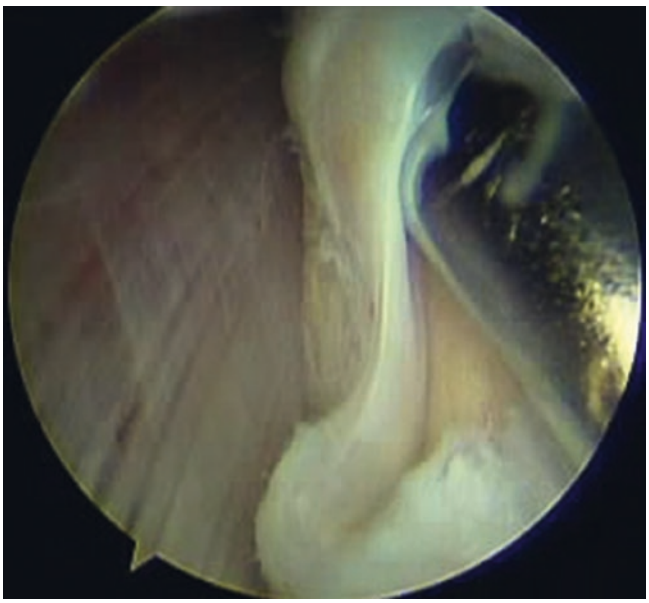

Fig. 8.12 Clean the cystic wall tissue with a shaver

emptying the cystic fluid, only the cystic wall tissue is left (Fig. 8.11). Use a shaver to clean the cystic wall tissue (Fig. 8.12), or use nucleus pulposus pliers to take out the cystic wall tissue (Fig. 8.13). Check whether there is bleeding, and use radiofrequency to stop bleeding.

Fig. 8.13 Take out the cystic wall tissue with nucleus pulposus pliers

Fig. 8.14 Suck out the liquid from the popliteal cyst under endoscopy

8.4.3 Intracapsular Exfoliation

Endoscopy was inserted into the cavity of the popliteal cyst to suck out the liquid (Fig. 8.14). After repeated irrigation with saline, the cysts were observed. The walls of the cysts were honeycomb like (Fig. 8.15), or dimple like (Fig. 8.16). It was also found that there was a channel between the popliteal cysts and the knee joint cavity (Fig. 8.17) and there were small free bodies in the cysts sometimes (Fig. 8.18).

Fig. 8.15 The wall of the cysts looks like honeycomb under endoscopy

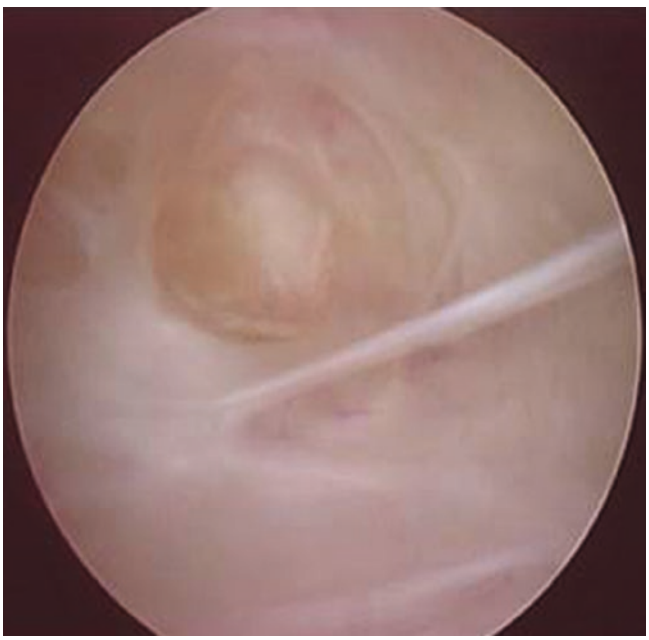

Fig. 8.16 The wall of the cysts looks like dimple under endoscopy

Lidocaine mixture adrenals was injected into the cyst wall tissue of popliteal cyst under endoscopy (Fig. 8.19), so that the cyst wall tissue could be easily separated from the surrounding tissue (Fig. 8.20). The blunt stripper was inserted between the cyst wall and the surrounding tissue and then peeled around the cyst under endoscopy (Fig. 8.21). After the

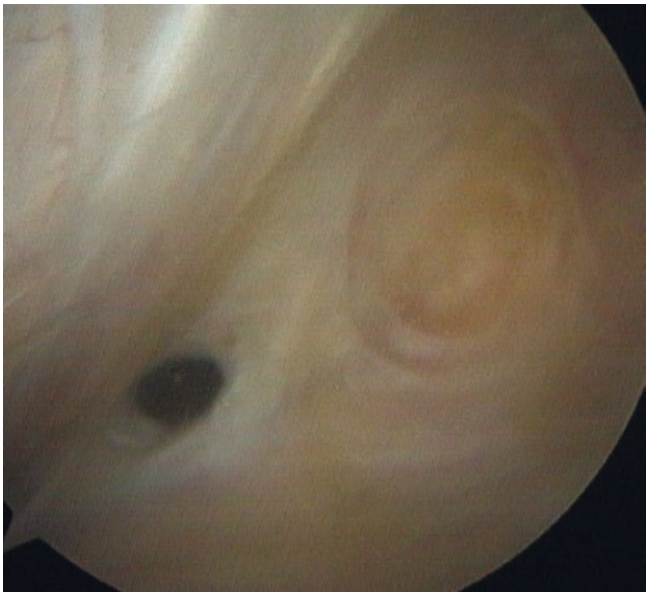

Fig. 8.17 There was a channel between the popliteal cysts and the knee joint cavity

Fig. 8.18 There were free bodies in the cysts

cyst wall and the surrounding tissue were completely separated (Fig. 8.22). Nucleus pulposus forceps or shaver were used to clean the cystic wall (Fig. 8.23), and radiofrequency was used to stop bleeding. The cyst and the channel do not need to be closed. If necessary, put a negative pressure drainage tube to lead out the liquid in the joint cavity.

After the cyst was removed, the patient turned over to supine position and underwent knee endoscopy. It was found that most of the patients with popliteal cyst had meniscus lesion (Fig. 8.24), osteoarthritis (Fig. 8.25), and synovitis (Fig. 8.26).

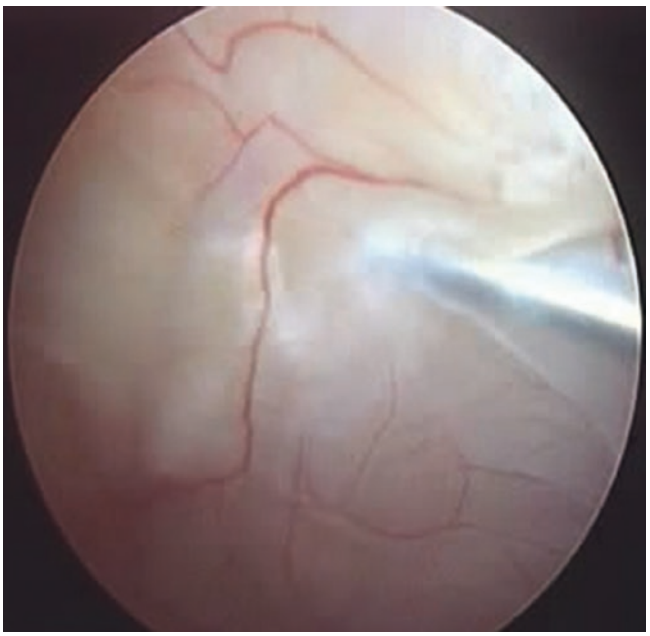

Fig. 8.19 Inject lidocaine mixture adrenals into the cyst wall tissue of popliteal cyst under endoscopy

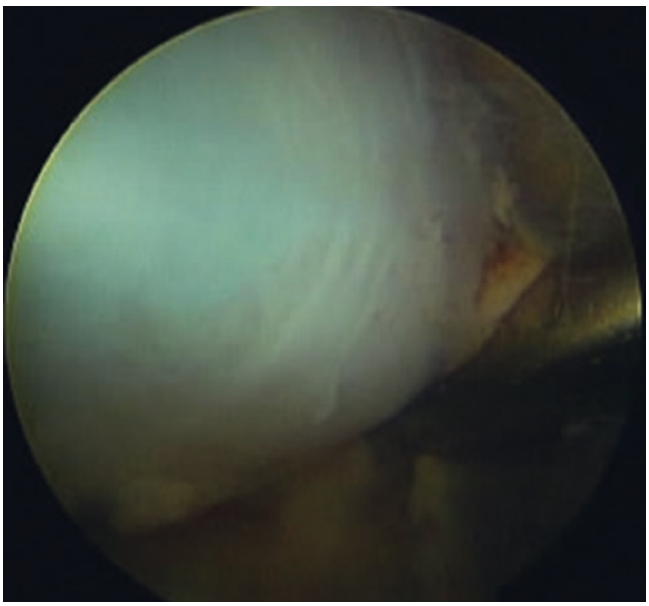

Fig. 8.21 Peel the cyst wall from the surrounding tissue under endoscopy

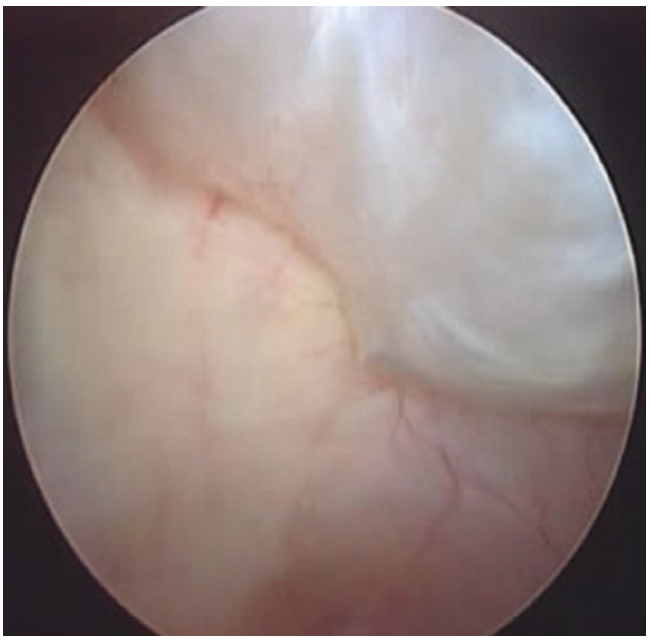

Fig. 8.20 Separate the cyst wall tissue from the surrounding tissue

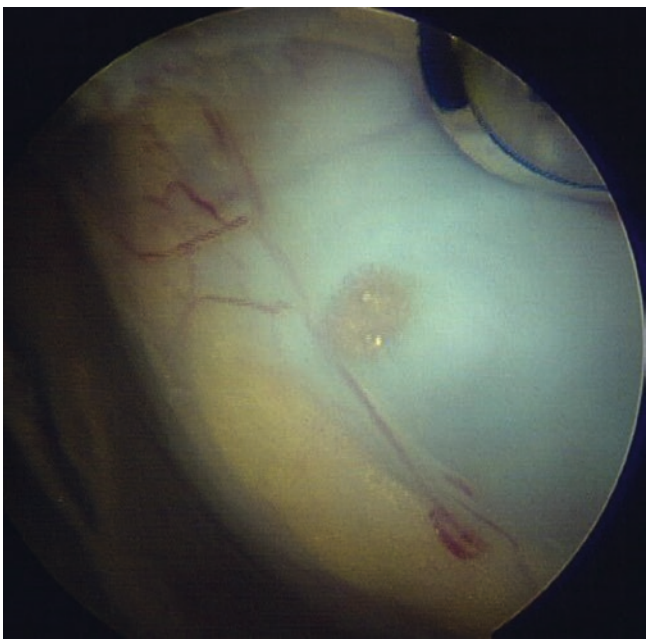

Fig. 8.22 The cyst wall and the surrounding tissue were completely separated

Fig. 8.23 Clean the cystic wall with nucleus pulposus forceps or shaver

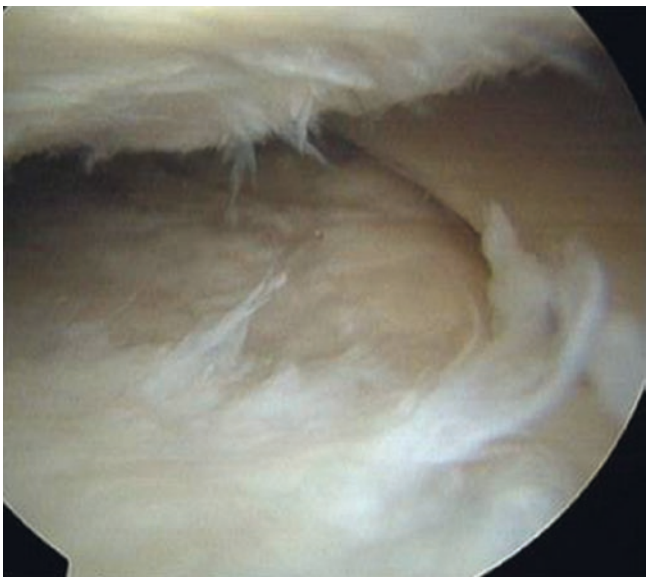

Fig. 8.25 Popliteal cyst with osteoarthritis

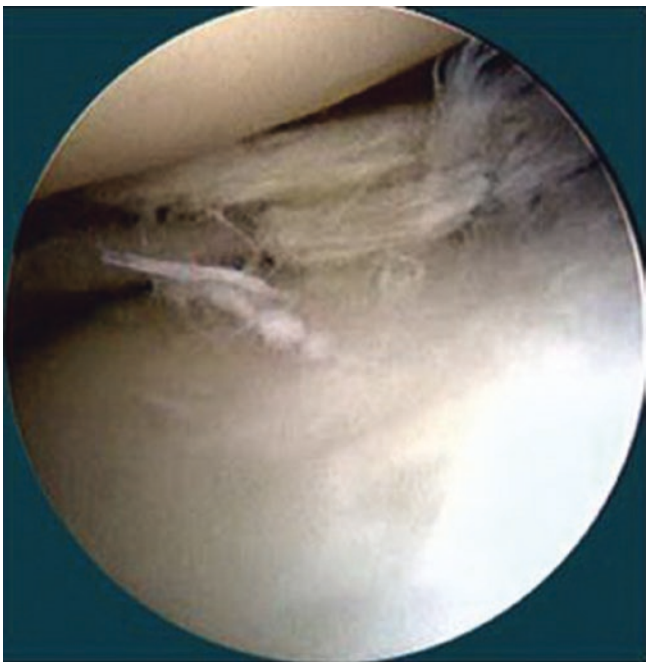

Fig. 8.24 Popliteal cyst with meniscus lesion

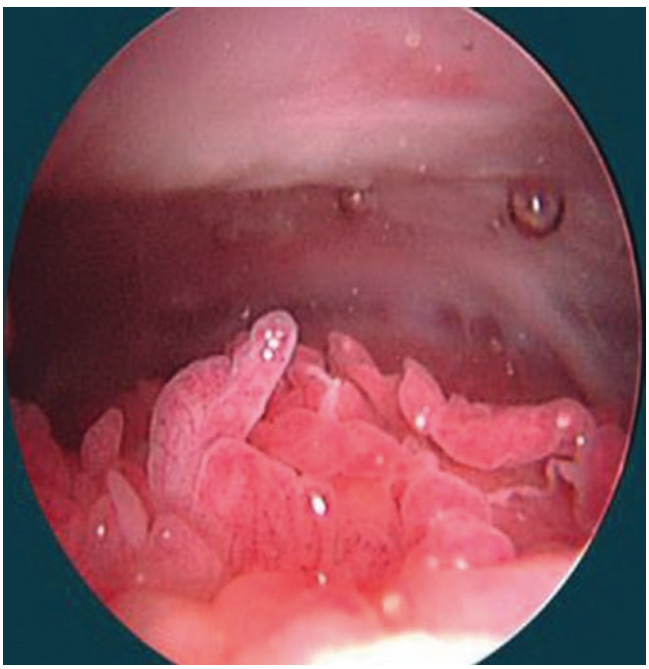

Fig. 8.26 Popliteal cyst with synovitis

8.5 Critical Points

1. The doctor should be familiar with the anatomy of the posterior tibial vessels and nerves in the popliteal region of the knee and avoid injuries them during surgery.
2. When removal of popliteal cysts under endoscopy, avoid blood vessels and nerves and does not need to be deliberately exposed.
3. After removal of the popliteal cyst, the knee joint should be cleaned up to avoid recurrence post operation.
4. Local anesthesia can be performed simultaneously for knee joint cleaning and popliteal cyst removal, so as not to affect the effect of local anesthesia.

Arthroscopic Curettage of Benign Bone Tumors

9

Yu-jie Liu and Feng Qu

9.1 Introduction

Benign bone tumors are often treated with open surgery, local curettage, or bone grafting, especially in the process of exposing the lesion by injuring the normal anatomical structure firstly, thereby resulting in large surgical trauma and bleeding. The arthroscopic minimally invasive technique can precisely remove the lesion with little trauma to the tissues surrounding the lesion. For benign bone tumors, arthroscopic curettage and bone grafting and carbonated hydroxyapatite filling the lesion can achieve good results [1].

9.2 Preoperative Preparation

Preoperative X-ray (Fig. 9.1), CT scan and CT value (Fig. 9.2), and MRI (Fig. 9.3) are helpful in the initial diagnosis of the lesion, further understanding of the extent of the lesion, and assessment of the amount of bone graft is benefited to guide surgery. It is necessary to use a fluoroscopy machine for positioning during the operation. General or epidural anesthesia was routinely carried out, and the sheets were routinely disinfected.

9.3 Operative Technique

Under fluoroscopy, drill the K-wire percutaneously into the bone lesion (Fig. 9.4). The hollow drill penetrates the bone wall along the guidewire (Fig. 9.5) [2, 3]. Apply a circular drill with a diameter of 5 mm to drill the lesion for pathological examination (Fig. 9.6). Insert the arthroscope into the lesion to observe the lesion (Fig. 9.7), [4] and use curettes to curette the bone tumor tissue (Fig. 9.8), and then grind of tumor bone wall with burr (Fig. 9.9), and the bone wall of the tumor lesion was cauterized under radiofrequency (Fig. 9.10) to reduce the chance of tumor recurrence [5, 6].

After debridement, carbonated hydroxyapatite may be implanted arthroscopically into the bone tumor lesion to prevent pathologic collapse fractures from thinning of the bone wall after tumor curettage (Fig. 9.11).

The advantage of implanted carbonated hydroxyapatite is that it can fill bone defect areas of arbitrary shape and size [6–8]; and out-of-bed activity may occur early after surgery (Fig. 9.12), thus reducing complications of bed rest. Small scope bone defects may also be treated arthroscopically with autogenous bone or allograft (Fig. 9.13).

9.4 Critical Points

1. The nature of the lesion must be clearly defined before surgery for benign bone tumors before arthroscopic surveillance surgery.
2. Fluoroscopy should be used to locate the bone tumor lesion before the operation, and the guide needle should be employed to impact the bone tumor lesion. A trephine should be used to open the window before inserting the arthroscope into the lesion.
3. The amount of bone graft and material was selected according to the size of the lesion cavity, and carbonated hydroxyapatite could fill lesions of any shape and size.

Y.-j. Liu (✉)
Department of Orthopedics, Chinese PLA General Hospital, Beijing, China

F. Qu
Beijing Tongren Hospital, Capital Medical University, Beijing, China

Y.-j. Liu et al. (eds.), *Advanced Application of Arthroscopy*, https://doi.org/10.1007/978-981-15-4684-6_9

Fig. 9.1 Lesion in distal Femur under X-ray

Fig. 9.3 MRI T1-weighted image exhibiting low signal intensity in the lesion

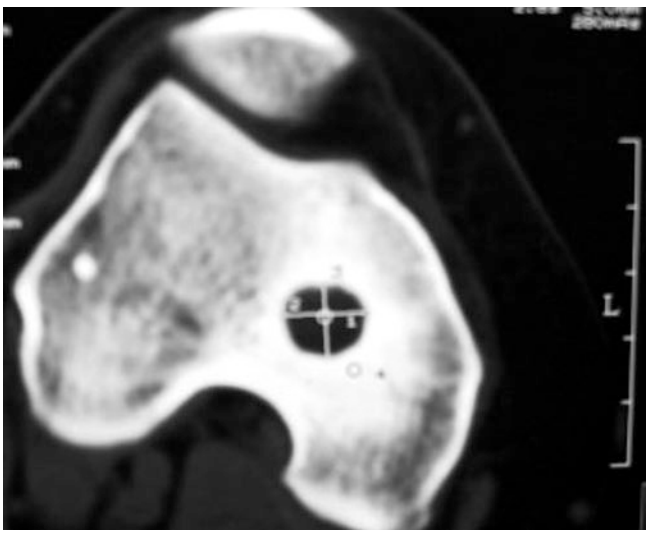

Fig. 9.2 Location, shape, and size of lesions on CT scan

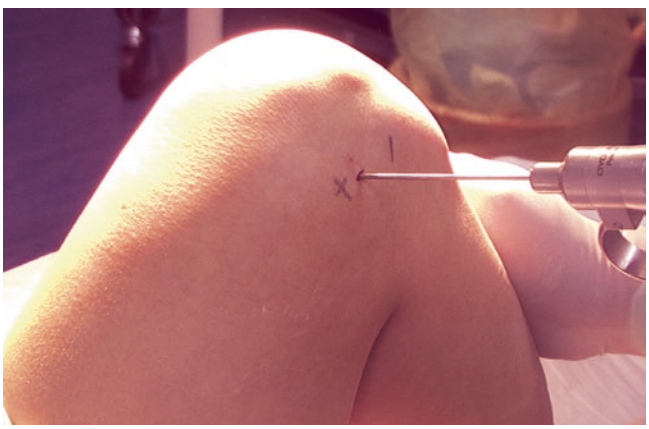

Fig. 9.4 Percutaneous drilling of bone lesions by Kirschner needles under fluoroscopy (X-ray)

Fig. 9.5 Hollow drill drilling bone tumor lesion along guidewire

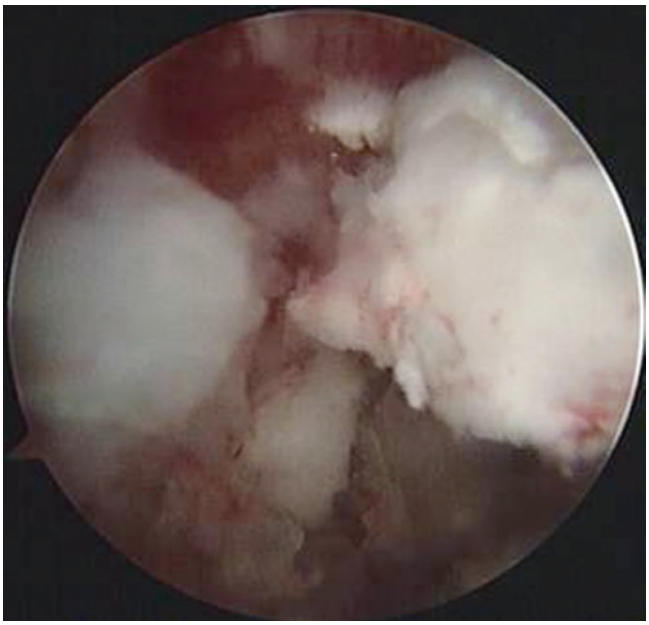

Fig. 9.7 Arthroscopic insertion into tumor lesion for observation

Fig. 9.6 Drilling tissue of tumor lesion with ring drill

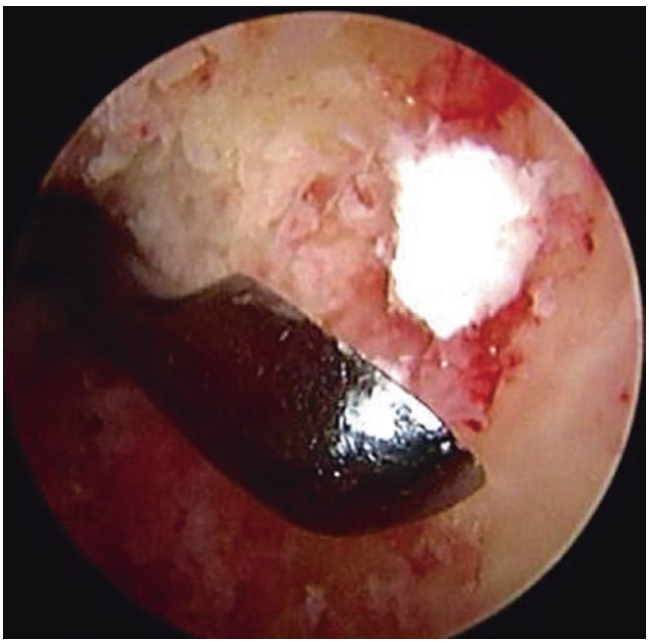

Fig. 9.8 Curettage of bone tumor tissue

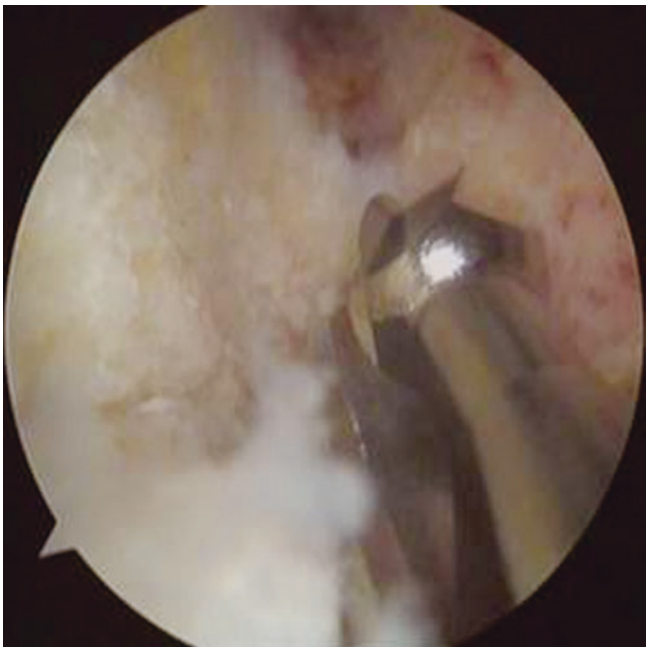

Fig. 9.9 Grinding of tumor bone tissue under arthroscopic surveillance

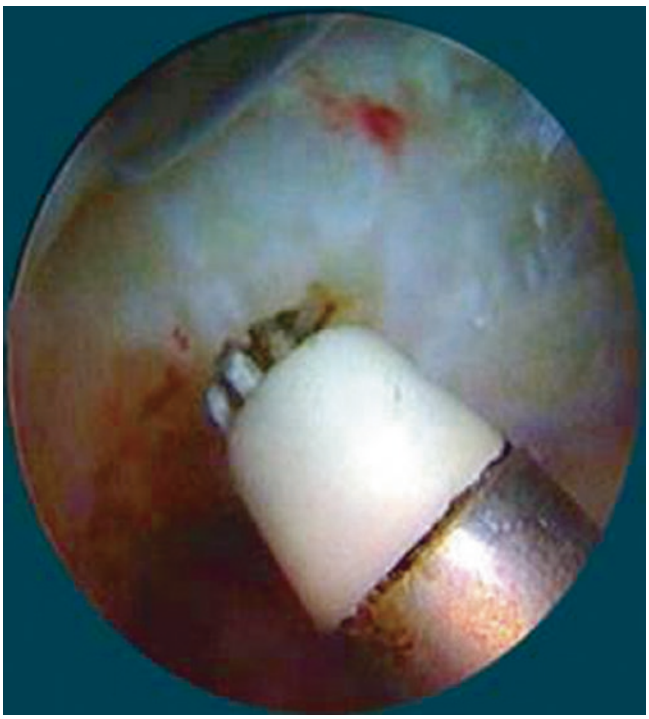

Fig. 9.10 Cauterizing of the bone wall of lesion with radiofrequency

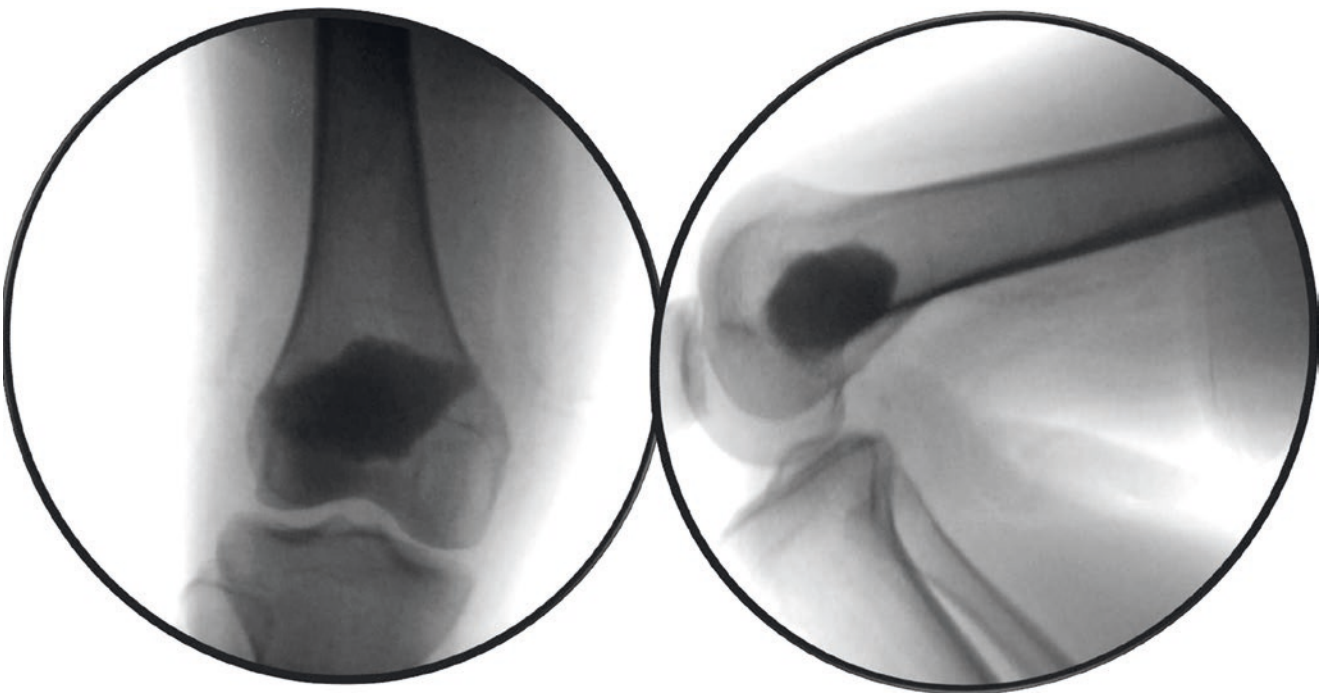

Fig. 9.11 Carbonated hydroxyapatite filled in bone defect area after removal of bone cyst lesion at lower end of femur

Fig. 9.12 Carbonated hydroxyapatite filled after arthroscopic curettage of calcaneal bone cysts

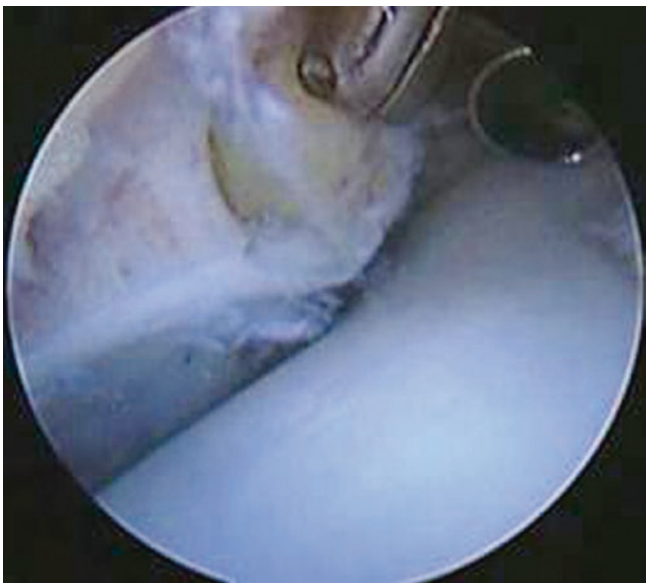

Fig. 9.13 Bone cyst in distal tibia of ankle joint. Implanted autogenous bone block after lesion curettage under arthroscopy

References

1. Cassidy C, Jupiter JB, Cohen M, et al. Norian SRS cement compared with conventional fixation in distal radial fractures. A randomized study. J Bone Joint Surg Am. 2003;85-A(11):2127–37.
2. Westendorff C, Hoffmann J, Troitzsch D, et al. Ossifying fibroma of the skull: interactive image-guided minimally invasive localization and resection. J Craniofac Surg. 2004;15(5):854–8.
3. El-Mowafi H, Refaat H, Kotb S. Percutaneous destruction and alcoholisation for the management of osteoid osteoma. Acta Orthop Belg. 2003;69(5):447–51.
4. Muckley T, Schutz T, Schmidt MH, et al. The role of thoracoscopic spinal surgery in the management of pyogenic vertebral osteomyelitis. Spine (Phila Pa 1976). 2004;29(11):E227–33.
5. Wiedemayer H, Sandalcioglu IE, Wiedemayer H, et al. The supraorbital keyhole approach via an eyebrow incision for resection of tumors around the Sella and the anterior skull base. Minim Invasive Neurosurg. 2004;47(4):221–5.
6. Yu-Jie L, Zhi-Gang W, Zhong-Li L, et al. Clinical application of arthroscopic technique in exterior joint surgery. Med J Chin People's Liberation Army. 2003;3:275–6.
7. Ke-ya MAO, Li-bo HAO, Pei-fu TANG, et al. The effect of different diameters powder on setting time and compressive stress of carbonated hydroxyapatite cement. J Med Biomech. 2004;1:6–9.
8. Ke-ya MAO, Pei-fu TANG, Li-bo HAO, et al. Skeletal repair by carbonated hydroxyapatite cement loaded with active peptides. Chin J Orthop Trauma. 2004;3:64–7.

Removal of Plate and Screws Under Endoscopy

10

Yu-jie Liu and Hai-peng Li

10.1 Introduction

Fractures of extremities are usually fixed with plates and screws. After fracture healing, plates and screws are always removed by conventional open surgery (Fig. 10.1). In 2001, the author designed the technique to remove the plate and screws under endoscopy [1]. The advantages of this technique include less bleeding, clear operative field, minimally invasive, shorter hospital stay, faster functional recovery, and no complications such as nerve and blood vessel injury. This technique enriches the indication of minimally invasive surgery and widens the application field of endoscopy.

10.2 Preoperative Preparation

Anesthesia is induced as a general anesthesia or nerve block anesthesia. In order to avoid intraoperative bleeding and ensure a clear operative field, 0.9% saline containing adrenaline (0.1% adrenaline 0.2 ml + 0.9% saline 50 ml) was injected between the plate and soft tissue before operation. During the operation, 3000 ml of 0.9% saline and 1 ml of 0.1% adrenaline were used for continuous perfusion.

10.3 Operative Technique

10.3.1 To Establish the Working Cavity for Endoscopy

Make a portal at one end of the original surgical incision, insert the stripper to peel along the plate, and make the working cavity for endoscopy (Fig. 10.2). Make another portal and insert the shaver at the other end of incision (Fig. 10.3). Shave and clean the tissue which affects the surgical field of vision (Fig. 10.4). The callus and scar tissue were removed along the surface of the plate by the periosteal stripper (Fig. 10.5). The tissue in the screw holes was cleaned by radiofrequency (Fig. 10.6) [2], and the screw holes were exposed clearly.

10.3.2 Screws Removal

The screwdriver was inserted to the screw cap vertically under the endoscopy (Fig. 10.7). Rotate the screwdriver to take out the screws one by one (Fig. 10.8). The endoscopic portal and the portal of instrument can be used interchangeably. Each portal can take out 3–4 screws. After all the screws

Y.-j. Liu (✉)
Department of Orthopedics, Chinese PLA General Hospital, Beijing, China

H.-p. Li
Department of Orthopedics, The 7th Medical Center of Chinese PLA General Hospital, Beijing, China

Y.-j. Liu et al. (eds.), *Advanced Application of Arthroscopy*, https://doi.org/10.1007/978-981-15-4684-6_10

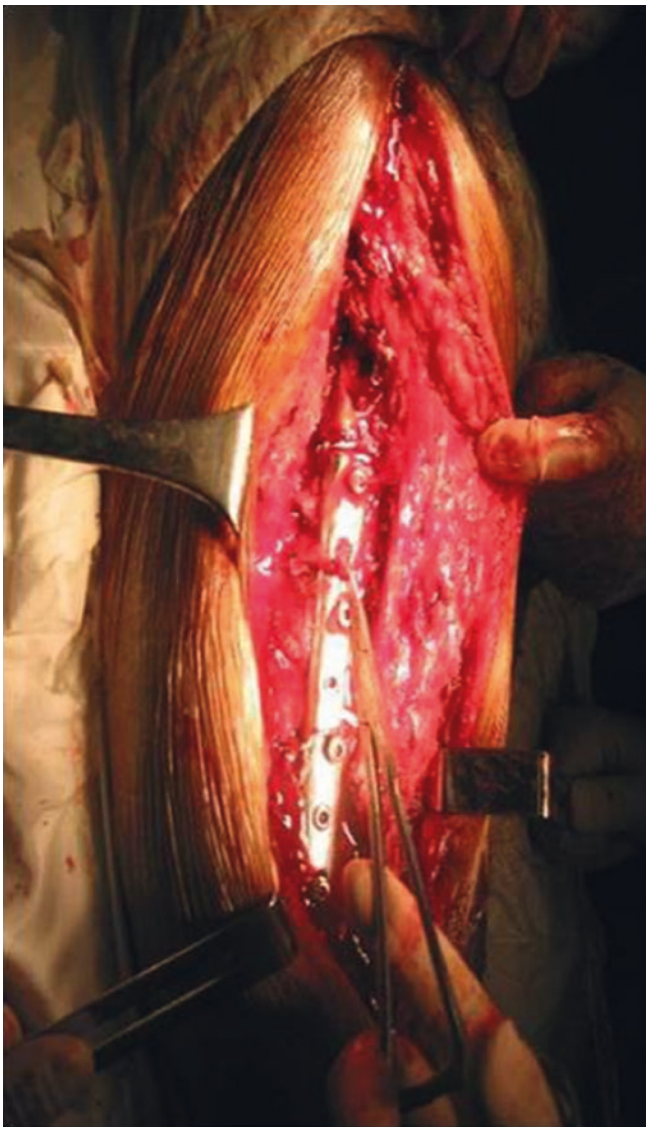

Fig. 10.1 The incision for removal of plates and screws by conventional open surgery

Fig. 10.2 Make portal and insert the stripper to peel tissue along the plate to make the working cavity for endoscopy

Fig. 10.3 Insert the endoscopy from the portal at end of the original surgical incision

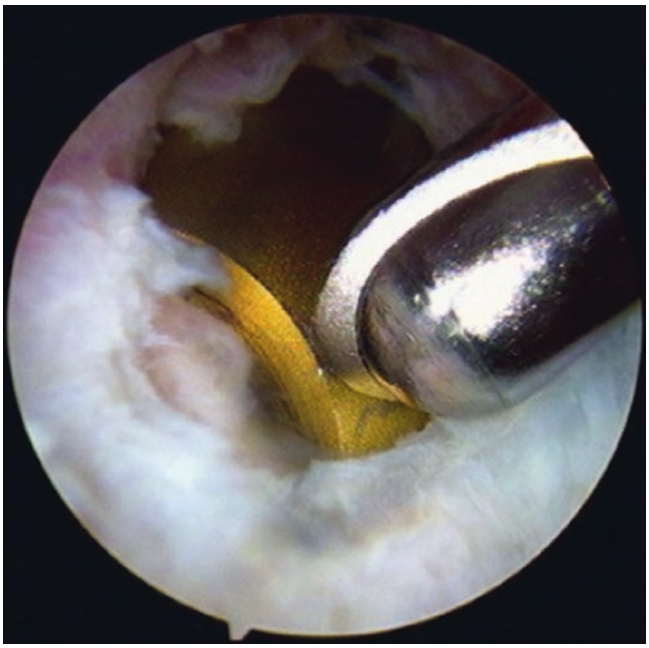

Fig. 10.4 Clean the tissue with shaver under endoscopy

Fig. 10.5 Remove the callus and scar tissue along the surface of the plate by the periosteal stripper

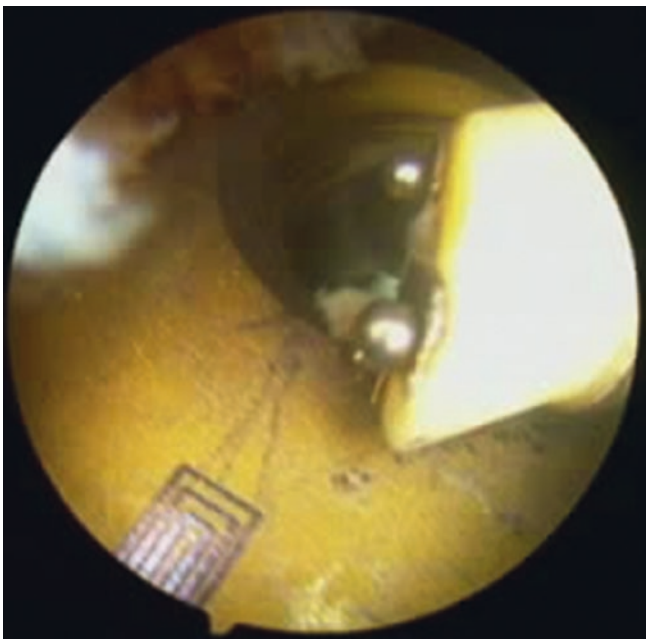

Fig. 10.6 Clean the tissue in the screw hole by radiofrequency

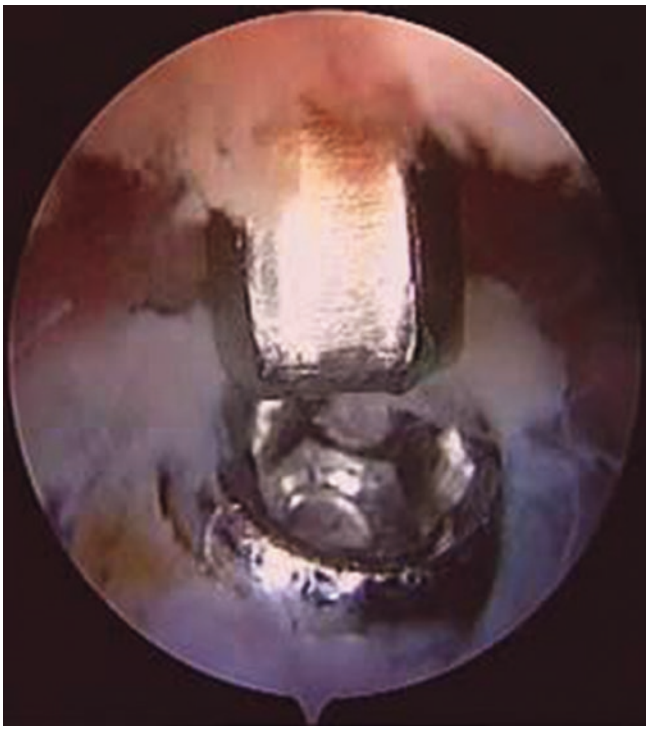

Fig. 10.7 Insert the screwdriver to connect the screw cap vertically under the endoscopy

are taken out, the periosteal stripping ion is used to insert at one end of the plate. After the plate is lifted loose, the plate (Fig. 10.9) is extracted from the incision of the other end. The portal can be suture or not (Fig. 10.10). One month after the operation, the patients can move under the protection of crutches.

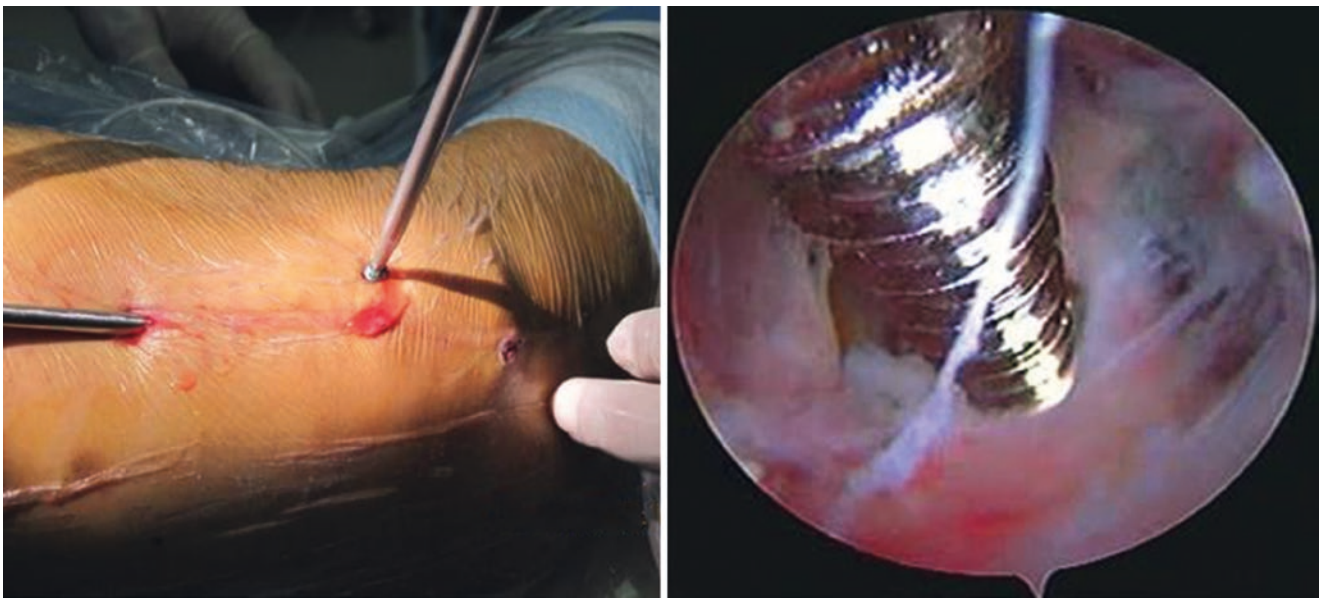

Fig. 10.8 Remove the screws

Fig. 10.9 Remove the plate

Fig. 10.10 The incision for endoscopy

References

1. Yujie L, Wang Z, Zhongli L. Clinical application of arthroscopy in extraarticular surgery. Med J Chin People's Liberation Army. 2003;28(3):275–6.
2. Yujie L, Wang Z, Jinpeng J, et al. Application and result of mini-trauma arthroscopic technique assisted in extra articular surgery. Orthop J Chin. 2004;12(21):1645–7.

Minimally Invasive Arthroscopy for Achilles Tendinopathy

11

Yu-jie Liu, Feng Qu, and Hai-peng Li

11.1 Introduction

The Achilles tendon, the most powerful tendon in the human body that carries and transmits the body's load, is formed by the joint of the gastrocnemius and soleus tendons and attached to the calcaneal tuberosity (Fig. 11.1) [1, 2]. Achilles tendinopathy may be associated with exercise overload, repeated accumulation of chronic fatigue injury, resulting in chronic damage to Achilles tendon fibers [3].

In the literature, 24.0–45.5% of Achilles tendinitis is reported, which is refractory to conservative treatment [4]. Conventionally, we use of open surgery for calcification cleaning, radiofrequency ablation, bone protrusion (Haglund's nodule) resection, and fixation of Achilles tendon insertion. The author designed and carried out radiofrequency ablation, debridement, and osteophyte grinding under arthroscopic surveillance to treat this disease in 2004 and received satisfactory clinical efficacy, which avoids tissue scarring and blood supply damage to the peritendinous tissue after open surgery [5] and is beneficial for lesion healing and early functional rehabilitation.

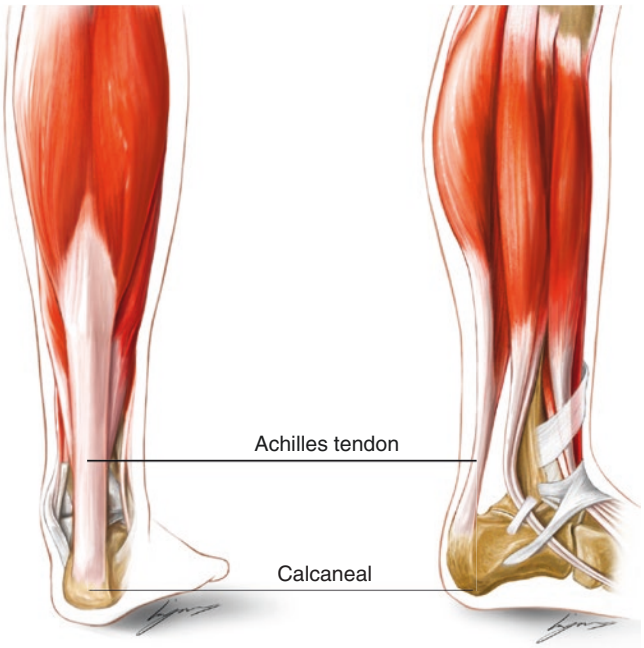

Fig. 11.1 Gross anatomy of Achilles tendon

11.2 Clinical Features

Plain radiographs show hyperostosis of the calcaneal tuberosity (Fig. 11.2) with calcification in the Achilles tendon (Fig. 11.3); CT displays worm-like changes in the calcaneal tuberosity (Fig. 11.4); and MRI exhibits mixed signals in the

Fig. 11.2 Hyperostosis of calcaneal tuberosity under plain X-ray

Y.-j. Liu (✉)
Department of Orthopedics, Chinese PLA General Hospital, Beijing, China

F. Qu
Beijing Tongren Hospital, Capital Medical University, Beijing, China

H.-p. Li
Department of Orthopedics, The 7th Medical Center of Chinese PLA General Hospital, Beijing, China

Y.-j. Liu et al. (eds.), *Advanced Application of Arthroscopy*, https://doi.org/10.1007/978-981-15-4684-6_11

Fig. 11.3 Hyperplastic calcified shadow at Achilles tendon attachment

Achilles tendon (Fig. 11.5) [6]. Ultrasonography disclosed partial rupture of Achilles tendon fibers and abnormal echo area of bursa and peritendinous tissue.

11.2.1 Clinical Typing

Achilles tendinopathy is classified into calcific tuberosity (Fig. 11.6), fibrous tear (Fig. 11.7), hypertrophic hypertrophy (Fig. 11.8), and calcaneal tuberosity hyperplasia (Haglund's deformity, Fig. 11.9) based on clinical, radiographic, and arthroscopic findings [7].

11.3 Preoperative Preparation

Prepare a 30° diameter 2.7-mm-wide angle arthroscope, radiofrequency plasma knife generator and timer, TOPAZ radiofrequency electrode blade (Fig. 11.10). The Achilles tendon anatomical outline, pain points, and surgical portals (Fig. 11.11) are marked preoperatively; and local infiltration anesthesia was performed with 2% lidocaine around the lesion and in the surgical approach (Fig. 11.12). A 10-mm

Fig. 11.4 Cortex of calcaneus at the attachment of Achilles tendon with worm-like changes by CT

lateral opening is made 20 mm proximal to the Achilles tendon pain point to create an arthroscopic and an instrument pathway (Fig. 11.13) [8]. Operative procedures were performed under arthroscopic surveillance.

11.4 Operative Technique

11.4.1 Calcified Nodular Type

Most of the patients suffered sudden onset, severe pain, sometimes at night, and could not be touched locally. X-rays

Fig. 11.5 Mixed signals in the Achilles tendon under MRI

Fig. 11.7 Achilles tendon fiber tear type

Fig. 11.6 Calcified nodule type

Fig. 11.8 Hyperplastic fertilizer

Fig. 11.9 Hyperplastic type of calcaneal tuberosity (Haglund's deformity)

Fig. 11.10 TOPAZ electrode blades

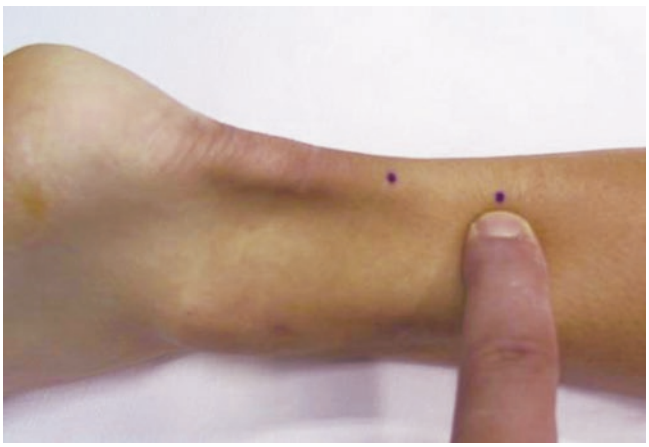

Fig. 11.11 Anatomical outline, pain points, and surgical approach of Achilles tendon marked before operation

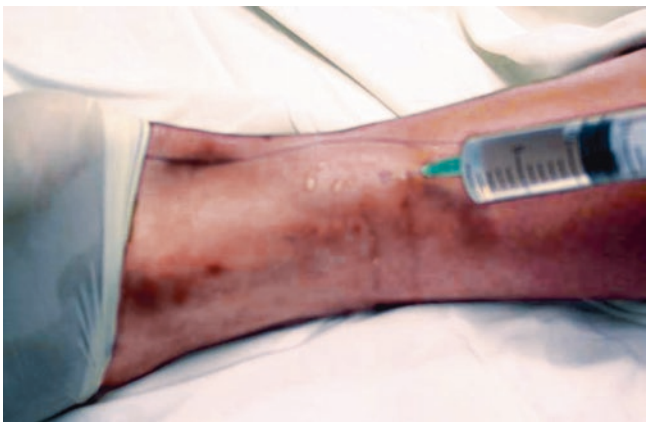

Fig. 11.12 Local infiltration anesthesia around lesion and surgical approach with 2% lidocaine

Fig. 11.13 A 10 mm lateral to both sides of Achilles tendon 20 mm proximal to lesion for arthroscopic and surgical access

display increased density of calcified shadows attached to the calcaneal tuberosity (Fig. 11.14), and MRI presents strip hyperintense calcifications in the Achilles tendon (Fig. 11.15). Arthroscopic exploration of the aponeurosis revealed rose-red hyperemia and edema (Fig. 11.16). The deep layer of the opened aponeurosis is a whitish lime-like slag of calcification (Fig. 11.17), and the calcified material is similar to calcified supraspinatus tendinitis of the shoulder.

After arthroscopic shaver cleaning, flush the released calcification with a large volume of saline. The edge of the calcified Achilles tendon lesion is then cleaned with a plasma knife (Fig. 11.18). The pain symptoms can be significantly relieved after the calcium material is cleaned. Immobilization was performed with a plaster cast or ankle brace for 3 weeks after surgery to allow healing of the injured Achilles tendon fibrous tissue and aid in functional rehabilitation.

Fig. 11.14 Calcified shadows of increased density in Achilles tendon at attachment of calcaneal tuberosity under X-rays

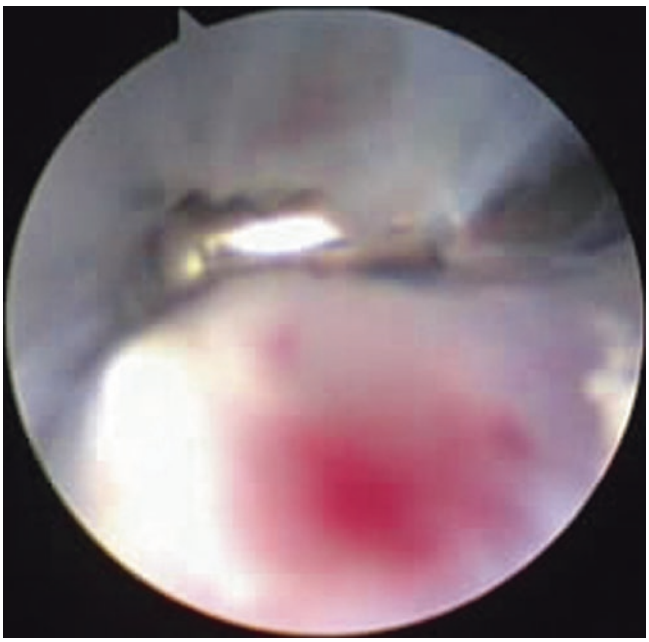

Fig. 11.16 Rose-red hyperemic area on surface of aponeurosis arthroscopy

Fig. 11.15 Striped hyperintense calcified signal in Achilles tendon tissue under MRI

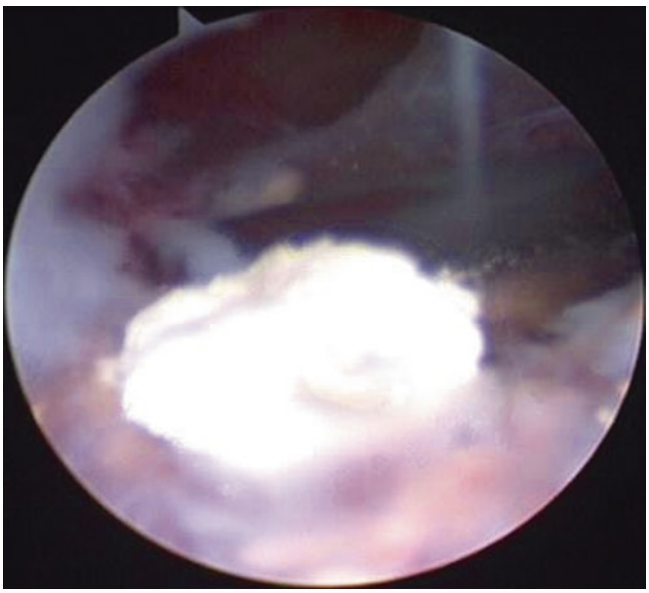

Fig. 11.17 Calcified substance with white lime slag in Achilles tendon

11.4.2 Fiber Tear Type

This type is mostly triggered by sports injury, which occurs in the middle third of the Achilles tendon, and there is no obvious positive manifestation on X-ray and CT scan. MRI may reveal structural derangements of the Achilles tendon tissue as high signal intensity (Fig. 11.19). Arthroscopic exploration reveals loss of Achilles tendon lustre, curling fibrous tissue, and disorganized structures (Fig. 11.20), partial rupture of Achilles tendon fibrous tissue defects (Fig. 11.21), and with deep continuity. Under the surveillance of arthroscope, shaver was used to clean up the broken, rough, and curly fiber and hypertrophic scar tissue. Radiofrequency ablation (Fig. 11.22) is followed by immobilization in a cast or brace for 3–4 weeks.

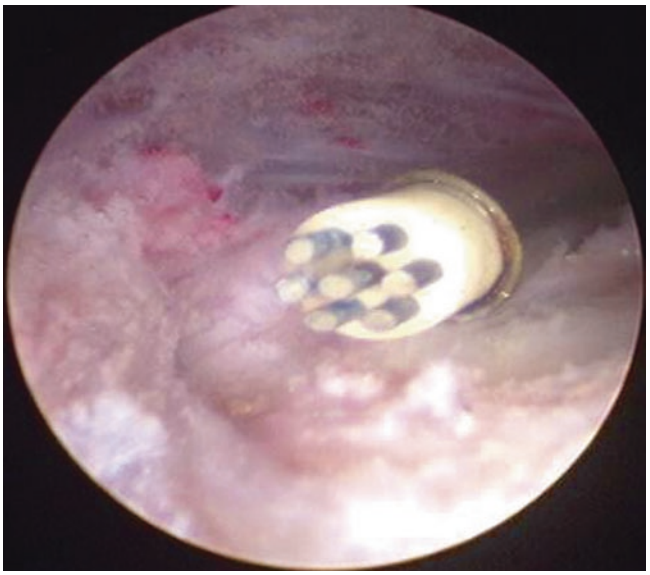

Fig. 11.18 Plasmakinetic debridement of calcified Achilles tendon edge

Fig. 11.19 Disordered structure of Achilles tendon fiber tear and tissue edema under MRI

11.4.3 Hypertrophic Type

Lesions occurred mainly in the tissues where the calcaneal tuberosity was attached to the Achilles tendon. Rough cracked skin with hyperpigmentation and hyper-

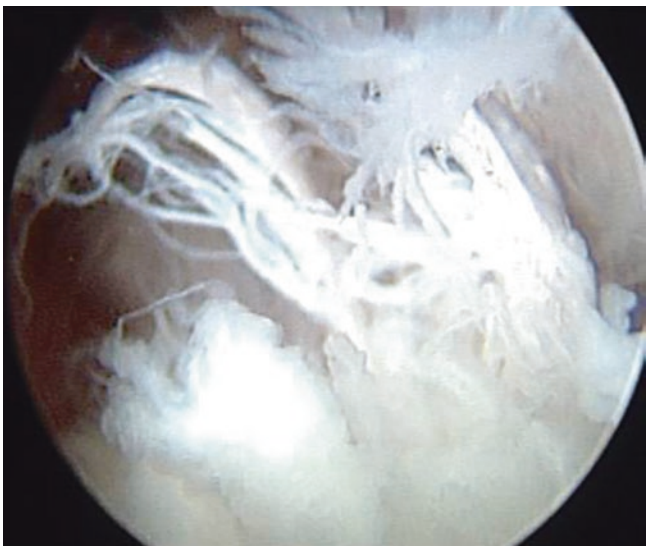

Fig. 11.20 Partial disruption of Achilles tendon tissue with curled fibers and disorganized structure under arthroscopic exploration

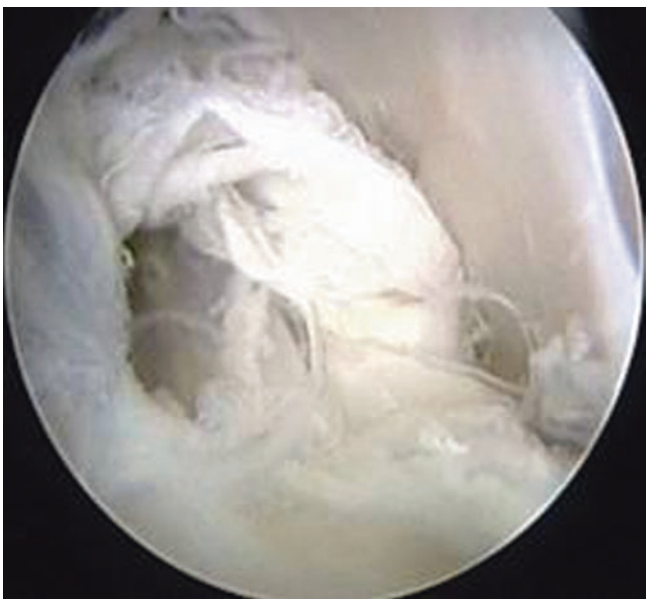

Fig. 11.21 Partial rupture and defect of fibrous tissue of Achilles tendon

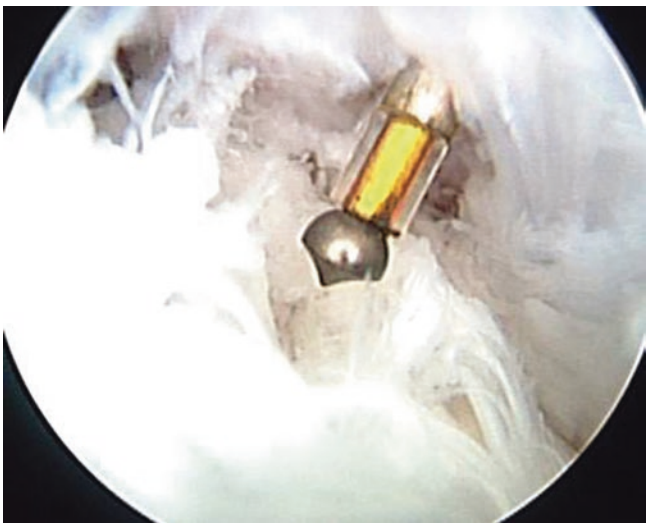

Fig. 11.22 Radiofrequency ablation technique

Fig. 11.23 Clinical manifestations of heel swelling, soft tissue hyperplasia and hypertrophy around calcaneal tuberosity

trophy around the calcaneal tuberosity are the clinical findings (Fig. 11.23). X-rays and CT scans show hyperostosis or worm-like changes in the calcaneal tuberosity (see Fig. 11.4). MRI demonstrates abnormal signal intensity in the Achilles tendon disorganization (Fig. 11.24) with

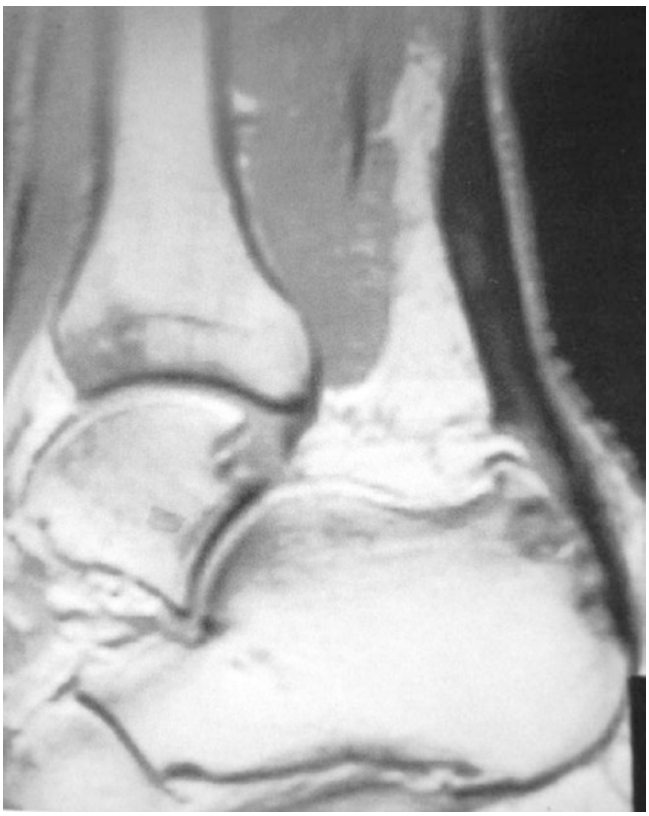

Fig. 11.24 Worm-like changed and signal abnormal Achilles tendon at the attachment of the calcaneal tuberosity under MRI

worm-like changes at the calcaneal tuberosity. Arthroscopic exploration reveals disorganized tissue at the calcaneal tuberosity Achilles tendon attachment (Fig. 11.25) and fibrous disruption and scar hyperplasia in some Achilles tendons (Fig. 11.26).

Fibrous scar tissue on the surface of Achilles tendon is cleaned by arthroscopy (Fig. 11.27). Radiofrequency ablation is performed at the attachment of Achilles tendon using TOPAZ (Fig. 11.28). It is vertically inserted into the deep layer of Achilles tendon to reach the calcaneal tuberosity with a treatment point at 3 mm interval. The treatment time is 0.5 s at each point, with pressure 5–8 g. The appearance of lesion area after treatment is mesh-like (Fig. 11.29) [9]. The incision of 3 mm was sutureless, externally dressed, and immobilized for 3 weeks with an ankle brace. Functional rehabilitation training was carried out gradually after operation. The swelling of the Achilles tendon tissue at the calcaneal tuberosity subsides by 6 weeks (Fig. 11.30).

11.4.4 Calcaneal Tubercle Hyperplasia (Haglund's Deformity)

Haglund's anomaly is defined as an abnormal protrusion of the posterosuperior calcaneal tubercle, accompanied by inflammation around the insertion of the Achilles tendon,

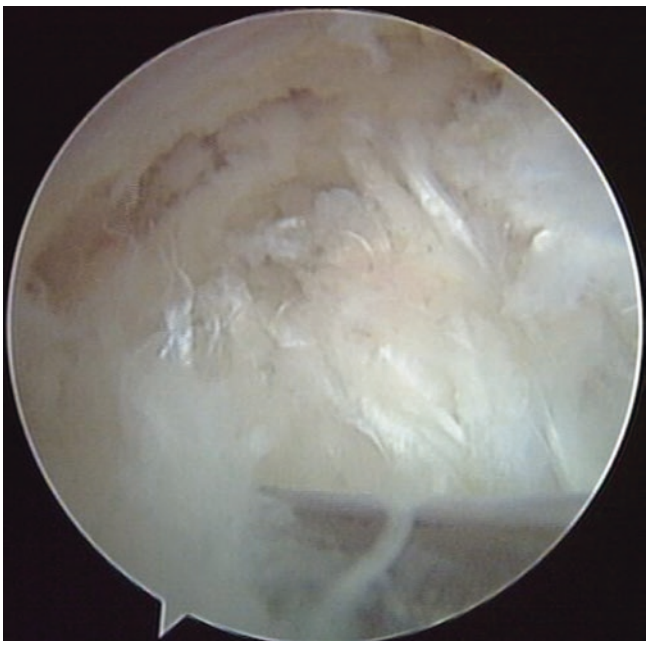

Fig. 11.25 Disorganized tissue at calcaneal tuberosity Achilles tendon attachment under arthroscopic exploration

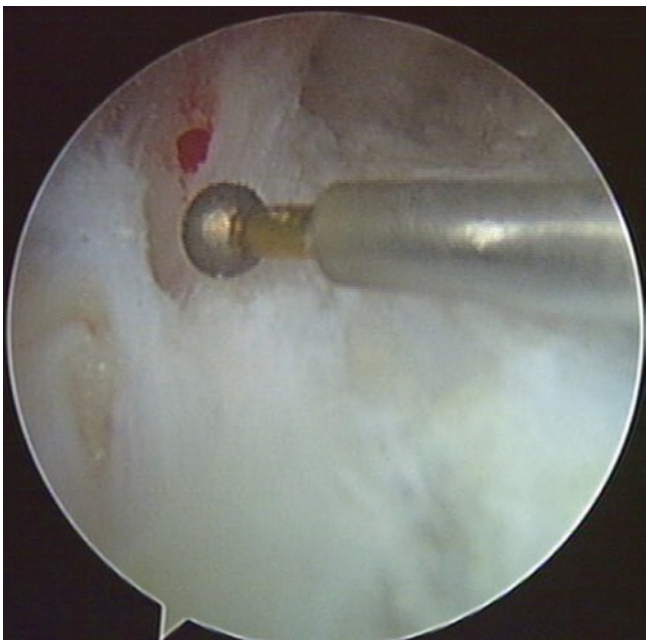

Fig. 11.27 Arthroscopic debridement of hypertrophic fibrous scar tissue of Achilles tendon

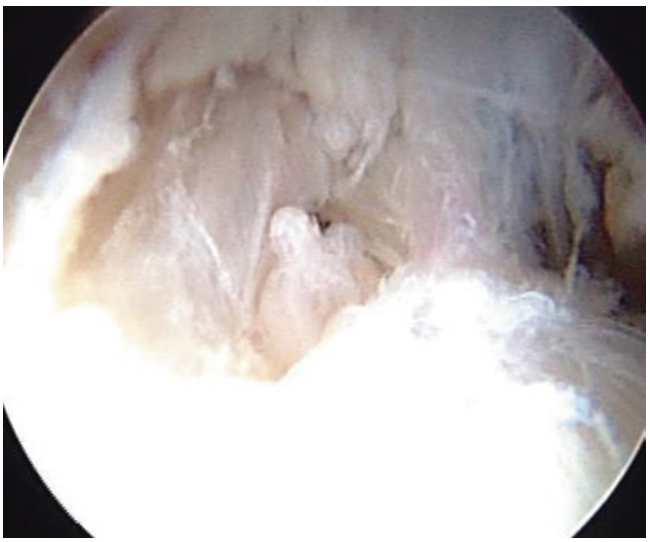

Fig. 11.26 Partial fracture and scar hyperplasia of Achilles tendon fibrous tissue

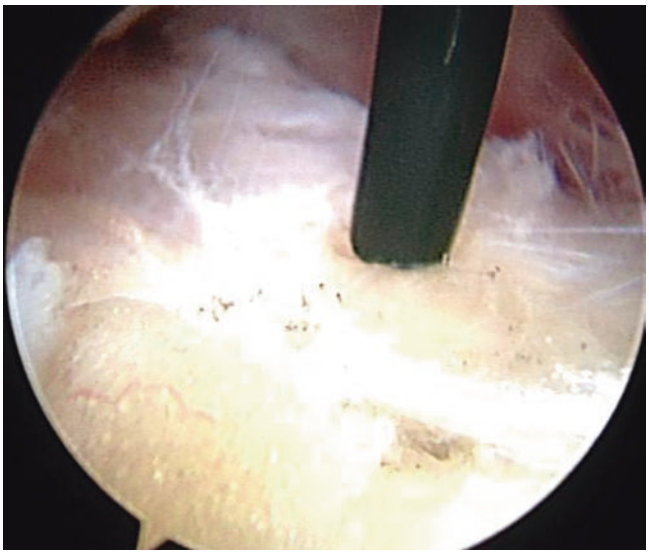

Fig. 11.28 TOPAZ radiofrequency ablation with vertical penetration into calcaneal tuberosity

and is a type of Achilles tendinopathy. The clinical manifestations were swelling and tenderness behind the Achilles tendon and limitation of dorsal extension of the foot. CT examination showed the superior posterior process of the calcaneus. MRI presented congestion and edema of the Achilles tendon.

The patient was placed in a prone position with the foot and ankle positioned distally to facilitate intraoperative passive ankle mobilization (Fig. 11.31). The distal end of the medial and lateral malleoli and the medial and lateral edges of the Achilles tendon were marked, and the posterior and posterior medial approaches were used for arthroscopic treatment of Haglund's deformity. The posterior arthroscopic approach was routinely selected slightly higher than the calcaneus.

Fig. 11.29 Topical mesh after TOPAZ radiofrequency ablation

Fig. 11.30 Rough swelling skin of right heel before treatment and swelling around calcaneal tuberosity subsided 6 weeks after operation

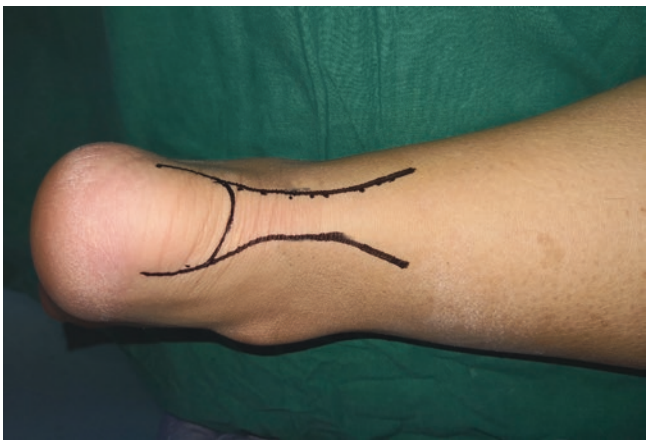

Fig. 11.31 Surgical position

The posterolateral surgical approach is first established, the skin is incised with a sharp knife and then punctured with a blunt tip awl and a cannula directed toward the posterosuperior calcaneal tubercle, and a 4 mm diameter, 30° angled arthroscope is inserted. The posterior internal approach is established under arthroscopic surveillance by first puncturing with a syringe needle to confirm proper position and angle, incising the skin 3 mm, and then separating the lacuna from the adipose tissue beneath the Achilles tendon (Fig. 11.32). After filling with water, a shaver blade is placed to clean the adipose tissue beneath the Achilles tendon, fully exposing the Achilles tendon, the Achilles tendon bursa, and the posterior bursa mucosa and superior anapophysis of the calcaneus (Fig. 11.33). The hyperemic bursa in front of the Achilles tendon was cleaned, and the ankle joint was moved passively to observe the impact of the posterior superior calcaneal tubercle and the Achilles tendon. Insert the needle of the syringe behind the Achilles tendon to the posterior superior tuberosity of the calcaneus under arthroscopic surveillance (Fig. 11.34), locate fluoroscopically to identify the area of osteophyte removal from the calcaneus (Fig. 11.35), abrade the osteophyte portion (Fig. 11.36), and perform a negative impact test and hind-

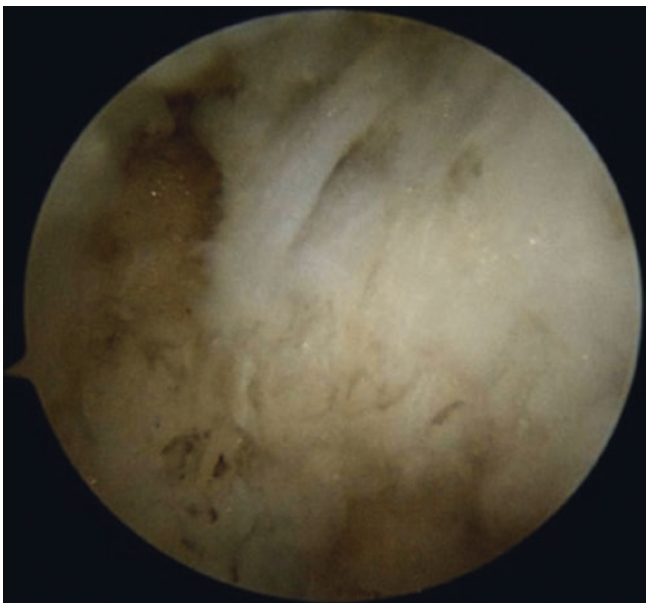

Fig. 11.32 Peel the posterior malleolus to create operating cavity

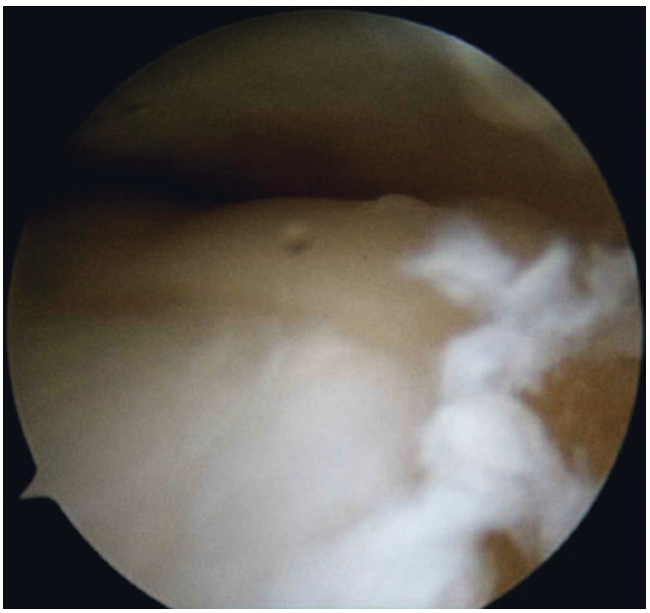

Fig. 11.34 Confirm the position of posterosuperior calcaneal tubercle under arthroscopic surveillance

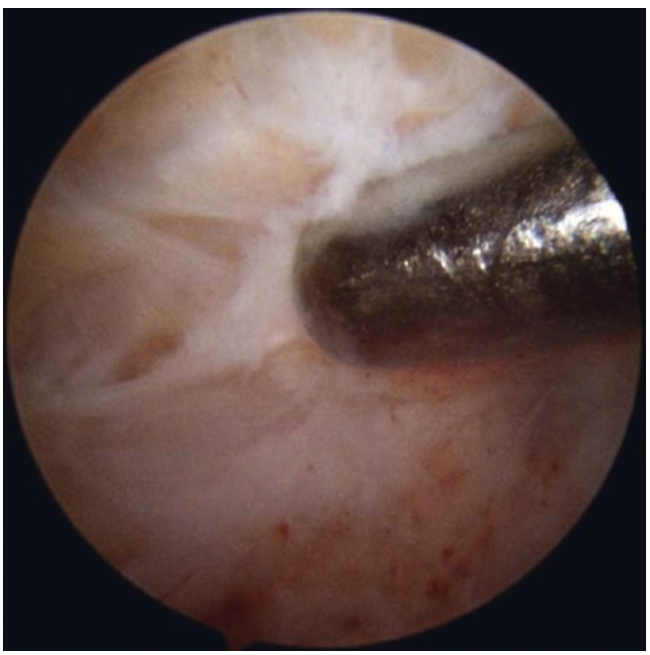

Fig. 11.33 Shaver debridement to expose Achilles tendon, Achilles bursa, and poster superior calcaneal process

Fig. 11.35 Location of the posterosuperior calcaneal tubercle under fluoroscopy

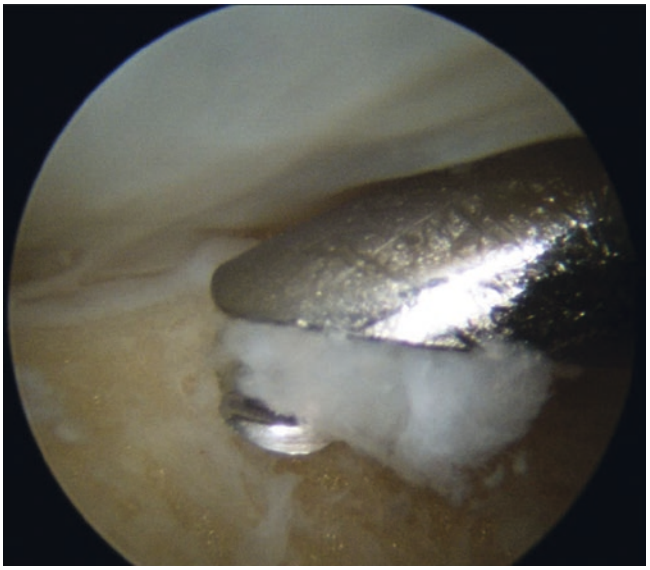

Fig. 11.36 Grinding and drilling to remove part of posterosuperior tuberosity of calcaneus

Fig. 11.37 Posterior superior calcaneal tuberoplasty

foot varus impact test (Fig. 11.37). Lesions in the superficial layers of the Achilles tendon were also managed in parallel. Note residual osteophytes at the posterolateral or posteromedial approach to the posterior superior calcaneal tuberoplasty (Fig. 11.38), resulting in residual postoperative symptoms [10].

Fig. 11.38 Residual osteophytes under CT 3D reconstruction

11.5 Critical Points

1. Imaging studies such as MRI are important for the preoperative diagnosis of Achilles tendinopathy and the development of treatment options.
2. Haglund's deformity preoperative 3D CT can show the extent and location of the bony prominence, facilitating the removal of the lesion during surgery.
3. Patients who frequently undergo local hormonal blockade are prone to Achilles tendon rupture or non-healing wounds.
4. Achilles tendon fiber tear pattern due to reduced strength of the Achilles tendon tissue, 4–6 weeks after surgery should be developed to prevent rupture.

References

1. Silva RT, et al. Medical assistance at the Brazilian juniors tennis circuita one-year prospective study. J Sci Med Sport. 2003;6:14–8.
2. Jarde O, et al. Surgical treatment of chronic Achilles tendiopathies: report of 52 cases. Rev Chir Orthop Reparatrice Appar Mot. 2000;86:718–23.
3. Thermann H, Benetos IS, Panelli C, Gavritlidis I, Feil S. Endoscopic treatment of chronic mid-portion Achilles tendinopathy: novel technique with short-term results. Knee Surg Sports Traumatol Arthrosc. 2009;17(10):1264–9.

4. Maquirriain J, Ayerza M, Costa Paz M, Muscolo DL. Endoscopic surgery in chronic achilles tendinopathies: a preliminary report. Arthroscopy. 2002;18(3):298–303.
5. Ahmed IM, Lagopoulos M, McConnell P, et al. Blood supply of the achilles tendon. J Orthop Res. 1998;16:591–6.
6. Maquirriain J. Endoscopic surgery in chronic achilles tendinopathies: a preliminary report. Arthroscopy. 2002;18:298.
7. Yu-Jie L, Zhi-Gang W, Zhong-Li L, et al. Arthroscopically assisted radiofrequency probe to treat achilles tendinitis. Chin J Surg. 2008;46(2):101–3.
8. McAllister JE, Hyer CF. Safety of Achilles detachment and reattachment using a standard midline approach to insertional enthesophytes. J Foot Ankle Surg. 2015;54(2):214–9.
9. James P, Tasto JP, Cummings J, Medlock V, Hardesty R, Amiel D. Microtenotomy using a radiofrequency probe to treat lateral epicondylitis. Arthroscopy. 2005;21:851–60.
10. Roth KE, Mueller R, Schwand E, et al. Open versus endoscopic bone resection of the dorsolateral calcaneal edge: a cadaveric analysis comparing three dimensional CT scans. J Foot Ankle Res. 2014;7(1):56.

Arthroscopic Percutaneous Suture of Achilles Tendon Ruptures

12

Yu-jie Liu and Feng Qu

12.1 Introduction

Achilles tendon is an important anatomic structure for maintaining standing, walking, running, and jumping. Achilles tendon ruptures (ATR) usually result from strain injury and local trauma after jump landing in sport tasks. The location of such a rupture commonly appears at Achilles tendon-calcaneus bone junction (Fig. 12.1) or gastrocnemius muscle-Achilles tendon junction (Fig. 12.2). Spontaneous ATR occurs during sports activities, making you feel like heel strike by a blunt object, or with a popping sound, followed by heel pain and immobility immediately.

12.2 Clinical Features

Physical examinations reveal swelling at the injury site of ATR with local ecchymosis, and local indentation can be touched. The patient is ordered to maintain a 90° knee flexion in the prone position. If the strength of Achilles tendon disappears featuring no ankle plantar flexion when a physician presses the triceps surae, a positive sign of Thompson's test will be confirmed (Fig. 12.3). Besides, the patient will also fail to stand tiptoe with one foot. Imageologically, ultrasonography and magnetic resonance imaging (MRI) are beneficial to the diagnosis (Fig. 12.4) [1].

An external fixation system as a conservative treatment for repairing ATR requires 6–8 weeks with high rates of nonunion and repeated rupture. However, an open surgery can inevitably damage the surrounding anatomic structures of Achilles tendon, usually bringing about insufficient blood supply, scar adhesion, non-healing wound, delayed wound healing, and infection [2]. Arthroscopic percutaneous suture of ATR is a minimally invasive method with a minimal surgical wound (Fig. 12.5) and successfully averts structural damage to surrounding tissues and local scar hyperplasia induced by an open surgery (Fig. 12.6) [3].

Fig. 12.1 Achilles tendon-calcaneus bone junction as a common rupture site

12.3 Preoperative Preparation

A patient is positioned prone. The chest, pelvis, and ankle are elevated. See to it that the ankle must be placed at the end of the operative table for arthroscopic surgery, and the shape of Achilles tendon, the rupture site, and the operative approach must be marked on the skin for an intraoperative observation (Fig. 12.7).

Y.-j. Liu (✉)
Department of Orthopedics, Chinese PLA General Hospital, Beijing, China

F. Qu
Beijing Tongren Hospital, Capital Medical University, Beijing, China

Y.-j. Liu et al. (eds.), *Advanced Application of Arthroscopy*, https://doi.org/10.1007/978-981-15-4684-6_12

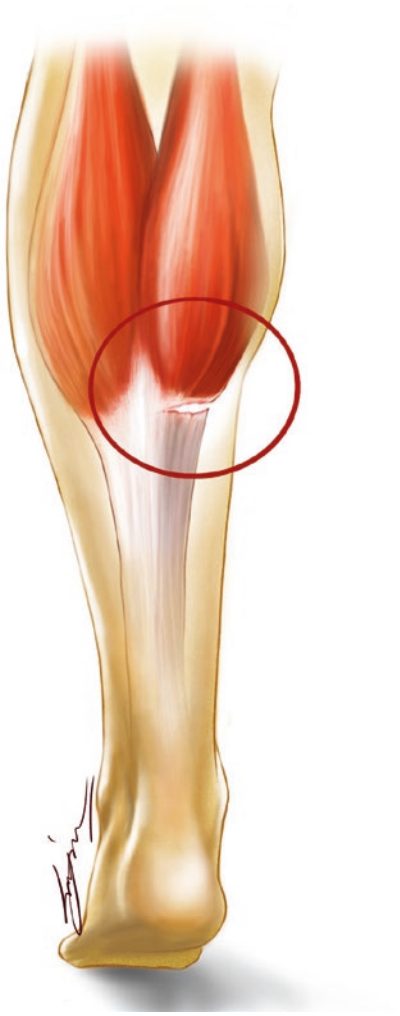

Fig. 12.2 Gastrocnemius muscle-Achilles tendon junction as a common rupture site

12.4 Operative Technique

Approximately at 5 cm proximal to the ruptured tendon two 3-mm incisions are made (Fig. 12.8) as operative tunnels for inserting arthroscope and surgical instruments, respectively. A trocar is used for blunt dissection of subcutaneous tissue around Achilles tendon, providing sufficient space for following procedures. As the arthroscope reaches the ruptured tendon, blood clots are found in the ruptured space (Fig. 12.9) and removed under arthroscopic vision. Subsequently, a moderate-sized cavity caused by the retracted tendon is revealed (Fig. 12.10), and the ruptured ends are impaired (Fig. 12.11).

The clots and the tissue of remnant at the ruptured ends of achillea tendon were removed under arthroscopy (Fig. 12.12). The knee is flexed at 90° with the ankle plantar flexion at 45°, making the torn ends closer (Fig. 12.13). The tendon is sutured with the modified Kessler method

Fig. 12.3 Thompson's test

Fig. 12.4 Discontinuous signals in Achilles tendon on MRI

(Fig. 12.14). Two epidural needles are percutaneously punctured across the torn Achilles tendon at 20 mm close to the proximal and distal ends perpendicular to the vertical axis of the tendon, bringing high-strength sutures piercing the ends. The sutures must remain stretched and be knotted under

Fig. 12.5 The skin incision of the arthroscopic percutaneous suture of ATR

Fig. 12.6 Arthroscopic surgery can prevent scar hyperplasia

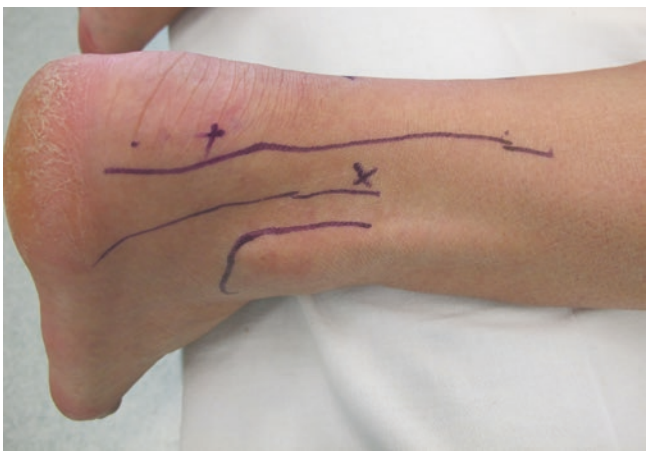

Fig. 12.7 The shape of Achilles tendon, the rupture site, and the operative approach have been marked before the arthroscopic surgery

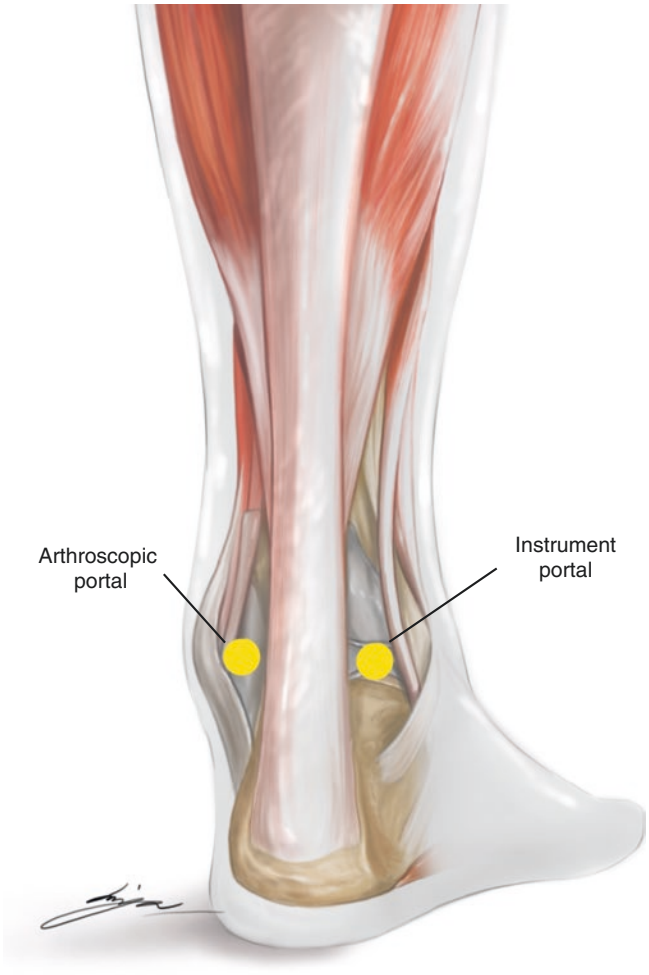

Fig. 12.8 Operative tunnels for arthroscope and surgical instruments

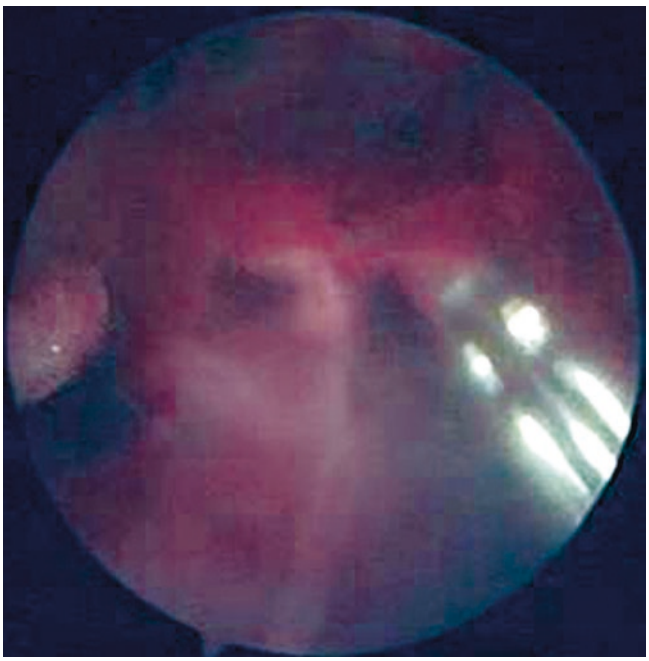

Fig. 12.9 Arthroscope reveals blood clots at the ruptured ends of Achilles tendon

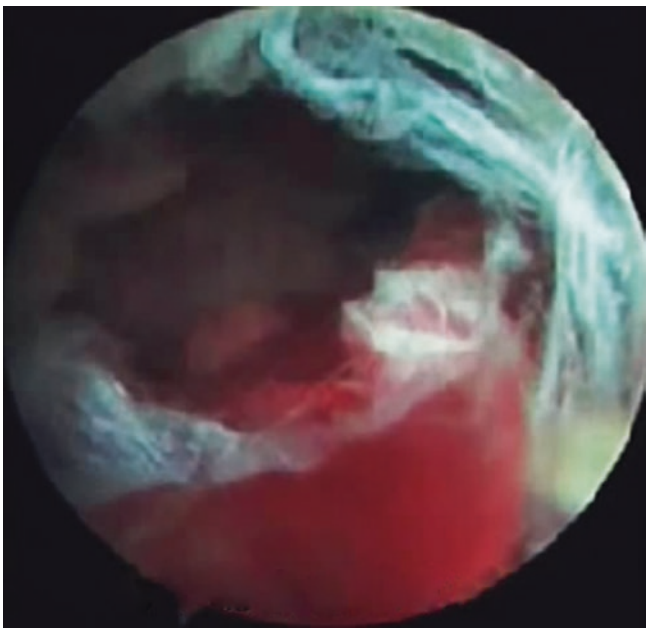

Fig. 12.10 Arthroscope reveals that a cavity is formed due to retracted ends of the ruptured Achilles tendon

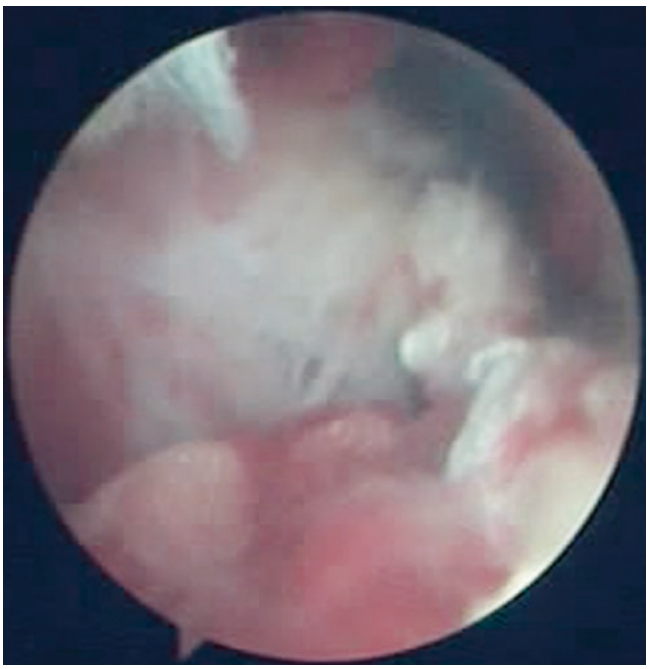

Fig. 12.12 Residual tissue is revealed after removing blood clots in the ruptured space of Achilles tendon under arthroscopic vision

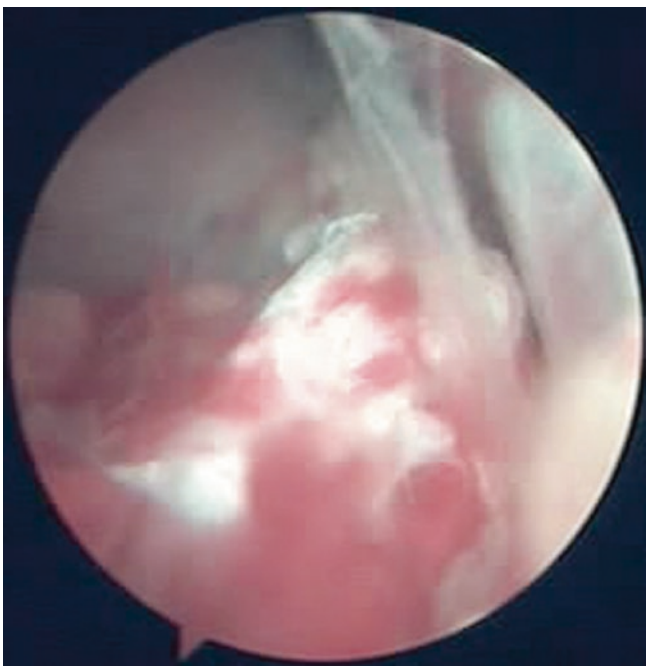

Fig. 12.11 Blood clots are removed and the ruptured ends are impaired

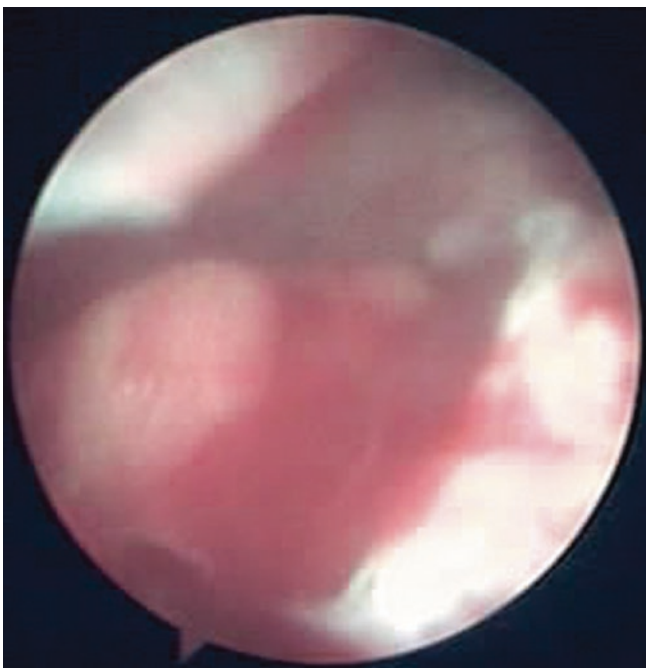

Fig. 12.13 Ankle plantar flexion to make the torn ends closer

clear arthroscopic vision (Fig. 12.15) [4]. After that, surgeons should examine whether the ruptured ends are properly overlapped under arthroscopic vision (Fig. 12.16). Postoperatively, ankle plantar flexion should be remained with brace or plaster immobilization for 4–6 weeks. The ankle should be gradually adjusted to the functional position by stages, and a walking boot is used for further protection. Partial weight bearing is permitted until 8 weeks after surgery, adding plantar flexion and walking over time. Heel raising can be allowed 3 months after surgery.

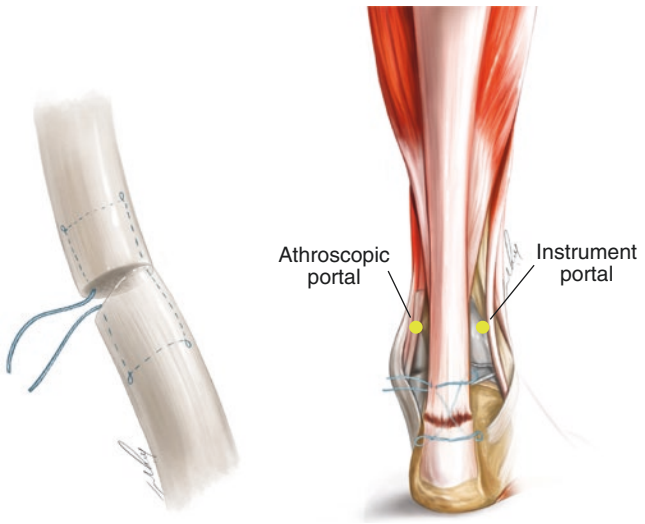

Fig. 12.14 The modified Kessler method is adopted to percutaneously suture the ruptured Achilles tendon

Fig. 12.15 The sutures are stretched and knotted extracorporally

12.5 Critical Points

1. Arthroscopic percutaneous suture is merely suitable for acute ATR and should be performed within about 1 week after the injury in case of malalignment due to tendon contractures. However, severe tendon contractures due to old rupture make the ruptured tendon difficult in overlapping, so the arthroscopic percutaneous suture is not suitable.
2. See to it that posterior tibial nerves and vessels of the medial ankle and lateral sural cutaneous nerve are undamaged.
3. Add sutures, if necessary, in ruptured tendon tissues according to the alignment of the ruptured tendon when modified Kessler tendon repair is performed. Postoperative brace or plaster immobilization is requisite for fear that sutures might be torn.
4. Because arthroscopic percutaneous suture of ATR is more demanding, experienced senior surgeons are demanded for completing the surgical procedures.

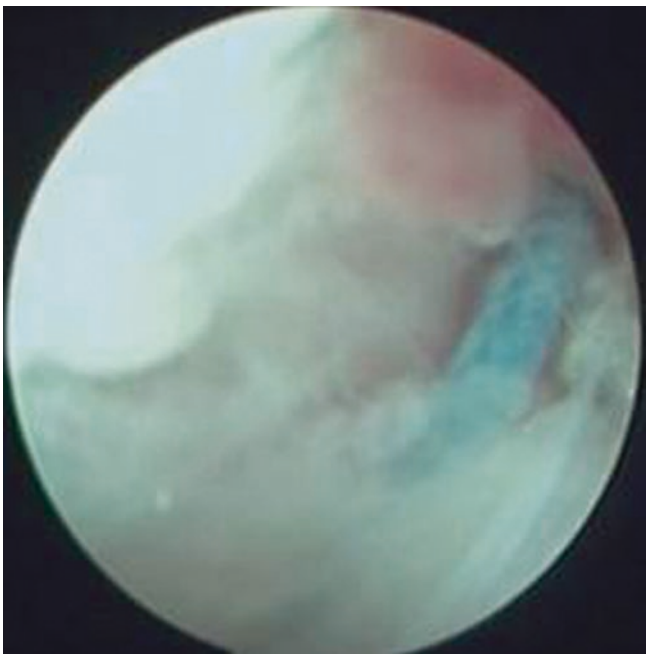

Fig. 12.16 Arthroscope reveals that the ruptured ends of Achilles tendon are properly overlapped

References

1. Aktas S, Kocaoglu B. Open versus minimal invasive repair with Achillon device. Foot Ankle Int. 2009;30(5):391–7.
2. Jung HG, Lee KB, Cho SG, et al. Outcome of achilles tendon ruptures treated by a limited open technique. Foot Ankle Int. 2008;29(8):803–7.
3. Yu-Jie L, Zhi-Gang W, Zhong-Li L, et al. Clinical application of arthroscopic technique in exterior joint surgery. Med J Chin People's Liberation Army. 2003;3:275–6.
4. Lim J, Dalal R, Waseem M. Percutaneous vs. open repair of the ruptured Achilles tendon-a prospective randomized controlled study. Foot Ankle Int. 2001;22(7):559–68.

13 Arthroscopic Minimally Invasive Surgery for Hallux Valgus Caused by Bunion

Yu-jie Liu and Feng Qu

13.1 Introduction

Hallux valgus deformity is mainly manifested by adduction of the first metatarsal bone, hallux valgus, and the second toe riding across the hallux (Fig. 13.1); the collapse of second, third metatarsal heads and the transverse arch of the foot and painful callus on the sole (Fig. 13.2). The above abnormal changes often cause pain in the big toe, the second, and third metatarsophalangeal joints and in more serious cases may affect wearing shoes and walking [1].

13.2 Clinical Features

Anterior and lateral X-ray films of the foot can be used to evaluate the presence and severity of arthritis in the first metatarsophalangeal joint [2–4]. Common measurement methods include hallux valgus angle (HVA, normal: 15–16°) (Fig. 13.3), first-second metatarsus intermetatarsal angle (IMA, normal: 8–10°) (Fig. 13.4); metatarsus distal metatarsal articular angle (DMAA, normal: 5–7°) (Fig. 13.5). The sesamoid position (SP) is also valuable for judging hallux valgus (Fig. 13.6). CT scan of foot weight loading position is also gradually applied to clinical imaging examination of hallux valgus [5–7], which has certain reference value.

According to the angle of measurement, the degree of hallux valgus can be divided into mild, moderate, and severe: mild: HVA $\leq 20°$, IMA $\leq 13°$; moderate: $20° < \text{HVA} \leq 40°$, $13° < \text{IMA} \leq 16°$; severity: HVA $> 40°$, IMA $> 16°$ [8, 9].

Fig. 13.1 Malformations of the second toe riding across the big toe in hallux valgus

13.3 Operative Technique

13.3.1 Open Surgery for Hallux Valgus

The treatment of hallux valgus usually adopts open surgery, using soft tissue surgical methods such as McBride, Du Vries-Mann and Silver, etc. [10]. Hallux valgus deformity

Y.-j. Liu (✉)
Department of Orthopedics, Chinese PLA General Hospital, Beijing, China

F. Qu
Beijing Tongren Hospital, Capital Medical University, Beijing, China

Y.-j. Liu et al. (eds.), *Advanced Application of Arthroscopy*, https://doi.org/10.1007/978-981-15-4684-6_13

Fig. 13.2 Painful callus on sole of patients with hallux valgus

Fig. 13.3 Hallux valgus angle

Fig. 13.4 First-second metatarsus intermetatarsal angle

can be corrected by excision of osteophyte on the medial side of the hallux, release of adductor pollicis muscle, and cleaning of bunion of thumb.

For patients with severe hallux valgus deformity, metatarsophalangeal arthritis debridement and osteotomy are required. Akin surgery, Chevron surgery, Scarf surgery, Ludloff surgery, Lapidus surgery, Reverdin surgery, Weil surgery, Keller surgery, and fusion of metatarsophalangeal joint [11, 12] are commonly used to correct the first-second metatarsus intermetatarsal angle and DMAA.

13.3.2 Arthroscopic Hallux Valgus Surgery

13.3.2.1 Surgical Indications

Arthroscopic hallux valgus surgery is suitable for patients with bunion of thumb and mild hallux valgus deformity as early main manifestations (Fig. 13.7), whose hallux valgus angle <20° IMA < 13°; the metatarsophalangeal articular cartilage is normal, without serious osteoarthritis, with good joint mobility and normal flexion and extension function.

13.3.2.2 Contraindications

This procedure is not suitable for the following patients: patients with severe hallux valgus deformity, with valgus angle >25°, or have Hammer toe with one or more toes (Fig. 13.8); patients with metatarsophalangeal joint disloca-

Fig. 13.5 Metatarsus distal metatarsal articular angle

Fig. 13.6 The sesamoid position

Fig. 13.7 Arthroscopic surgery is suitable for patients with mild hallux valgus complicated with bunion of thumb

Fig. 13.8 Patients with severe hallux valgus deformity accompanied by Hammer's toe are not suitable for arthroscopic surgery

Fig. 13.9 Local infiltration anesthesia is performed with the first metatarsophalangeal joint as the center

tion complicated with osteoarthritis; patients with the rigidity of metatarsophalangeal joints and limited mobility; patients with the history of surgery in first metatarsophalangeal joint and have local skin scar adhesion which makes arthroscopy difficult to enter; patients with local skin ulceration infection or foot fungus infection; and patients with diabetic foot and lower limb vascular diseases that lead to poor foot blood circulation and affect wound healing. None of the above patients is suitable for arthroscopic minimally invasive surgery.

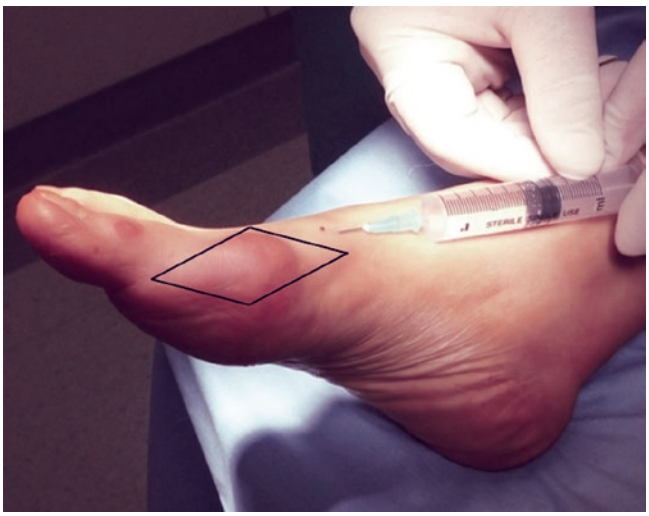

Fig. 13.10 The anesthesia range is a rhombus

13.3.2.3 Anesthesia and Position

The patient is in a supine position. Routine disinfection. Spread sterile sheet. Using 2% lidocaine, physiological saline and 0.75% ropivacaine to prepare 10–15 ml of 1:1:1 mixed solution as local infiltration anesthesia. Local skin infiltration anesthesia (Fig. 13.9) and intra-articular anesthesia are performed with the first metatarsophalangeal joint as the center, and the anesthesia range is a rhombus (Fig. 13.10).

Prepare the arthroscope with a diameter of 1.9 ~ 2.7 mm and a 30° wide angle, micro planer, and drill bit. Two surgical approaches are, respectively, made at the position near the first metatarsal head 3 cm; the arthroscope is inserted into the joint cavity (Fig. 13.11). Establish the working channel of surgical instruments under arthroscope monitoring (Fig. 13.12). Due to the narrow gap of the first metatarsophalangeal joint, drainage is difficult, which will affect the visual field. A thick injection needle can be inserted to increase the liquid perfusion and circulation (Fig. 13.13), to make the visual field clearer [13, 14].

13.3.2.4 Operation Method

Arthroscopic examination revealed celluloid bursitis of thumb (Fig. 13.14) and osteophyte hyperplasia of the first metatarsophalangeal joint (Fig. 13.15). The hyperplastic synovial tissue is cleaned by an equal radio-frequency ion knife (Fig. 13.16); the osteophyte hyperplastic in the first

Fig. 13.11 Insert the puncture cone into the articular cavity

Fig. 13.13 A thick injection needle can be inserted to increase the liquid perfusion and circulation

Fig. 13.12 Establish working channel under arthroscope monitoring

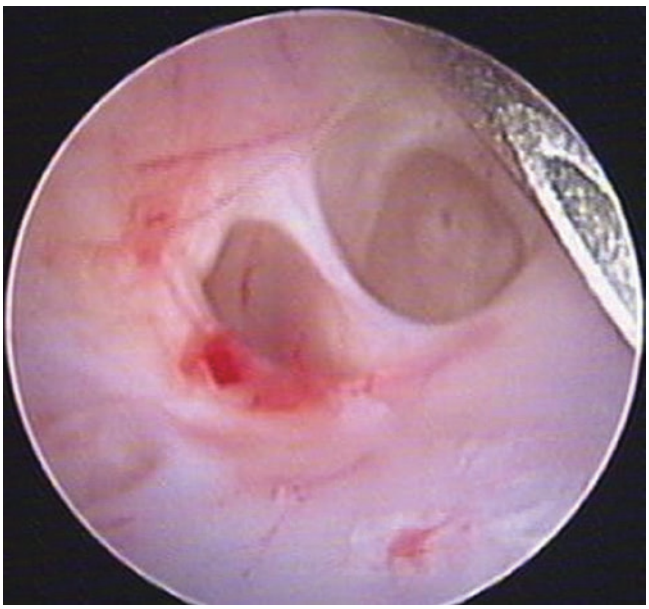

Fig. 13.14 Thumb bursitis of the metatarsophalangeal joint is honeycomb-shaped

metatarsophalangeal joint is cleaned by planing and drilling (Fig. 13.17). Investigate whether the ground osteophyte wound is flat or not (Fig. 13.18). During the operation, special attention should be paid to protect the vascular nerves near the metatarsophalangeal joint to avoid injury (Fig. 13.19).

A small incision is made on the dorsal side between the first and second toes to release adductor pollicis muscle, and the wound doesn't need to be sutured. After the operation, cover the incision with gauze, wrap up the bandage or orthopedic strap in a figure of "8" (Fig. 13.20), and fix it in the hallux valgus position.

13.4 Critical Points

1. In preoperative selection, bunion of thumb with mild hallux valgus should be taken as the surgical indication, and the surgical indication cannot be blindly expanded.
2. Pay attention to protect the vessels and nerves near the metatarsophalangeal joint to avoid injury.

Fig. 13.15 Osteophyte hyperplastic in the first metatarsophalangeal joint

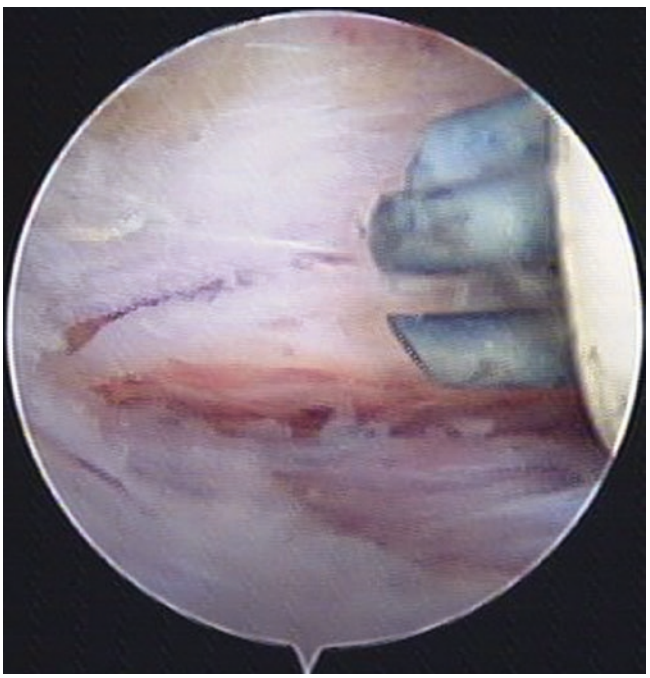

Fig. 13.16 The hyperplastic synovial tissue in the first metatarsophalangeal joint is cleaned by an equal radio-frequency ion knife

Fig. 13.17 Grinding of osteophyte hyperplasia in the first metatarsophalangeal joint with a drill

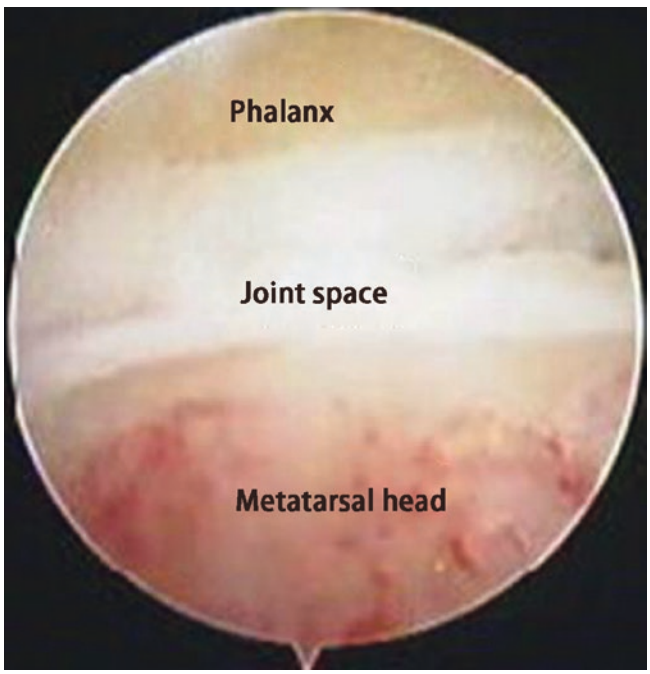

Fig. 13.18 The bone surface is flat after osteophyte grinding

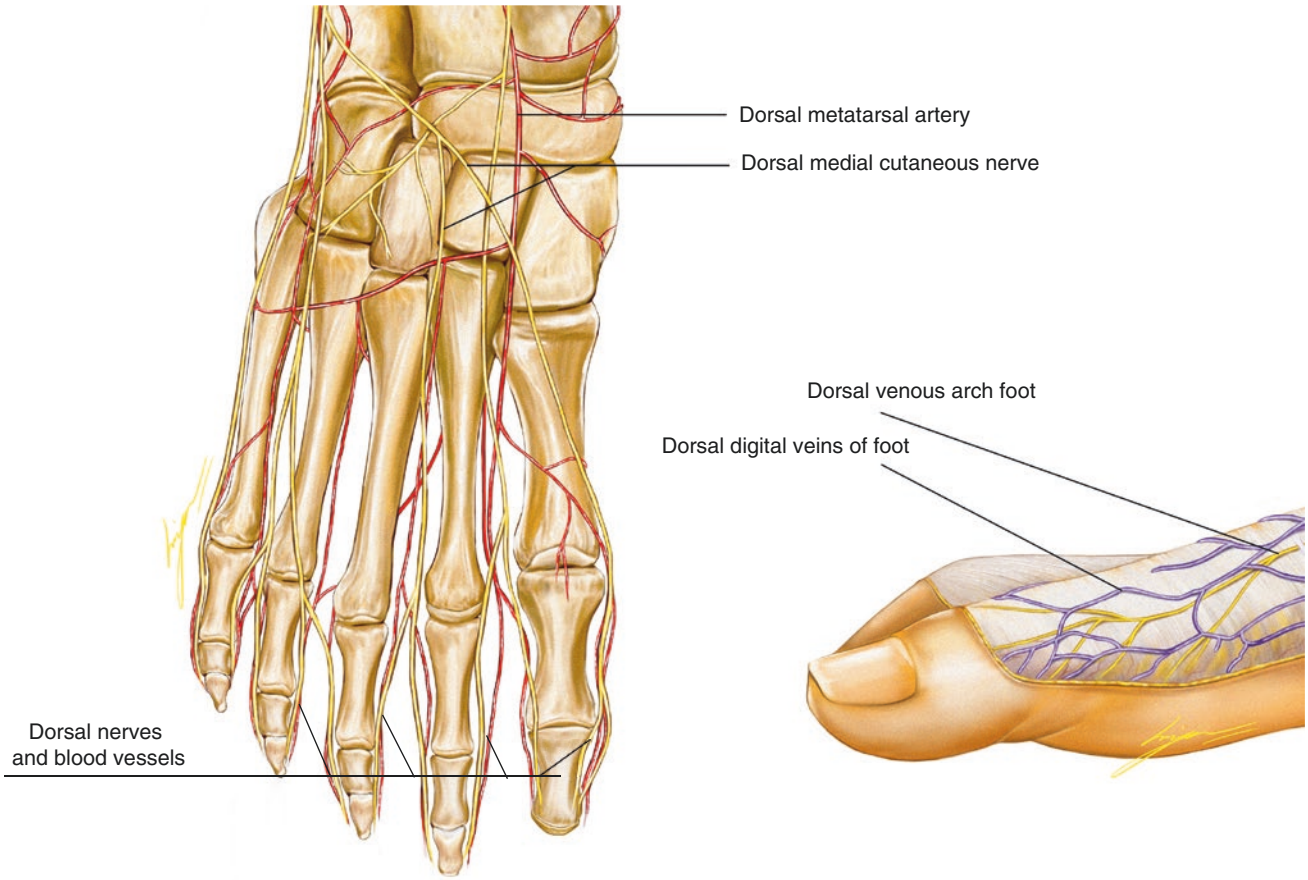

Fig. 13.19 Schematic diagram of blood vessels and nerves near metatarsophalangeal joint

Fig. 13.20 Orthopedic band fixation after hallux valgus surgery

References

1. Coughlin MJ. Hallux valgus. J Bone Joint Surg Am. 1996;78:932–66.
2. Lee JS, Kim KB, Jeong JO, et al. Correlation of foot posture index with plantar pressure and radiographic measurements in pediatric flatfoot. Ann Rehabil Med. 2015;39(1):10–7.
3. Mittag F, Leichtle U, Meisner C, et al. Proximal metatarsal osteotomy for hallux valgus; an audit of radiologic outcome after single screw fixation and full postoperative weightbearing. J foot Ankle Res. 2013;6:22.
4. Coughlin MJ, Jones CP. Hallus valgus: demographics, etiology and radiographic assessment. Foot Ankle Int. 2007;28(7):759–77.
5. Coughlin MJ, Roger A. Mann award. Juvenile hallux valgus: etiology and treatment. Foot Ankle Int. 1995;16(11):682–97.
6. Geng X, Wang C, Ma X, et al. Mobility of the first metatarsal cuneiform joint in patients with and without hallux valgus: in vivo three-dimensional analysis using computerized tomography scan. J Orthop Surg Res. 2015;10:140.
7. Dhinsa B, Walker R, Jones I. Technique to test flexor hallucis longus after Akin osteotomy. Ann R Coll Surg Engl. 2016;98(2):156.
8. Deenik AR, de Visser E, Louwerens JW, et al. Hallus valgus angle as main predictor for correction of hallus valgus. BMC Musculoskelet Disord. 2008;9:70.
9. Wang Z, Baoguo J, Kanglai T, Jianzhong Z. Expert consensus on the surgical treatment of hallux valgus. Chin J Bone Joint Surg. 2018;11(2):87–95.
10. Cemil K, Hasan O, Haluk A, et al. The effectiveness of distal soft tissue procedures in hallux Valgus. J Orthopaed Traumatol. 2008;9:117–21.

11. Swanson AB, de Groot Swanson G. Use of grommets for flexible hinge implant arthroplasty of the great toe. Clin Onhop Relat Ras. 1997;34(10):87–94.
12. Mroczek KJ, Miller SD. The modified oblique Keller procedure: a technique for dorsal approach interposition arthroplasty sparing the flexor tendons. Foot Ankle Int. 2003;24(7):521.
13. Lui TH, Chan KB, et al. Endoscopic distal soft-tissue release in the treatment of hallux valgus: a cadaveric study. Arthroscopy. 2010;26(8):1111–6.
14. Lui TH. Arthroscopy and endoscopy of the foot and ankle indications for new techniques. Arthroscopy. 2007;23(8):889–902.

Part II

Arthroscopic Minimally Invasive Techniques

14 Arthroscopic Prying Reduction and Fixation for the Greater Tuberosity Fractures

Yu-jie Liu, Chang-ming Huang, and Shao-hua Ding

14.1 Introduction

The incidence of greater tuberosity fracture of the humerus was 15 ~ 30% [1–3]. Anteroposterior shoulder joint radiography, and axial radiography can confirm the diagnosis (Fig. 14.1). Three-dimensional CT reconstruction is helpful to evaluate the condition of bone fracture displacement (Fig. 14.2), and shoulder joint MRI examination would be helpful to diagnosis of Bankart injury or rotator cuff injury [1, 3–5].

Accordingly the condition of bone fracture displacement can be divided into displaced fracture and undisplaced fracture. Neer use open surgical reduction internal fixation to treat greater tuberosity fracture of humerus which displacement >1 cm. Study shows even fracture fragments of greater tuberosity of humerus mild displacement; there will be acromion impingement syndrome when the shoulder joint is moving. Prying reduction and fixation under arthroscopy, operative wound smallness and would be helpful to early functional rehabilitation [6, 7].

Fig. 14.1 Radiography shows anterior shoulder dislocation

14.2 Operative Technique

14.2.1 The Treatment of Greater Tuberosity Fracture of Humerus with Prying Reduction and Fixation Under Arthroscopy

After general anesthesia, the patients were posed at lateral position, limb abduction 60°, traction weight 3–4 KG. Before surgery, mark acromion, coracoid process, bone landmarks of greater tuberosity of humerus and arthroscopic surgical portal. For operation field clear, arthroscopic perfusate contains 0.1% adrenaline 1 ml per 3000 ml normal saline, for continuous lavation.

Operative approach: Posterolateral corner of acromion downward 10 mm and then inward 10 mm, it's a "soft point" behind the shoulder joint, used as arthroscopic posterior portal (Fig. 14.3); the lateral or anterior side of the shoulder joint is the operating channel.

Routinely examine scapula glenoid, cartilage, and rotator cuff for any damage; probe the condition of bone fracture displacement (Fig. 14.5). Notice under the acromion 4–5 cm, there is axillary nerve (Fig. 14.4) prevent injury.

Clean up the bone chip, old hematocele, and scar tissue, debridement was performed on the fracture surface, to make

Y.-j. Liu (✉)
Department of Orthopedics, Chinese PLA General Hospital, Beijing, China

C.-m. Huang
Department of Orthopedics, The 73 Group Army Hospital, Chenggong Hospital Affiliated to Xiamen University, Xiamen, China

S.-h. Ding
Department of Orthopedics, Medical Center of Ningbo, Lihuili Hospital, Ningbo, China

Y.-j. Liu et al. (eds.), *Advanced Application of Arthroscopy*, https://doi.org/10.1007/978-981-15-4684-6_14

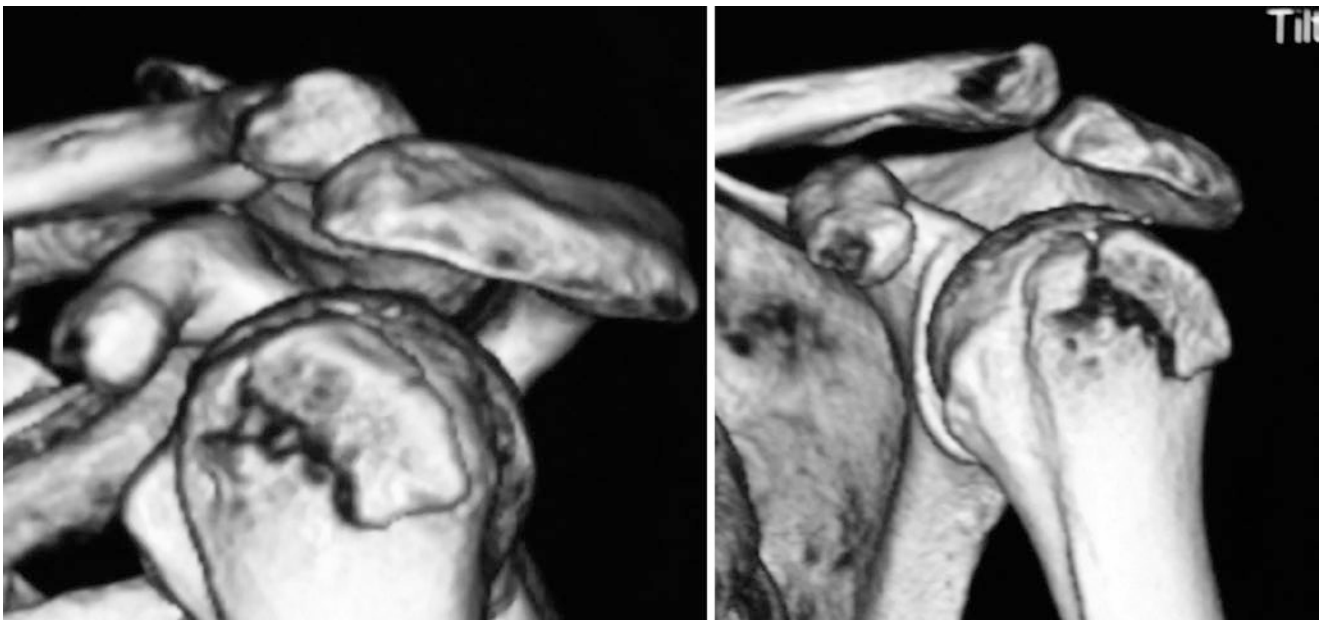

Fig 14.2 Three-dimensional CT reconstruction is helpful to evaluate the condition of bone fracture displacement

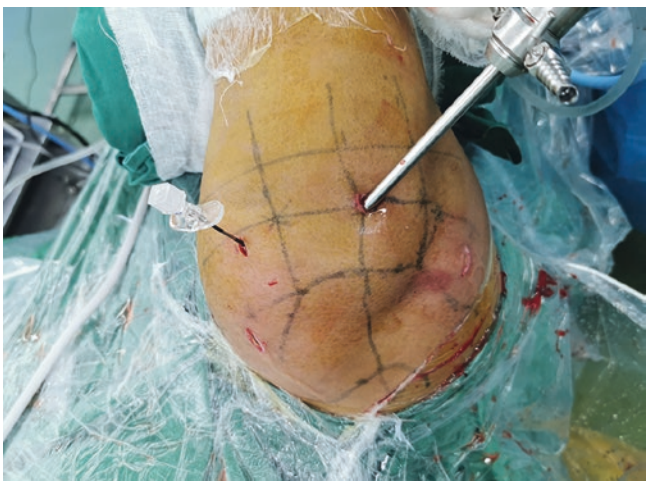

Fig. 14.3 Posterior portal of shoulder arthroscopy

it fresher, and poking reduction of the fracture fragment was watched by arthroscopy (Fig. 14.5). Take care to protect rotator cuff tissue when prying reduction of the fracture fragment, in order to avoid damage. After anatomical reduction of the fracture, fixing the fracture fragment by percutaneous Kirschner wire fixation observing depth and angle of Kirschner wire entry into the bone by X-ray, hold the Kirschner wire at a 45-degree angle toward humeral shaft. Choose titanium alloy cannulated screws of suitable length or absorbable screws to fix fracture fragment (Fig. 14.6). Driving screws into bone alone Kirschner wire, for increase adhesive ability of screws, screws must bite contralateral

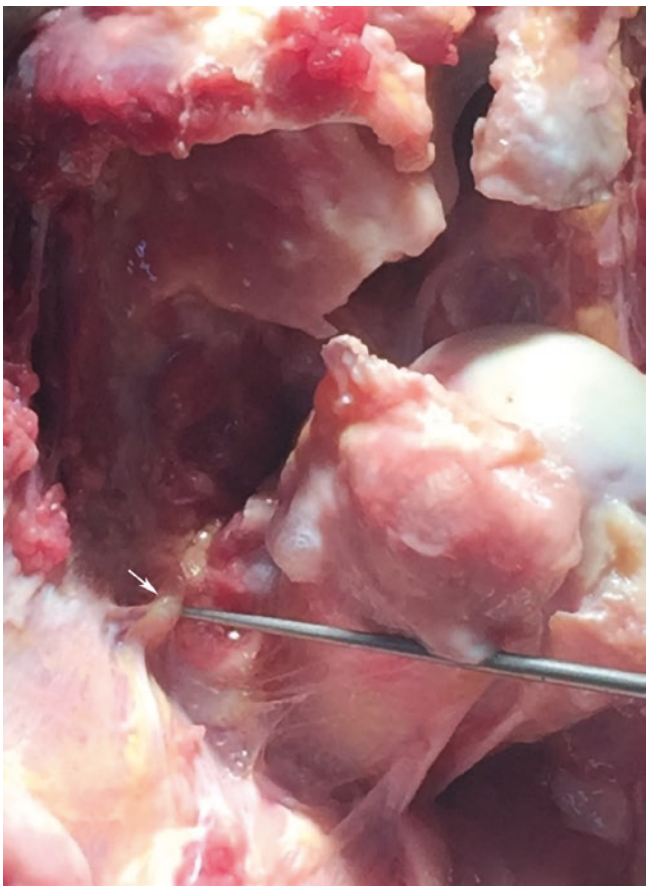

Fig. 14.4 Notice not to injure the axillary nerve, which pass under the acromion 4–5 cm

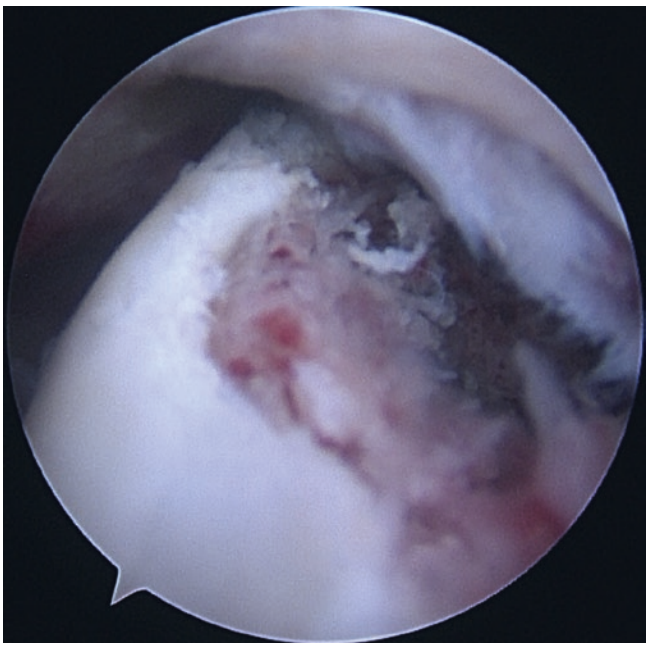

Fig. 14.5 Poking reduction of the fracture fragment was watched by arthroscopy

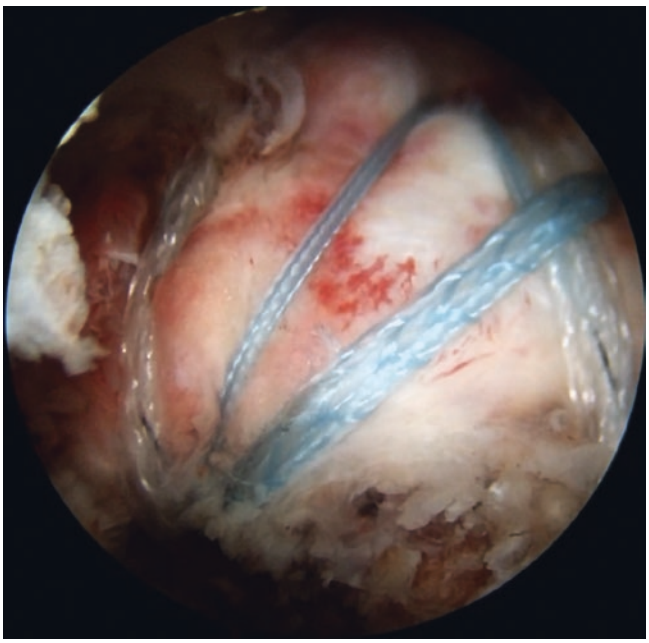

Fig. 14.7 Suture across the rotator cuff tissue, fixing the rotator cuff and fracture fragment in network

Fig. 14.6 Choose titanium alloy cannulated screws of suitable length to fix fracture fragment

cortex of bone and guide pin and screws avoid injure articular cartilage and glenoid labrum tissue.

14.2.2 Suture Anchor Fixation of Greater Tuberosity Fracture

After the reduction of fracture fragment, crossing the Kirschner wire into fracture fragment for temporary fixation, driving a suture anchor into the normal bone structure of greater tubercles of the humerus, suture across the rotator cuff tissue, fixing the rotator cuff and fracture fragment in network (Fig. 14.7) and fixing the other end of the suture with outside suture anchor (Fig. 14.8). Check and confirm the anatomical reduction of fracture fragment, fixed rigidly, and then remove the arthroscope and instruments. After operation, use sling or brace to immobilize upper limb according to the situation. Radiography shows well reduction of fracture postoperatively (Fig. 14.9).

14.3 Postoperative Treatment

Routine affected limb suspension and immobilization 4 ~ 6 weeks after operation; during this period, patients can do shoulder joint abduction, lift, bend, and rotation passively. Do suspension pendulum motion at 7 ~ 10 days after operation, lift affected limb 30° ~ 45° passively. Patients should avoid shoulder joint abduction and lift forwardly within 6 weeks [1, 2, 8].

14.4 Critical Points

1. Intra-articular fracture must anatomical reduction, in order to avoid greater tuberosity fracture fragment moving and impact the acromion.
2. During prying reduction and fixation, avoid separating the fracture fragment and rotator cuff tissue.

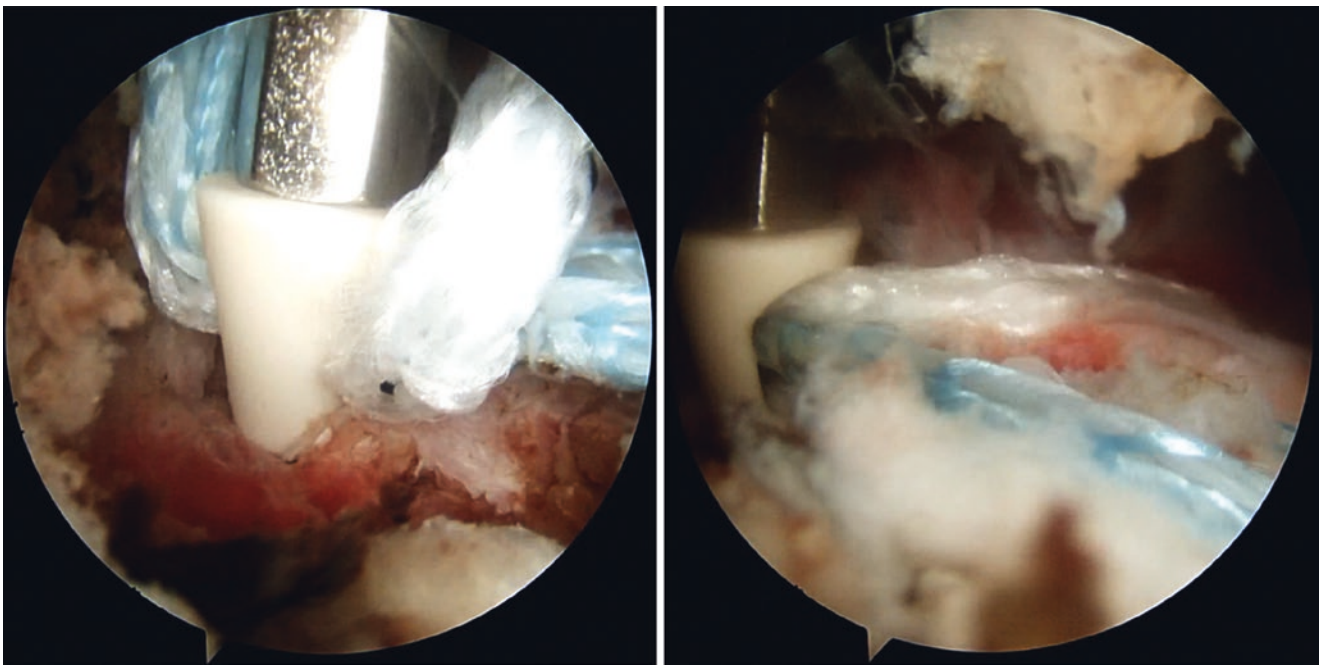

Fig. 14.8 Fixing the other end of the suture with outside suture anchor

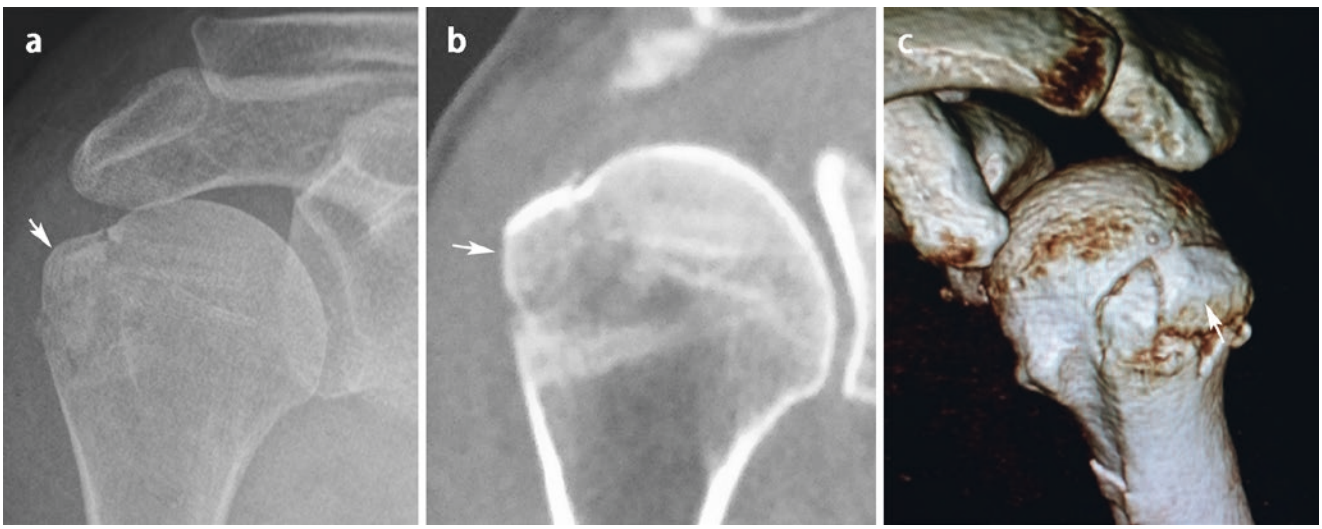

Fig. 14.9 X-ray (**a**) and CT (**b**, **c**) images show the fracture reduction as well

3. Anchor fixation should keep away from osteoporosis zone, in order to avoid pulling the anchor out.
4. It should prevent from anchor penetrating the articular surface of the humeral head, in order to avoid injure the bone cartilage.
5. During the implantation of outside anchor, you should avoid injure axillary nerve.

References

1. Ji JH, Kim WY, Ra KH. Arthroscopic double-row suture anchor fixation of minimally displaced greater tuberosity fractures. Arthroscopy. 2007;23(10):1133.el–4.
2. Song HS, Williams GR Jr. Arthroscopic reduction and fixation with suture-bridge technique for displaced or comminuted greater tuberosity fractures. Arthroscopy. 2008;24(8):956–60.

3. Carrera EF, Matsumoto MH, et al. Fixation of greater tuberosity fractures. Arthroscopy. 2004;20(8):109–11.
4. Bhatia DN, de Beer JF, et al. The bony partial articular surface tendon avulsion lesion: an arthroscopic technique for fixation of the partially avulsed greater tuberosity fracture. Arthroscopy. 2007;23(7):786.el–6.
5. Bahrs C, Lingenfelter E, Fischer F, et al. Mechanism of injury and morphology of the greater tuberosity fracture. J Shoulder Elb Surg. 2006;15(2):140–7.
6. Meier SW, Meier JD. The effect of double-row fixation on initial repair strength in rotator cuff repair: a biomechanical study. Arthroscopy. 2006;22(11):1168–73.
7. Platzer P, Thalhammer G, Oberleitner G, et al. Displaced fractures of the greater tuberosity: a comparison of operative and nonoperative treatment. J Trauma. 2008;65(4):843–8.
8. Ji J-H, et al. Arthroscopic fixation technique for comminuted, displaced greater tuberosity fracture. Arthroscopy. 2010;26(5):600–9.

Arthroscopic Reduction and Fixation of Bony Bankart Lesions

15

Yu-jie Liu and Chang-ming Huang

15.1 Introduction

Anterior and inferior dislocation of the shoulder joint (Fig. 15.1) often occur in training wound and sport injury, and it is often combined with glenoid cavity fracture also called bone bankart injury. This kind of injury accounts for 5.4 ~ 70% of traumatic instability of the glenohumeral joint [1–4]. It has a strong impact on the stability of shoulder joint.

15.2 Imaging Examinations

Due to the cover of the humeral head, it is difficult to find the fracture in front of the glenoid from X-ray. Three-dimensional CT reconstruction of the shoulder joint (Fig. 15.2) is useful to determine the degree of glenoid labrum coloboma of the shoulder joint, and MRI (Fig. 15.3) is useful to diagnose the degree of compression bone defect of the humeral head and rotator cuff injury [5].

15.3 Operative Technique

15.3.1 Anesthetic Position and Portal

General anesthesia, the beach chair position (Fig. 15.4) or the lateral position (Fig. 15.5), traction weight 3–5 kg. The posterior portal (Fig. 15.6) incision is made 1.5 cm medial and 1.5 cm distal to the posterolateral corner of the acromion, slightly lateral to the soft spot [6].

Fig. 15.1 Anterior dislocation of the shoulder joint

15.3.2 Investigation of the Shoulder Joint

Investigate the anatomical structure of the rotator cuff and glenohumeral joint, to observe whether there were Hill-Sachs injury (Fig. 15.7), Bankart injury (Fig. 15.8) of the glenoid cavity, and SLAP (Fig. 15.9) above the back of the humeral head under arthroscopy. The anterior superior and anterior inferior portals were established under arthroscopic direct visualization. The anterior superior portal will be used to the observation of labrum complex injury, fracture fragment displacement, bankart injury soft tissue release, bone reduction, and anchor implantation (Fig. 15.10).

Y.-j. Liu (✉)
Department of Orthopedics, Chinese PLA General Hospital, Beijing, China

C.-m. Huang
Department of Orthopedics, The 73 Group Army Hospital, Chenggong Hospital Affiliated to Xiamen University, Xiamen, China

Y.-j. Liu et al. (eds.), *Advanced Application of Arthroscopy*, https://doi.org/10.1007/978-981-15-4684-6_15

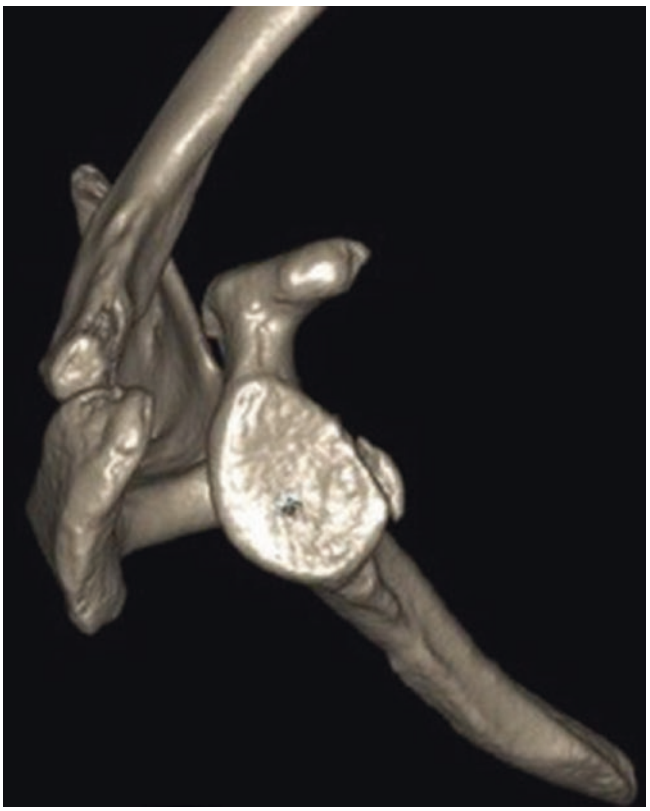

Fig. 15.2 Anterior bony bankart lesions of the shoulder

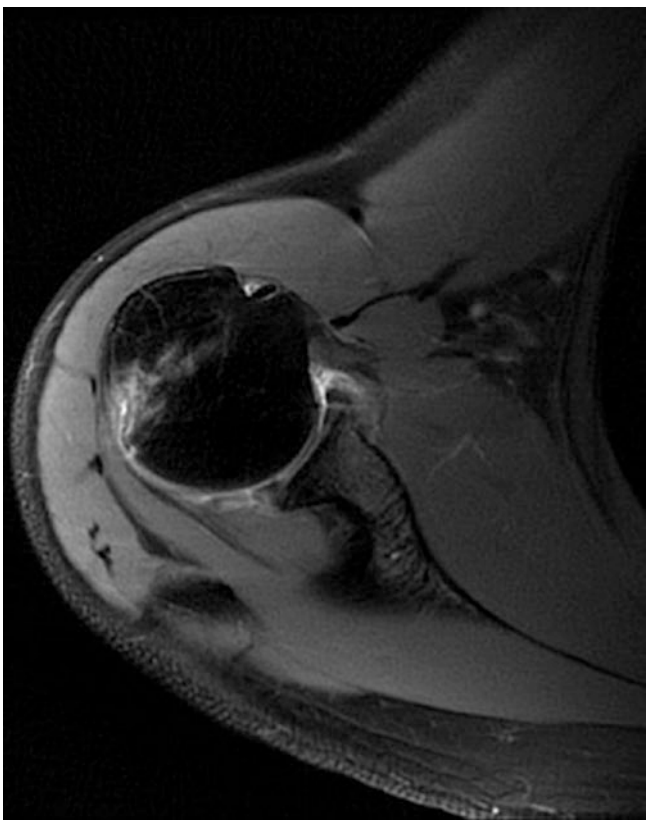

Fig. 15.3 Anterior bankart of the shoulder and humeral head injury

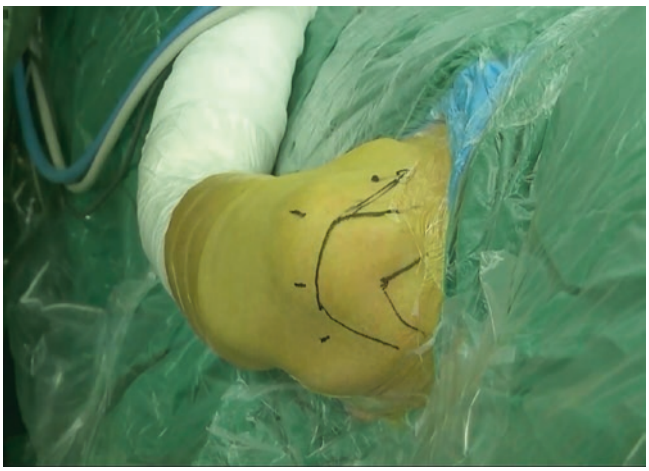

Fig. 15.4 The beach chair position

Fig. 15.5 The shoulder joint is maintain abduction 30–45° and traction, with an axillary roll under arm

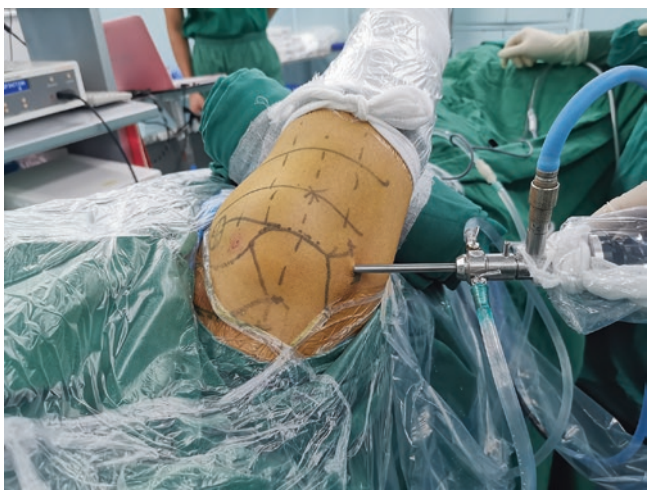

Fig. 15.6 The posterior portal incision is made 1.5 cm medial and 1.5 cm distal to the posterolateral corner of the acromion, slightly lateral to the soft spot

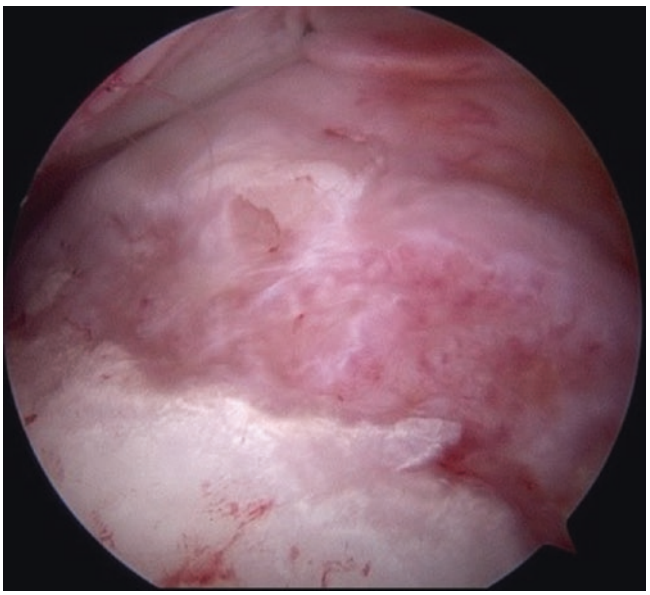

Fig. 15.7 Hill-Sachs injury

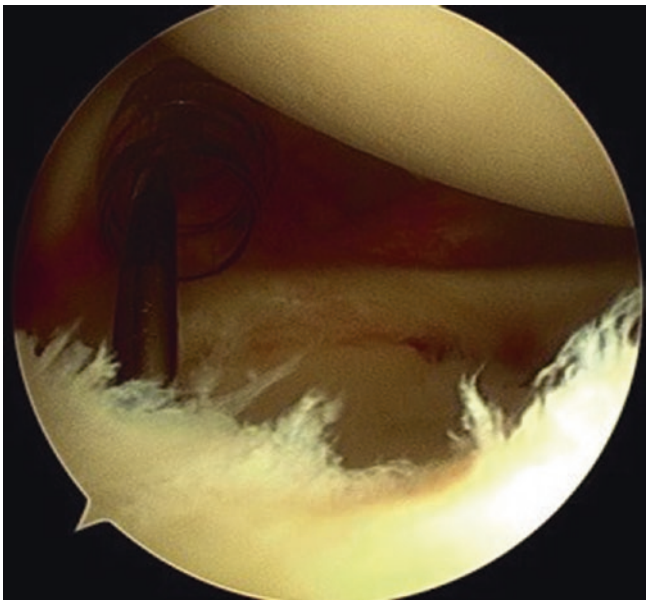

Fig. 15.9 SLAP lesions

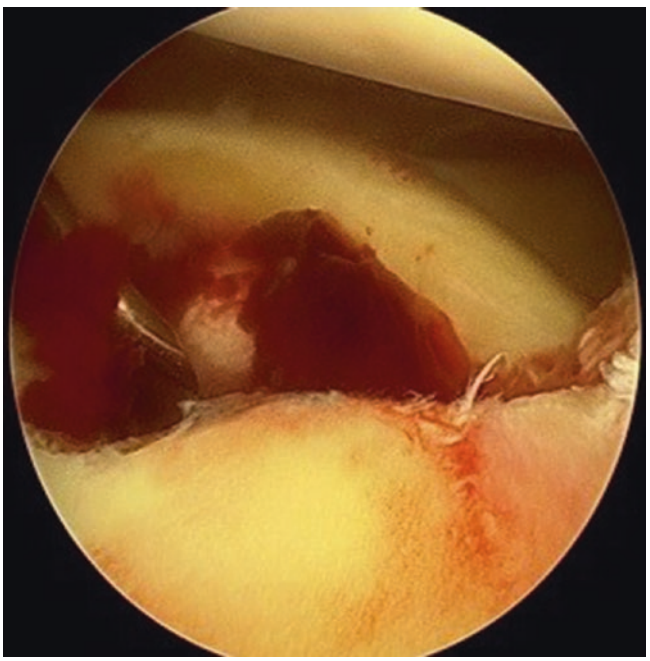

Fig. 15.8 Bony bankart lesions, fracture fragment displacement

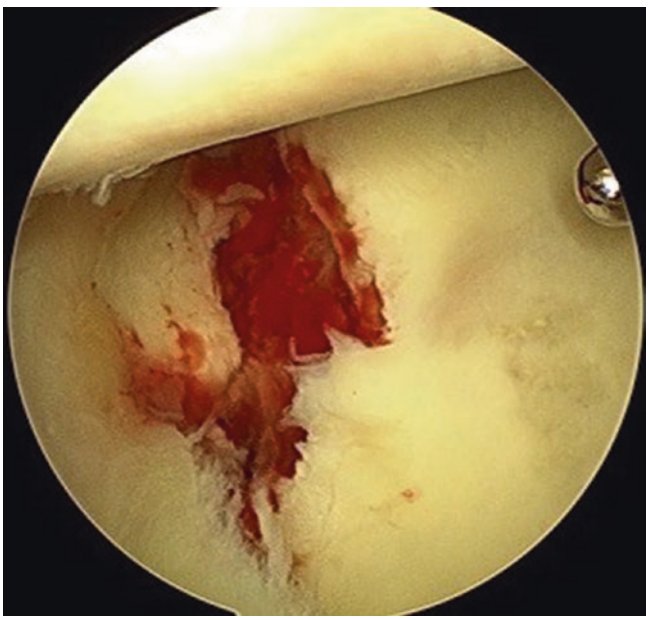

Fig. 15.10 Anterior superior portal was used to observe the bankart injury

15.3.3 Reconstruct Bony Bankart Lesions

If the bankart injury is combined with the posterior instability and Hill-Sachs injury, you should repair the posterior instability and Hill-Sachs injury first, drilling into the suture anchor, and then handle the anterior bony bankart injury.

For the suture repair of labrum of bone bankart injury, the repair plan should be evaluated and designed according to the conditions of labrum injury and fracture and the occupational conditions of the patients. General fracture block of glenoid shoulder <25% feasible suture of labrum to repair bankart injury; if the bone defect of the glenoid shoulder is >25%, Bristow-Latarjet surgery is required [7–9].

The scar tissue was first cleaned and then soft tissue released (Fig. 15.11), and the cartilage at the edge of the glenoid was removed for 3–4 mm, so as to make the fracture wound fresh and conducive to healing. Anchors were drilled into the the edge of the glenoid, and the avulsion bone was generally fixed from the bottom up. The suture under the

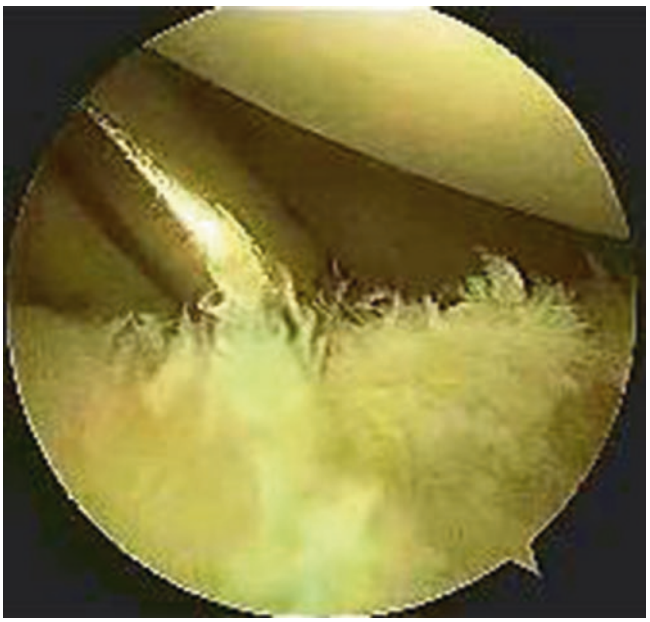

Fig. 15.11 Bankart injury scar tissue is cleaned and released

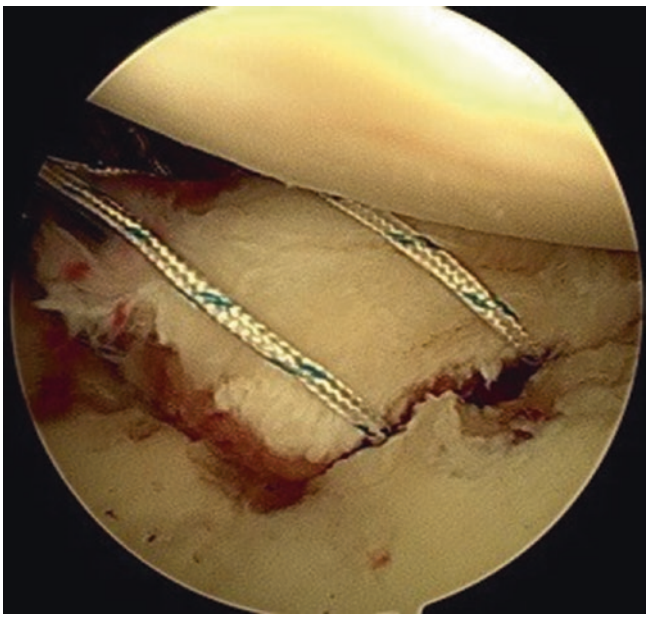

Fig. 15.13 Suture was introduced to wrap the fracture block

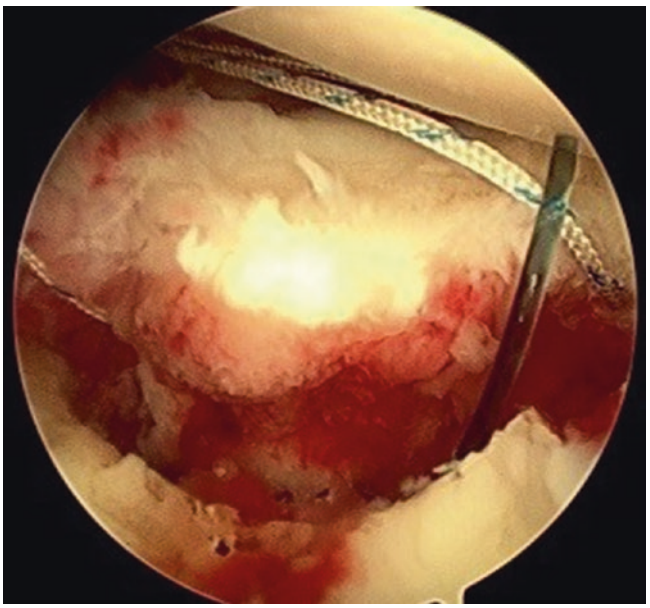

Fig. 15.12 The suture hook passes around the fracture block to release a PDS line

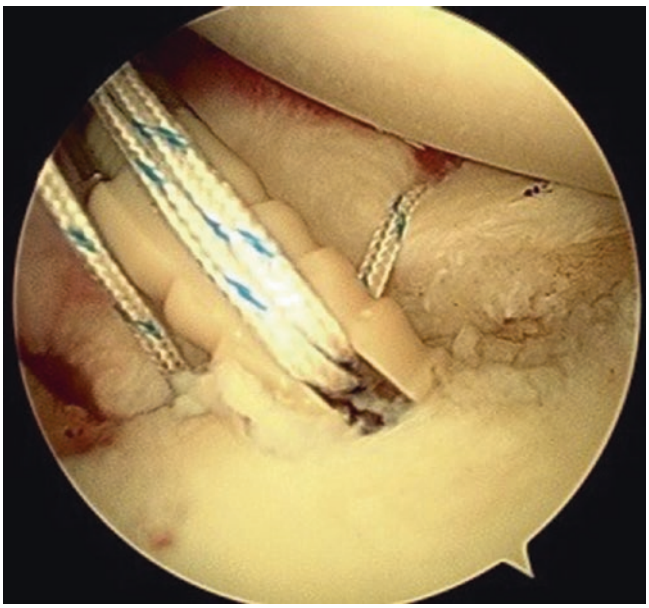

Fig. 15.14 Unknotted anchors fix the suture

bone passed through or bypassed the bone and soft tissue for knotting and fixation. The sequence of fixation is that the first anchor should be place at the lower edge of the fracture block, the second anchor is place at the middle of the fracture block, and the third anchor is place the upper edge of the fracture block.

The second anchor can be used as a suture hook to bypass the fracture block (Fig. 15.12), pass a PDS thread through the suture, tie a knot around the bone, and fix it (Fig. 15.13). You can also use unknotted anchors to fix the suture (Fig. 15.14). Finally, the posterior portal (Fig. 15.15) and the anterior superior portal (Fig. 15.16) were used to check whether the suture fixation of the fracture block was firm. If the fracture block is too large for the suture hook to bypass the fracture block, the suture hook can be threaded through the bone block or through the drilled bone block pierced with a Kirschner, which we also can perform from the posterolat-

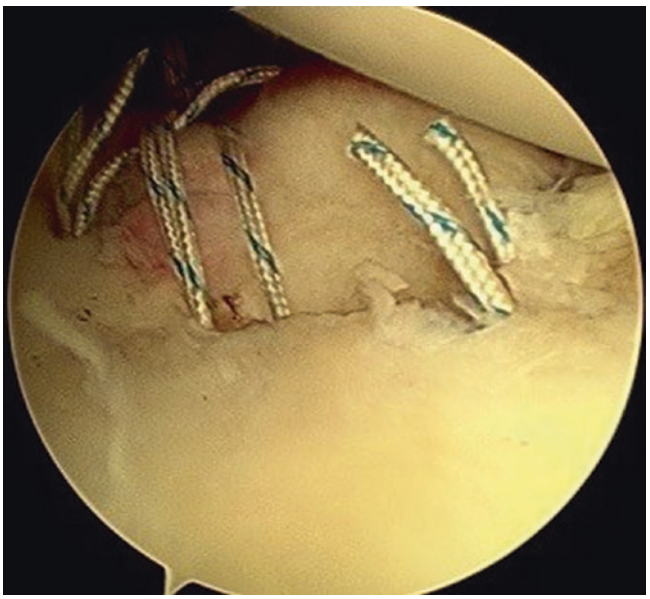

Fig. 15.15 After the reduction and fixation of bony bankart lesions

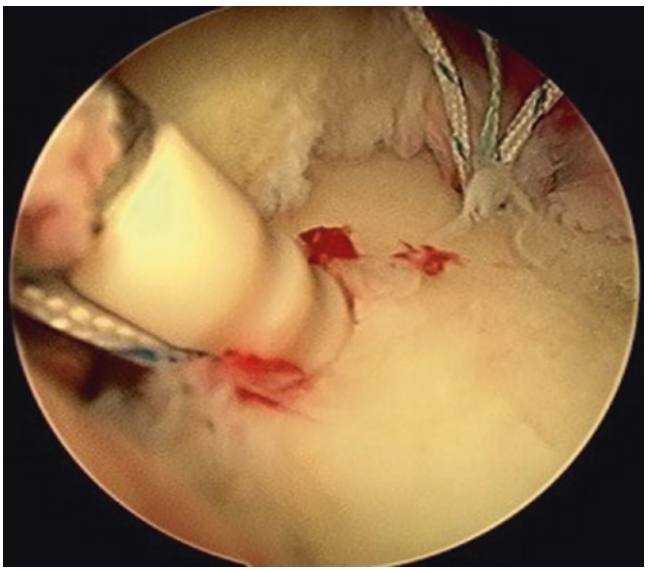

Fig. 15.17 Suture on bankart injury combined with SLAP

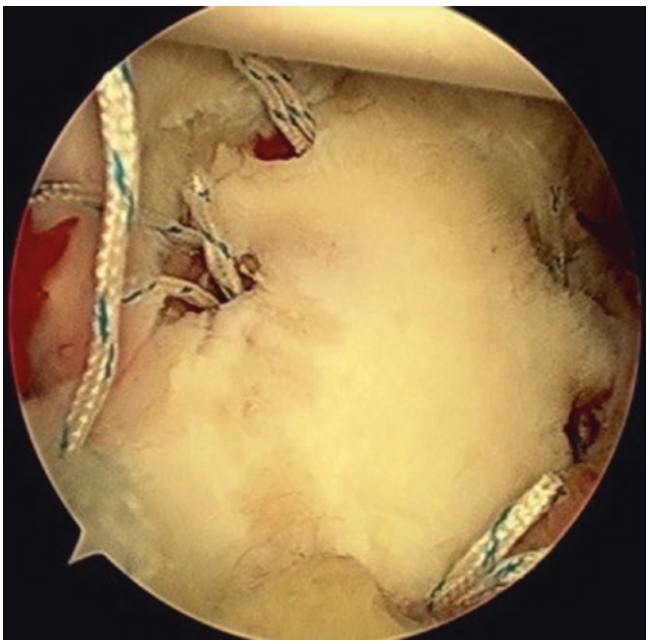

Fig. 15.16 Use the anterior superior portal to observe the condition after repair the shoulder joint anterior and posterior instability

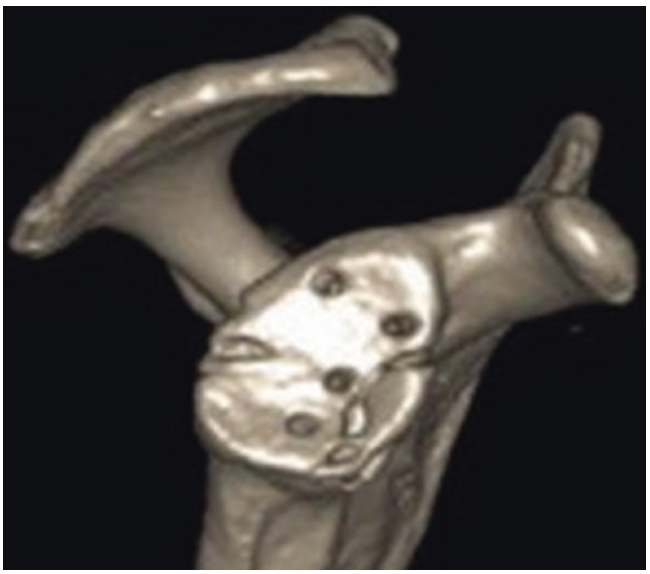

Fig. 15.18 Three-dimensional CT shows the anchor position and fracture reduction

eral portal. The type and number of anchors implanted should be determined according to the condition of the fracture block. Generally, moderate injuries require 3–4 anchors. We can choose single row or double row seam according to the situation. It must be careful, because there are important vascular and nerve structures in front of the scapula. If there is a SLAP injury, it can be repaired at the same time (Fig. 15.17).

15.4 Postoperative Treatment

After surgery, three-dimensional CT should be routinely reexamined (Fig. 15.18) to determine the position of the anchor and the reduction of the fracture block (Fig. 15.19).

Postoperative functional training was conducted according to the rehabilitation exercise procedure; correct rehabilitation training is helpful to postoperative recovery of shoulder joint function. Use sling or triangle towel suspend your

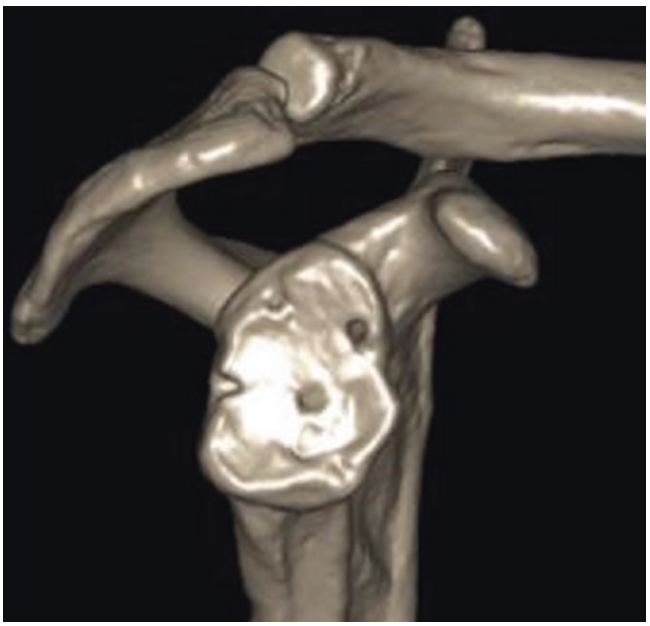

Fig. 15.19 Four years after the operation, three-dimensional CT showed good fracture healing and smooth joint surface

affected limb 4–6 weeks to protect the shoulder. Generally, arm swing exercise was started 1 week after the operation. After 2 weeks, initiate passive or active assisted range-of-motion exercises.

References

1. Porcellini G, Campi F, Paladini P. Arthroscopic approach to acute bony Bankart lesion. Arthroscopy. 2002;18(7):764–9.
2. Mologne TS, Provencher MT, Menzel KA, Vachon TA, Dewing CB. Arthroscopic stabilization in patients with inverted pear glenoid: results in patients with bone loss of the anterior glenoid. Am J Sports Med. 2007;35(8):1276–83.
3. Millett PJ, Horan MP, Martetschlager F. The "bony Bankart bridge" technique for restoration of anterior shoulder stability. Am J Sports Med. 2013;41(3):608–14.
4. Cameron SE. Arthroscopic reduction and internal fixation of an anterior glenoid fracture. Arthroscopy. 1998;14(7):743–6.
5. Bigliani LU, Newton PM, Steinmann SP, Connor PM, McLlveen SJ. Glenoid rim lesions associated with recurrent anterior dislocation of the shoulder. Am J Sports Med. 1998;26(1):41–5.
6. Kim YK, Cho SH, Son WS, Moon SH. Arthroscopic repair of small and medium-sized bony Bankart lesions. Am J Sports Med. 2014;42(1):86–94.
7. Sugaya H, Moriishi J, Kanisawa I, Tsuchiya A. Arthroscopic osseous Bankart repair for chronic recurrent traumatic anterior glenohumeral instability: surgical technique. J Bone Joint Surg Am. 2006;88(Suppl 1, Pt 2):159–69.
8. Sugaya H, Moriishi J, Kanisawa I, Tsuchiya A. Arthroscopic osseous Bankart repair for chronic recurrent traumatic anterior glenohumeral instability. J Bone Joint Surg Am. 2005;87:1752–60.
9. Boileau P, Villalba M, Hery JY, et al. Risk factors for recurrence of shoulder instability after arthroscopic Bankart repair. Arthroscopy. 2006;88:1755–63.

Treatment of Fracture of Radial Head with Arthroscopic Prying Reduction and Fixation

16

Yu-jie Liu and Chang-ming Huang

16.1 Introduction

The fracture of the radial head is mainly caused by indirect violence. When falling, pronation of forearm, straightening of elbow joint, palms on the ground, excessive valgus of the elbow, vertical transmission of violence to the radial head and the humeral head, resulting in radial head or neck fracture [1–3] (Fig. 16.1).

Fracture closed reduction difficult and maintain the anatomic position of radial head with external fixation. It is difficult, so most of us choose open reduction or radial head resection. Under arthroscopy, fracture can be visualized. The clinical effect is good through prying reduction and internal fixation. Some fractures are difficult to reduction and fixation, and open surgery is needed [4–9].

16.2 Clinical Feature

16.2.1 Imaging Examinations

X-ray shows a fracture of the radial head with a cap at an angle (Fig. 16.2), radial head split fracture (Fig. 16.3), or displacement of fracture block outward and downward (Fig. 16.4).

16.2.2 Fracture Classification

In 1954, Mason classifies radial head fractures into four types according to the severity and displacement of the fracture (Fig. 16.5):

Fig. 16.1 Mechanism of fracture is vertical conduction of hand support, impact of humeral head and radial head

- Type I: Minor or marginal fracture, no displacement or slight displacement, fracture line through the edge of radial head or split, or the fracture line passes through the articular surface obliquely.
- Type II: Marginal fracture, displacement, and fracture range more than 30%, and small pieces of bone or cartilage may be embedded in the fracture space.
- Type III: Comminuted fracture of the capitulum radialis, the capitulum radialis is often burst and displaced to all sides, and collapse fracture may also occur.
- Type IV: Comminuted fracture of capitulum radialis with dislocation of elbow joint.

Mason suggested non-surgical treatment for type I radial head fracture, and type III fracture requires small head of radius resection because it can easily block the rotation of forearm [6–8, 10, 11].

Y.-j. Liu (✉)
Department of Orthopedics, Chinese PLA General Hospital, Beijing, China

C.-m. Huang
Department of Orthopedics, The 73 Group Army Hospital, Chenggong Hospital Affiliated to Xiamen University, Xiamen, China

Y.-j. Liu et al. (eds.), *Advanced Application of Arthroscopy*, https://doi.org/10.1007/978-981-15-4684-6_16

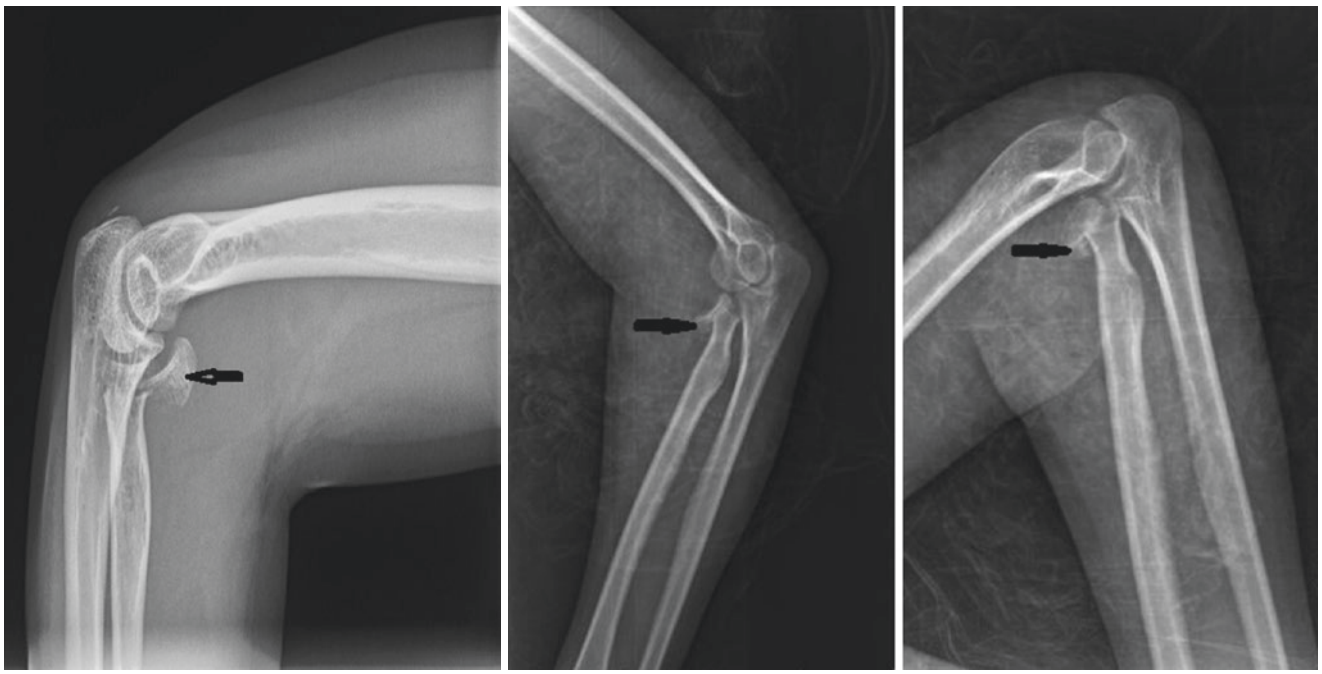

Fig. 16.2 Fracture of the radial head with a cap at an angle

Fig. 16.3 Radial head split fracture

Fig. 16.4 Displacement of fracture block outward and downward

Fig. 16.5 Mason radial head fracture classification

16.3 Operative Technique

16.3.1 Arthroscopic Prying Reduction and Fixation

General anesthesia or nerve block anesthesia. Operative position (Fig. 16.6): lateral or prone position, preoperative marker bone markers of the elbow, the movement of nerve vessels, and the entrance of the arthroscope [12] (Fig. 16.7).

16.3.2 Arthroscopic Approach to Elbow

Radial head, lateral epicondyle of the humerus, and olecranon of ulna constitute an isosceles triangle; the middle is soft. Establish the lateral channel of elbow joint here (Fig. 16.8). The soft access for arthroscopic exploration and operation of elbow.

Using inside-out technology under arthroscopic monitoring, the front inner approach is established by guiding the exchange rod. Arthroscopy in the anterior internal passage, to explore the injury of radial head, capitulum of the humerus, trochlear, coro-

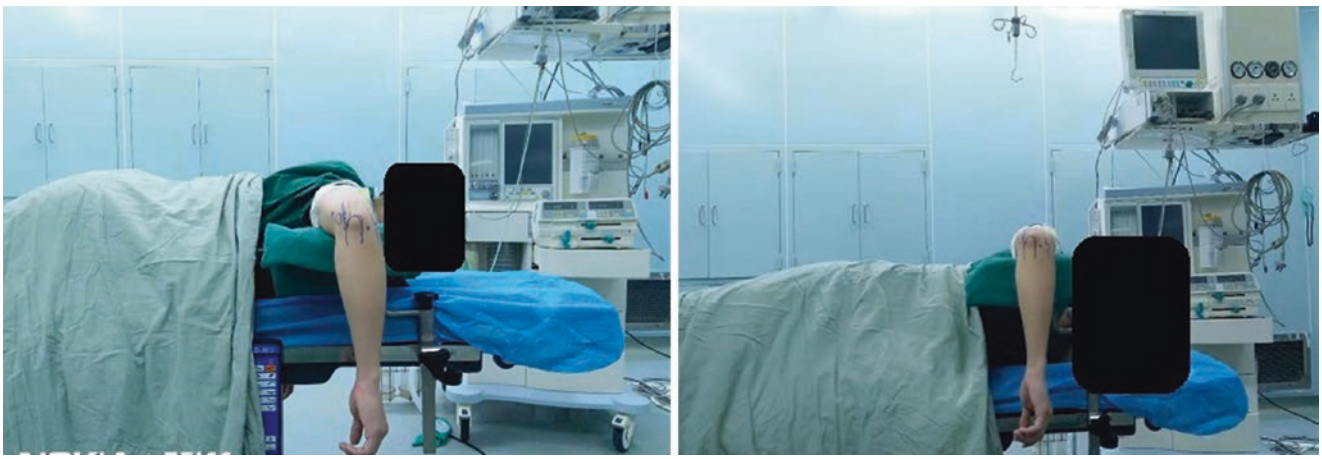

Fig. 16.6 Operation position: lateral position or prone position

Fig. 16.7 Preoperative marker bone markers of the elbow, the movement of nerve vessels, and the entrance of the arthroscope

Fig. 16.8 Lateral epicondyle of the humerus and olecranon of ulna constitute an isosceles triangle; the middle is soft

Fig. 16.9 Observation of radial head and capitulum of the humerus through anteromedial channel

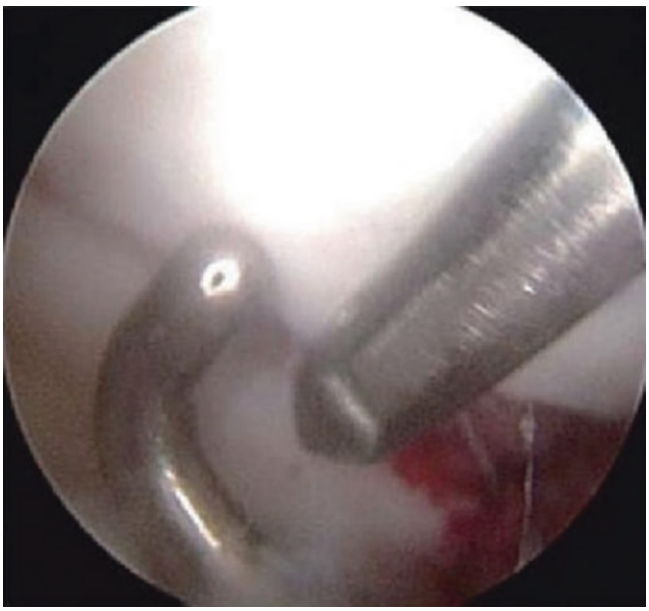

Fig. 16.10 Lateral approach of elbow joint for prying reduction of radial head fracture

noid process, and internal and external joint capsule. Forearm rotation can further observe the radial head fracture and displacement (Fig. 16.9) and monitor the whole operation.

Through the elbow joint lateral soft point approach, the forearm supination position, the use of sledge device to the radial head fracture collapse or displacement of sledge reduction (Fig. 16.10). For the reduction of radial head

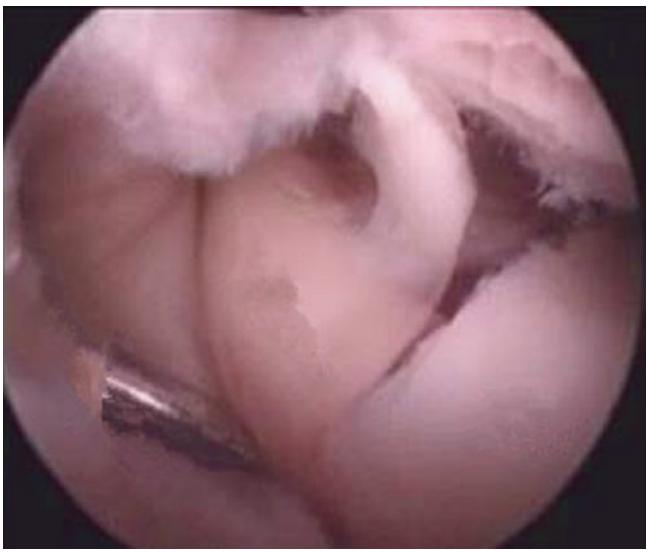

Fig. 16.11 Anatomic reduction of articular cartilage surface of radial head fracture after sledging

fracture, it is important to observe whether the step or collapse after fracture has been corrected and whether the articular cartilage surface has been anatomically reduced (Fig. 16.11).

The vertical fracture line of 1–2 Kirschner wires can be closed and drilled into the bone cortex of the opposite side through the anterolateral approach (Fig. 16.12). It is not recommended to use steel plate and screw fixation; otherwise it will affect elbow joint movement (Fig. 16.13). After fixation, arthroscopy was used to explore the reduction of fracture, wash the bone debris in joint cavity, and take X-ray films of elbow joint (Fig. 16.14), After the operation, fixed in the functional position with a brace or plaster, rechecked every 1–2 weeks and conducted functional training guidance (Fig. 16.15).

16.4 Critical Points

Pay attention to the protection of the annular ligament and the radial nerve muscle branch in the treatment of radial head fracture.

If the comminuted fracture of the radial head cannot be anatomically reduced, the replacement or resection of the radial head is feasible. It is not recommended to fix it with steel plate and screw.

After the operation, the elbow was bent 90 ° and protected by a neutral brace or plaster, and the functional exercises were reviewed and guided regularly every week to prevent the long-term fixation after the operation and avoid the elbow joint stiffness.

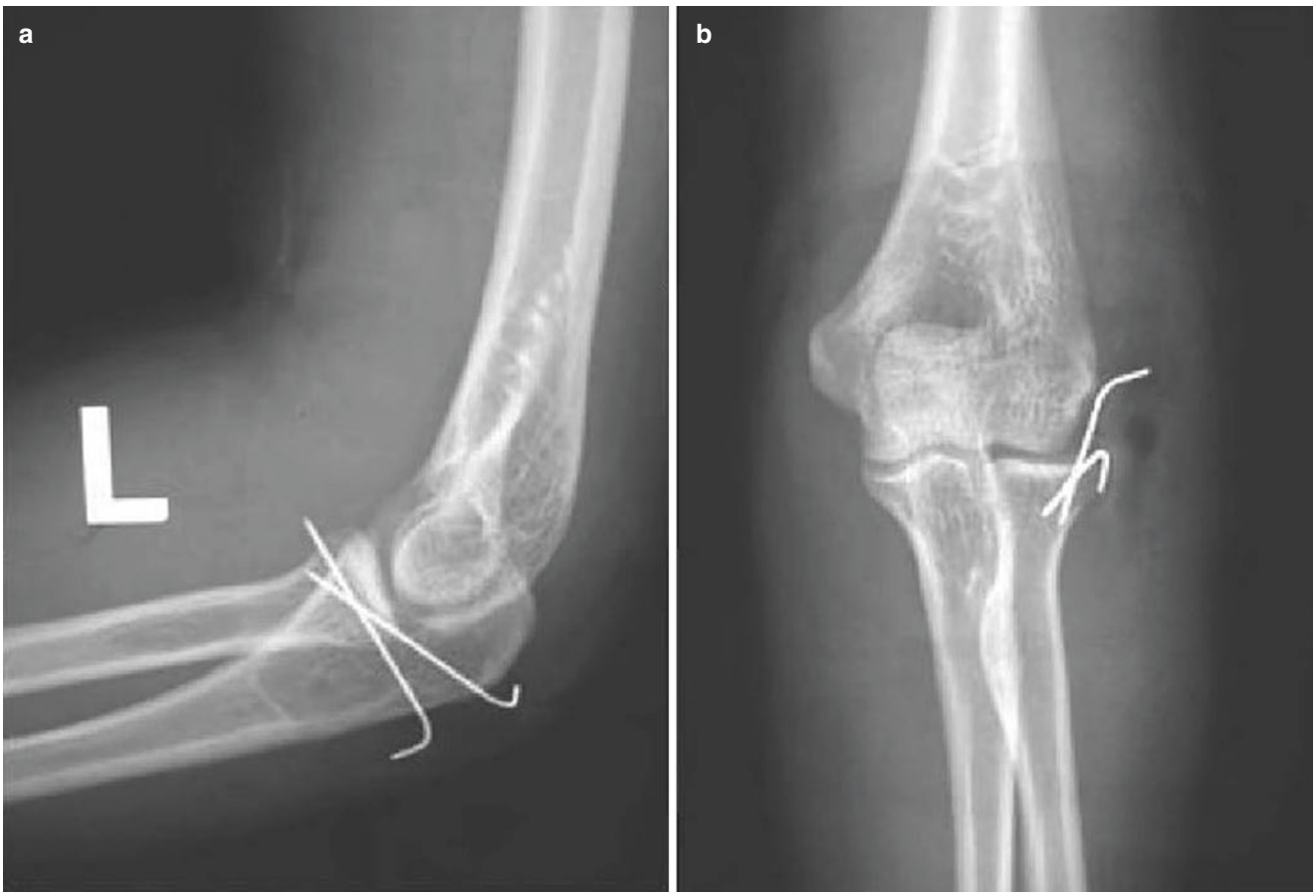

Fig. 16.12 X-ray in anteroposterior (**a**) and side position (**b**) of elbow joint shows vertical fracture line fixation of 2 Kirschner wires by anterolateral approach

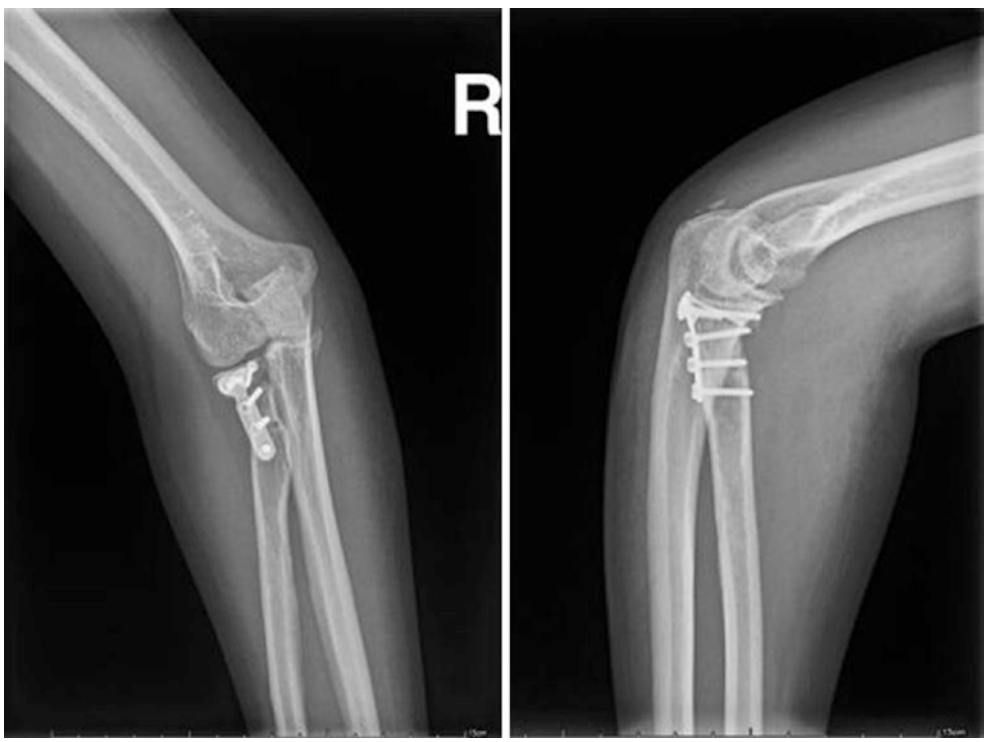

Fig. 16.13 Limited elbow joint selection after plate and screw fixation

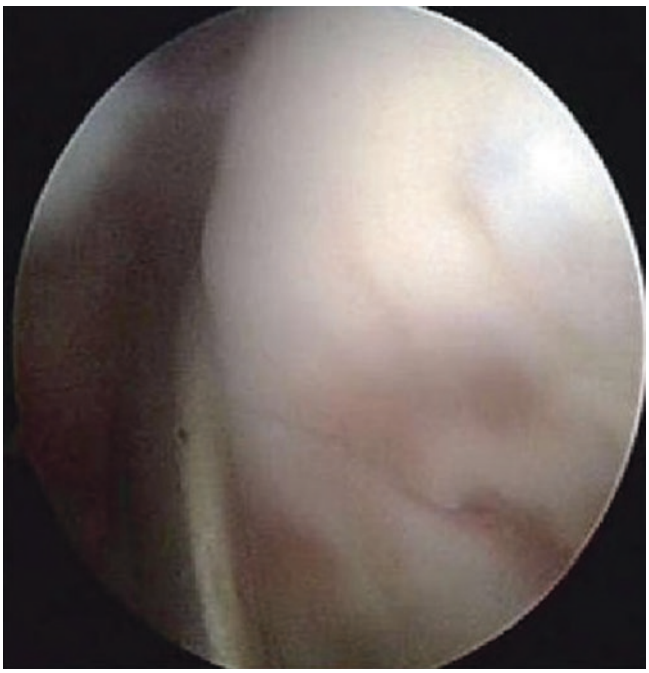

Fig. 16.14 Anatomical reduction of radial head fracture after arthroscopic prying reduction

Fig. 16.15 After the operation, the patients were instructed in functional exercises, and their activities returned to normal

References

1. Dodson C, Williams RJ NS 3rd, et al. Elbow arthroscopy. J Am Acad Orthop Surg. 2008;16(10):574–85.
2. Haddad N, Chebil M, Mili W, et al. Technique and indications of elbow arthroscopy. A twelve-cases report. Tunis Med. 2009;87(2):120–2.
3. Michels F, Pouliart N, Handelberg F. Arthroscopic management of Mason type 2 cadial head fractures. Knee Surg Sports Traumatol Arthrosc. 2007;15(1):1244–50.
4. Ikeda M, Sugiyama K, Kang C, et al. Comminuted fractures of the radial head, comparison of resection and internal fixation. J Bone Joint Surg (Am). 2005;87(1):76–84.
5. Ertilrer E, Seckin F, Akman S, et al. The results of open reduction and screw or K-wire fixation for isolated type III radial head fractures. Acta Orthop Traumatol Ture. 2010;44(1):20–6.
6. Burkhart KJ, Nowak TE, Appelmann P, et al. Screw fixation of radial head fractures: compression screw versus lag screw-A biomechanical comparison. Injury. 2010;4(10):1015–9.
7. Ozkan Y, Oztrk A, Ozdcmir RM, et al. Open reduction and internal fixation of radial head fractures. Uius Travma Acil Cerrahi Derg. 2009;15(3):249–55.
8. Nalbaotoglu U, Kocaoglu B, Gereli A, et al. Open reduction and internal fixation of Mason type III radial head fractures with and without an associated elbow dislocation. Hand Surg (Am). 2007;32(10):1560–8.
9. Businger A, Ruedi TP, Sommer C. On-table reconstruction of comminuted fractures of the radial head. Injury. 2010;4(6):583–8.
10. Miller MC, Wirtz DC, et al. Replacement of the comminuted radial head fracture by a bipolar radial head prosthesis. Oper Orthop Traumatol. 2011;23(1):37–45.
11. Hotchkiss RN. Displace fractures of the radial head: internal fixation or excision? J Am Acad Orthop Surg. 1997;5:1–10.
12. Atesok K, Doral MN, Whipple T, et al. Arthroscopy-assisted fracture fixation. Knee Surg Sports Traumatol Arthrosc. 2011;19(2):320–9.

Arthroscopic Treatment of Avulsion Fracture of the Tibial Intercondylar Eminence

17

Chun-bao Li and Yu-jie Liu

17.1 Introduction

The tibial intercondylar eminence fracture classification was proposed by Meyers and Mckeeverin 1959, according to the intercondylar eminence fracture displacement (Fig. 17.1): Type I, the tibial intercondylar eminence fracture is no obvious shift, the front of fracture bone is just arise; Type II, the 1/3 or 1/2 before the tibial intercondylar eminence fracture bone is arise, looks like a "beak" in the lateral X ray film. Type IIIA, the whole tibial intercondylar eminence fracture bone is arise from the base and no contact with the tibia; Type IIIB, the whole tibial intercondylar eminence fracture bone is arise from the base and with rotating shift.

17.2 Surgery Treatment of Tibial Intercondylar Eminence Fracture

The deformity healing or non-union rate of tibial intercondylar eminence fracture is 50% to 90% [1]. As the anterior cruciate ligament relaxing relaxation resulting in the instability of the knee joint, deformed healing of the fractures is prone to the impact between intercondylar fossa (Fig. 17.2). McLennan first reported on arthroscopy reduction and fixation for tibial intercondylar eminence fracture in 1982. In the early days, steel wires were often used for fixation. The main problems were the cutting of bones by the wire, wire fracture, or failure of fixation. Screw fixation is mostly used for

Fig. 17.1 Meyers-Mckeever tibial intercondylar eminence fracture classification schematic diagram

C.-b. Li · Y.-j. Liu (✉)
Department of Orthopedics, Chinese PLA General Hospital, Beijing, China

Y.-j. Liu et al. (eds.), *Advanced Application of Arthroscopy*, https://doi.org/10.1007/978-981-15-4684-6_17

the fixation of fracture. However, because of the tibial condyle is cancellous bone, the screw fixation is easy to loosen and pulled out, which cause fixation failure. At present, screw and wire fixing methods have gradually been replaced by other fixing methods. High-strength suture tension band fixation method is used for adolescent tibial intercondylar eminence fracture, which has little damage to the epiphyseal plate. This method can also be used for comminuted fractures and without suture removal [2].

17.3 Neckwear-Knot-Loop-Ligature Fixation Technique

After general anesthesia or epidural anesthesia, the affected knee was bent at the end of the bed by 90 °in supine position. Firstly, cleaned up the blood and bone fragments of the joint under arthroscopy (Fig. 17.3). It is usually found that the anterior meniscus and transverse knee ligament were embedded between the fractures, which affect the fracture reduction (Fig. 17.4). The probe is used to gently pulled them away, then the fracture can be reset by skidding (Fig. 17.5).

The anterior cruciate ligament tibial tunnel locator was used on medial and lateral sides of the anterior cruciate ligament attachment site (Fig. 17.6), and a 2.2 mm diameter guide needle was used to drill the tunnel from both sides of the tibial tubercle for backup (Fig. 17.7). A shoulder suture was used to bypass the ACL and pass at the junction of the ACL and the bone pedicle (Fig. 17.7). Then a No. 5 Ethibond suture which tied a double-strand suture like a tie knot at the junction of ACL and bone (Fig. 17.8) is passed. The two wires were passed from the tibial tunnel on both sides of the fracture block and tighten the suture to tie the two sides of the tibial tubercle. According to the shape of tibial intercondylar eminence fracture, single or double tie ligature can be used for ligature fixation. Generally, single tie ligature is used for large and single fracture (Fig. 17.9); double tie knot fixation technique is used for comminuted fractures (Fig. 17.10).

Arthroscopy was used to investigate the stability of the fracture after the operation, and it was protected by a chuck brace after the operation. Functional training was performed according to the rehabilitation procedure. The X-ray examination of the knee joint shows that the fracture could acquire good healing 3 month after the operation (Fig. 17.11) on average.

Fig. 17.2 Deformed healing of the fractures are prone to the impact between intercondylar fossa

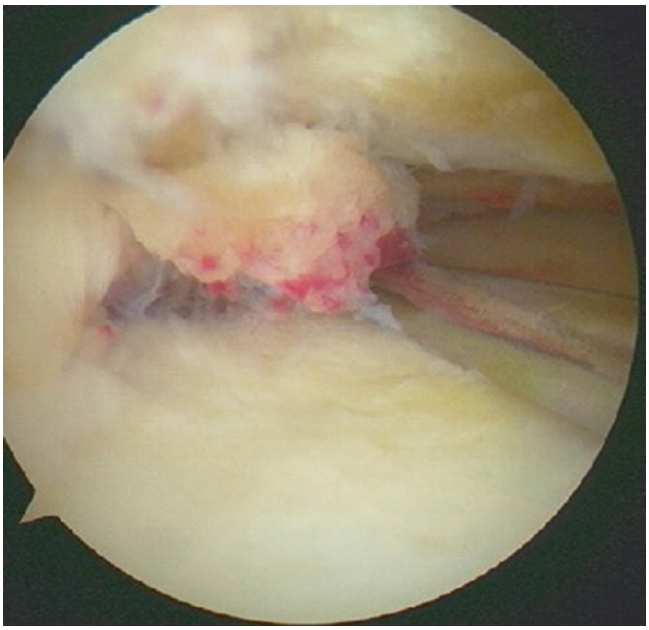

Fig. 17.3 Clean up the blood and bone fragments in the joint

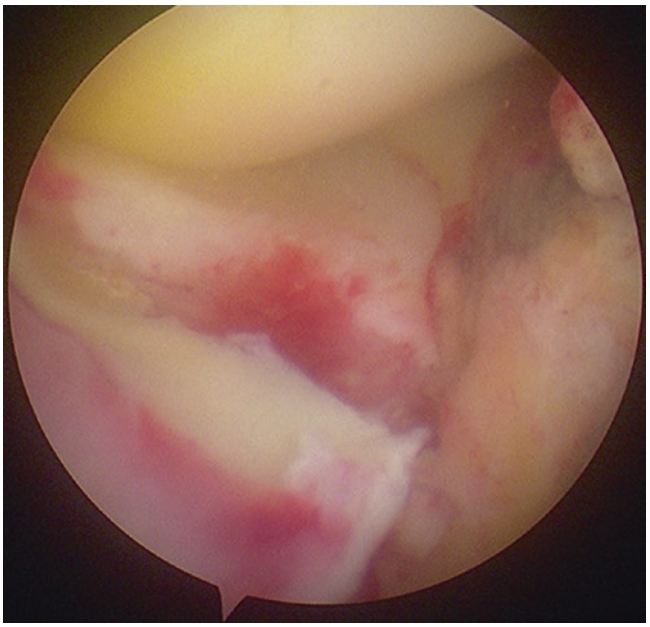

Fig. 17.4 Anterior meniscus and transverse knee ligament embedded in the fracture space, affecting the fracture reduction

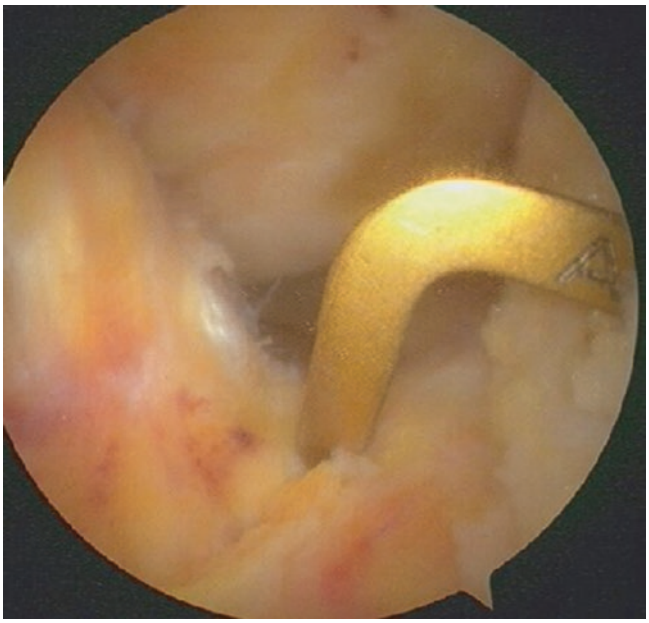

Fig. 17.6 Anterior cruciate ligament tibial tunnel locator pre-drilled tibial tunnel

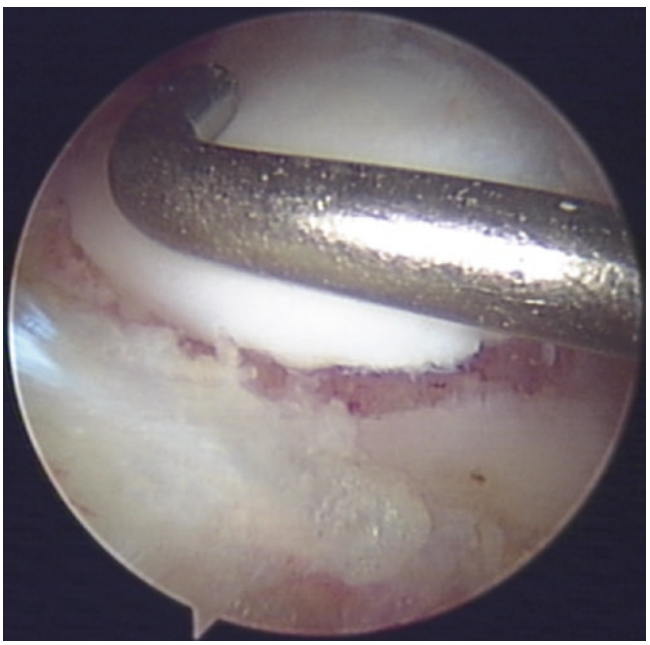

Fig. 17.5 Arthroscopy probe pulled meniscus and transverse knee ligament away, fracture reduction

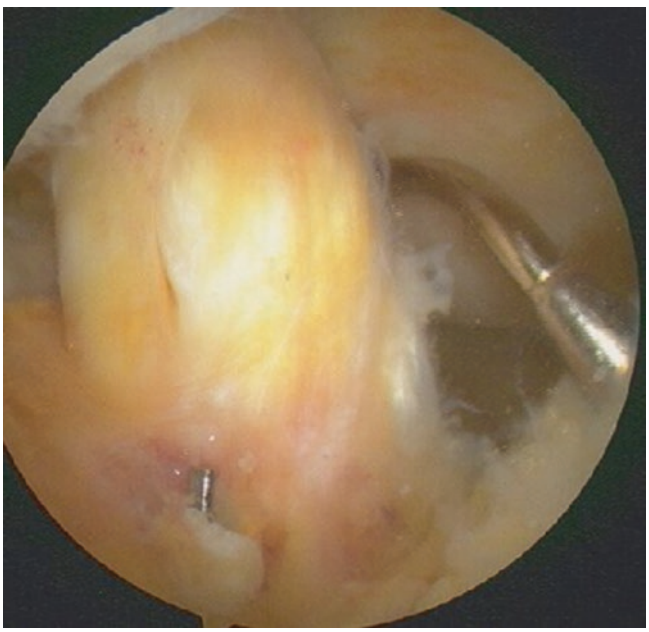

Fig. 17.7 Using a stapler to bypass the ACL

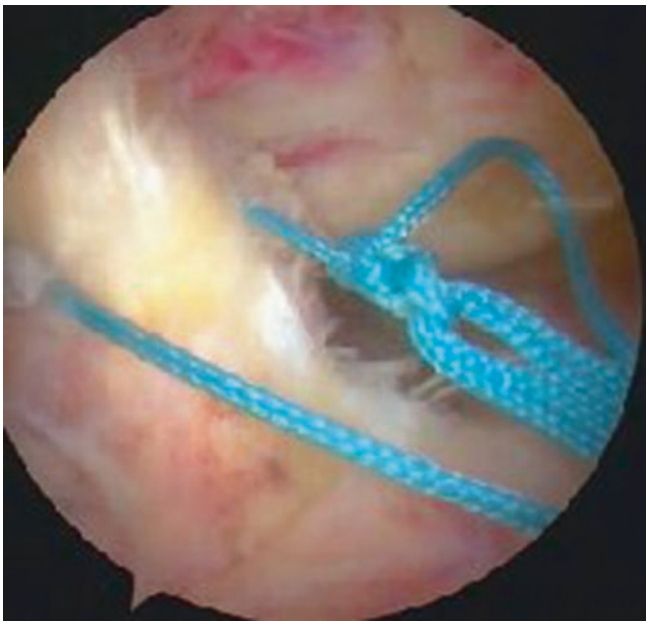

Fig. 17.8 Passing No. 5 Ethibond suture which tied a double-strand suture like a tie knot at the junction of ACL and bone

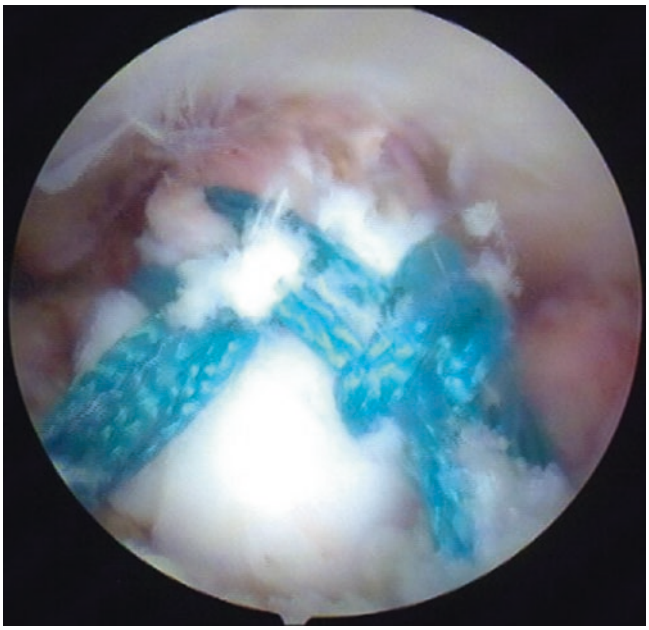

Fig. 17.10 Double tie knot fixation is used for comminuted fracture

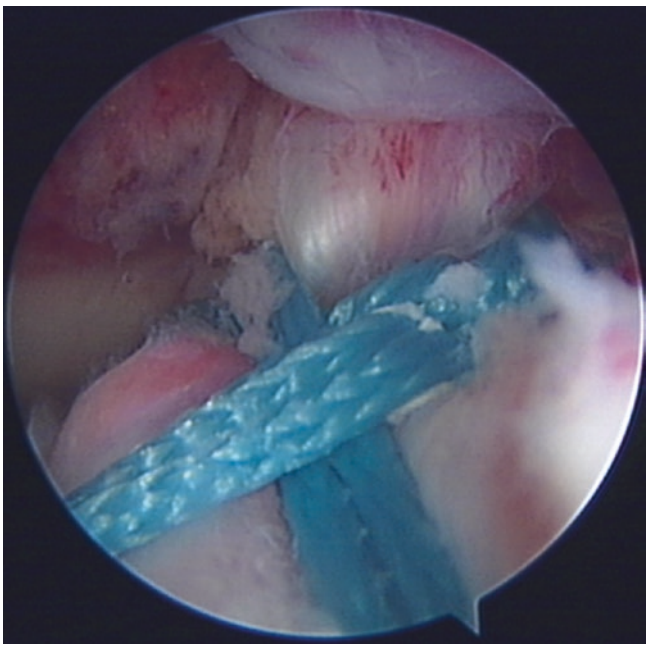

Fig. 17.9 Single tie knot ligature is used for large fractures

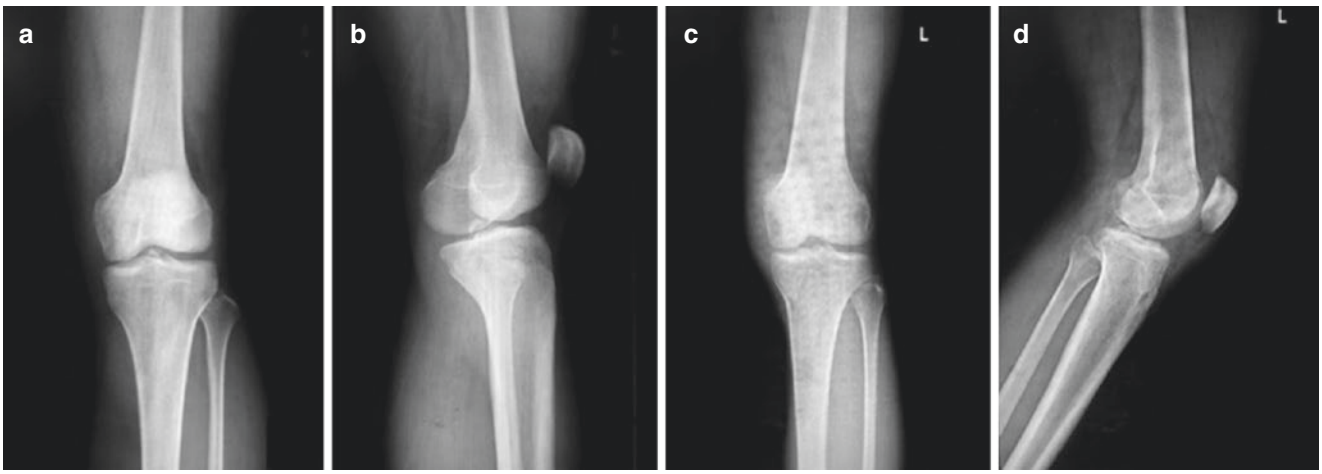

Fig. 17.11 X-ray examination shows good fracture reduction and healing. (**a**) preoperative anteroposterior position X-ray of left knee; (**b**) preoperative lateral position X-ray of left knee; (**c**) anteroposterior position X-ray of left knee 3 months after operation; (**d**) lateral position X-ray of left knee 3 months after operation

References

1. Osti L, Buda M, Soldati F, Del Buono A, Osti R. Arthroscopic treatment of tibial intercondylar eminence fracture: a systematic review of different fixation methods. Maffulli N Br Med Bull. 2016 Jun;118(1):73–90.
2. Liu YJ, Wang JL, et al. Arthroscopic reduction and fixation of tibial intercondylar eminence avulsion fracture using nonabsorbable suture with neckwear knot loop ligature. Zhong Guo Xiu Fu Chong Jian Wai Ke Za Zhi. 2011;25(08):903–6.

Treatment of Tibial Plateau Fractures with Prying Reduction and Fixation Under Arthroscopy

18

Yu-jie Liu and Chang-ming Huang

18.1 Introduction

Tibial plateau fractures often occur in traffic injuries, falling injuries, and sports injuries. It is easy to be complicated with vascular and nerve, ligament injury of knee joint and compartment syndrome; improper treatment seriously affects the function. The literature reported that tibial plateau fractures accounted for about 4% of systemic fractures, combined with anterior cruciate ligament injury (32%) and meniscus injury (47%) [1–6]. Radiographs of anterior and lateral position and oblique position of knee joint are helpful to the diagnosis of tibial plateau fracture (Fig. 18.1). However, it is difficult to judge the condition of fracture collapse, displacement, and articular surface injury. CT scanning with three-dimensional reconstruction can accurately evaluate the compression fracture of the tibial plateau (Fig. 18.2), articular surface collapse, and bone mass displacement (Fig. 18.3). MRI can not only observe the fracture but also accurately judge the soft tissue injury such as meniscus, cruciate ligament, and medial and lateral collateral ligament (Fig. 18.4).

Fig. 18.1 Radiograph shows fracture of tibial plateau

18.2 Schatzker Classification of Tibial Plateau Fractures

Schatzker classification (Fig. 18.5) has important guiding value for the treatment of tibial plateau fractures [7–8].

- Type I tibial plateau fracture: Mostly seen in young patients, it is a wedge-shaped or split fracture of the lateral condyle, and the bone mass is not compressed, usually caused by valgus and axial stress.
- Type II tibial plateau fracture: The injury mechanism is similar to type I. However, the lateral condyle of the tibial plateau is wedge-shaped or split with compression fracture because osteoporosis cannot resist the strong external force.
- Type III tibial plateau fracture: Lateral condyle compression fracture caused by axial stress, located in the lateral tibial plateau.
- Type IV fracture of medial condyle of tibial plateau: Split compression fracture of tibial plateau caused by varus stress position and axial compression force.
- Type V fracture of the medial and lateral tibial plateau: It usually occurs when the split compression fracture of the

Y.-j. Liu (✉)
Department of Orthopedics, Chinese PLA General Hospital, Beijing, China

C.-m. Huang
Department of Orthopedics, The 73 Group Army Hospital, Chenggong Hospital Affiliated to Xiamen University, Xiamen, China

Y.-j. Liu et al. (eds.), *Advanced Application of Arthroscopy*, https://doi.org/10.1007/978-981-15-4684-6_18

Fig. 18.2 CT shows tibial plateau compression fracture

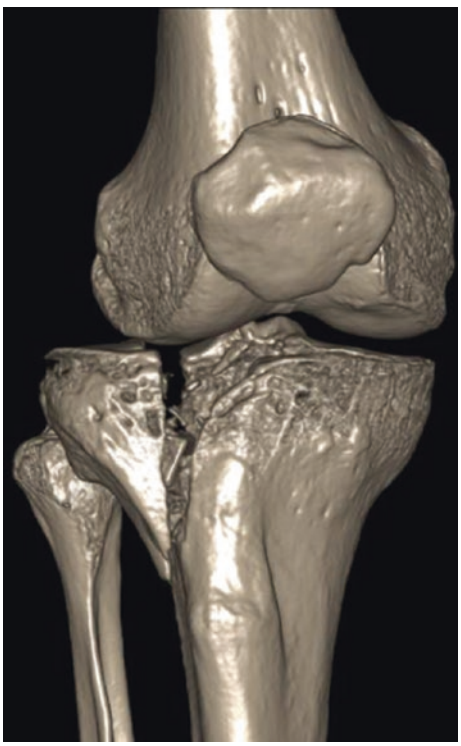

Fig. 18.3 CT shows tibial plateau fracture articular surface collapse

Fig. 18.4 MRI shows tibial plateau fracture with ligament and soft tissue injury

plateau is caused by axial violence in the straightened position of the knee joint.

- Type VI tibial plateau fracture: Compression and insertion of medial and medial condyle caused by high energy combined with violence, and the fracture was separated from the shaft.

18.3 Operative Technique

18.3.1 Arthroscopic Prying Reduction for the Treatment of Tibial Plateau Fracture

The patients were treated with general anesthesia or epidural anesthesia. The patients were taken from supine position; pneumatic tourniquet was put on their thighs and disinfected routinely.

The anterior medial and anterolateral working portals of the knee joint were established to remove the intra-articular hemorrhage. Detect fracture displacement under arthroscopy (Fig. 18.6), detect ligament, meniscus cartilage, and other tissues for injury, and use probe to detect the displacement of articular fracture fragments (Fig. 18.7).

First, closed manipulation, by squeezing the split fracture block forcefully from the side of the tibial plateau, and then

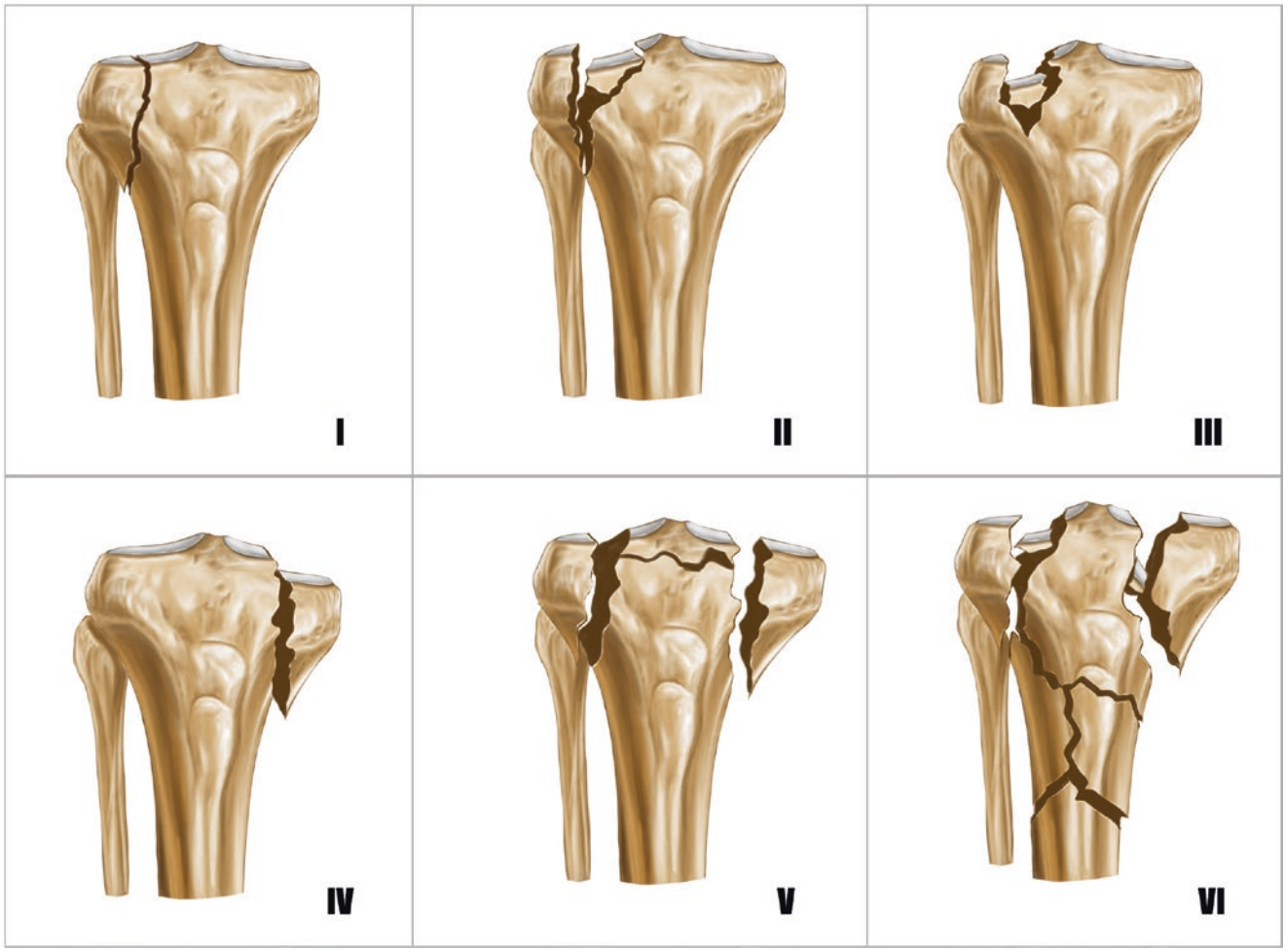

Fig. 18.5 Schatzker classification of tibial plateau fracture

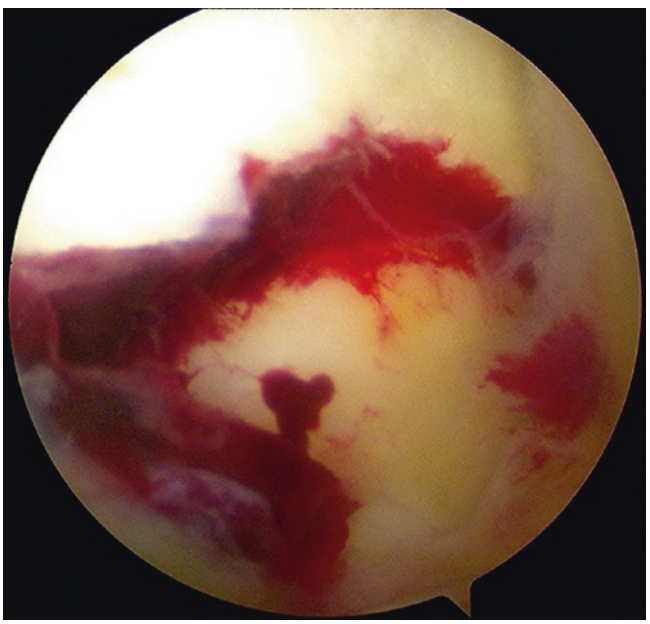

Fig. 18.6 Exploration of articular cartilage surface collapse under arthroscopy

Fig. 18.7 Arthroscopic exploration of tibial plateau fractures. The articular surface is step-off

Fig. 18.8 Fixing with reduction forceps

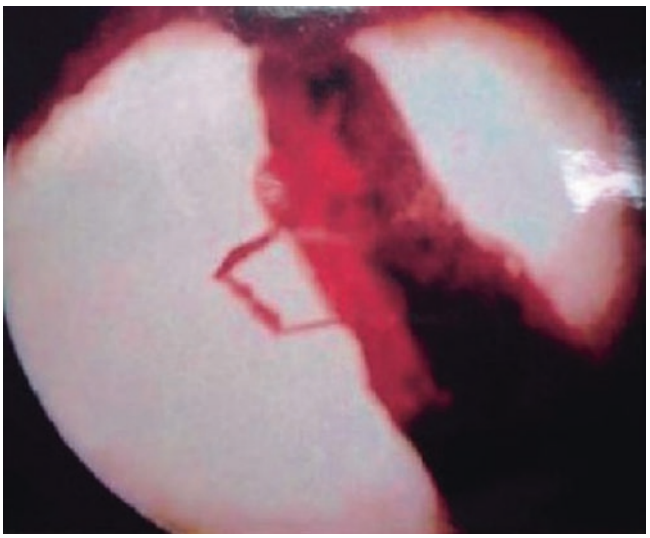

Fig. 18.9 Fracture displacement of tibial plateau under arthroscopy

squeezing and fixing with reduction forceps (Fig. 18.8). The displacement of the subchondral bone and cartilage surface was observed under arthroscopy (Fig. 18.9). At the 2–3 cm under the medial and lateral joint line, one or two Kirschner wires were inserted into the fracture block through the metaphysis, and the top pressure fracture block was pried upward, and after the fracture was anatomically reduced (Fig. 18.10). The cancellous bone tension compression screw is screwed into the 2–3 cm vertical fracture line under the

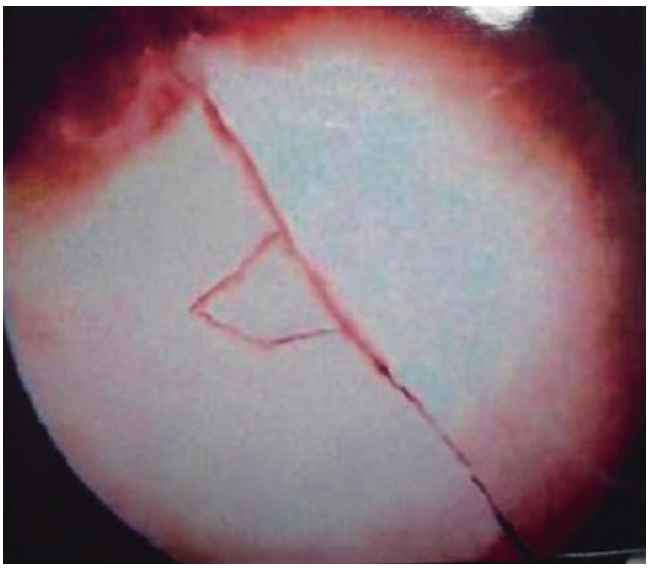

Fig. 18.10 Prying reduction of fracture block to dissection position under arthroscopy

Fig. 18.11 Fixation of fracture block with lag screw

articular surface (Fig. 18.11). The screw bites the contralateral bone cortex firmly and can be fixed with one screw or two screws according to the situation [9].

18.4 Treatment of Schatzker I-IV Type Tibial Plateau Collapse Fracture

The fracture collapse of the tibial plateau was shown by CT (Fig. 18.12). A bone window was opened at the anterior and inferior 3–5 cm of the external articular tibial plateau to align the collapse direction, and the collapsed bone was slowly lifted from the window with a metal rod (Fig. 18.13). The reduction of the collapsed fracture was observed under arthroscopy (Fig. 18.14). The collapsed bone cavity was filled with iliac bone or artificial bone, and then the supporting bone mass was fixed with two to three lag screws.

For Schatzker V-VI type fractures, arthroscopic reduction can be performed (Fig. 18.15). Be careful not to cut open the articular capsule so as not to affect the filling of the articular cavity and endoscopic surgery.

18.4.1 Postoperative Treatment

After operation, arthroscopic irrigation was used to remove free bone fragments, cartilage fragments, and blood clots, so as to reduce postoperative joint adhesion and osteoarthritis. Arthroscopic surgery can understand the specific location and scope of the collapse and displacement of the articular surface, look directly at the reduction of the cartilage of the tibial plateau, find other tissue injuries in the joint in time, and do the corresponding surgical treatment.

Fig. 18.12 CT shows fracture collapse of tibial plateau

Immediately after the operation, the patients were protected by knee brace and cold compress with ice bag. For those who are firmly fixed with supporting plate after reduction, crutches are allowed to move in a non-weight-bearing state, which is beneficial to the recovery of joint function after operation.

Fig. 18.13 Periosteal exfoliator inserted into fracture collapse area prying and crown prying collapse fracture

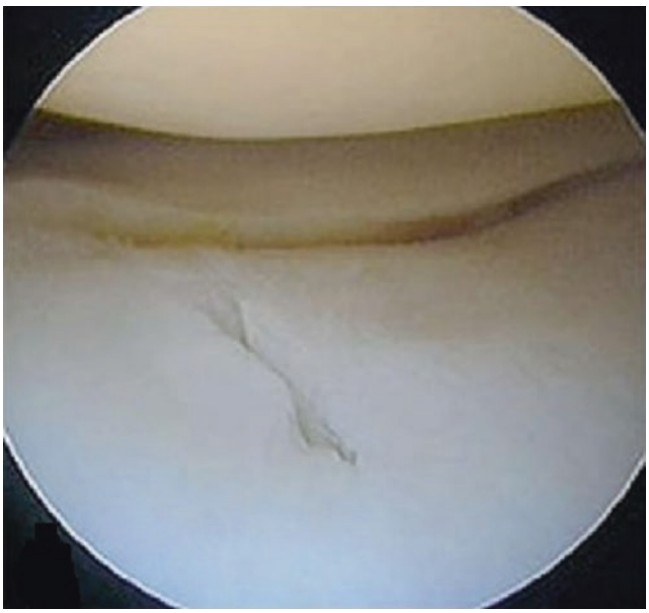

Fig. 18.14 Good reduction of fracture after exploration and prying under arthroscopy

Fig. 18.15 X-ray film after arthroscopic internal fixation of tibial plateau fracture

18.5 Critical Points

1. The perfusion fluid of tibial plateau fracture will infiltrate into the interstitial chamber along the fracture space, which can easily lead to limb swelling. In order to prevent the occurrence of fascial compartment syndrome, put an elastic bandage on the leg.
2. The use of the tibial metaphysis to open the window and press the collapsed fracture block is beneficial to the reduction of the fracture.
3. Before the screw is crossed and fixed, it needs to be explored again by arthroscopy to confirm that the articular surface must be anatomic reduction.

References

1. Abdel-Hamid MZ, Chang CH, et al. Arthroscopic evaluation of soft tissue injuries in Tibial plateau fractures: retrospective analysis of 98 cases. Arthroscopy. 2006;22(6):669–75.
2. Bernfeld B, Kligman M, Roffman M. Arthroscopic assistance for unselected tibial plateau fractures. Arthroscopy. 1996;12(5):598–602.
3. Gill TJ, Moezzi DM, Oates KM, Steret W. Arthroscopic reduction and internal fixation of tibial plateau fractures in skiing. Clin Orthop Rel Res. 2001;383:243–9.
4. Ercin E, Bilgili MG, Basaran SH, Kural C, Avkan MC. Arthroscopic treatment of medial femoral condylar coronal fractures and nonunions. Arthroscopic Tech. 2013;2(4):e413–5.
5. Hartigan DE, McCarthy MA, Krych AJ, Levy BA. Arthroscopic-assisted reduction and percutaneous fixation of tibial plateau fractures. Arthroscopic Tech. 2015;4(1):e51–5.
6. Yoon YC, Oh JK, Oh CW, Sahu D, Hwang JH, Cho JW. Inside out rafting K-wire technique for tibial plateau fracture. Arch Orthop Trauma Surg. 2012;132(2):233–7.
7. Schatzker J. Fractures of the Tibial plateau. In: The Rationale of Operative Fracture Care. Berlin: Springer-Verlag; 1987. p. 279–95.
8. Schatzker J, McBroom R, Bruce D. The tibial plateau fracture. The Toronto experience 1968–1975. Clin Orthop Relat Res. 1979;138:94–104.
9. Afsar T, Oguz S, et al. Arthroscopic technique for treatment of Schatzker type III tibia plateau fractures without fluoroscopy. Arthrosc Tech. 2017;6(1):e195–9.

Arthroscopic Poking Reduction and Fixation of Ankle Fractures

19

Yu-jie Liu and Feng Qu

19.1 Introduction

The type of injury in ankle joint depends on force levels as it receives. Internal rotational forces can bring about medial and lateral malleolus fracture and osteochondral fractions of the talus (Fig. 19.1) [1]. Plain film radiography and CT reveal significant diagnostic values in fracture diagnosis and location (Fig. 19.2) and MRI in ankle ligament damage (Fig. 19.3) [2, 3].

19.2 Clinical Features

Comminuted burst fracture of distal tibia, or pilon fracture, often results from high-energy vertical forces in distal tibia due to jumping or tumbling from high places (Fig. 19.4). Rüedi and Allgôwer have divided ankle pilon fracture into three types (Fig. 19.5).

- Type I: Cleavage fracture without displacement but with fracture line in the articular surface of ankle
- Type II: Cleavage fracture with displacement and fracture line in the articular surface of ankle
- Type III: Severe comminuted fracture with fracture line in the metaphysis and the articular surface of ankle

External fixation and open surgery are conventional treatments for ankle fractures (Fig. 19.6). However, the narrow surgical field in an open surgery can hardly make comminuted fractured fragments of joint or cartilage injuries visible, not to mention the anatomical restoration of ankle fractures. Ankle arthroscope allows surgeons to remove fractured fragments in the joint space, and the anatomical restoration can be achieved precisely, thus restoring a smooth articular surface with normal anatomy in case of osteoarthritis after surgery [4].

19.3 Arthroscopic Poking Reduction and Internal Fixation of Ankle Fractures

The patient is positioned supine or prone according to fracture location, using a sterile pneumatic tourniquet in an ankle arthroscope. Either general anesthesia or femoral nerve block anesthesia can be applied. Surgical approach and relevant vessels and nerves should be marked. The ankle is routinely prepared and draped.

Intra-articular hematoma and synovial tissues that block the arthroscopic vision must be removed (Fig. 19.7). Comminuted fractured bones in the joint space are eliminated (Fig. 19.8). An arthroscopic observation reveals the rupture of the distal part of anterior tibiofibular ligament with widened distal tibiofibular joint space (Fig. 19.9) and distal tibial fracture with displacement and step-shape bone defects (Fig. 19.10).

Comminuted fractured bones are grafted in the defect area under arthroscopic vision, and periosteal stripping is used to expand fracture spaces for further poking by k-wire and manipulative reduction (Fig. 19.11). The reduction standard of comminuted fracture is a smooth cartilaginous surface (Fig. 19.12). Screw fixation is used vertical to the fracture line (Fig. 19.12) [5]. An external fixator can be selected depending on the evaluation of ankle fractures (Fig. 19.13). Meanwhile, ligament injuries should be repaired during the arthroscopic surgery (Fig. 19.14), with ankle immobilization brace and reexamination of X-ray postoperatively.

Y.-j. Liu (✉)
Department of Orthopedics, Chinese PLA General Hospital, Beijing, China

F. Qu
Beijing Tongren Hospital, Capital Medical University, Beijing, China

Y.-j. Liu et al. (eds.), *Advanced Application of Arthroscopy*, https://doi.org/10.1007/978-981-15-4684-6_19

Fig. 19.1 Internal rotational forces lead to medial and lateral malleolus fracture, and some cases are accompanied by osteochondral fractions of the talus

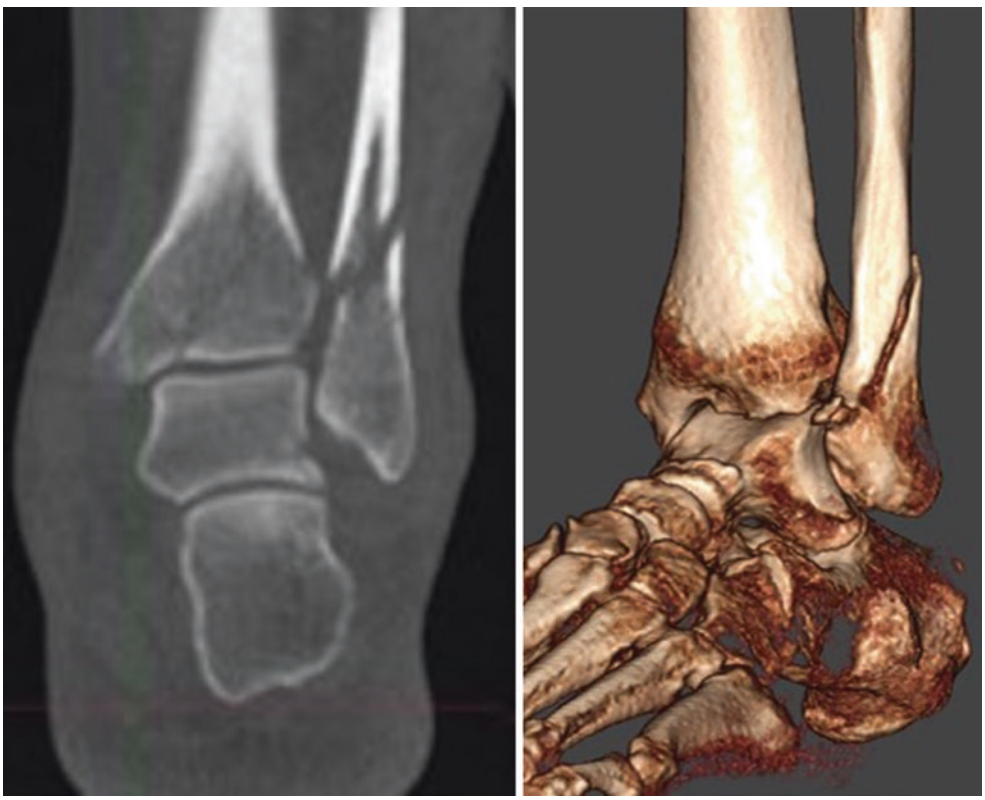

Fig. 19.2 Three-dimensional (3D) CT reveals ankle fracture displacement

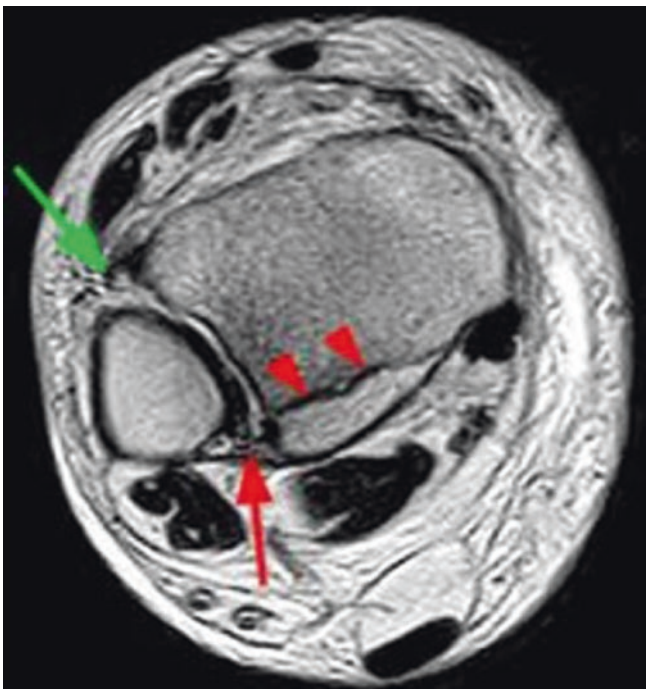

Fig. 19.3 MRI reveals posterior malleolus fracture of the ankle with ligament damage

19.4 Critical Points

1. The best time window of arthroscopic surgery for ankle fractures is within 24 hours after fracture, in the condition of no soft-tissue swelling. Poking reduction is suitable for a fresh fracture, but not an old one.
2. Ankle fractures with distal tibiofibular ligament or talofibular ligament injury can be repaired simultaneously.
3. If a compression fraction of ankle is accompanied by bone defects, bone graft for bone defect will be needed with brace or plaster immobilization postoperatively for fear of early weight bearing.

Fig. 19.4 X-ray shows comminuted fracture of ankle involving tibiotalar joint

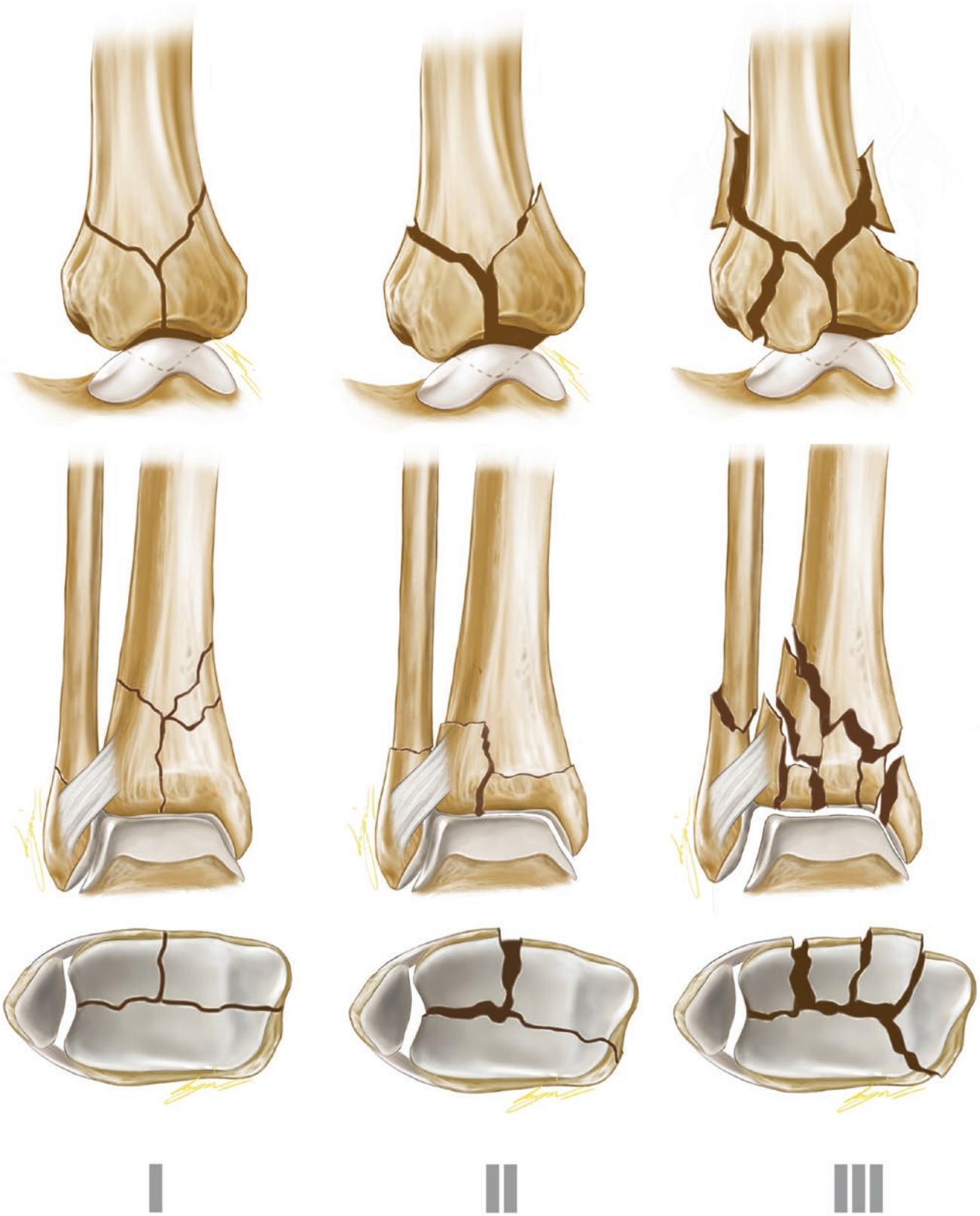

Fig. 19.5 The classification of pilon fracture

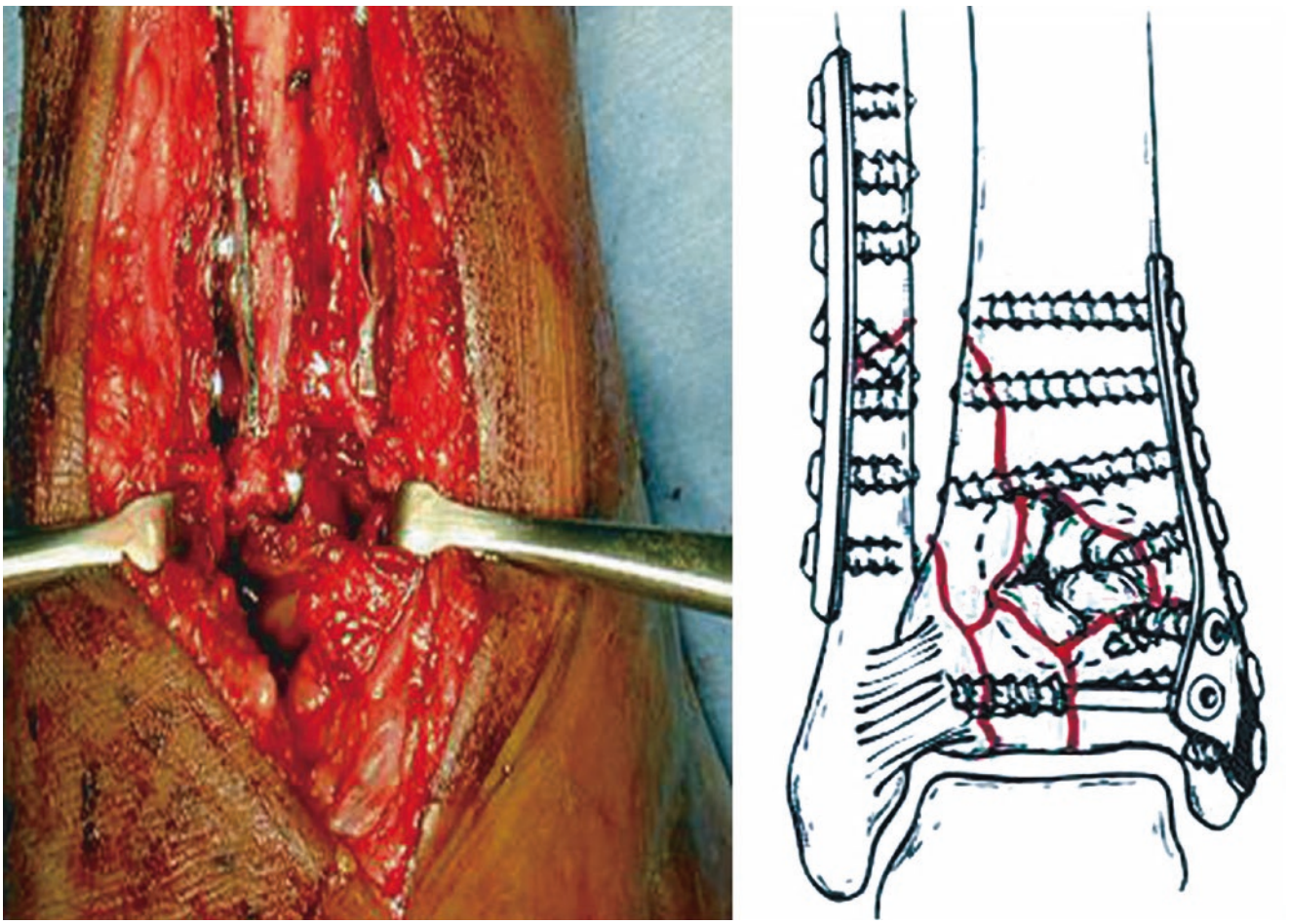

Fig. 19.6 An open surgery for ankle fractures

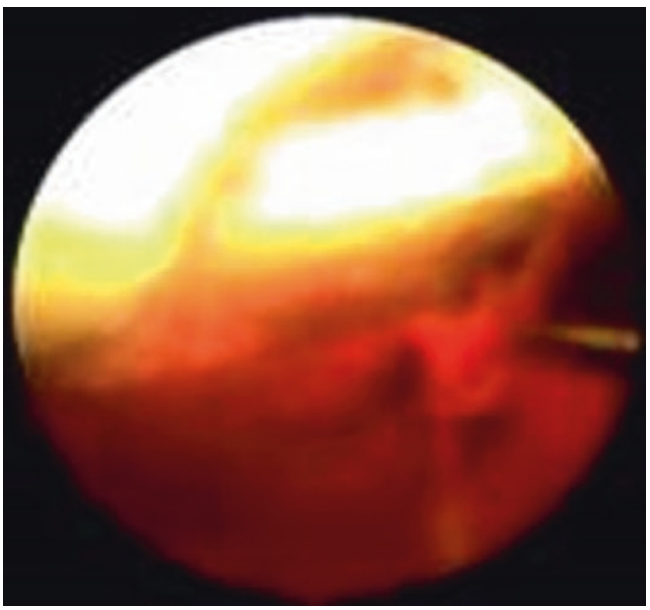

Fig. 19.7 Intra-articular hematoma is removed under arthroscopic vision

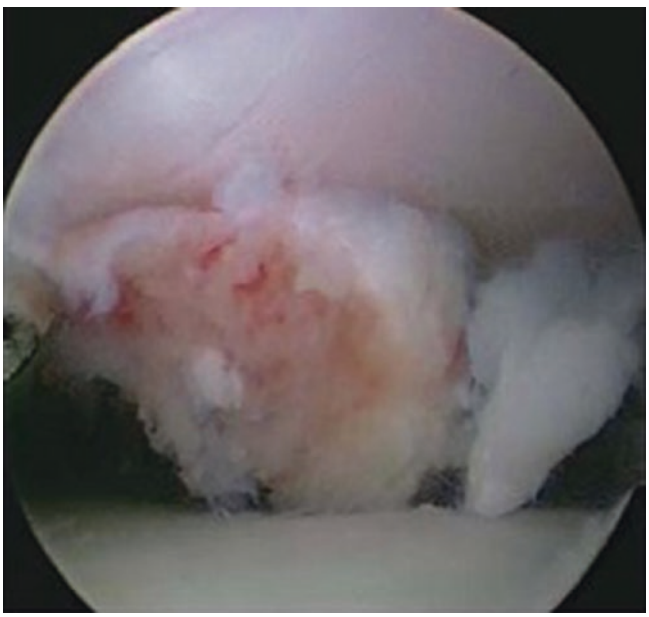

Fig. 19.8 Comminuted fractured bones in the joint space are eliminated

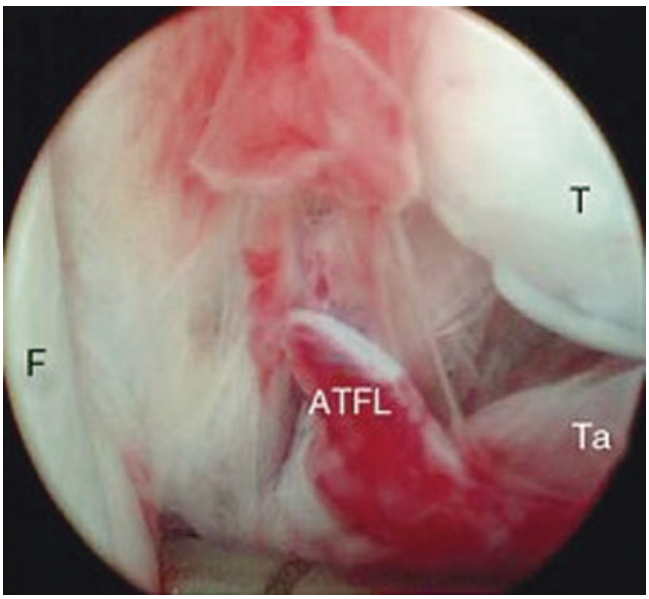

Fig. 19.9 An arthroscopic observation reveals the rupture of the distal part of anterior tibiofibular ligament with widened distal tibiofibular joint space

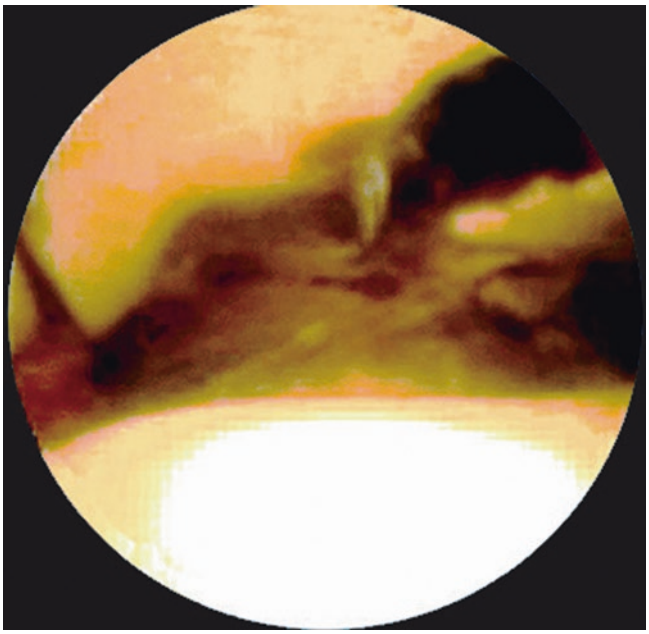

Fig. 19.10 Comminuted fracture of the ankle joint near distal tibia with displacement

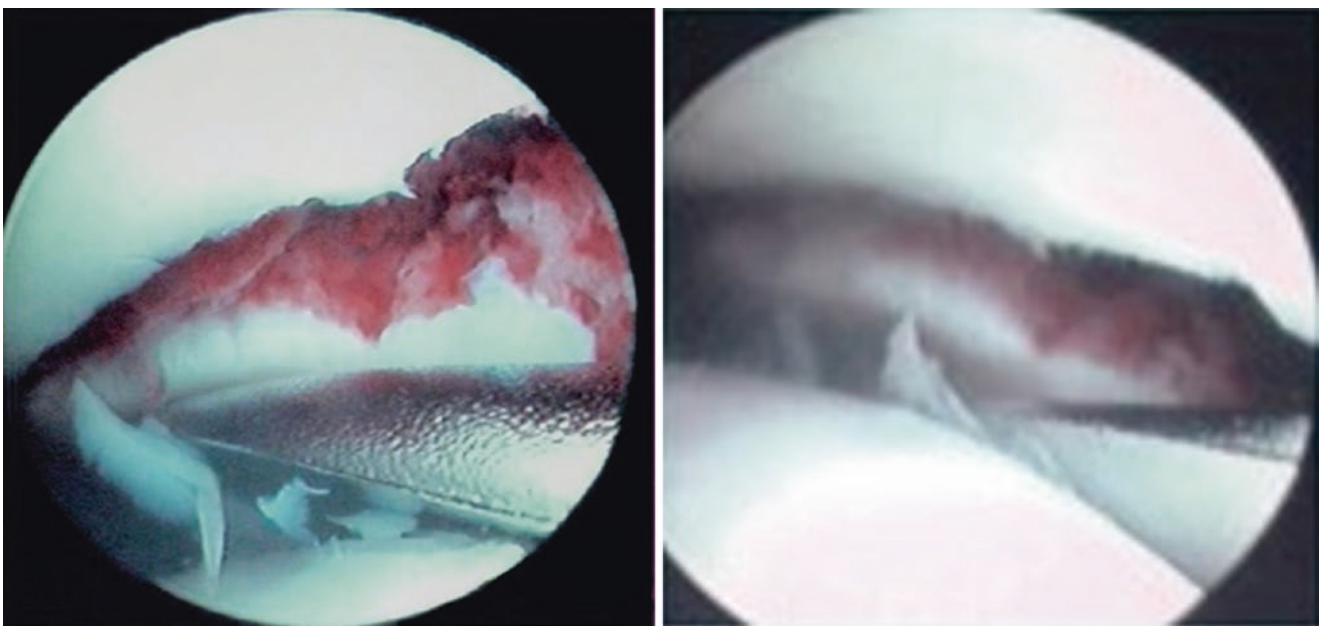

Fig. 19.11 Fracture displacement with step-shape bone defects

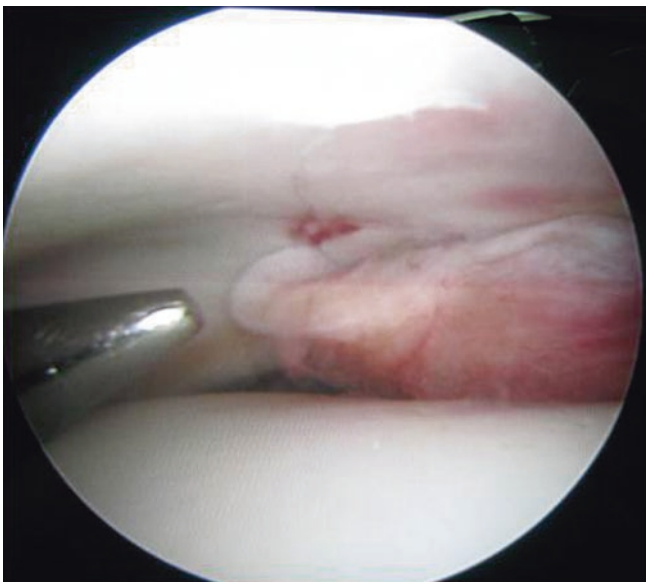

Fig. 19.12 Restored cartilaginous surface of the ankle joint after poking reduction

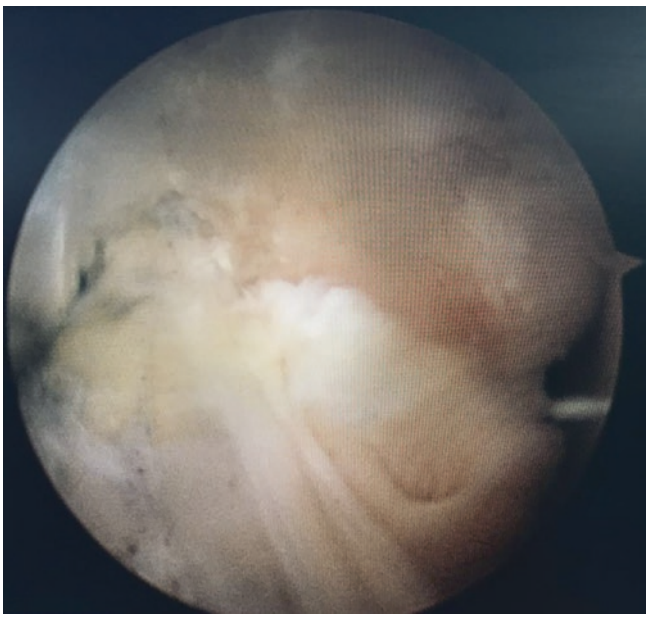

Fig. 19.14 Ligament injuries should be repaired during the arthroscopic surgery

Fig. 19.13 Lag screw fixation for fracture fragments, with an external fixator if necessary

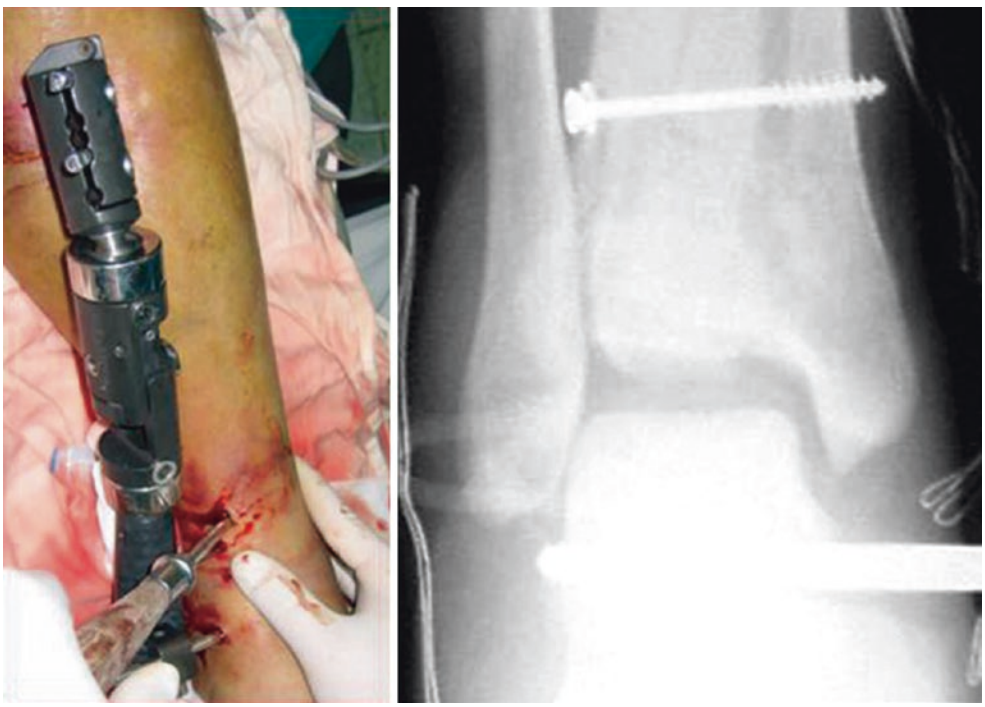

References

1. Tao S, Liu Y, Guo Y, et al. Treatment of Pilon fracture with external fixation under arthroscopy. Chinese J Orthop Trauma. 2004;6(10):1112–5.
2. Leontaritis N, Hinojosa L, Panchbha Vi VK. Arthroscopically detected intra-articular lesions associated with acute ankle fractures. J Bone Joint Surg Am. 2009;91(2):333–9.
3. O'Loughlin PF, Heyworth BE, Kennedy JG. Current concepts in the diagnosis and treatment of osteochondral lesions of the ankle. Am J Sports Med. 2010;38(2):392–404.
4. Bonasia DE, Rossi R, Saltzman CL, et al. The role of arthroscopy in the management of fractures about the ankle. J Am Acad Orthop Surg. 2011;19(4):226–35.
5. Dodd A, Simon D, Wilkinson R. Arthroscopically assisted transfibular talar dome fixation with a headless screw. Arthroscopy. 2009;25(7):806–9.

Part III

Innovative Technology for Repair and Reconstruction of Joint Injuries

Reconstruction of Anterior Cruciate Ligament with Tendon Knot Press-Fitted Technique

20

Yu-jie Liu and Hai-peng Li

20.1 Introduction

During the surgery of anterior cruciate ligament reconstruction, the fixation methods can be divided into direct fixation and indirect fixation according to the fixation position of the tendon and the relationship between the graft and the bone tunnel. Direct fixation methods included interface screw and Rigidfix cross nail. Indirect fixation included button steel plate, transfix suspension, and PEG fixation [1]. The cost of either fixation method is high for patients. The author designed the technique of tendon knot press-fitted method to reconstruct ACL and achieved good results [2, 3].

20.2 Preoperative Preparation

20.2.1 Design of Stepped Drill

The self-designed stepped drill and stepped impactor for the femur tunnel: the diameter of the stepped drill at the distal end (1/3) is 7 mm, and the length is 8 mm; the diameter of the proximal part (2/3) is 10 mm, and the length is 10 mm. The diameter of the stepped impactor is 1 mm thicker than that of the drill (Fig. 20.1).

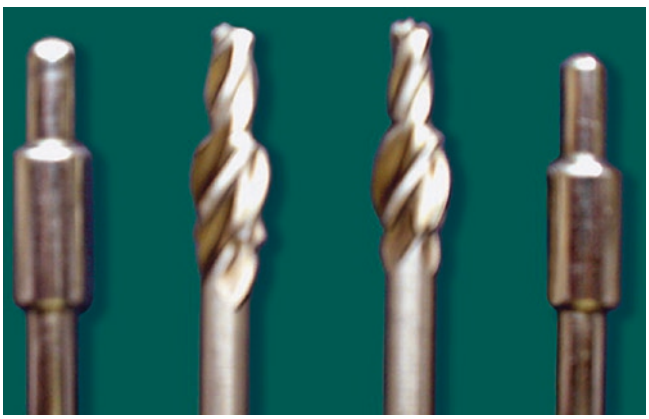

Fig. 20.1 The self-designed stepped drill and stepped impactor for the femur tunnel

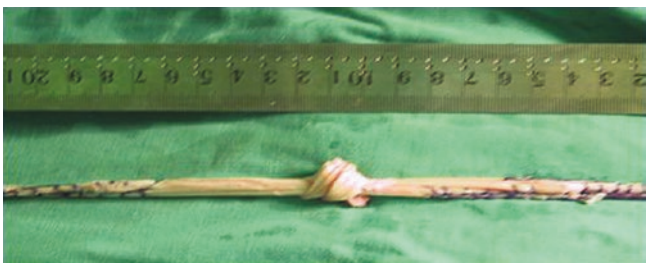

Fig. 20.2 Hamstring tendon knot

20.2.2 Tendon Knot Graft Preparation

20.2.2.1 Hamstring Tendon Knot Preparation

Semitendinosus tendon and gracilis tendon were harvested, and then weave suture and maximally tightened the tendon under cyclic manual loading. Measure the diameter of four-strand tendon, generally 7–8 mm in diameter and 8–9 cm in length, and make the knot at the middle of the tendon (Fig. 20.2).

20.2.2.2 Tendon Knot with Bone Plug Preparation

Semitendinosus tendon and gracilis tendon were harvested, and then make the knot in the middle of the tendon. The bone plug is taken out from the femoral tunnel and remodeled into a 5 mm × 10 mm bone block. Insert the bone plug into the

Y.-j. Liu (✉)
Department of Orthopedics, Chinese PLA General Hospital, Beijing, China

H.-p. Li
Department of Orthopedics, The 7th Medical Center of Chinese PLA General Hospital, Beijing, China

Y.-j. Liu et al. (eds.), *Advanced Application of Arthroscopy*, https://doi.org/10.1007/978-981-15-4684-6_20

tendon knot and then suture the tendon to fix the bone plug [4]. The final shape of tendon knot with bone plug is "T" shape (Fig. 20.3).

20.2.2.3 The Quadriceps Tendon-Patellar Bone Autograft Preparation

The skin and subcutaneous tissue were cut in the middle of the upper of the patella to expose the tendon and the upper 2/3 of the patella. The tendon with patella block was harvested with 9–10 cm long, 7–8 mm wide, 9–10 mm in diameter, and 10 mm in length, which was made into a cylindrical shape [5] (Fig. 20.4).

Fig. 20.3 Tendon knot with bone plug

Fig. 20.4 The quadriceps tendon-patellar bone autograft

Fig. 20.5 Measure the diameter of bone block and tendon graft

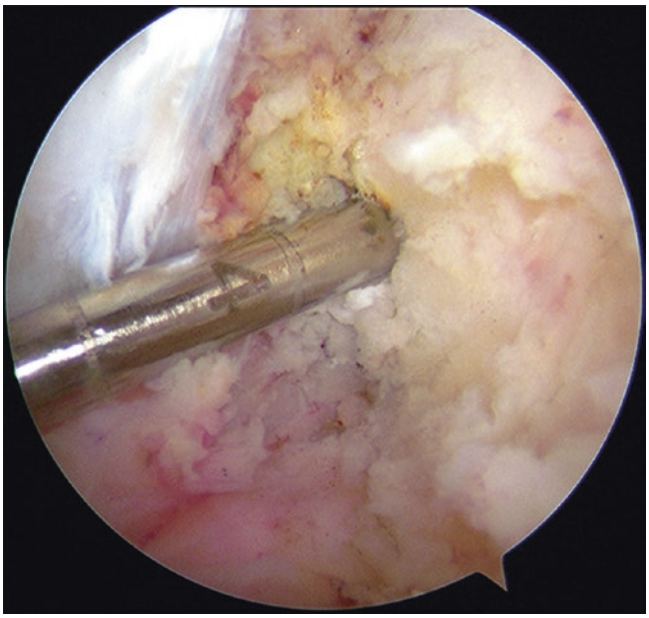

Fig. 20.6 The guide Kirschner was inserted into the femoral footprints of the ACL

The diameter of bone block and tendon graft was measured by measuring sleeve (Fig. 20.5), so as to select the equal diameter of stepped drill.

20.3 Operative Technique

20.3.1 Femoral Tunnel Preparation

The knee was flexed 110°, and the ACL femoral drill guide was placed through anteromedial portal. The guide Kirschner (Fig. 20.6) was inserted into the footprints of the ACL femoral intercondylar fossa. The guide Kirschner was drilled from the anterolateral side of the junction of the femoral lateral

Fig. 20.7 Make the femoral tunnel with the stepped drill along the guide Kirschner

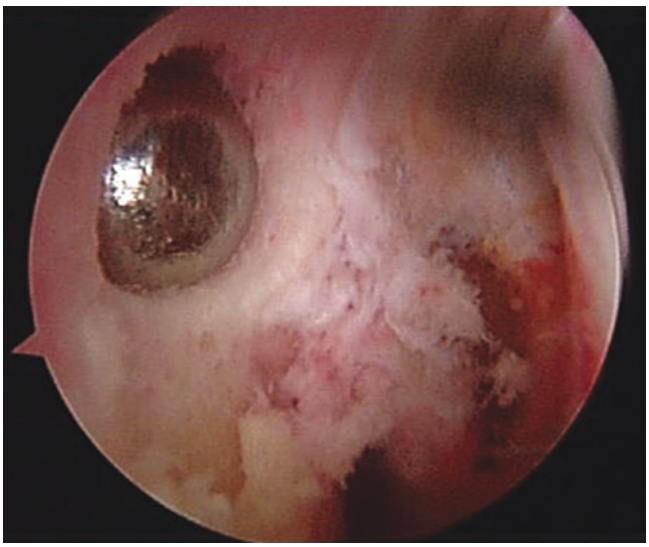

Fig. 20.8 Use the femoral tunnel impactor to punch into the tunnel from the external epicondyle of the femur

condyle. Select the equal diameter stepped drill to the tendon graft and drill the tunnel (Fig. 20.7) along the guide Kirschner from the external epicondyle of the femur to the bone cortex of the intercondylar fossa of the femur. Then use the femoral tunnel impactor to punch into the tunnel from the external epicondyle of the femur (Fig. 20.8), so as to compact the peripheral wall of the tunnel. After forming, the femoral tunnel is in bottleneck shape (Fig. 20.9).

20.3.2 Tibial Tunnel Preparation

The tibial guide is used for positioning at the center of the native ACL tibial footprint under arthroscopic monitoring

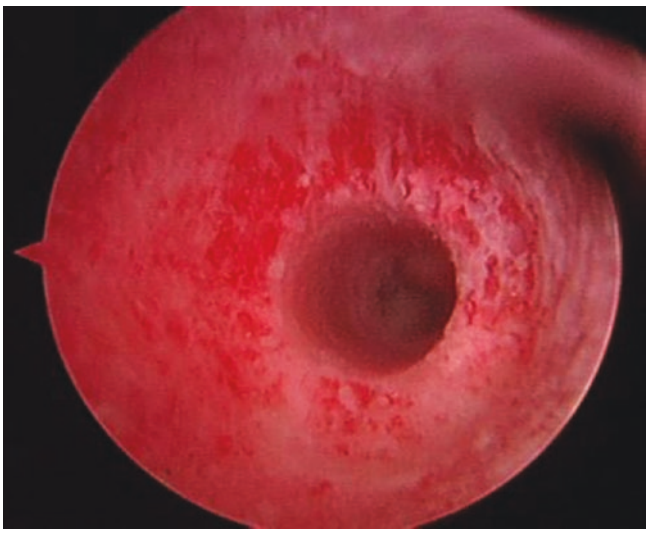

Fig. 20.9 The femoral tunnel is in bottleneck shape

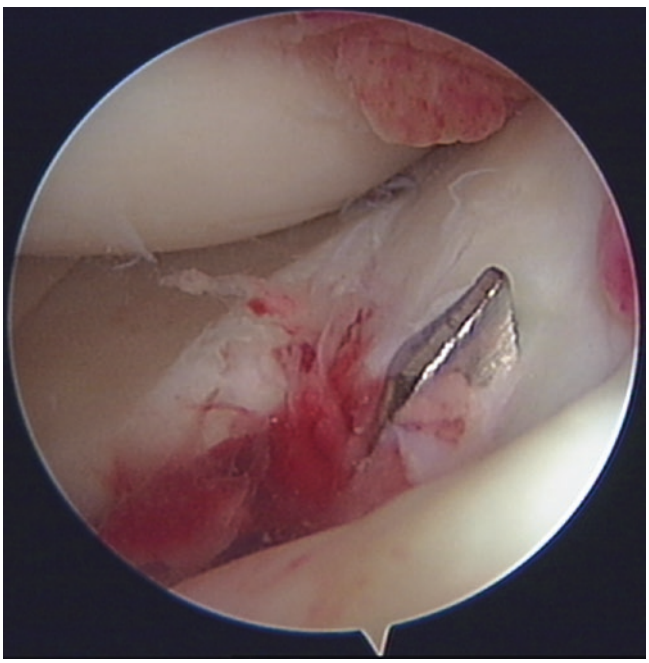

Fig. 20.10 Put the tibial guide at the center of the native ACL tibial footprint

(Fig. 20.10), and the tibial tunnel is drilled with the same drill diameter as tendon graft. If the bone thrombus tendon knot is made, the cylindrical bone block is drilled along the guide needle with a ring drill for standby.

After the preparation of the tibial tunnel, a 4.5-mm drill hole was made 1 cm distal to the tibial end of the tunnel. A bone bridge was created by tunneling under the bone with a right-angle clamp. Penetrate the steel wire through bone tunnels and use the tibial bone bridge as fixation for tendon graft (Fig. 20.11).

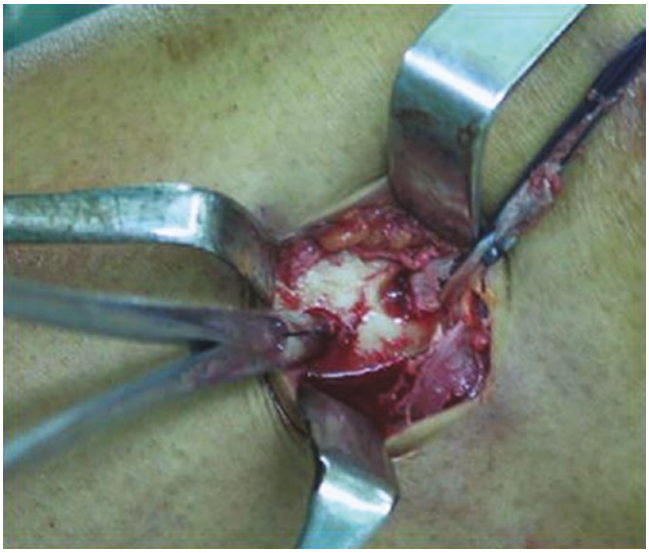

Fig. 20.11 Make a tibial bone bridge at 1 cm distal to the tibial end of the tunnel

Fig. 20.12 The tendon knot is embedded into the stepped femur tunnel

20.3.3 Tendon Graft Passage

The drawn suture runs through the tibial tunnel from the femur tunnel. The tendon graft is pulled into the femur and tibial tunnel from the outside of the femur stepped tunnel. The impactor is inserted above the femur tunnel. The tendon knot is embedded into the stepped femur tunnel and hammered to be firm (Fig. 20.12). The surgeon pulls the tendon from the tibial end and flexes and extends the knee joint for 20 times. The suture at the end of tendon shall be threaded and knotted at the upper and lower part of tibial bone bridge respectively (Fig. 20.13). Absorbable interface screws or pegs can also be used to fix the tibial side. The bone mass extracted from the bone tunnel can be filled back into the cavity from the external mouth of the femoral tunnel.

Fig. 20.13 Tract the end of tendon from the tibial bone bridge respectively

20.4 Critical Points

1. The tendon must be pretensioned to avoid the relaxation of tendon creep after surgery.
2. The tendon knot should be placed in the middle of the tendon. If it is placed at the end, it is easy to fail to fix the tendon knot.
3. The diameter of the bone tunnel should be consistent with the tendon knot, so as to avoid the influence of the thickness of the tunnel and tendon on the implantation.
4. The tendon knot is embedded in the neck to achieve firm compression fixation.

References

1. Chang L, Yujie L. Research progress of graft fixation in arthroscopic anterior cruciate ligament reconstruction. Chin J Laparoscopic Surg (Electronic Edition). 2013;6(1):48–52.
2. Yujie L, Wang Z, Wang Y. Anterior cruciate ligament reconstruction using semitendinosus and gracilis tendons knot and bone lock-bolt implant fixation under arthroscope. Chinese J Trauma. 2003;19(3):167–9.
3. Yujie L, Wang Z, Zhongli L. Anatomic reconstruction of ACL single bundle injury with press-fitted method. China J Su rg. 2006;44(24):1724–5.

4. Yujie L, Wang Z, Zhongli L. Arthroscopically assisted combined anterior cruciate ligament reconstruction with an implant fixation of hamstrings tendons knot and bone bolt press-fit technique. China J Orthop. 2004;24(3):133–6.

5. Yujie L, Peifu T, Wang Z. Arthroscopically assisted combined anterior cruciate ligament reconstruction with quadriceps tendons and patella bone lock bolt an implant-free and press-fit technique. Orthop J China. 2005;13(4):264–6.

Anterior Cruciate Ligament Reconstruction with Remnant-Preserving Technique

21

Yu-jie Liu and Hai-peng Li

21.1 Introduction

ACL is divided into anteromedial bundle (AMB) and posterolateral bundle (PLB) (Fig. 21.1). The anteromedial bundle (AMB) can resist the tibial forward movement during the flexion of the knee joint, and the posterolateral bundle (PLB) can stabilize the knee joint during the extension position. The stability of knee joint will be affected by partial or complete injury of ACL.

In the past, most of the ACL reconstruction were performed by removing the residual ligament. However, the author selected different reconstructions to preserve the residual according to the type of ACL injury and achieved good results [1]. The results show that the preservation of ACL remnant bundle, remnant end, or remnant root is beneficial to the restoration of proprioception, revascularization, and promotion of tendon bone healing [2].

Surgery was conducted in patients with supine position under general anesthesia or epidural nerve block anesthesia. The status of the ACL remnant, meniscus, and articular cartilage was determined. Reconstruction plan was made after arthroscopic evaluation according to the type of ACL injury. The ipsilateral or contralateral hamstring tendons were used as ACL reconstruction materials.

The following are different types of remnant-preserving technique: ACL single-bundle reconstruction with retaining healthy bundle; ACL reconstruction with suturing the long stump and suspension fixation; ACL reconstruction with binding fixation in the short stump to the graft; ACL reconstruction with the tendon graft through the middle of stump; and ACL avulsion injury by suture avulsion end and suspension fixation, fix in the avulsion fracture of the tibial intercondylar eminence with suture tie knot.

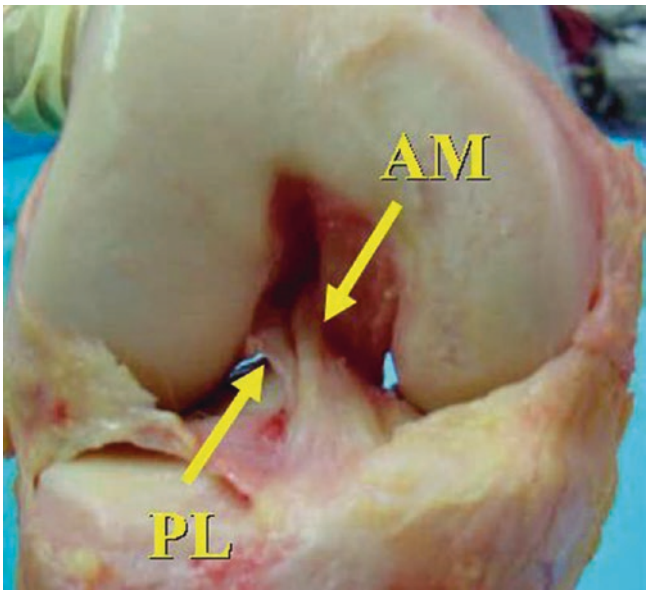

Fig. 21.1 ACL is divided into anteromedial bundle (AMB) and posterolateral bundle (PLB)

21.2 Operative Technique

21.2.1 Reconstruction of the Posterolateral Bundle with the Preserved Anteromedial Bundle

Taking the posterolateral bundle injury of ACL as an example, this paper describes the method of reconstructing the damaged bundle by retaining the healthy bundle. Arthroscopic evaluation showed that the anteromedial bundle of ACL was

Y.-j. Liu (✉)
Department of Orthopedics, Chinese PLA General Hospital, Beijing, China

H.-p. Li
Department of Orthopedics, The 7th Medical Center of Chinese PLA General Hospital, Beijing, China

Y.-j. Liu et al. (eds.), *Advanced Application of Arthroscopy*, https://doi.org/10.1007/978-981-15-4684-6_21

normal and the posterolateral bundle was damaged (Fig. 21.2). Hamstring tendon was harvested as graft.

At the back of the anteromedial bundle, the radiofrequency was used to expose the footprint of the posterolateral bundle as the location point of the tibial tunnel. The ACL tibial guide was used to check whether the position was correct and whether there was impingement. According to the diameter of the tendon, drill the tibial tunnel (Fig. 21.3). At the femoral side, select the footprint to drill the femoral tunnel (Fig. 21.4). After the EndoButton loop was connected with the tendon, tract the tendon from the tibia tunnel to the femur tunnel and fix the femoral end of the graft with EndoButton. Re-tensioning was facilitated by several cyclic motions of the knee. The tibial end of the graft was fixed with interface screw or Rigidfix. The tension and stability of ACL graft and remaining residual bundle after reconstruction were evaluated (Fig. 21.5) [3, 4].

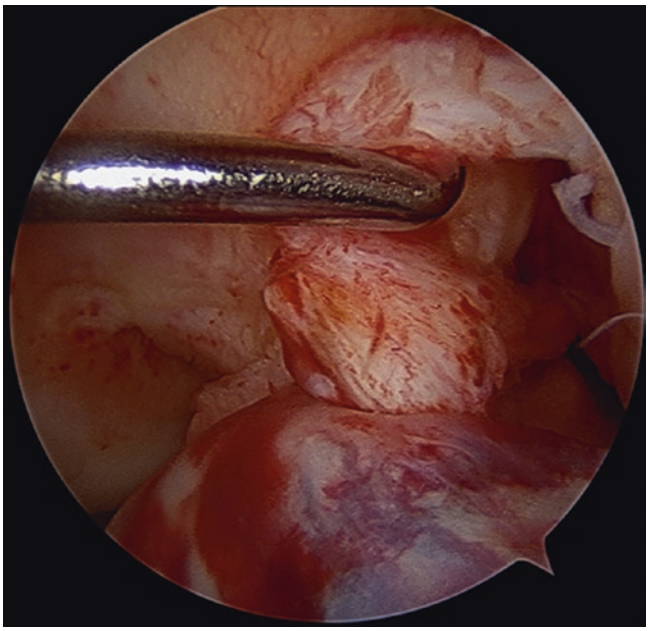

Fig. 21.2 Posterolateral bundle of ACL was injured, and the anteromedial bundle was normal

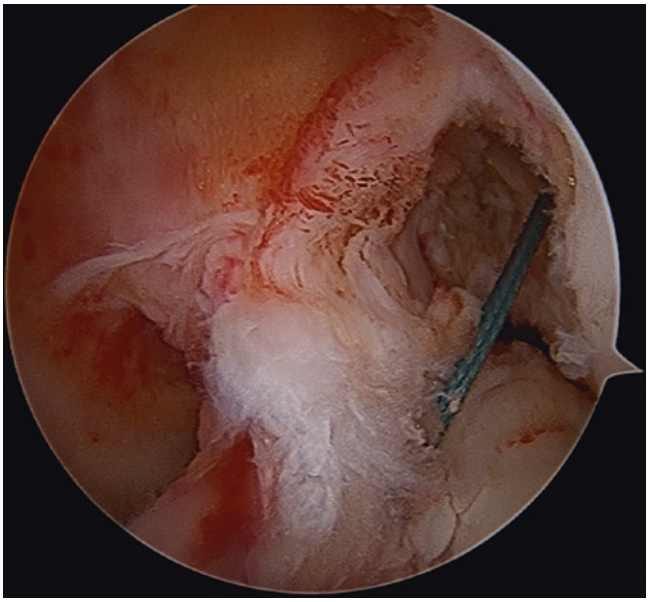

Fig. 21.4 Drill the femoral tunnel and preserve the anteromedial bundle of ACL

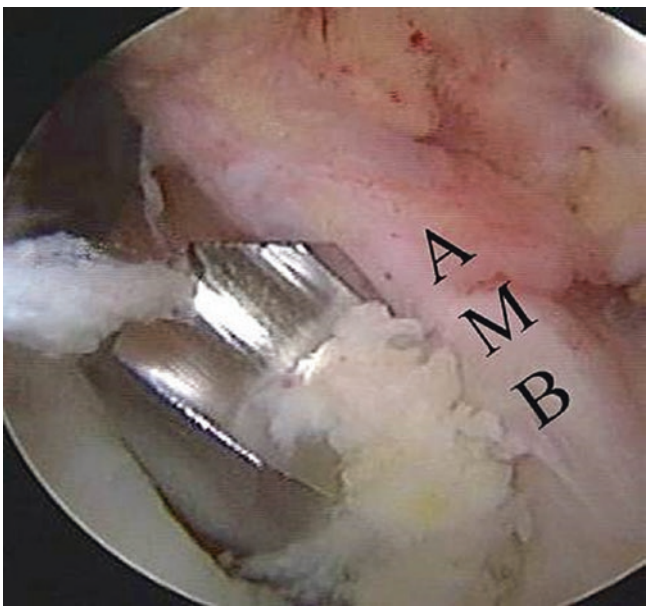

Fig. 21.3 Drill the tibial tunnel and preserve the anteromedial bundle of ACL

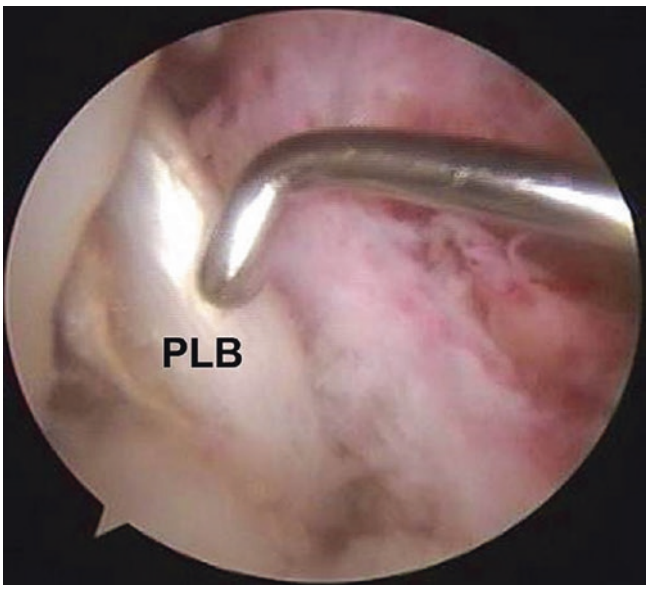

Fig. 21.5 Reconstruct the posterolateral bundle of ACL and preserve the anteromedial bundle

21.2.2 ACL Reconstruction with Suturing the Long Stump and Suspension Fixation

The injury of ACL is often at the femoral attachment, and the surrounding synovium or membranous tissue of ACL is attached to the femoral insertion. It can be found that the femoral insertion of ACL was void with probe hook (Fig. 21.6). The length of damaged ACL is similar to that of normal ACL.

Before drilling the femoral tunnel, the residual end of ACL should be slightly free and then sutured ligament with suture hook (Fig. 21.7), and the tail end of suture should be led out. When drilling tibial tunnel, we should avoid ACL anteromedial bundle and drill at the attachment point of the posterolateral bundle to protect the fibers of ACL anteromedial bundle. The femoral tunnel was selected at the anatomic point of ACL. After the tunnels are drilled, the Rigidfix guider is placed to drill the nail bone tunnel, and then the tendon graft is pulled into the femoral tunnel from the tibial tunnel. The suture of the stump and the tendon graft are pulled out of the femoral tunnel together (Fig. 21.8). The suture is tied and fixed outside the femoral tunnel. The tibia and the femur sides can be respectively fixed with Rigidfix (Fig. 21.9). The tendon graft was completely covered by the stump (Fig. 21.10). The residual synovium and capillaries should not be cleaned, so as not to affect the blood supply of the graft and creeping substitution after reconstruction.

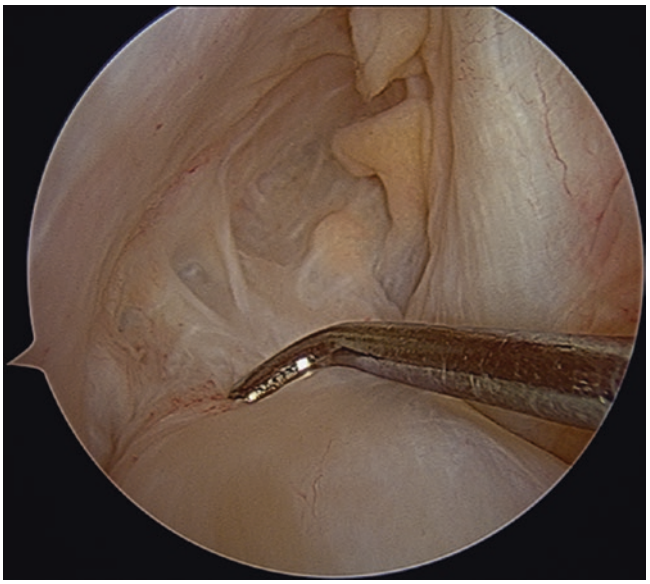

Fig. 21.6 The femoral attachment of ACL is injured and the internal void of ACL can be found with probe hook

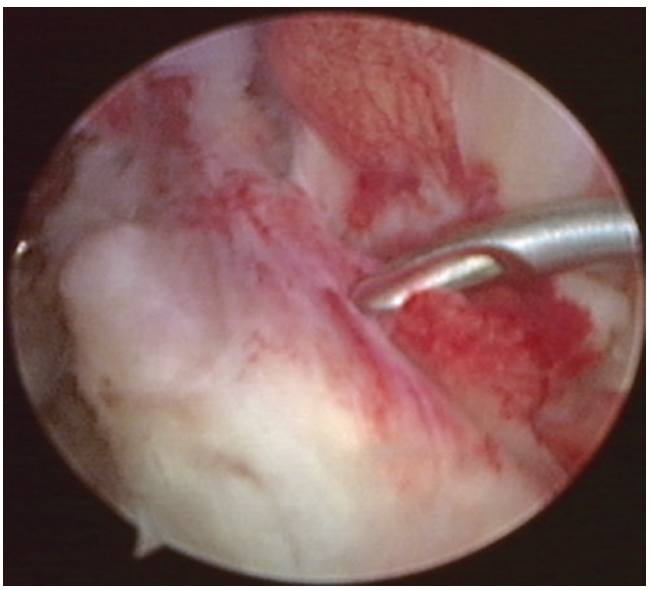

Fig. 21.7 Suture the residual ligament of ACL with suture hook

21.2.3 ACL Reconstruction with Binding Fix in the Short Stump to the Tendon Graft

The surgery steps of ACL reconstruction with short stump are basically the same as described above. As the length of the remnant is only 2/3 of the normal ACL, it can't be suspended and fixed in the femoral tunnel, so after ACL reconstruction, the author uses the suture hook to bind the remnant of ACL and fix it in front of the tendon graft (Fig. 21.11), which can improve the tension of the remnant and prevent the tendon from slipping down to form the bull's eye sign (Fig. 21.12) [5].

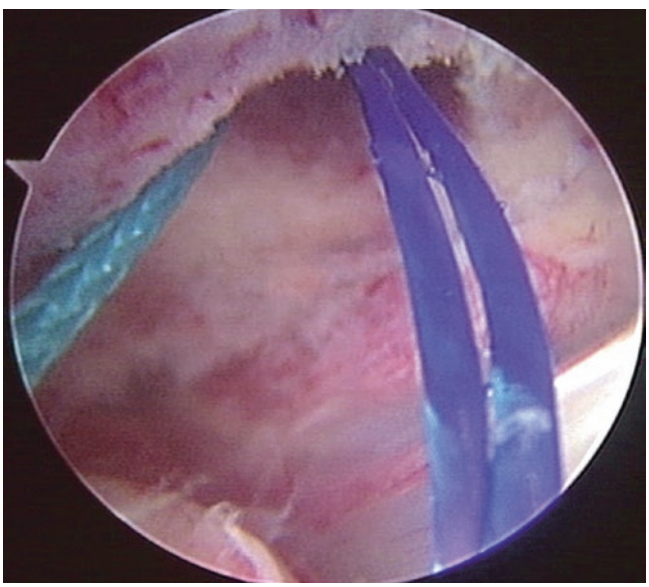

Fig. 21.8 The suture of the stump and the tendon graft is pulled out of the femoral tunnel together

Fig. 21.9 The tibia and femur sides of tendon graft was fixed with Rigidfix respectively

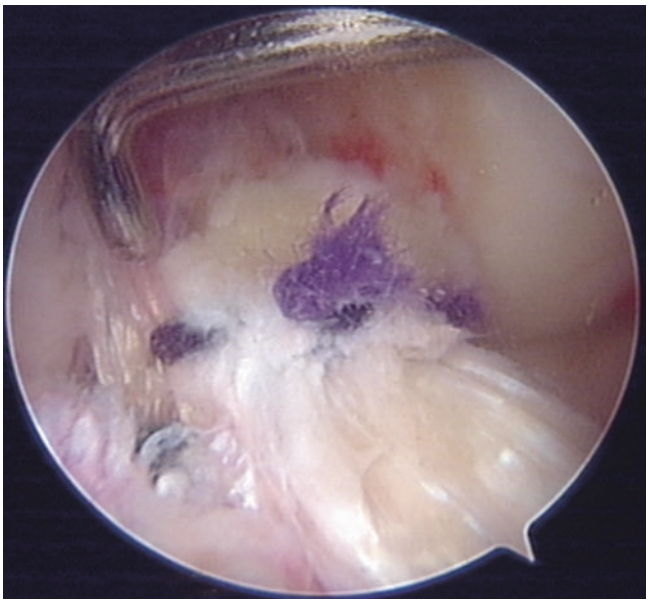

Fig. 21.11 Suture the remnant of ACL and fix it in front of the tendon graft

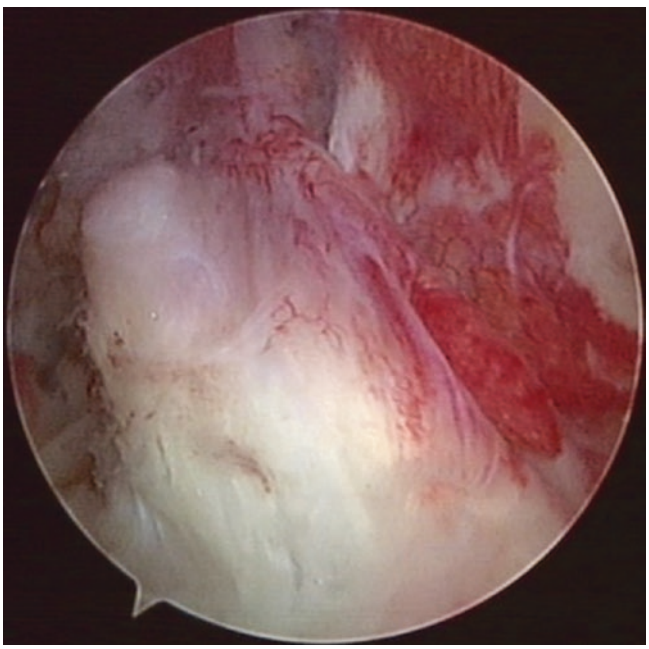

Fig. 21.10 The tendon graft was completely covered by the stump

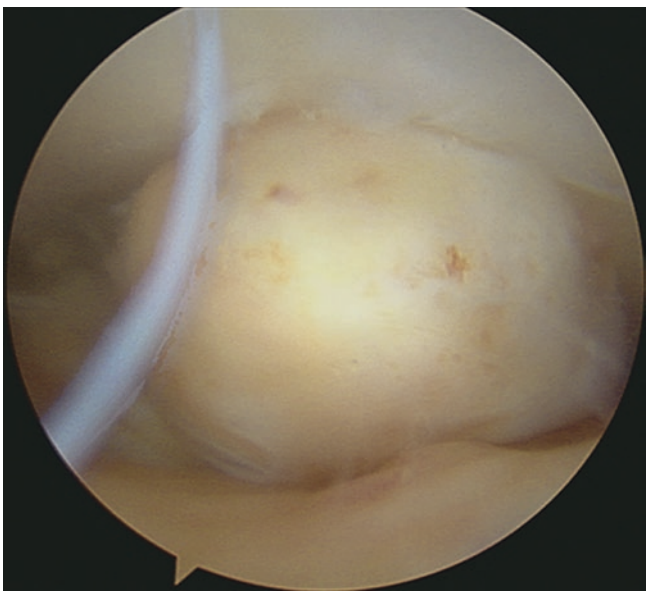

Fig. 21.12 The remnant of ACL slips down to form the bull's eye sign

21.2.4 ACL Reconstruction with Residual Root Preservation

Most of the ACL injury left only the residual roots of ACL as the ligament was absorbed (Fig. 21.13). The key point of the residual root preservation surgery is to place the tibial guide on the center of residual root, drill the tibial tunnel in the middle (Fig. 21.14), preserve the fibers around the residual root, and the graft passes through the middle of the ACL residual root (Fig. 21.15). There are blood vessels and neurosensors on the remaining roots, which are helpful for the ligament to restore proprioception and revascularization and prevent the joint fluid from infiltrating into the bone tunnel to affect the tendon bone healing.

Fig. 21.13 The residual roots of ACL as the ligament of ACL was absorbed

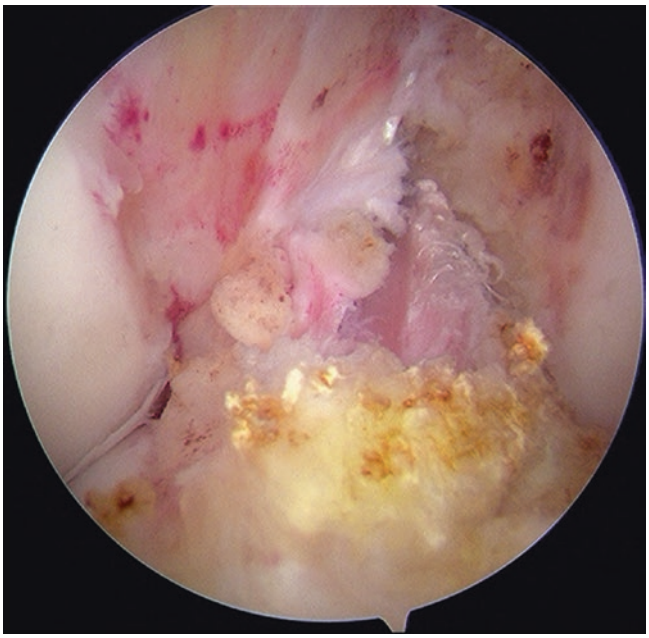

Fig. 21.15 The graft passes through the middle of the ACL residual root

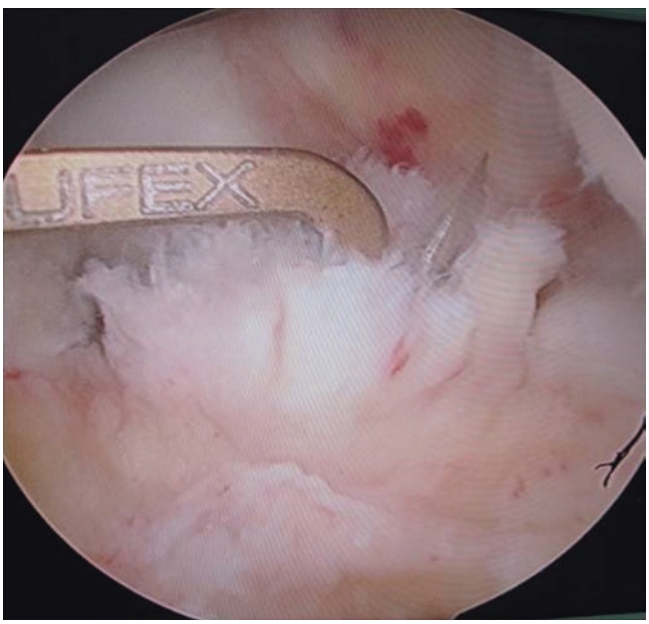

Fig. 21.14 Drill the tibial tunnel with residual root preservation

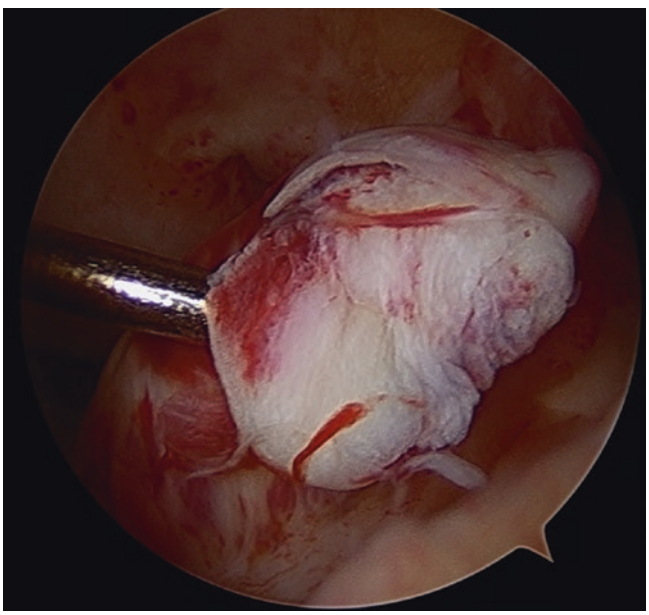

Fig. 21.16 The single bundle of ACL is tear from the femur insertion

21.2.5 Insertion Injury of Single Bundle of ACL Treated by Suture Ligament and Fix In Situ

When the knee joint is sprained, the single bundle of ACL is easy to tear from the femur insertion (Fig. 21.16) or tibia insertion (Fig. 21.17), resulting in ACL partial injury or fiber elongation (Fig. 21.18). Because of ACL relaxation and low tension, it affects the stability of knee joint. The author sutures the ligament at the insertion (Fig. 21.19), drilled a 4 mm diameter bone tunnel at the in situ attachment point, then passed the suture with ligament through the bone tunnel, tightened it outside of the femur, and fixed it with Endobutton.

For the avulsed fibers of ACL at the insertion on the tibial side, suture the ACL fibers (Fig. 21.20). Drill a 3 mm diameter bone tunnel in situ with the ACL tibial guide (Fig. 21.21), then guide the suture to the front of tibial tubercle, and knot and fix it on the bone bridge.

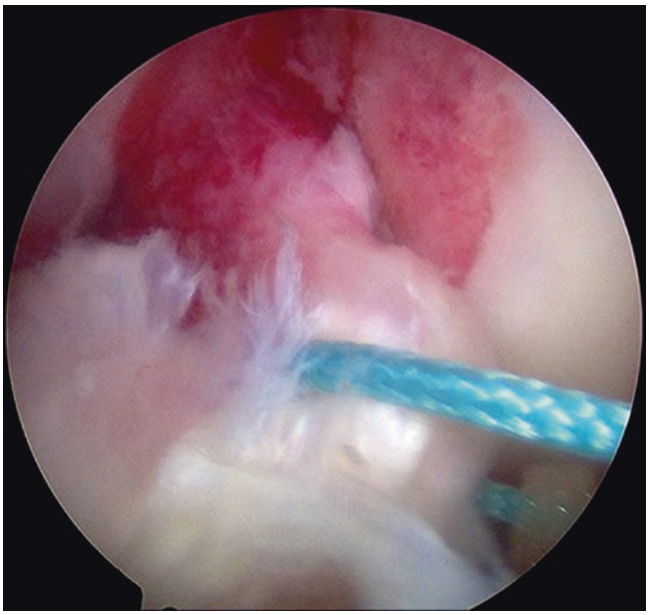

Fig. 21.17 The single bundle of ACL is tear from tibia insertion

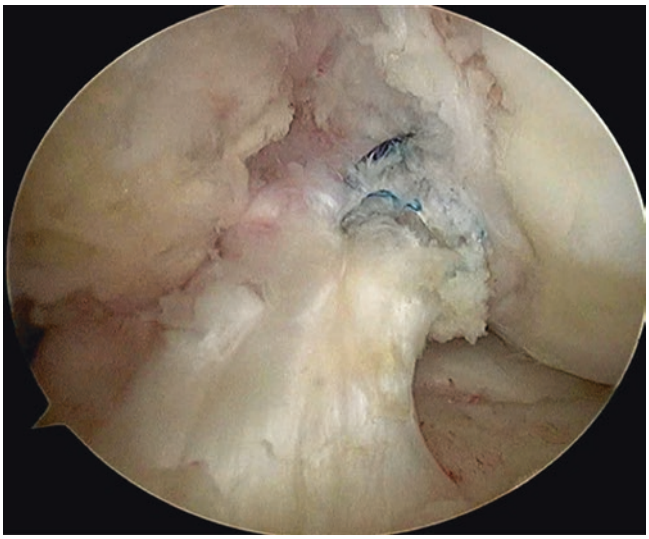

Fig. 21.19 Sutures the ligament of ACL

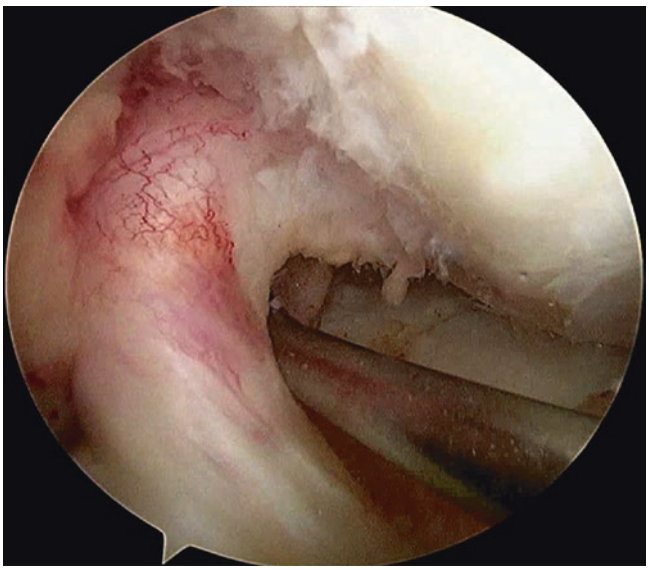

Fig. 21.18 Partial injury of ACL or ligament elongation

Fig. 21.20 Suture the fibers of ACL at the insertion on the tibial side

21.2.6 Fix the Avulsion Fracture of the Tibial Intercondylar Eminence with Suture Tie Knot

When the knee joint is seriously injured, ACL will pull tibial intercondylar eminence and cause avulsion fracture (Fig. 21.22). Because the anterior horn of meniscus or transverse ligament of the knee is embedded between the fracture blocks (Fig. 21.23), it is difficult to anatomize and reposition with conservative treatment. The author used single tie knot (Fig. 21.24) or double tie knot to suture and binding fixation (Fig. 21.25) to treat ACL tibial avulsion fracture and achieved good results.

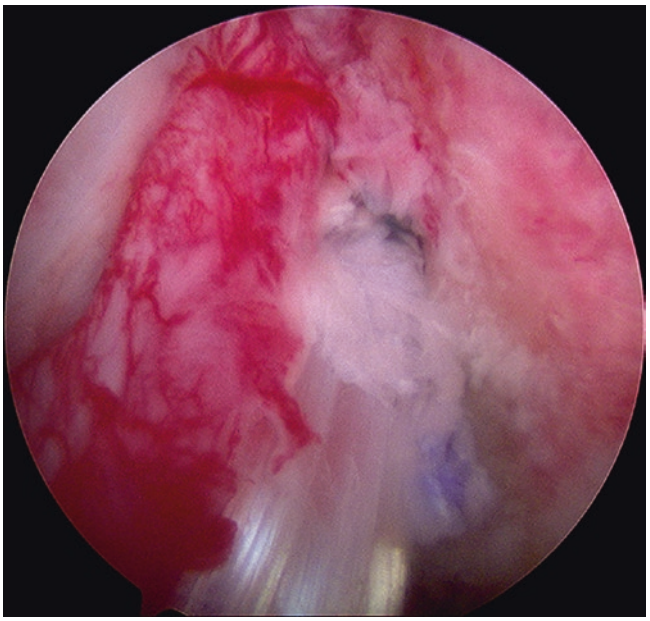

Fig. 21.21 Drill the bone tunnel in situ at the tibial guide

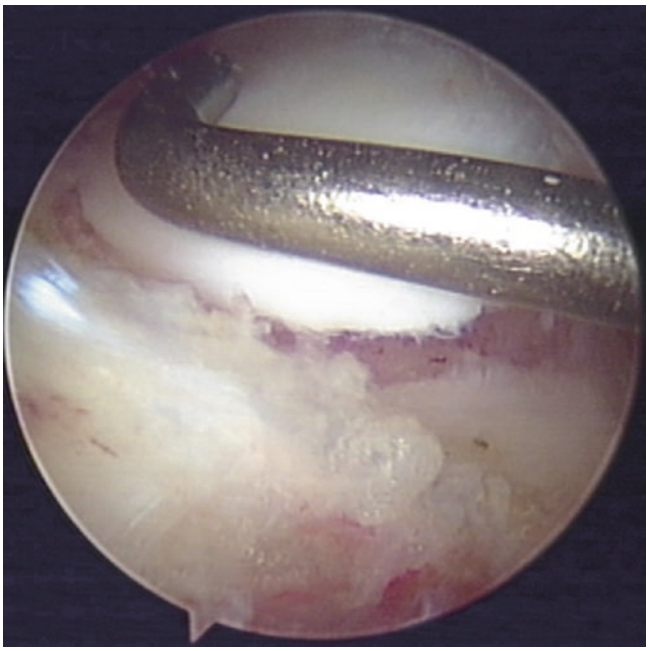

Fig. 21.23 The anterior horn of meniscus or transverse ligament is embedded between the fracture blocks

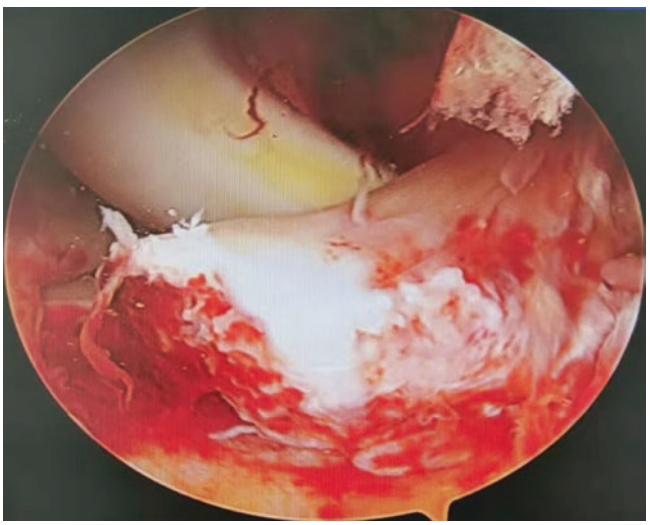

Fig. 21.22 The tibial intercondylar eminence avulsion fracture of ACL

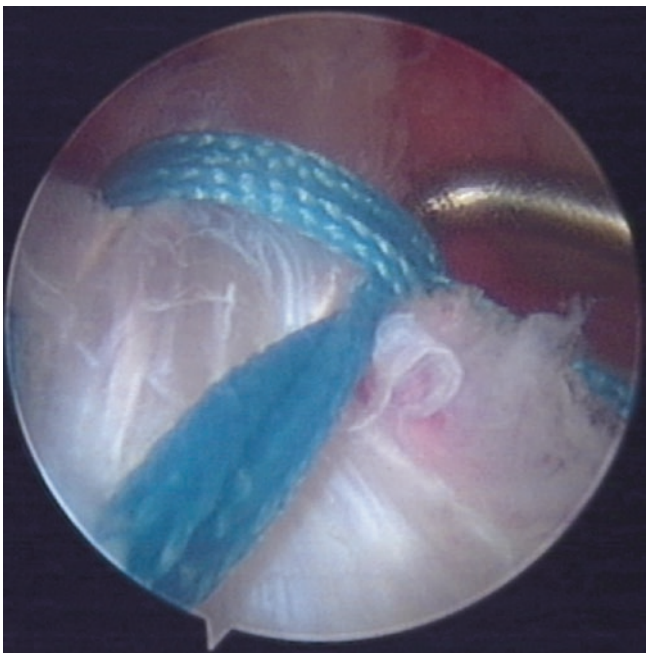

Fig. 21.24 Fix the tibial intercondylar eminence avulsion fracture single tie knot

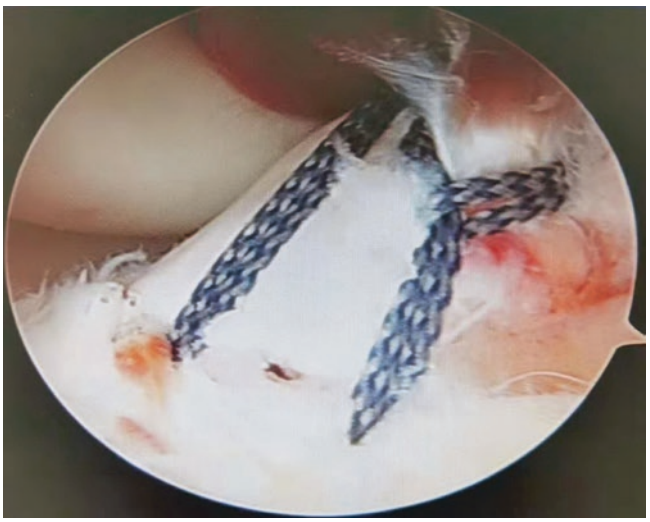

Fig. 21.25 Fix the tibial intercondylar eminence avulsion fracture double tie knot

References

1. Yujie L. Recognition of reconstruction of cruciate ligament with remnant preservation. China J Orthop Trauma. 2013;26(5):357–9.
2. Zhicao L, Yujie L, Bin S. An experimental study on anterior cruciate ligament reconstruction with remnants and remaining bundle preservation. Chinese J Reparative Reconstr Surg. 2009;3:282–6.
3. Yujie L, Zhicao L, Haipeng L. Value of reconstruct anterior cruciate ligament for remaining anteromedial or posterolateral bundle and ruptured fiber. Orthopedic Journal of China. 2008;16(2):89–91.
4. Wei Q, Junliang W, Feng Q. Arthroscopic reconstruction of anterior cruciate ligament with preservation of the remnant bundle. China J Orthop Trauma. 2013;26(5):376–80.
5. Jingbin Z, Yujie L, Guoping L. Research advances in anterior cruciate ligament reconstructions with remnant preservation. China J Orthop Trauma. 2013;26(5):441–4.

22 Femoral and Tibial Fixation with Cross-Pin System in Anterior Cruciate Ligament Reconstruction by Using Semitendinosus and Gracilis

Yu-jie Liu and Wei Qi

22.1 Introduction

Good clinical outcomes have been achieved by using RigidFix cross-pin system (Depuy Mitek, Raynham, MA, USA) in the femoral fixation of hamstring tendons in ACL reconstruction [1–5]. We have applied the femoral RigidFix cross-pin system in the femoral and tibial fixation with semitendinosus and gracilis graft since 2006 [6]. Based on the biomechanical tests and clinical observations, the feasibility and reliability of this method have been proved. The fixation points are close to the original attachment of the ACL which could avoid the longitudinal and lateral oscillation of the tendon graft. Applying the cross-pin system in the tibia fixation could avoid cutting the graft which is caused by the interference screw fixation. The graft is in full contact with the tunnel which could be beneficial to the bone-tendon healing. The RigidFix cross-pin system both on femur and tibia is a safe and efficient fixation method for the ACL reconstruction [1, 2, 7–10].

22.2 Patient Positioning Setup and Graft Harvest

After general or spinal anesthesia, the patient is placed in the supine position. A routine diagnostic arthroscopy is performed around the joint. Meniscectomy or meniscal repair and treatment for cartilage lesions are performed if necessary. Then, the gracilis and semitendinosus are harvested to obtain a length of 18 cm at least. The tendons are made into four to six strands. The diameter of the tendon graft is 7 to 9 mm, and the length is 90 to 100 mm (Fig. 22.1). No. 2 Ethibond suture is applied to suture the tibial and femoral portions of the tendon with whipstitches to achieve 30 mm prospectively (Fig. 22.2). A line is marked on the graft 30 mm distal to the end of the femoral portion. Attach two no. 5 Ethibond sutures to the end of the femoral portion to lead and pass the graft (Fig. 22.3).

Y.-j. Liu (✉) · W. Qi
Department of Orthopedics, Chinese PLA General Hospital, Beijing, China

22.3 Operative Technique [6]

22.3.1 Femoral Tunnel Preparation

Through the anteromedial (AM) portal, a transportal ACL femoral guide is seated at the center of the ACL footprint. Then, a straight 2.4-mm guide pin is drilled through the guide and exited on the lateral side of the knee while keeping the knee in a hyperflexion position. Read the scale on the guide pin to measure the length of the femoral tunnel. An endoscopic drill bit is selected which matches the graft diameter, and the femoral tunnel is produced by the drill with a depth of 30 mm (Fig. 22.4).

22.3.2 Tibial Tunnel Preparation

The tibial guide is seated at the center of the intercondylar ACL remnant of the tibia through the AM portal. A 2.4-mm guide pin is drilled through the guide and exited at the center of the ACL footprint (Fig. 22.5). Then, a cannulated drill whose diameter is equal to the diameter of the graft is run through the guide pin (Fig. 22.6).

22.3.3 Femoral Cross-Pin Channels Preparation

Place the knee in the 90° of flexion. The RigidFix cross-pin guide frame is inserted in the femoral tunnel through the AM portal (Fig. 22.7). Insert the cross-pin sleeves

Y.-j. Liu et al. (eds.), *Advanced Application of Arthroscopy*, https://doi.org/10.1007/978-981-15-4684-6_22

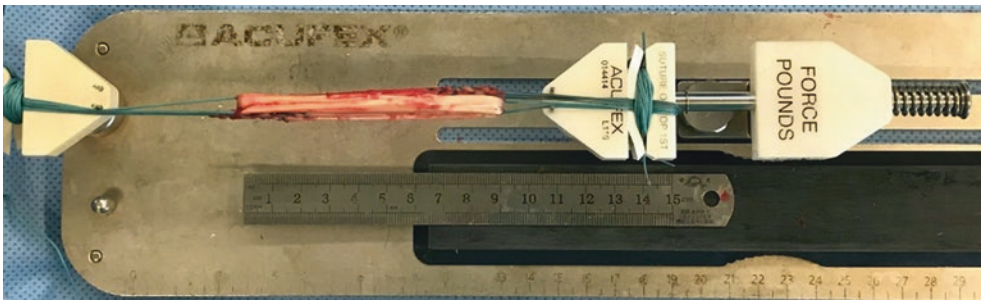

Fig. 22.1 Pretensioning the six-strands tendon graft, the length is 90 mm

Fig. 22.2 Pretension the graft, and the femoral and tibial portions of the tendon graft are sutured by whipstitches to achieve 30 mm

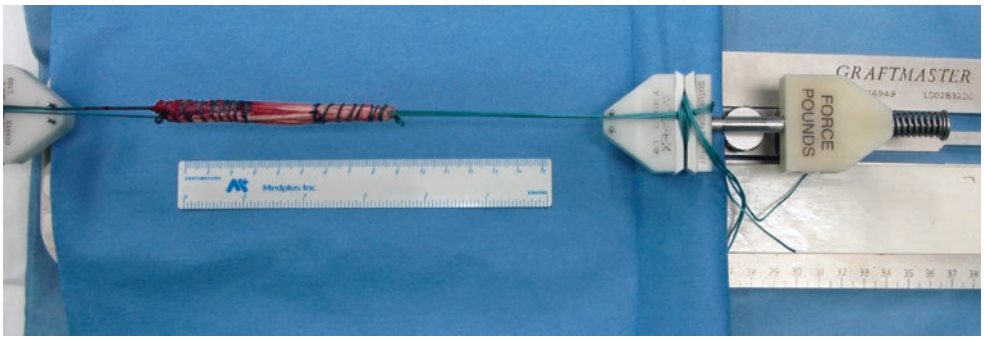

Fig. 22.3 Place a line 30 mm from the end of the femur on the graft, and two no. 5 Ethibond sutures are attached to lead the graft. *(Reprinted with permission from Elsevier and Copyright Clearance Center)*

Fig. 22.4 Drill the femoral tunnel with a depth of 30 mm through the AM portal

through the jig and stab two incisions at the drilling points. Drilling should be performed slowly and firmly without pushing too hard; otherwise the sleeves could easily miss the locking aperture in the tunnel. A 2.4-mm guide pin is inserted into the sleeve (Fig. 22.8) to check if the hole is in the center of the tunnel (Fig. 22.9). The femoral sleeve-trocar assembly is removed, and then insert an arthroscope into the femoral tunnel to check if the cross pins will be placed in the center of the tunnel (Fig. 22.10); otherwise, the tunnel of the cross pins should be recreated (Fig. 22.11).

22.3.4 Tibial Cross-Pin Channels Preparation

Insert the RigidFix cross-pin guide frame into the tibial tunnel. The top of the guide is about 5 mm beneath the tibial plateau (Fig. 22.12a). The insertion points of the cross-pin sleeves should be a little bit anterior to the center of the lateral tibia to protect the peroneal nerve (Fig. 22.12b). The same method as the femoral cross-pin channels preparation to check if the cross pins will be placed in the center of the tibial tunnel.

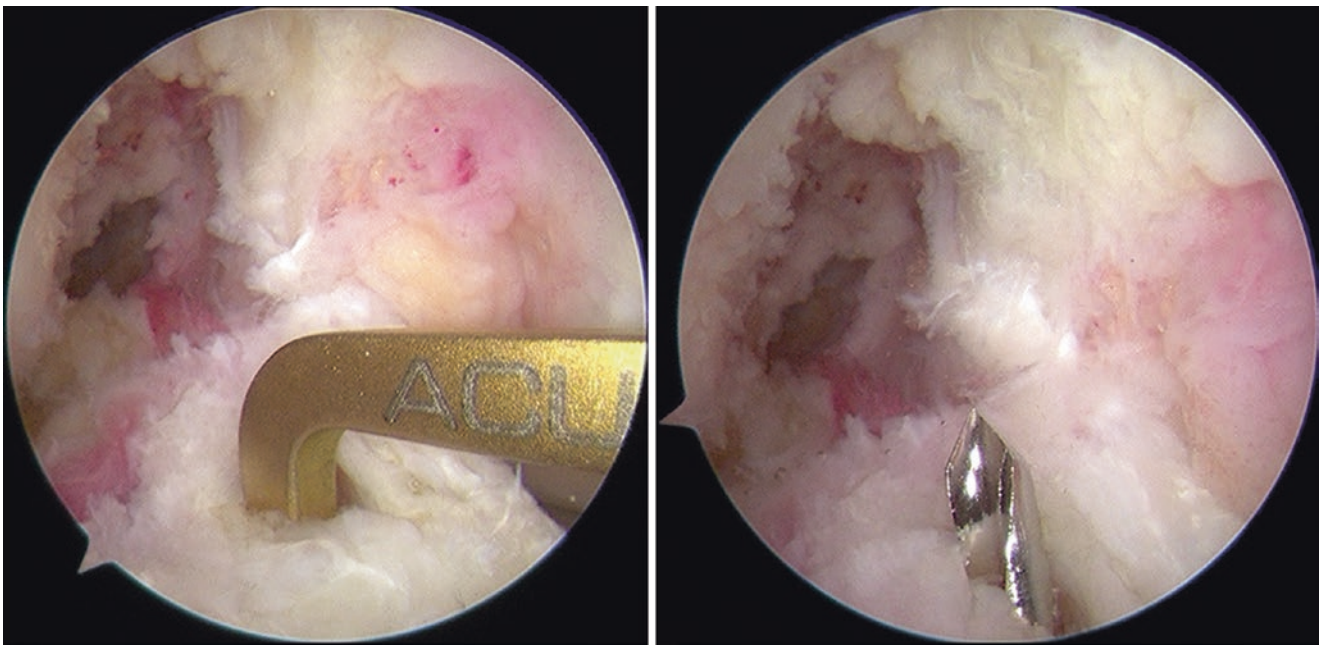

Fig. 22.5 Positioning the tibial tunnel at the center of the footprint of ACL remnant on the tibia

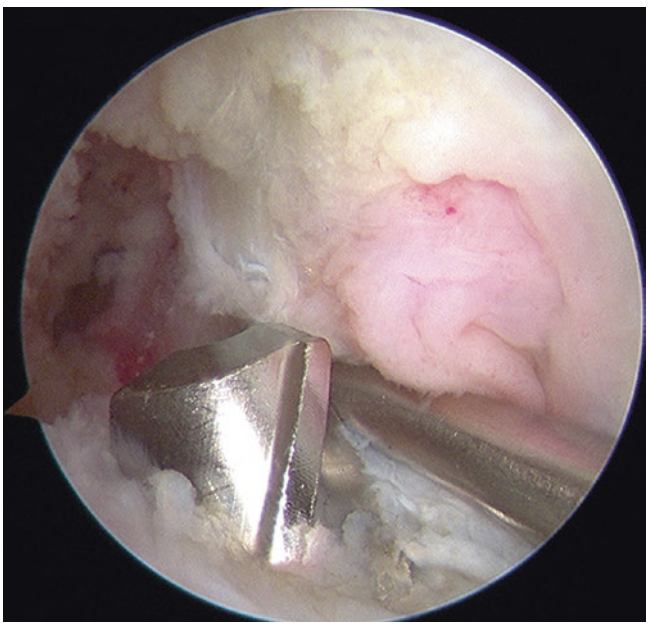

Fig. 22.6 The tibial tunnel was made by a tibial drill

Fig. 22.7 Drill the cross-pin hole femur through the AM portal

22.3.5 Graft Passage and Fixation

The two no. 5 Ethibond traction sutures of the femoral portion are passed through the femoral tunnel, and the quadriceps and skin are pierced by a passing pin. The no. 5 sutures are pulled until the 3-mm marking line reaches the entrance of the femoral tunnel. A guide pin was inserted into the cross-pin sleeves to feel the "soft touch" (Fig. 22.13). Two cross pins were punched through the sleeves from the proximal to the distal end of the femur to

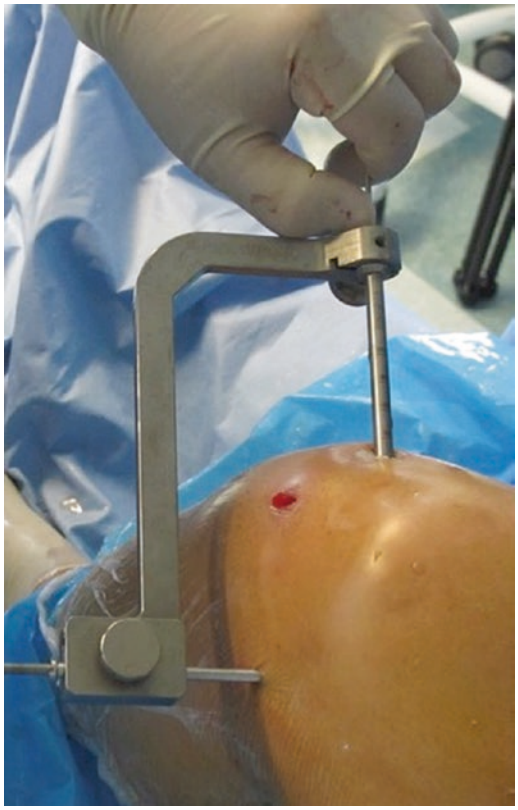

Fig. 22.8 Insert a 2.4-mm guide pin into the sleeve and feel a hard touch in the end

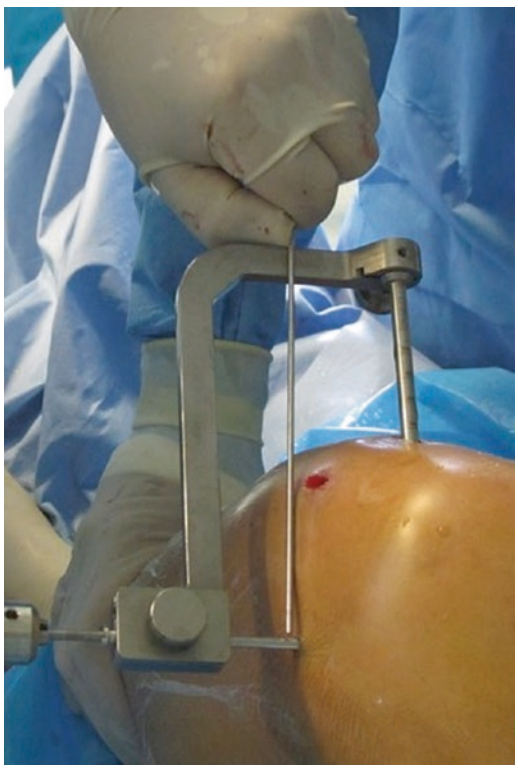

Fig. 22.9 Pull out the guide pin to check if the cross-pin hole is in the center of the tunnel

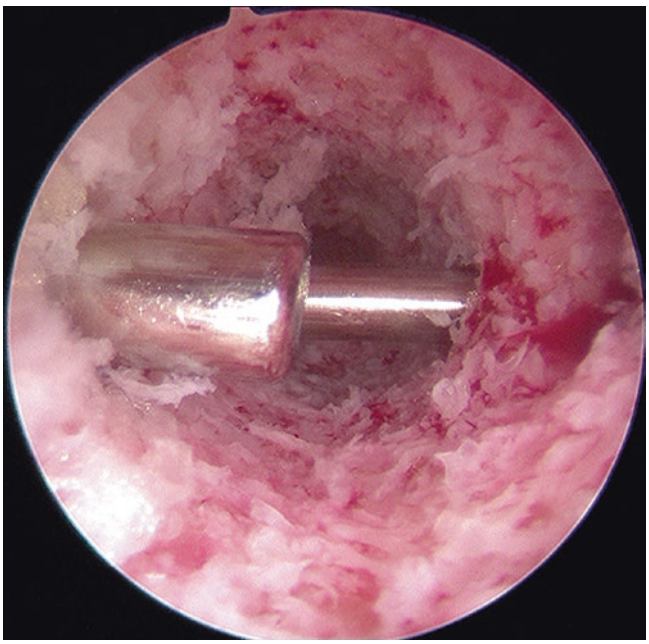

Fig. 22.10 Two guide pins are inserted into the cross-pin channels to check if the pins will be placed in the center of the tunnel

fix the femoral portion of the graft with the knee in 90° of flexion. With the knee in 30° of flexion and tensioning the graft through the tibial end of the graft, fix the tibial portion of the graft from the proximal to distal end by another two cross pins (Fig. 22.14). With flexion and extension of the knee joint, to check there is no impingement between the reconstructed ACL and intercondylar notch or PCL (Fig. 22.15).

22.4 Critical Points

The fixation strength of the cross-pin system would be affected by severe osteoporosis.

- Isotonic tension must be accomplished in multiple strands of the tendon graft; otherwise, the reconstructed ACL would be loosening.
- Drilling the femoral tunnel through the anteromedial portal may result in fracture of the posterior cortex of the femoral tunnel so that the correct angle and depth of the insertion should be made.
- The cross-pin drilling points of the tibia should be 10 mm anteriorly to the fibula head which could avoid the injury of the peroneal nerve.

The guide pins should be placed through the center hole of the guide rod; otherwise, if it slips over the surface of the guide rod, the cross pin will deviate from the center of the cross section of the tunnel and may miss the tendon, consequently affecting the stability of the fixation.

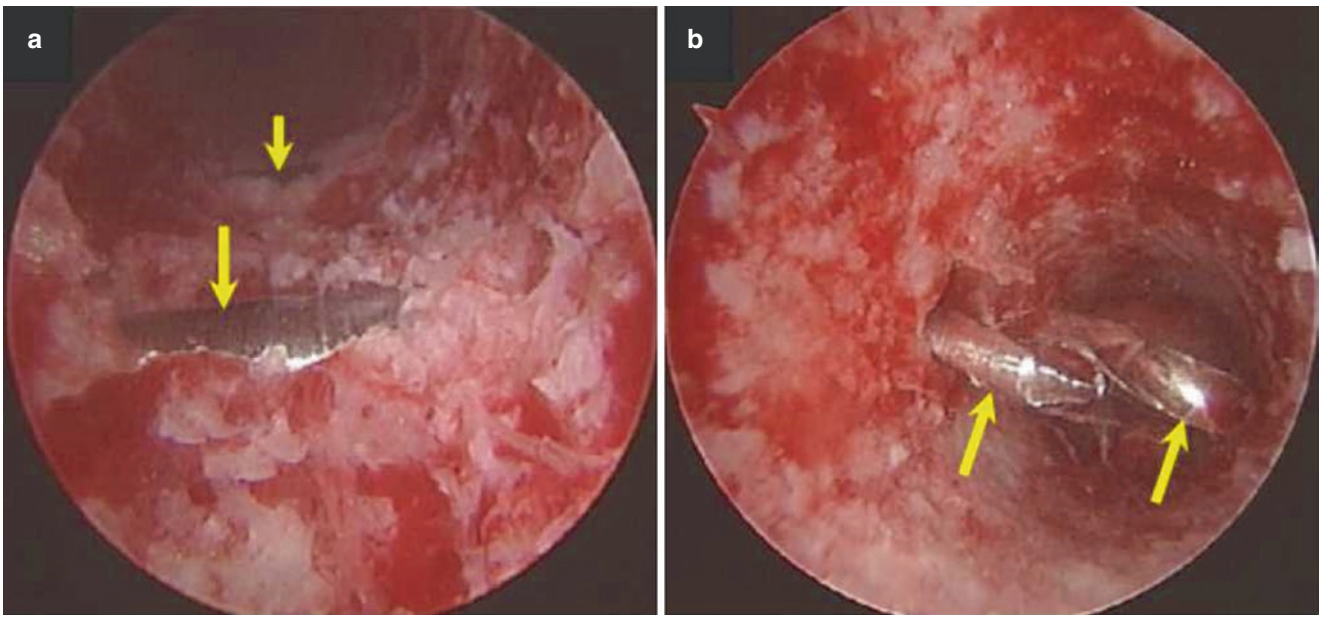

Fig. 22.11 (**a**) The cross pins (arrows) are not in the center of the tunnel. (**b**) Recreate the cross-pin holes and insert the arthroscope into the tunnel to check if the recreated cross-pin holes are in the center. *(Reprinted with permission from Elsevier and Copyright Clearance Center)*

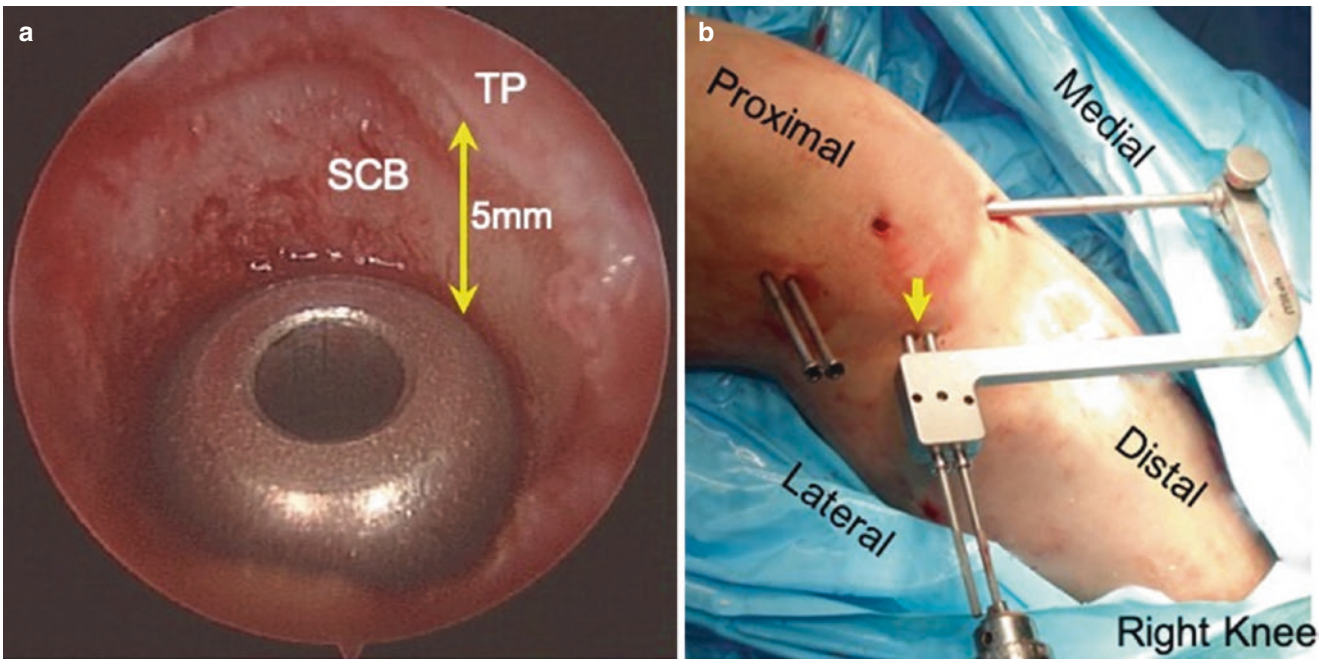

Fig. 22.12 (**a**) Insert the cross-pin guide into the tibial tunnel at the level of 5 mm beneath the articular surface of the tibial plateau (TP); the top of the guide reaches the subchondral bone (SCB) at the proximal entrance of the tibial tunnel. (**b**) The jig of the guide frame and the cross-pin sleeves are placed at the anterolateral of the right tibia (arrow) to create the tibial tunnel. *(Reprinted with permission from Elsevier and Copyright Clearance Center)*

Fig. 22.13 Feel the "soft touch" on the graft which is placed in the tunnel by using a guide pin

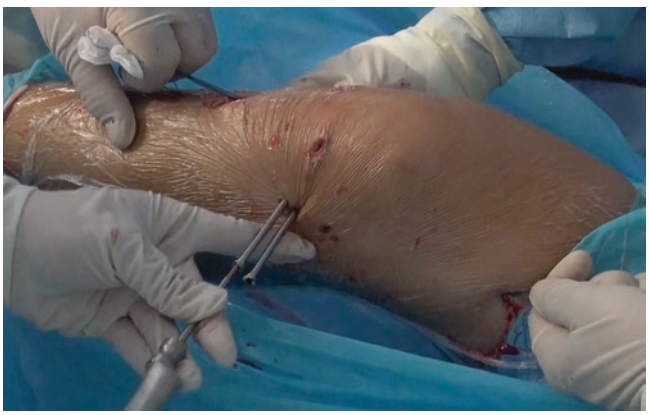

Fig. 22.14 Punch the cross pins under the tension on the graft

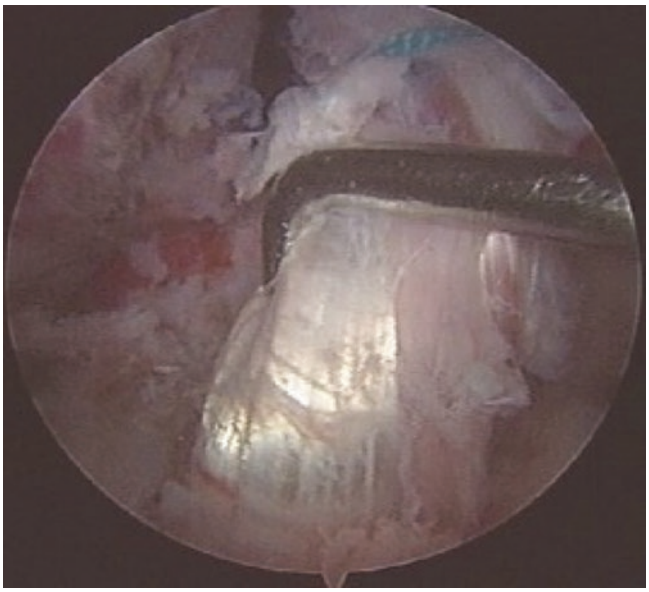

Fig. 22.15 Check the tension of the tendon graft and whether there is an intercondylar collision with flexion and extension of the knee joint

References

1. Monaco E, Labianca L, Speranza A, Agro AM, Camillieri G, D'Arrigo C, et al. Biomechanical evaluation of different anterior cruciate ligament fixation techniques for hamstring graft. J Orthop Sci. 2010;15(1):125–31. https://doi.org/10.1007/s00776-009-1417-9.
2. Harilainen A, Sandelin J. A prospective comparison of 3 hamstring ACL fixation devices--Rigidfix, BioScrew, and Intrafix--randomized into 4 groups with 2 years of follow-up. Am J Sports Med. 2009;37(4):699–706. https://doi.org/10.1177/0363546508328109.
3. Cinar BM, Akpinar S, Hersekli MA, Uysal M, Cesur N, Pourbagher A, et al. The effects of two different fixation methods on femoral bone tunnel enlargement and clinical results in anterior cruciate ligament reconstruction with hamstring tendon graft. Acta Orthop Traumatol Turc. 2009;43(6):515–21. https://doi.org/10.3944/AOTT.2009.515.
4. Bai L, Wang J, Fu Y. Anterior crucial ligament reconstruction with allograft hamstring fixed by Rigidfix and Intrafix anchorages. Zhongguo Xiu Fu Chong Jian Wai Ke Za Zhi. 2007;21(8):882–5.
5. Ahn JH, Park JS, Lee YS, Cho YJ. Femoral bioabsorbable cross-pin fixation in anterior cruciate ligament reconstruction. Arthroscopy. 2007;23(10):1093–9. https://doi.org/10.1016/j.arthro.2007.04.017.

6. Qi W, Liu Y, Xue J, Li H, Wang J, Qu F. Applying cross-pin system in both femoral and Tibial fixation in anterior cruciate ligament reconstruction using hamstring tendons. Arthrosc Tech. 2015;4(5):e397–402. https://doi.org/10.1016/j.eats.2015.03.018.
7. Bellisari GE, Kaeding CC, Litsky AS. Mechanical evaluation of cross pins used for femoral fixation of hamstring grafts in ACL reconstructions. Orthopedics. 2010;33(10):722. https://doi.org/10.3928/01477447-20100826-08.
8. Wu JL, Yeh TT, Shen HC, Cheng CK, Lee CH. Mechanical comparison of biodegradable femoral fixation devices for hamstring tendon graft--a biomechanical study in a porcine model. Clin Biomech (Bristol, Avon). 2009;24(5):435–40. https://doi.org/10.1016/j.clinbiomech.2009.02.003.
9. Marks P, O'Donnell S, Yee G. A pilot clinical evaluation comparing the Mitek bone-tendon-bone cross pin and bioabsorbable screw in anterior cruciate ligament reconstruction fixation, a randomized double blind controlled trial. Knee. 2008;15(3):168–73. https://doi.org/10.1016/j.knee.2007.11.004.
10. Castoldi F, Bonasia DE, Marmotti A, Dettoni F, Rossi R. ACL reconstruction using the Rigidfix femoral fixation device via the anteromedial portal: a cadaver study to evaluate chondral injuries. Knee Surg Sports Traumatol Arthrosc. 2008;16(3):275–8. https://doi.org/10.1007/s00167-007-0459-9.

Applying Allogeneic Cortical Bone Press-Fit Screw in Fixation of Anterior Cruciate Ligament Reconstruction

23

Yu-jie Liu and Wei Qi

23.1 Introduction

There are many fixation methods in anterior cruciate ligament reconstruction by using multiple hamstring tendons. The extra cortical fixation such as Endobutton is widely used (Fig. 23.1). The extra cortical fixation has the largest strength, no cutting of the graft, and full contact between graft and tunnel; however, the fixation point is far from the anatomic insertion of the ACL on the femur which could lead to the bungee and the windshield-wiper effect (Fig. 23.2), [1–6]. How to avoid the disadvantages above is a critical problem.

A previous research reported combining a bioabsorbable screw in the distal femoral tunnel with the extra cortical fixation to avoid tunnel enlargement [7]. However, the disadvantages of the bioabsorbable screw are obvious (Fig. 23.3) such as cutting the graft. In order to solve the above problems, we designed the allogeneic cortical bone press-fit screw (ACBPS, Fig. 23.4). The biomechanical and biological experiments have proved the ACBPS has satisfied biomechanical properties (Fig. 23.5) and biological features (Fig. 23.6). The ACBPS would be accomplished creeping substitution eventually in the bone tunnel [8]. Since 2011, we combined ACBPS with the extra cortical fixation in the clinic (Fig. 23.7) which has achieved the expected effects (Fig. 23.8).

23.2 Preparation of the ACBPS

The allogeneic femoral cortical bones were made into 5–6 mm diameter and 20 mm length ACBPSs. These screws were stored at −80 °C preservation after gamma-irradiation sterilization.

Y.-j. Liu (✉) · W. Qi
Department of Orthopedics, Chinese PLA General Hospital, Beijing, China

23.3 Patient Positioning Setup and Graft Harvest

After general or spinal anesthesia, the patient is placed in the supine position. A routine diagnostic arthroscopy is performed around the joint. Meniscectomy or meniscal repair and treatment for cartilage lesions are performed if necessary. Then, the gracilis and semitendinosus are harvested to obtain a length of 18 cm at least. The tendons are made into 4–6 strands. The tendon graft is 7 to 9 mm in diameter and 90 to 100 mm in length, and pretensioning the tendon graft with 80 pounds for 15 minutes.

23.4 Operative Technique

23.4.1 Femoral Tunnel Preparation

Through the anteromedial (AM) portal, a transportal ACL femoral guide is seated at the center of the ACL footprint.

Fig. 23.1 Different kinds of extra cortical fixation methods

Y.-j. Liu et al. (eds.), *Advanced Application of Arthroscopy*, https://doi.org/10.1007/978-981-15-4684-6_23

Fig. 23.2 Tunnel enlargement after ACLR by using extra cortical fixation

Fig. 23.3 The tendon graft has been cut by the interference screw

Fig. 23.4 The allogeneic cortical bone press-fit screw (ACBPS)

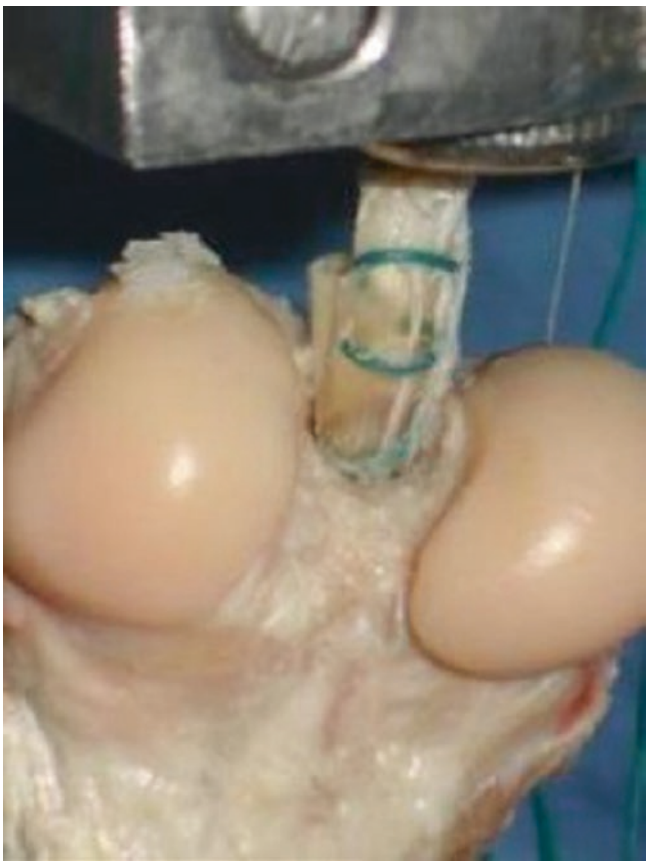

Fig. 23.5 Biomechanical test of the ACBPS in ACLR

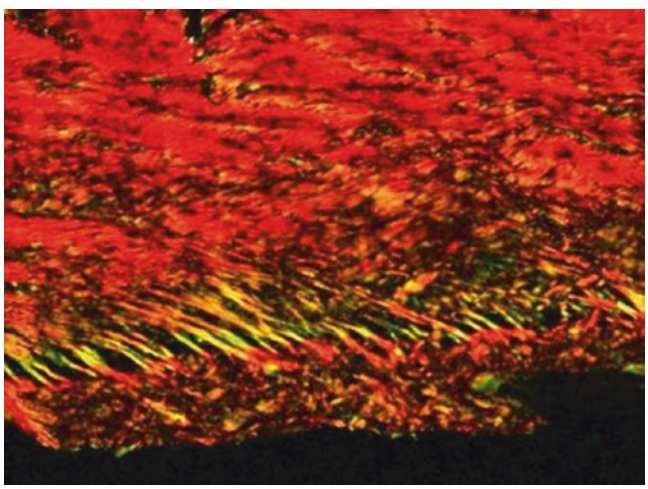

Fig. 23.6 The biological experiment shows a good bone-tendon healing

Then, a straight 2.4-mm guide pin is drilled through the guide and exited on the lateral side of the knee while keeping the knee in a hyperflexion position. Read the scale on the guide pin to measure the length of the femoral tunnel. A 4.5 mm endoscopic drill is used to drill the passing tunnel. An endoscopic drill bit is selected which matches the graft diameter, and the femoral tunnel is produced by the drill. Depth is calculated according to the length of the passing tunnel and the size of the Endobutton loop.

23.4.2 Tibial Tunnel Preparation

The tibial guide is seated at the center of the intercondylar ACL remnant of the tibia through the AM portal. A 2.4-mm guide pin is drilled through the guide and exited at the center of the ACL footprint. Then, a cannulated drill whose diameter is equal to the diameter of the graft is run through the guide pin.

23.4.3 Graft Passage

A line is marked on the graft 6 mm distal to the total channel length which indicates the rotation point for the Endobutton. Attach two #5 Ethibond sutures to one outside hole of the Endobutton device to lead and pass the Endobutton device. Attach a #2 polyester suture to the opposite outside hole of the Endobutton device to rotate the Endobutton device as it exits the femoral cortex. All sutures are passed through the femoral tunnel, and the quadriceps and skin are pierced by a passing pin. The #5 sutures are pulled until the marking line reaches the entrance of the femoral tunnel, and the #2 polyester suture is pulled, rotating the Endobutton device and feeling a "seesaw" to make sure the Endobutton is rotated. Pull the opposite end of the graft on the tibia until the "seesaw" feeling disappears, which means the Endobutton is on the outer femoral cortex and locked.

23.4.4 Graft Tensioning

Cycle the knee through a range of motion prior to tibial fixation to pretension the graft.

23.4.5 Tibial Fixation

Before fixing the tibial side, with flexion and extension of the knee joint, check if there is no impingement between the reconstructed ACL and intercondylar notch or PCL. Tension the graft, and with the flexion of the knee at 20–30°, fix the graft by the interference screw.

23.4.6 ACBPS Insertion

If the washer is used for tibial fixation only, two ACBPSs can be used. Tension the graft and punch an ACBPS into the distal part of the femoral (Fig. 23.7a) and tibial (Fig. 23.7b) tunnel, respectively.

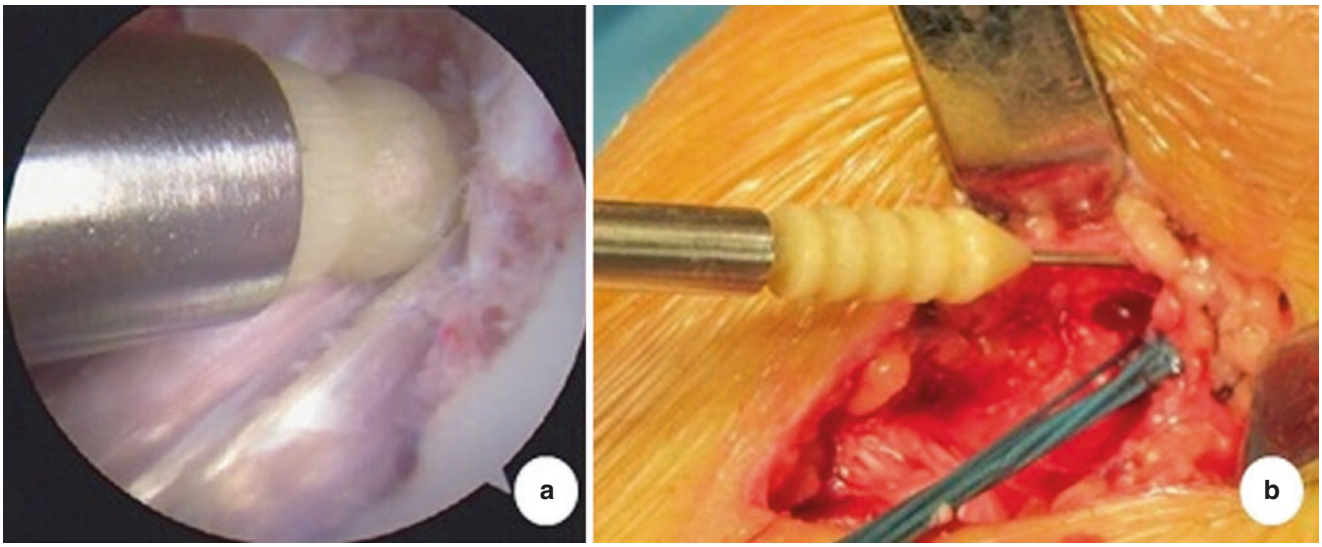

Fig. 23.7 (**a**) Punching an ACBPS into the distal femoral tunnel under arthroscope. (**b**) Punching an ACBPS into the distal tibial tunnel

Fig. 23.8 AP view of X-ray of a right knee (ACBPS both in femoral and tibial tunnel, 1-year postoperation). The X-ray shows there was no tunnel enlargement and bone-graft healing was excellent

23.5 Critical Points

- Isotonic tension must be accomplished in multiple strands of the tendon graft; otherwise, the reconstructed ACL would be loosened.
- The insertion point of the ACBPS should be at the anterolateral part of the entrance of the femoral tunnel to protect the posterior wall.
- A guidewire is applied to maintain the punching direction toward the long axis of the tunnel, which prevents the ACBPS from broken.
- ACBPS combine with the extra cortical fixation is suitable for the shorter graft or the revision cases.
- Tension the graft while punching the ACBPS in order to avoid the loosening of the fixation or the graft.

References

1. Cheung P, Chan WL, Yen CH, Cheng SC, Woo SB, Wong TK, et al. Femoral tunnel widening after quadrupled hamstring anterior cruciate ligament reconstruction. J Orthop Surg (Hong Kong). 2010;18(2):198–202. https://doi.org/10.1177/230949901001800213.
2. Choi NH, Oh JS, Jung SH, Victoroff BN. Correlation between endobutton loop length and tunnel widening after hamstring anterior cruciate ligament reconstruction. Am J Sports Med. 2013;41(1):101–6. https://doi.org/10.1177/0363546512466384.
3. Choi NH, Son KM, Yoo SY, Victoroff BN. Femoral tunnel widening after hamstring anterior cruciate ligament reconstruction with bioabsorbable transfix. Am J Sports Med. 2012;40(2):383–7. https://doi.org/10.1177/0363546511425883.

4. Fauno P, Kaalund S. Tunnel widening after hamstring anterior cruciate ligament reconstruction is influenced by the type of graft fixation used: a prospective randomized study. Arthroscopy. 2005;21(11):1337–41. https://doi.org/10.1016/j.arthro.2005.08.023.
5. Klein JP, Lintner DM, Downs D, Vavrenka K. The incidence and significance of femoral tunnel widening after quadrupled hamstring anterior cruciate ligament reconstruction using femoral cross pin fixation. Arthroscopy. 2003;19(5):470–6. https://doi.org/10.1053/jars.2003.50106.
6. Sabat D, Kundu K, Arora S, Kumar V. Tunnel widening after anterior cruciate ligament reconstruction: a prospective randomized computed tomography--based study comparing 2 different femoral fixation methods for hamstring graft. Arthroscopy. 2011;27(6):776–83. https://doi.org/10.1016/j.arthro.2011.02.009.
7. Lind M, Feller J, Webster KE. Bone tunnel widening after anterior cruciate ligament reconstruction using EndoButton or EndoButton continuous loop. Arthroscopy. 2009;25(11):1275–80. https://doi.org/10.1016/j.arthro.2009.06.003.
8. Qi W, Li CB, Wang JL, Zhu JL, Liu YJ. Experimental study of tendon graft fixation in anterior cruciate ligament reconstruction with cortical press-fit bolt in rabbits. Zhonghua Yi Xue Za Zhi. 2013;93(19):1503–6.

Applying Allogenetic Cortical Bone Cross-Pin in Fixation of Anterior Cruciate Ligament Reconstruction

24

Yu-jie Liu and Wei Qi

24.1 Introduction

One of the benefits of applying cross-pin system in anterior cruciate ligament reconstruction (ACLR) is that the fixation points are close to the anatomic attachments of the ACL (Fig. 24.1) which could lower the risk of the graft in the bone tunnel subject to longitudinal movement, which causes the bungee effect, and transverse movement, which causes the windshield-wiper effect. Applying cross-pin system in the tibial fixation could avoid cutting the graft which is caused by the interference screw fixation. The graft is in full contact with the tunnel which could be beneficial to the bone-tendon healing.

However, metal and bioabsorbable fixation devices have been widely used in ACLR including cross-pin systems (Fig. 24.2). Previous researches reported that disadvantages associated with the use of bioabsorbable cross-pin are the risk of fracture due to degenerative mechanical strength, defect of bone caused by degeneration of bioabsorbable materials, higher cost, and the undesirable biological response [1–4] (Fig. 24.3). The bioabsorbable materials cannot be absorbed completely (Fig. 24.4), and the metal materials will remain in the body permanently. In order to achieve the advantages and avoid the disadvantages of the cross-pin system, we designed the allogenetic cortical bone cross-pin (ACBCP) as a fixation device for ACLR (Fig. 24.5). The biomechanical and biological experiments have proved the ACBCP is as good as the Rigidfix cross-pin system (Figs. 24.6, 24.7, and 24.8). Meanwhile, the clinical application of ACBCP has been achieved the expected effects (Figs. 24.9, 24.10, and 24.11).

Operative Technique and Critical Points are the same as the previous parts of Sect. 3.

Y.-j. Liu (✉) · W. Qi
Department of Orthopedics, Chinese PLA General Hospital, Beijing, China

Y.-j. Liu et al. (eds.), *Advanced Application of Arthroscopy*, https://doi.org/10.1007/978-981-15-4684-6_24

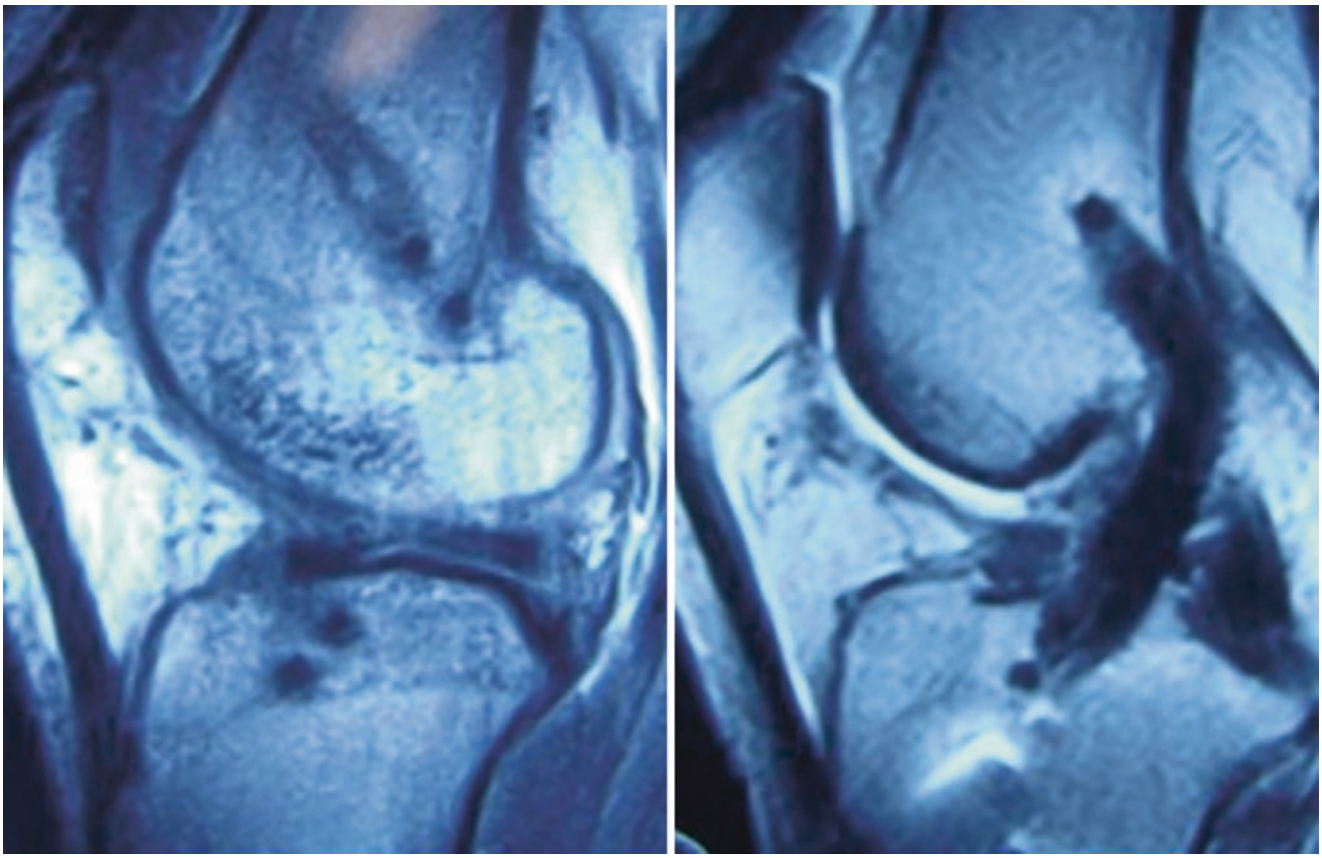

Fig. 24.1 The MRI shows the fixation points are close to the anatomic ACL attachments

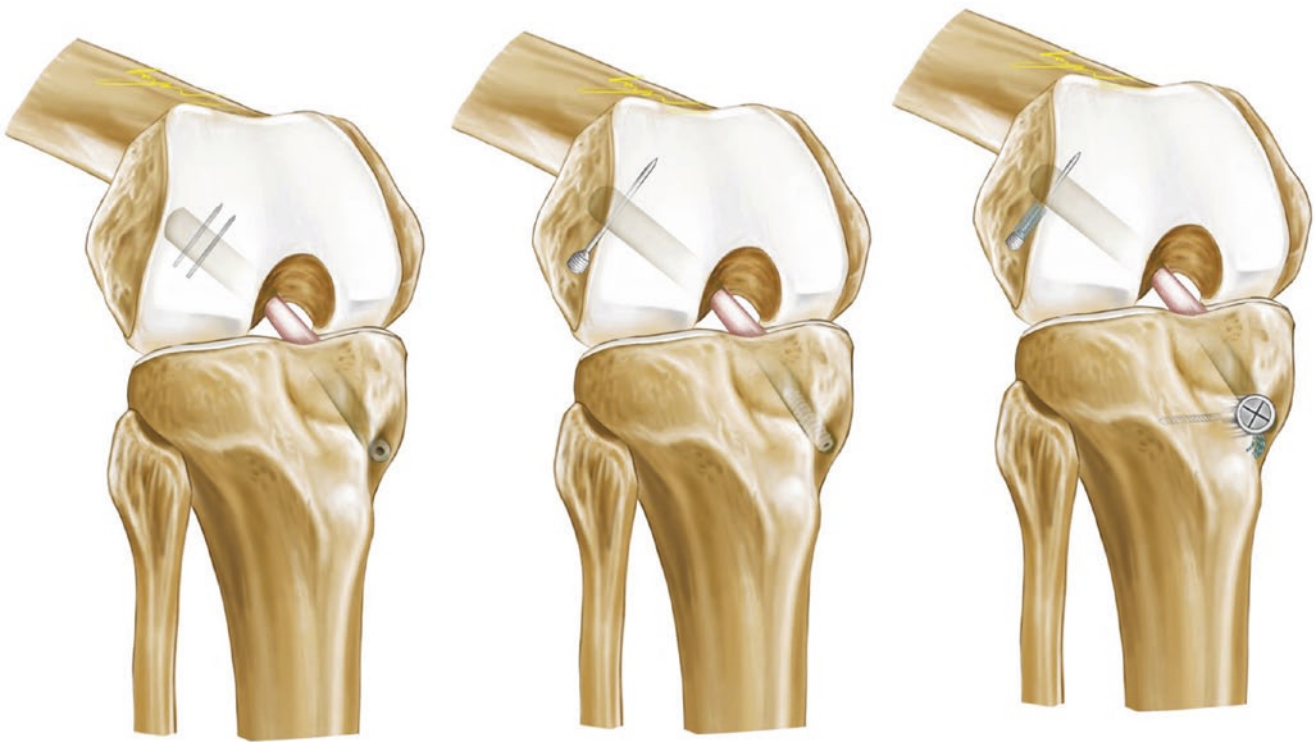

Fig. 24.2 The commonly used cross-pins in the clinic

Fig. 24.3 Aseptic inflammation caused by the bioabsorbable screw

Fig. 24.4 A bioabsorbable screw was not absorbed at 4 years

Fig. 24.5 The allogenetic cortical bone cross-pin (ACBCP)

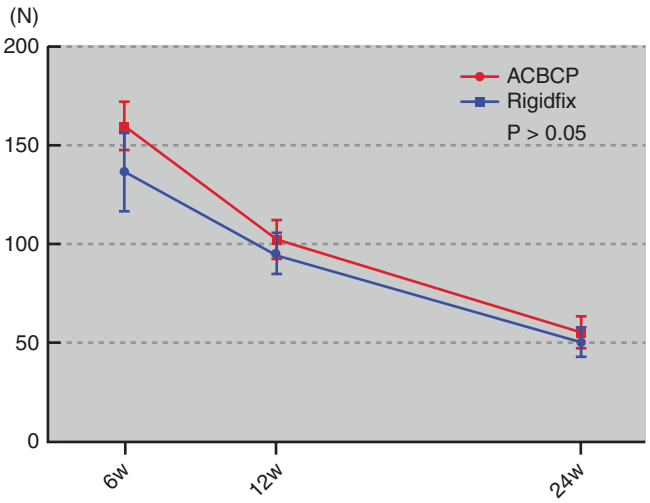

Fig. 24.6 The in vivo biomechanical experiment shows the fixation strength of ACBCP is as good as Rigidfix cross-pin in sheep

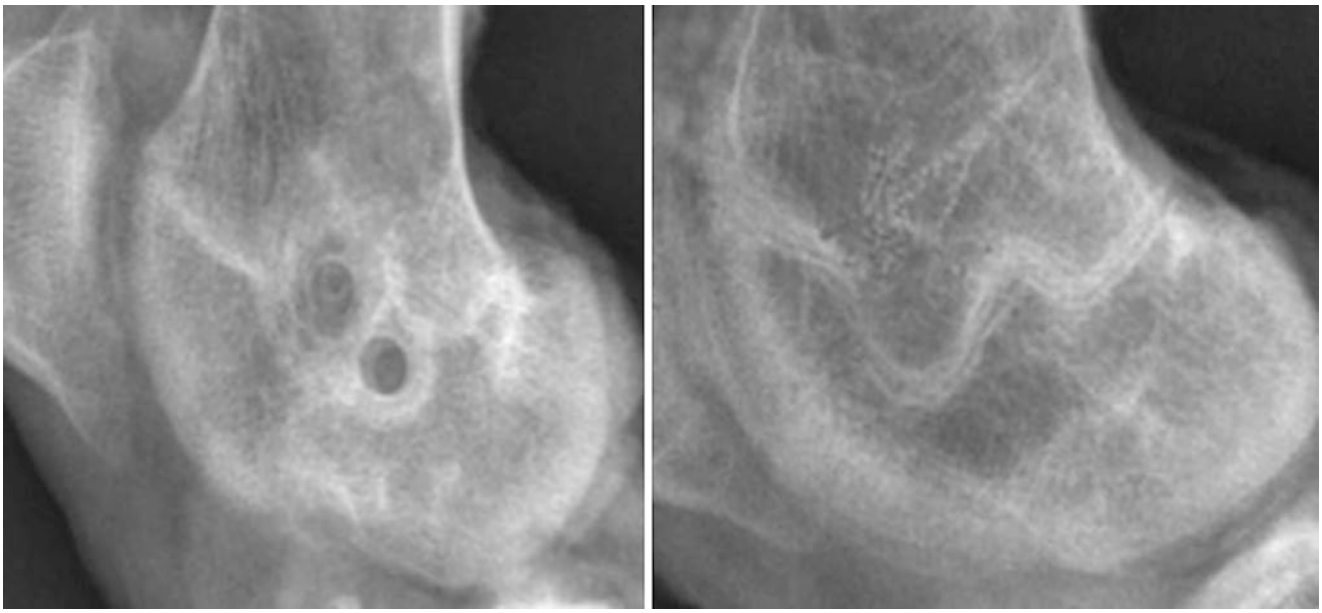

Fig. 24.7 The X-ray of sheep (24 weeks postoperation) shows the Rigidfix cross-pin hole still could be seen (left), and the creeping substitution of ACBCP (right) had been accomplished

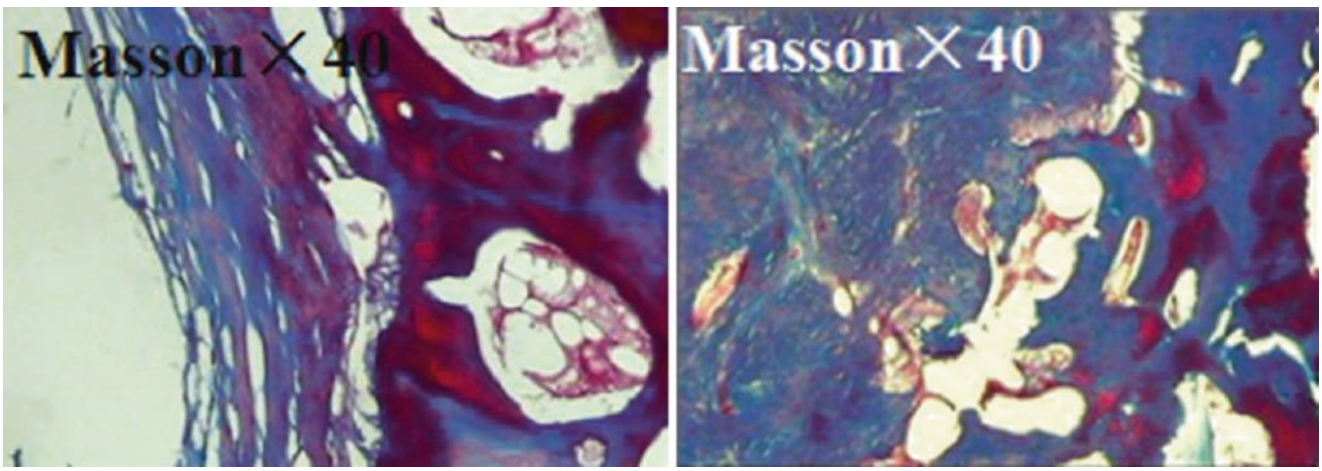

Fig. 24.8 The border of the Rigidfix cross-pin still can be recognized at 24 weeks postoperation (left); however, the border of the ACBCP was hard to recognized (right)

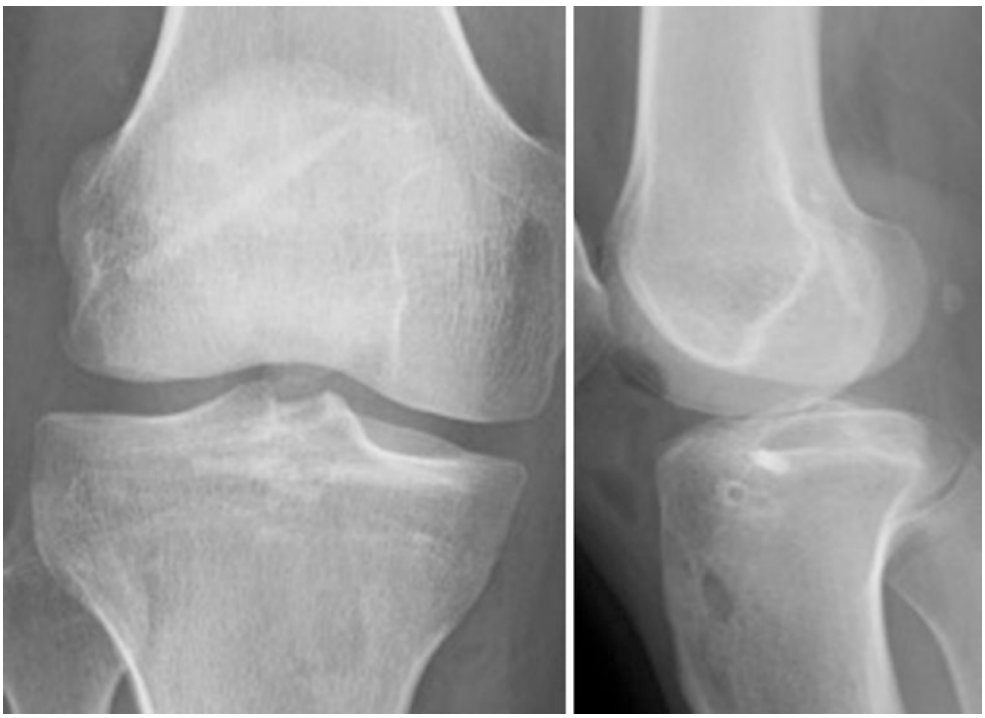

Fig. 24.9 Clinical application of the ACBCP in the femur and tibia (X-ray, 1-day postoperation)

Fig. 24.10 Clinical application of the ACBCP in the femur and tibia (X-ray, 4 weeks postoperation)

Fig. 24.11 Creeping substitution between the ACBCP and tunnel could be recognized after 1 year in a CT scan

References

1. Moisala AS, Jarvela T, Paakkala A, Paakkala T, Kannus P, Jarvinen M. Comparison of the bioabsorbable and metal screw fixation after ACL reconstruction with a hamstring autograft in MRI and clinical outcome: a prospective randomized study. Knee Surg Sports Traumatol Arthrosc. 2008;16(12):1080–6. https://doi.org/10.1007/s00167-008-0593-z.
2. Chevallier R, Klouche S, Gerometta A, Bohu Y, Herman S, Lefevre N. Bioabsorbable screws, whatever the composition, can result in symptomatic intra-osseous tibial tunnel cysts after ACL reconstruction. Knee Surg Sports Traumatol Arthrosc. 2019;27(1):76–85. https://doi.org/10.1007/s00167-018-5037-9.
3. Weiss KS, Weatherall JM, Eick J, Ross JR. Delayed Tibial osteomyelitis after anterior cruciate ligament reconstruction with hamstrings autograft and bioabsorbable interference screw: a case report and review of the literature. Case Rep Orthop. 2017;2017:6383526. https://doi.org/10.1155/2017/6383526.
4. Pereira H, Correlo VM, Silva-Correia J, Oliveira JM, Reis RL, Espregueira-Mendes J. Migration of "bioabsorbable" screws in ACL repair. How much do we know? A systematic review. Knee Surg Sports Traumatol Arthrosc. 2013;21(4):986–94. https://doi.org/10.1007/s00167-013-2414-2.

Bone Bio-Anchors for Repairing Rotator Cuff Tear

25

Yu-jie Liu and Ming Lu

The rotator cuff is a sleeve-like structure made of the tendons of the subscapular muscle, supraspinatus muscle, infraspinatus muscle, and teres minor muscle in the greater tuberosity of the humeral head [1]. Degeneration is liable to develop in the vascular insufficiency zone of the tendons of the supraspinatus and infraspinatus muscles 10–15 mm proximal to the end of the greater tuberosity. In addition, an impact or a trauma to the acromion can also result in degeneration [2]. A suture anchor is conventionally used for repair of the rotator cuff tears [3]. Metal anchors implanted can only stay in the body permanently, while absorbable anchors are high-value consumables made of polylactic acid materials, and their degradation may lead to decreased fixation strength, inflammatory response, and osteolytic defects in the body [4]. Therefore, we have designed and used an allogeneic cortical anchor to repair rotator cuff tear and achieved good results [4].

Cortical bone anchors are bio-embedded with high fixation strength and good histocompatibility [4]. The use of this anchor is beneficial for tendon-bone healing, avoids the use of high-value consumables, reduces medical cost, and eases patients' financial burden [4].

25.1 Preparation of Bone Anchors

Bone anchors, prepared by a biological company, were sealed with plastic bags followed by irradiation using gamma rays and then stored at −80 °C.

The first generation of bone anchors was 4–5.5 mm in diameter and 7.0 mm in length, with a coniform tip and a columnar protrusion at the tail embedded into the implant. The anchor had two threading holes with a diameter of 1 mm and could be penetrated with two no. 2 Ethibond nonabsorbable braided threads for suture tissue (Fig. 25.1).

The second generation of bone anchors was bullet-shaped, with a diameter of 4–5.5 mm and a length of 9.0 mm. Moreover, lateral suture holes and suture grooves were designed to be convenient for the insertion of bone anchors and suture sliding (Fig. 25.2).

The third generation of bone anchors was 4–5.5 mm in diameter and 8.0 mm in length. To increase the friction and pull-out resistance, the anchor body had three to four crossings and two suture holes (Fig. 25.3).

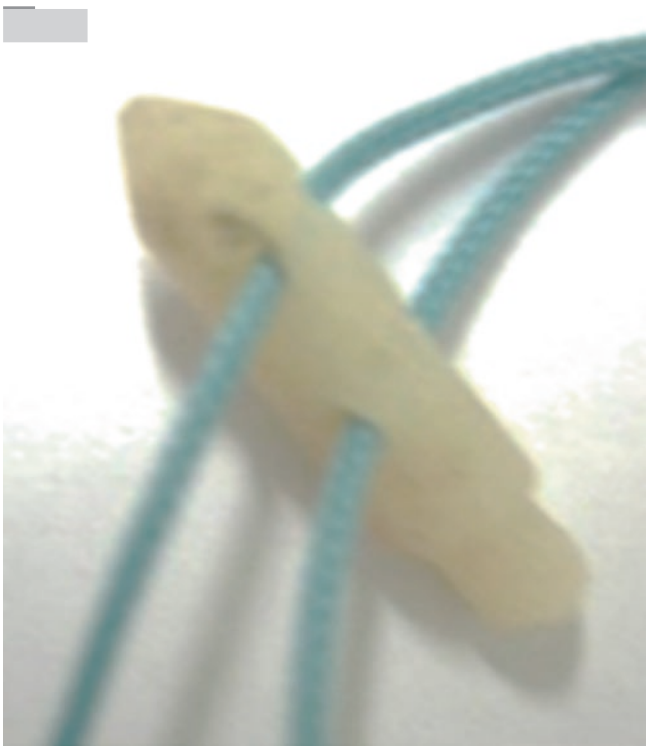

Fig. 25.1 First generation of bone anchors

Y.-j. Liu (✉)
Department of Orthopedics, Chinese PLA General Hospital, Beijing, China

M. Lu
The Fourth Comprehensive Service and Support Center of the PLA Beijing Administration of Veterans Service Affairs Department, Beijing, China

Y.-j. Liu et al. (eds.), *Advanced Application of Arthroscopy*, https://doi.org/10.1007/978-981-15-4684-6_25

Fig. 25.2 Second generation of bone anchor

Fig. 25.3 Third generation of bone anchor

We performed biomechanical experiments on bone anchors, metal anchors, and absorbable anchors. Studies have indicated no significant difference in the maximum pull-out load intensity and failure state between bone anchor and control groups ($P > 0.1$). Animal experiments showed complete healing in the recipient region after bone anchor implantation, and the bone anchor could be used as a material for rotator cuff and Bankart leisure repair [4].

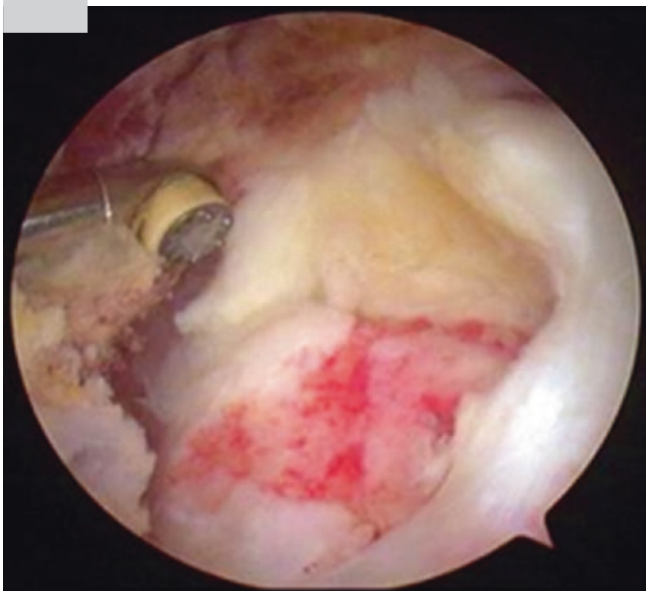

Fig. 25.4 A video for exploring rotator cuff tear and clearing the greater tuberosity of the humeral head

25.2 Essentials for the Operation

25.2.1 Preoperative Preparation

After general anesthesia, the patient was placed in the lateral position, and the affected limb was under the traction of 3–5 kg. Bony landmarks of the shoulder joint and the surgical entrance were marked preoperatively. A soft spot of the posterior shoulder joint was set as arthroscopy entrance, and the anterior and anterolateral entrance was as the entrance for surgical instruments.

25.3 Surgical Methods

A 30° arthroscopy was used to sequentially probe the tear of the rotator cuff (Fig. 25.4), as well as the presence or absence of acromion impacts followed by acromioplasty (Fig. 25.5). Hyperplasia was detected at the greater tuberosity of the humeral head (Fig. 25.6). Hyperplasia-induced osteophyma was grinded to reveal the U-shaped tear of the rotator cuff (Fig. 25.7).

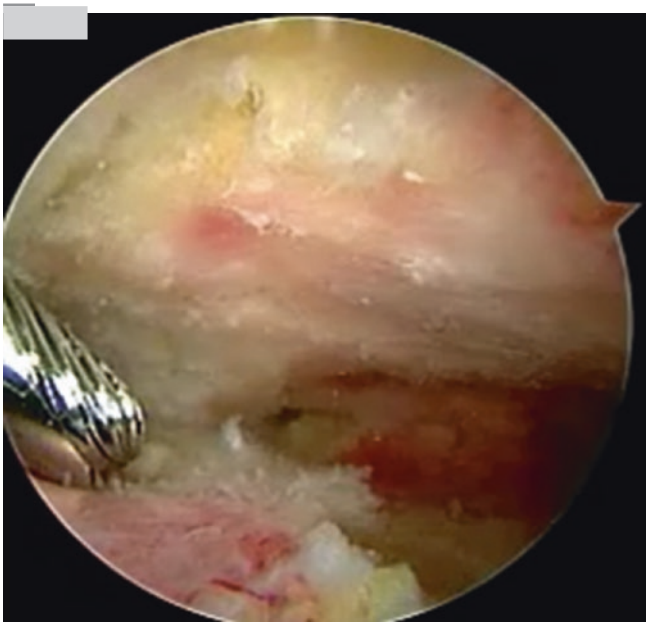

Fig. 25.5 Acromioplasty under arthroscopy

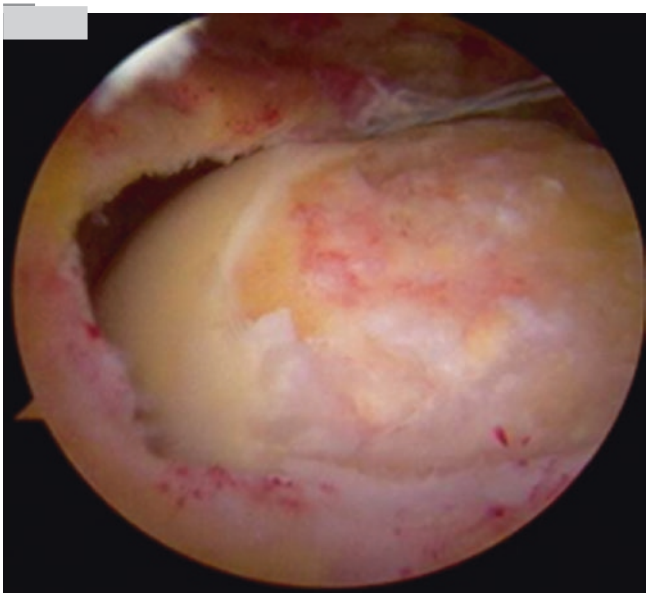

Fig. 25.7 A U-shaped tear of the rotator cuff after grinding osteophyma of the greater tuberosity of the humeral head

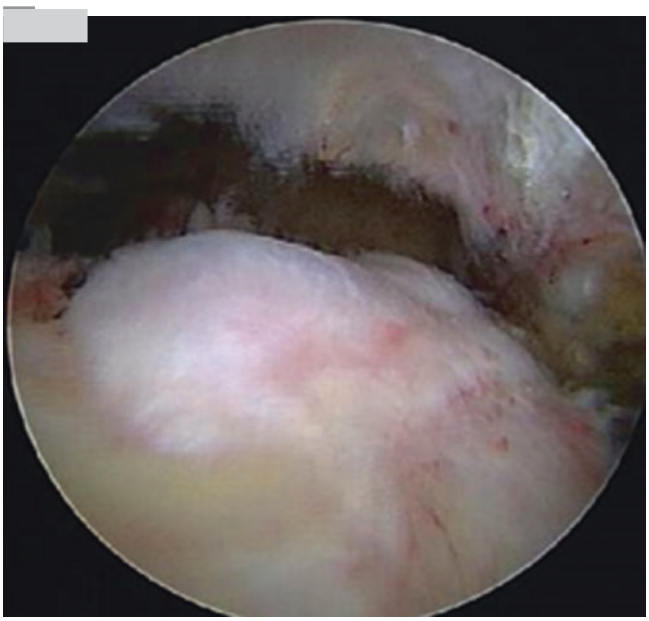

Fig. 25.6 Exploration on osteophyma of the greater tuberosity of the humeral head

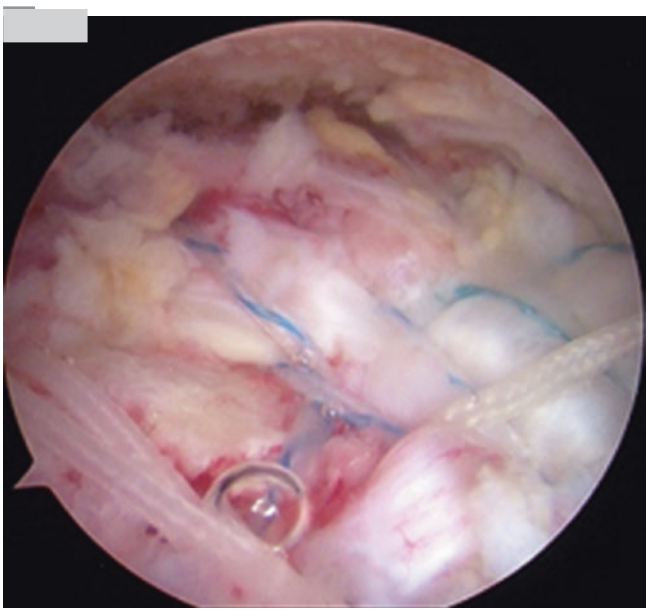

Fig. 25.8 The teared rotator cuff was stitched side to side from U-shape to T-shape

25.4 Implantation of Bone Anchors into the Rotator Cuff

For a huge rotator cuff tear, the rotator cuff was sutured side to side: from a U-shaped tear to a V-shaped and then to a T-shaped (Fig. 25.8). Under arthroscopy, we cleared the foot-print zone of rotator cuff via the anterolateral approach of the lower shoulder joint. A hole opener was used to prefabricate the anchor channel (Fig. 25.9), along which the bone anchor was gradually struck into the greater tuberosity through an arthroscopic cannula (Fig. 25.10). We then pulled the suture to check whether the bone anchor was fixed firmly and sutured the rotator cuff with a suture hook (Fig. 25.11). The rotator cuff was well-sutured (Fig. 25.12), and the postoperative rehabilitation was proceeded.

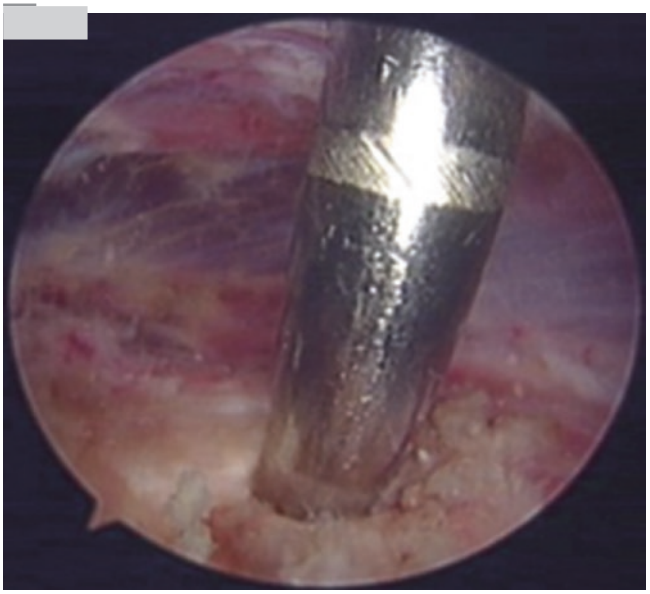

Fig. 25.9 Prefabrication of anchor holes in the foot-print zone of the rotator cuff of the greater tuberosity

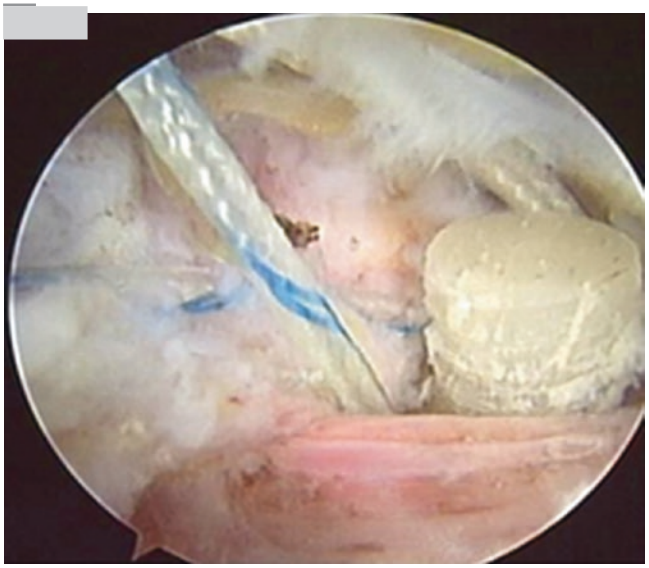

Fig. 25.11 Bone anchor implanted into the greater tuberosity of the humeral head and sutured rotator cuff

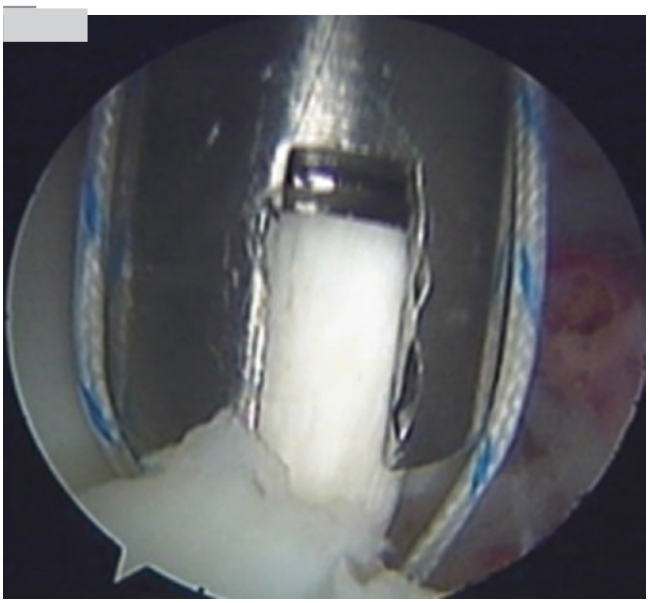

Fig. 25.10 The bone anchor was gradually struck via the cannula into the greater tuberosity

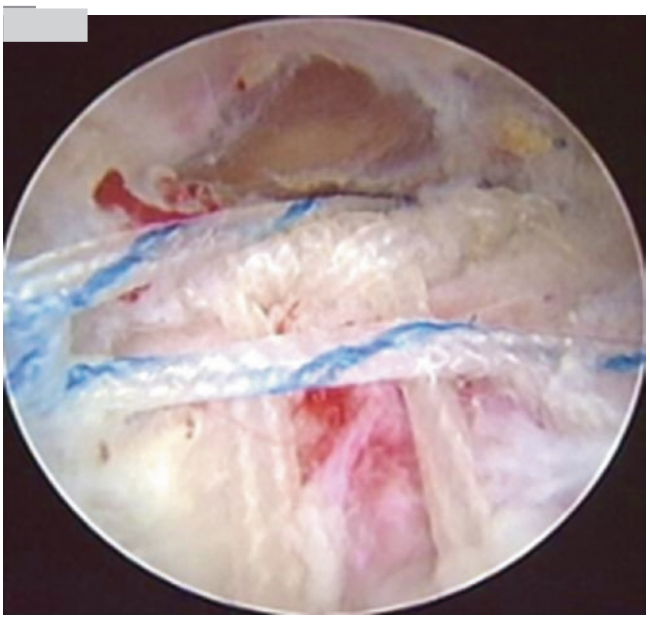

Fig. 25.12 Suture of the rotator cuff

Bone anchor double-row fixation technique for repairing the rotator cuff: Inner-row bone anchors were implanted into the intertubercular sulcus near the edge of the articular surface of the humeral head (Fig. 25.13), and then the rotator cuff was sutured. Outer-row bone anchors were inserted at the bone bed of the greater tuberosity of the humeral head (Fig. 25.14).

Double-row fixation makes full contact between the rotator cuff tissue and the bone bed, increases the tendon-bone contact area, reduces the load of each anchor, and improves the mechanical strength.

Postoperatively, plain X-ray films showed a gradual creep substitution after bone anchor insertion, and the bone anchor was fused with the recipient area after 16 weeks (Fig. 25.15).

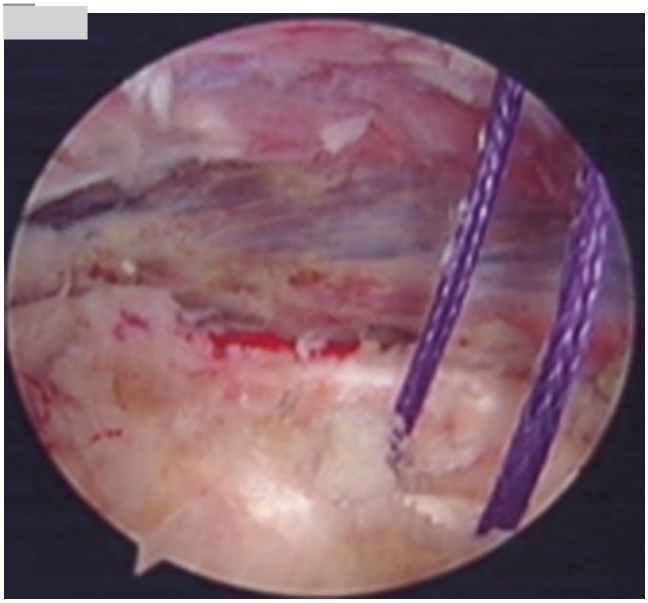

Fig. 25.13 Inner-row bone anchors near the edge of humeral head articular surface

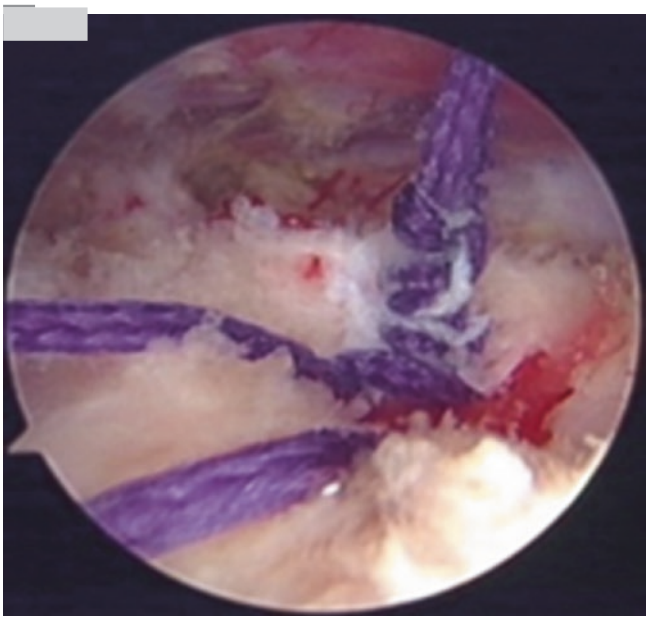

Fig. 25.14 Outer-row bone anchors in the greater tuberosity of the humeral head

Fig. 25.15 Creeping substitution at different time points after bone anchor fixation for repairing rotator cuff tear

25.5 Critical Points

1. For patients with osteoporosis, special attention should be paid to the risk of pulling out the anchor. Dispersion of stress can be achieved by double-row anchor fixation.
2. The inner-row anchor should be inserted at the anatomical neck of the humeral head, where the anchor is easy to pull out because of the relatively thick cortex.
3. To increase the stability of fixation, the number of anchors can be increased in patients with osteoporosis as appropriate.

References

1. Cooper A, Ali A. Rotator cuff tears. Orthopaedics III: Upper Limb. Surgery (Oxford). 2013;31(4):168.
2. Jarrett CD, Schmidt CC. Arthroscopic treatment of rotator cuff disease. J Hand Surg Am. 2011;36(9):1541–52. quiz 1552
3. Schmidt CC, Jarrett CD, Brown BT. Management of rotator cuff tears. J Hand Surg Am. 2015;40(2):399–408.
4. Liu Y, Wang Y, Wang L. Practical Operative of Arthroscopy. Beijing: People's military surgeon press; 2011.

Repair of Bankart Lesion with Biological Bone Anchors

26

Yu-jie Liu and Ming Lu

26.1 Introduction of Bankart Lesion

The shoulder is one of the most mobile and unstable joints in the body [1]. Shoulder dislocations represent 50% of all joint dislocations and 95% of which are anterior dislocation of the shoulder [2]. In 1923, Perthes and Bankart described anterior dislocation of the shoulder with lesion of the anterior inferior glenoid labrum of the shoulder, which is called Bankart lesion [3].

X-ray examination contributes to the diagnosis of shoulder dislocation (Fig. 26.1) and Hill-Sachs lesion, as well as humeral head fracture (Fig. 26.2) [3]. Three-dimensional CT reconstruction is of great value in the diagnosis of glenoid fracture (Fig. 26.3) [3]. MRI of the shoulder is of great significance in the diagnosis of rotator cuff tear, glenoid labrum lesion, and Hill-Sachs injury (Fig. 26.4) [4].

Anterior inferior shoulder subluxation often results in glenohumeral ligament, glenoid labrum complex, shoulder capsule, or Hill-Sachs lesions. All these lesions need to be repaired with absorbable anchors, PEEK suture anchors, and metal anchors (Fig. 26.5). If should dislocation occur again after surgery, it will be difficult to remove the anchors and implant the glenoid anchors.

Fig. 26.1 X-ray image of shoulder dislocation

26.2 Preparation of Bone Anchors

In 2005, we developed an allogeneic bone anchor for Bankart lesion. The bone anchors were made of allogeneic cortical bone. Bone anchors have been modified in different periods. Some bone anchors were engraved with transverse lines in the body to increase friction, and the lateral grooves were convenient for suture sliding (Fig. 26.6). Animal experiments showed that allogeneic bone had a natural three-dimensional structure with good bone conductivity, osteoinduction, and histocompatibility. The elastic modulus of allogeneic bone anchor was similar to human skeleton. The tensile strength of allogeneic bone anchor was comparable to that of metal anchor, absorbable anchor, or PEEK anchor. Different types of bone anchors have achieved good clinical results in the repair of Bankart lesion.

26.3 Key Points of Operation

26.3.1 Preoperative Preparation

Preoperative routine X-ray and three-dimensional CT reconstruction of the shoulder were performed to determine

Y.-j. Liu (✉)
Department of Orthopedics, Chinese PLA General Hospital, Beijing, China

M. Lu
The Fourth Comprehensive Service and Support Center of the PLA Beijing Administration of Veterans Service Affairs Department, Beijing, China

Y.-j. Liu et al. (eds.), *Advanced Application of Arthroscopy*, https://doi.org/10.1007/978-981-15-4684-6_26

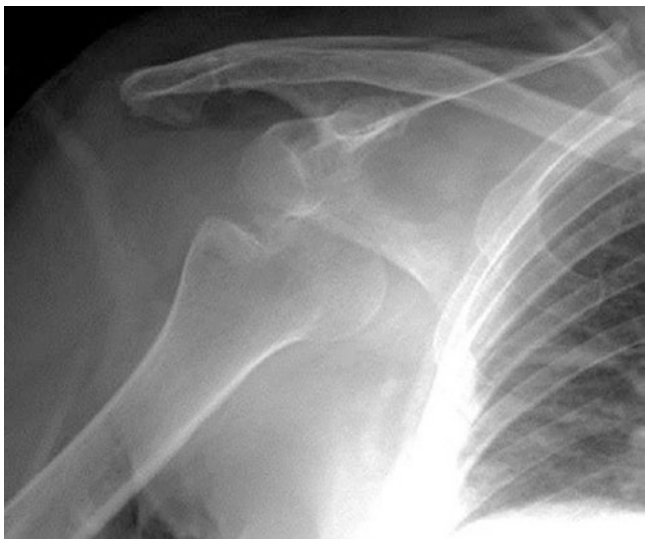

Fig. 26.2 Hill-Sachs humeral head fracture

Fig. 26.3 Three-dimensional reconstruction of glenoid fracture

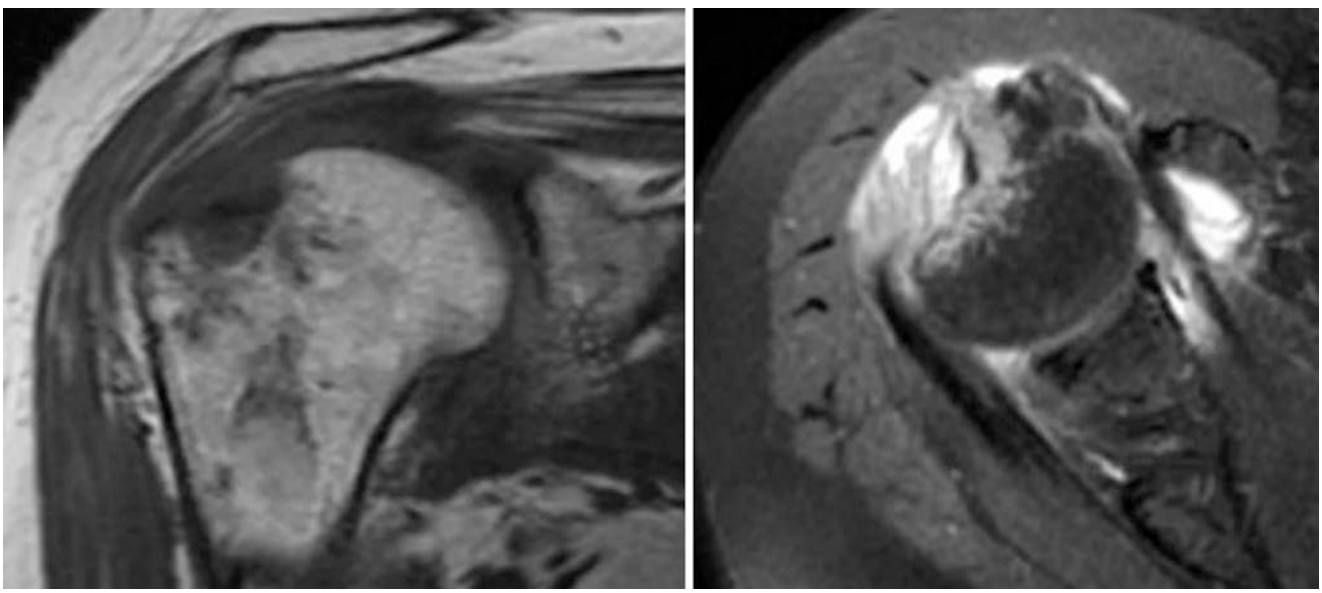

Fig. 26.4 MRI displaying Hill-Sachs lesion and rotator cuff tear

whether there was bone defect in glenoid and humeral head as well as the type of Bankart lesion. If necessary, MRI of shoulder joint should be performed to understand the injury of glenoid labrum, rotator cuff, and Hill-Sachs lesion. After general anesthesia, the affected limb was subjected to 5–6 kg traction in lateral position.

26.3.2 Surgical Approach

Arthroscopy was performed though standard posterior approach. First, glenohumeral joint and Bankart lesion in the shoulder were identified (Fig. 26.7). The glenoid capsule-glenohumeral ligament-glenoid labrum complex was fully released by stripping the scar tissue with a bone spatula (Fig. 26.8). The wound of the glenoid bone was cleaned up by radiofrequency or gouging to fresh the wound of the glenoid bone.

26.4 Repair of Bankar Lesion

The location of implant was designed according to the size of glenoid labrum lesion. The cartilage of 2–3 mm in width at the edge of the glenoid labrum was removed. A hole was drilled at the edge of the glenoid labrum with a drill with the

Fig. 26.5 Implantation of anchors in the shoulder for repair of Bankart lesion

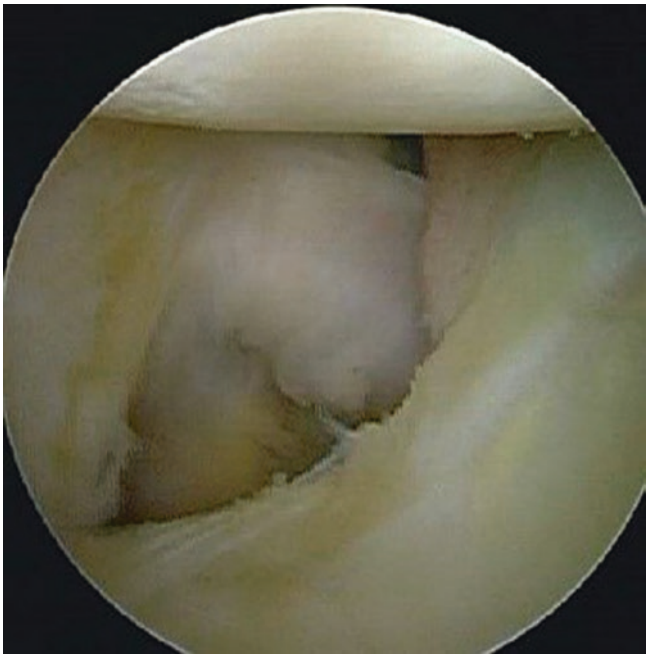

Fig. 26.7 Arthroscopy indicated Bankart lesion

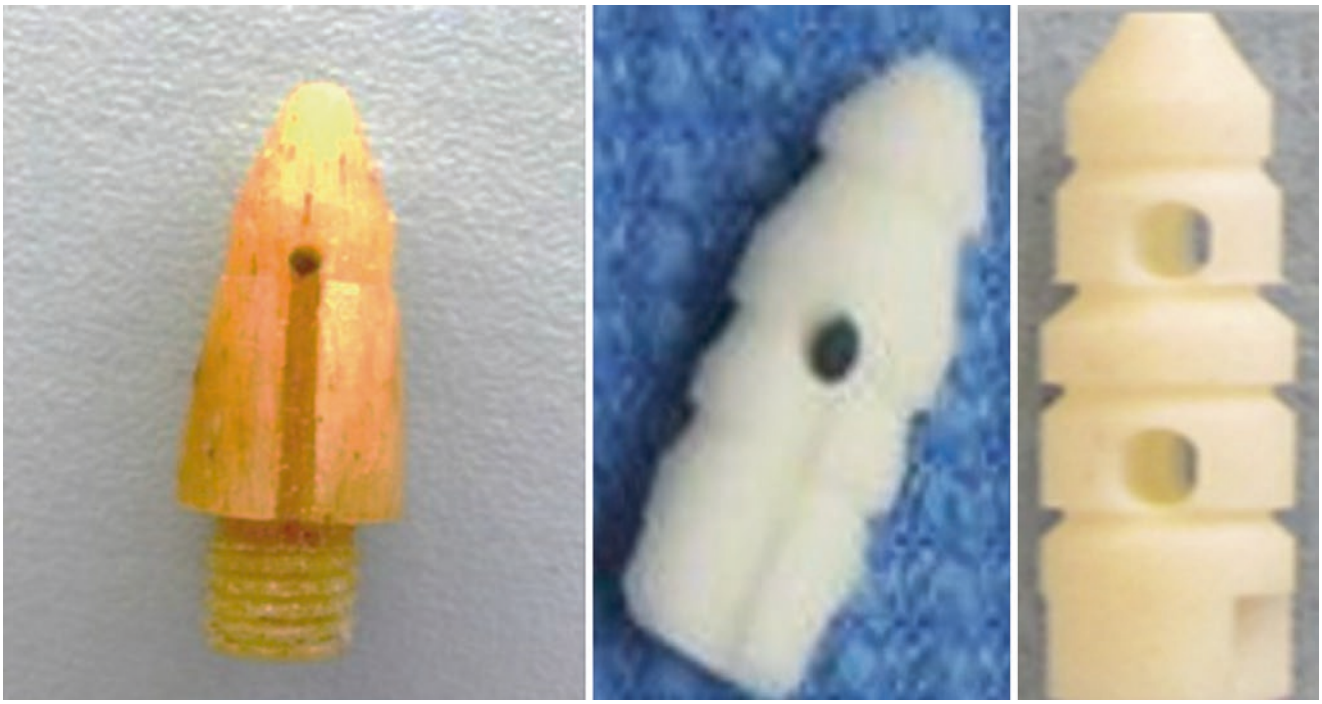

Fig. 26.6 Different types of bone anchors

same diameter as that of the bone anchor (Fig. 26.9). The bone anchor was inserted into the inner opening of the bone hole through the channel with a holder and gently tapped into the bone hole (Fig. 26.10). The tail of the anchor was buried in the cortical bone of the glenoid labrum (Fig. 26.11). The suture on the anchor was introduced to pass through the glenoid labrum with the suture hook and then knotted to tighten the anterior joint capsule (Fig. 26.12).

Bone anchors were inserted into the glenoid labrum from bottom to top and then sutured to repair Bankart lesion.

Routine X-ray and three-dimensional CT reconstruction were performed after surgery (Fig. 26.13). Slings were used

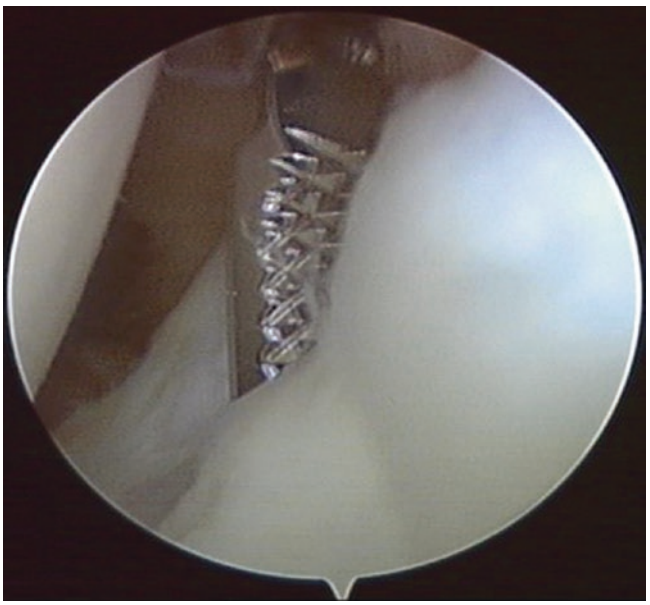

Fig. 26.8 Removal of the wound surface of Bankar lesion with a bone spatula

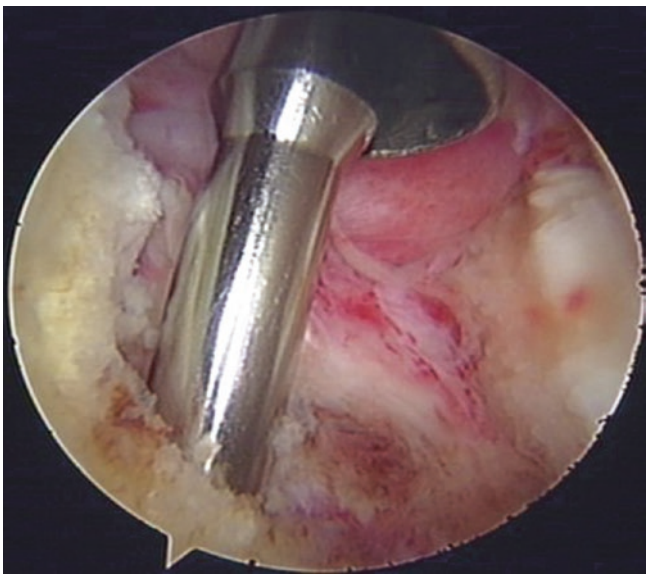

Fig. 26.9 Drilling the nail path of prefabricated anchor

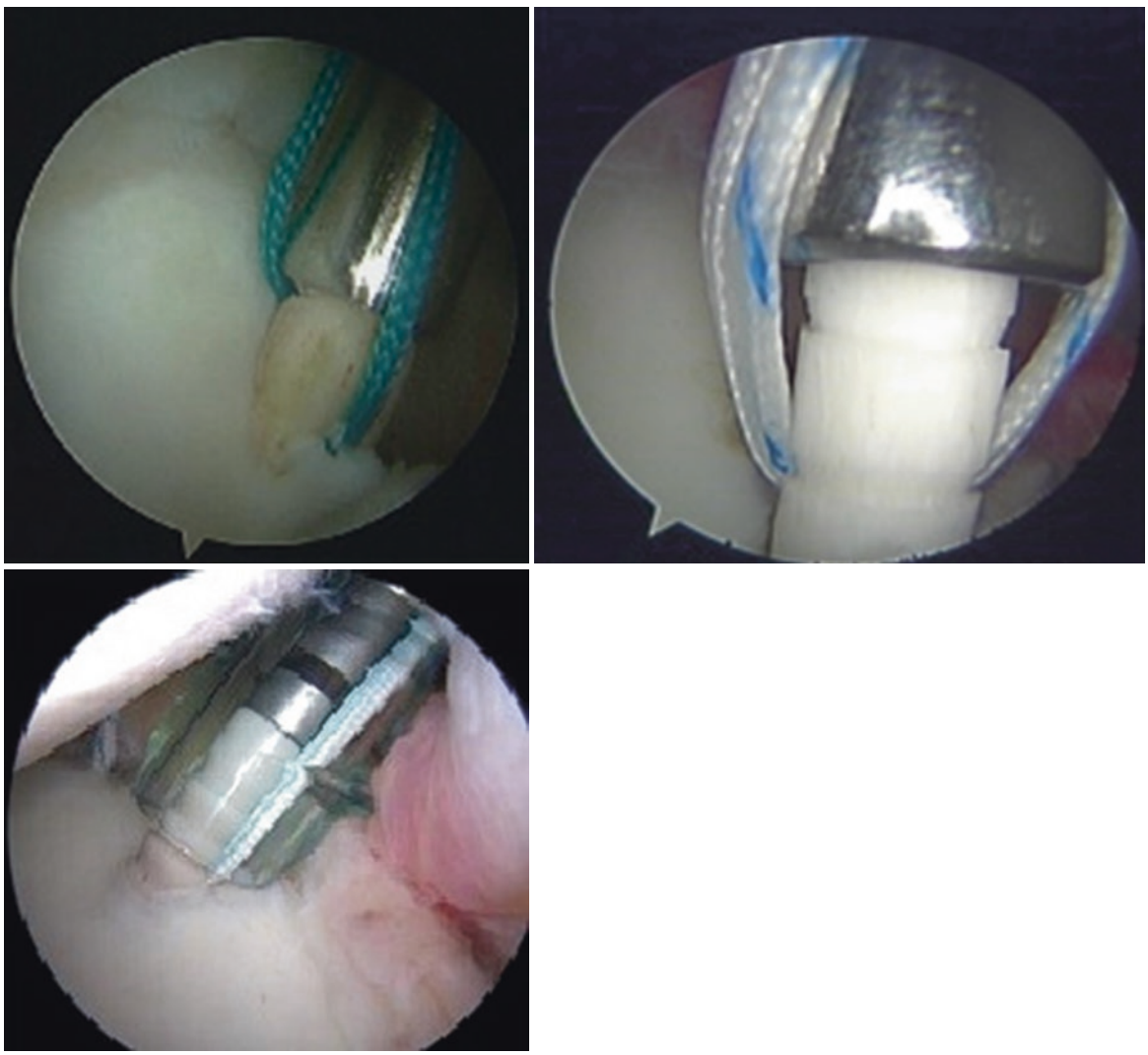

Fig. 26.10 Implantation of different types of bone anchors into bone hole

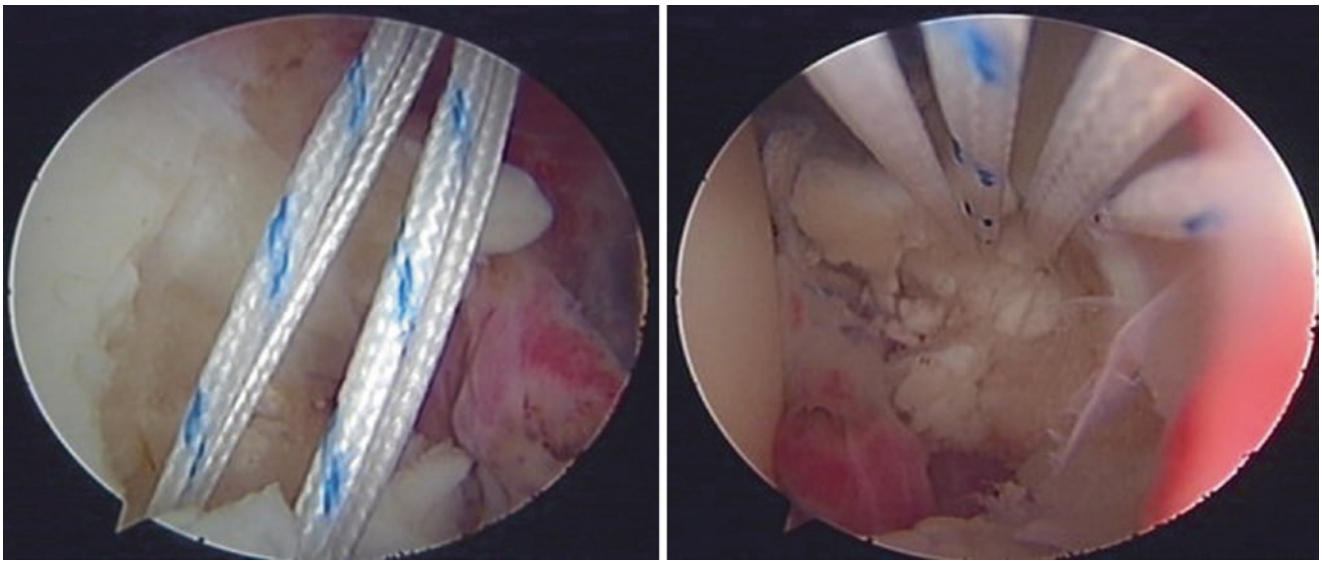

Fig. 26.11 Hammering the bone anchor into the cortex of the glenoid labrum, without exposure of anchor tail

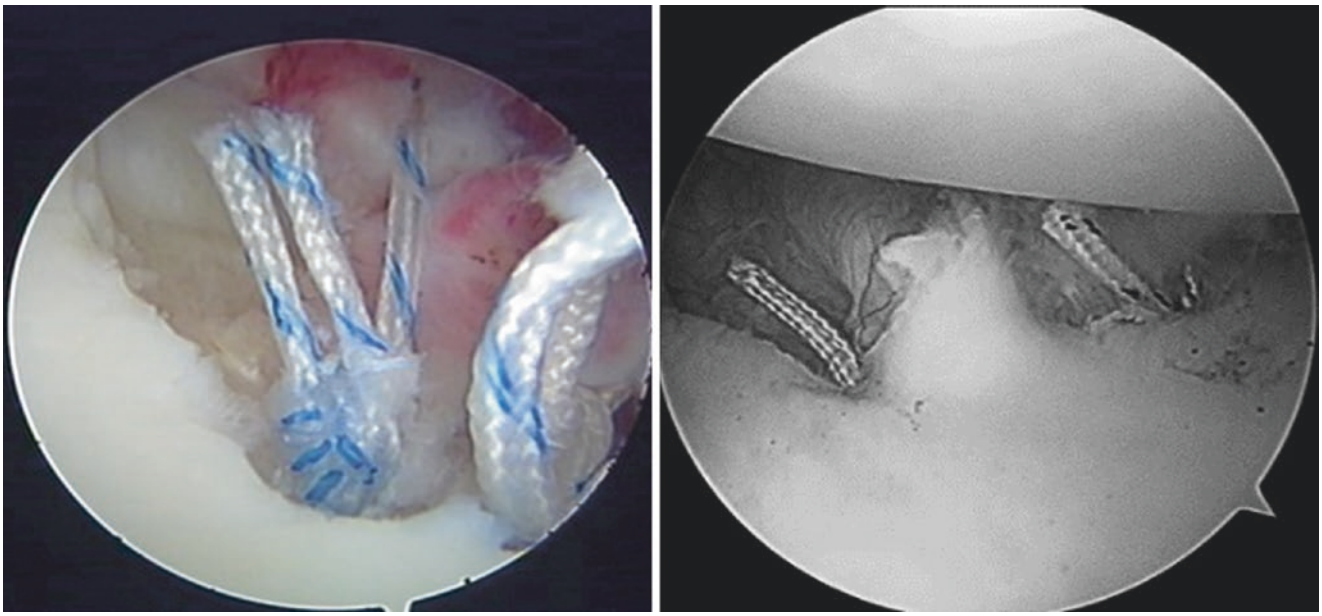

Fig. 26.12 Anchor implantation and suture for tightening anterior joint capsule

Fig. 26.13 Postoperative X-ray of the shoulder displays that the position of anchor in the glenoid region was good

to break the dislocated shoulder for 4–6 weeks. Function exercise was performed under the guidance of a rehabilitation physician.

26.5 Critical Points

1. The diameter of the drill should be matched with that of the anchor to avoid difficult anchor implantation and poor anchor control.
2. The bone of the anchor is brittle. Pay attention not to use too much force during the process of anchor implantation to avoid anchor crushing.
3. The tail end of the anchor should be hit into the cortex of the glenoid region of the shoulder to avoid wearing the cartilage of the humeral head.

References

1. Yamamoto N, Muraki T, An KN, et al. The stabilizing mechanism of the Latarjet procedure: a cadaveric study. J Bone Joint Surg Am. 2013;95(15):1390–7.
2. Memon M, Kay J, Cadet ER, Shahsavar S, Simunovic N, Ayeni OR. Return to sport following arthroscopic Bankart repair: a systematic review. J Shoulder Elb Surg. 2018;27(7):1342–7.
3. Randelli P, Cucchi D, Butt U. History of shoulder instability surgery. Knee Surg Sports Traumatol Arthrosc. 2016;24(2):305–29.
4. Liu Y, Wang Y, Wang L. Practical Operative of Arthroscopy. Beijing: People's military surgeon press; 2011.

27 Autologous Scapular Bone Block with Bone Allograft Pins for Bony Bankart Lesion

Yu-jie Liu and Ming Lu

Shoulder dislocation with bony Bankart lesion (Fig. 27.1) seriously impacts shoulder stability. Currently, open surgery or arthroscopic Latarjet-Bristow surgery (Fig. 27.2) [1] is often used for restoring the shoulder stability [2]. Although this surgery has better outcomes, the autologous coracoid process of the shoulder is taken as a bone graft, which results in a series of complications, including brachial plexus injury, tendon and ligament injuries after the coracoid process is removed, and instability of the anterior and superior shoulder joints, screw breakage (Fig. 27.3), bone nonunion (Fig. 27.4), or screw displacement due to infected bone resorption (Fig. 27.5) [3].

Herein, we describe the technique of autologous scapular bone block with allograft bone pins and suturing for repair of the shoulder joint after a bony Bankart lesion [4]. Literature review and anatomical studies have indicated that there is no important tissue structure around the scapula (Fig. 27.6). Scapular bone block for repair of bony Bankart lesion has the advantages of convenient material extraction and no significant impact on the shoulder joint. Therefore, good clinical efficacy can be achieved [4].

27.1 Surgical Procedures

27.1.1 Preoperative Preparation

Enrolled patients were interviewed about their medical history, and a physical examination was performed to record the mobility of the shoulder join. Imaging examination of the shoulder joint was performed to determine the location, range, and size of the glenoid defect. CT reconstruction was performed to measure the quality of the bone (Fig. 27.7). Magnetic resonance imaging was performed to assess the histologic and structural damage of the shoulder joint. Preoperatively, the coracoid process, acromion process, clavicle, acromioclavicular joint, and scapula were marked for surgical examination (Fig. 27.8).

27.1.2 Preparation of Autologous Scapular Bone Block

After general anesthesia, the patient was placed in the lateral position, and the affected limb was abducted under traction. Then, routine disinfection and draping were performed. Arthroscopic exploration of the shoulder joint was performed to assess the glenoid defect. Then, bone block from the scapular spine was harvested for surgical repair. A 2–3 cm incision was made along the inner 1/3 of the scapular spine to expose the scapular spine after peeling off the soft tissue and periosteum (Fig. 27.9). Bone block was harvested as required (Fig. 27.10), which was then trimmed in accordance with the shape of the glenoid defect and drilled (Fig. 27.11). Bone allograft pins with a diameter of 3.3 mm were inserted into the bone holes (Fig. 27.12). The incision at the donor site was sutured.

27.1.3 Bone Grafting and Fixation

Damaged anterior articular capsule and labrum were dissociated under arthroscopy, and the bone bed of the scapular spine was detected, cleaned, and freshened (Fig. 27.13). The skin was cut from 3 cm from the outer edge of the coracoid process to the wrinkles of the armpit. Then, the deltoid and pectoralis major muscles were medially separated. Then, the subscapularis muscle and surrounding tissue were pulled apart using a hook, and the shoulder joint capsule was cut until the glenoid defect was exposed. The prepared bone

Y.-j. Liu (✉)
Department of Orthopedics, Chinese PLA General Hospital, Beijing, China

M. Lu
The Fourth Comprehensive Service and Support Center of the PLA Beijing Administration of Veterans Service Affairs Department, Beijing, China

Y.-j. Liu et al. (eds.), *Advanced Application of Arthroscopy*, https://doi.org/10.1007/978-981-15-4684-6_27

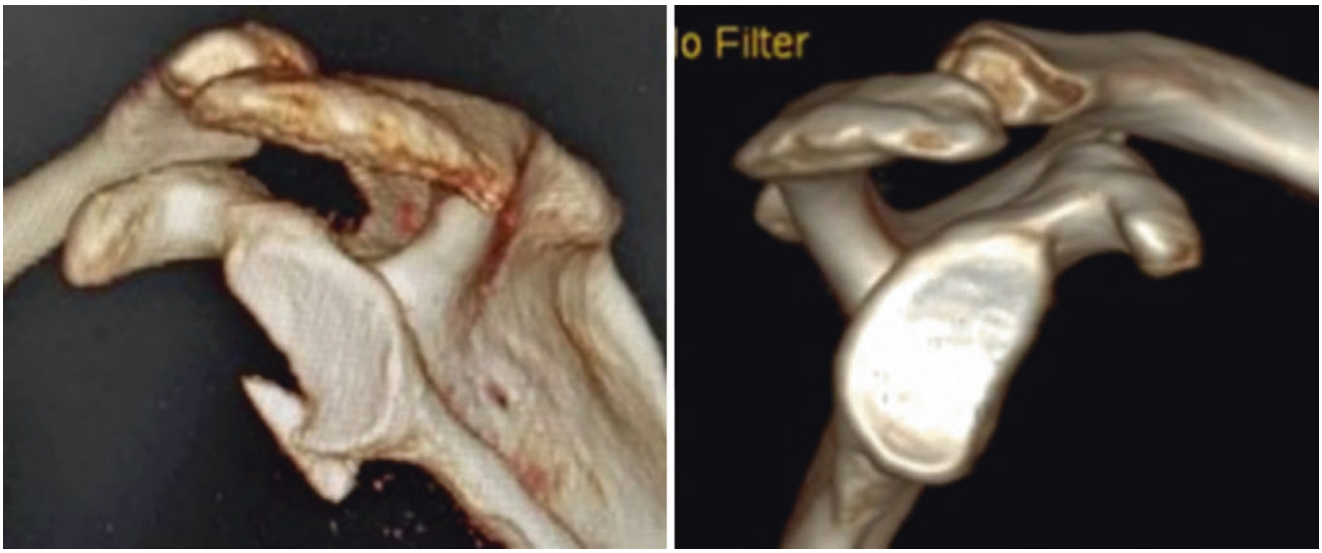

Fig. 27.1 Bony Bankart lesion

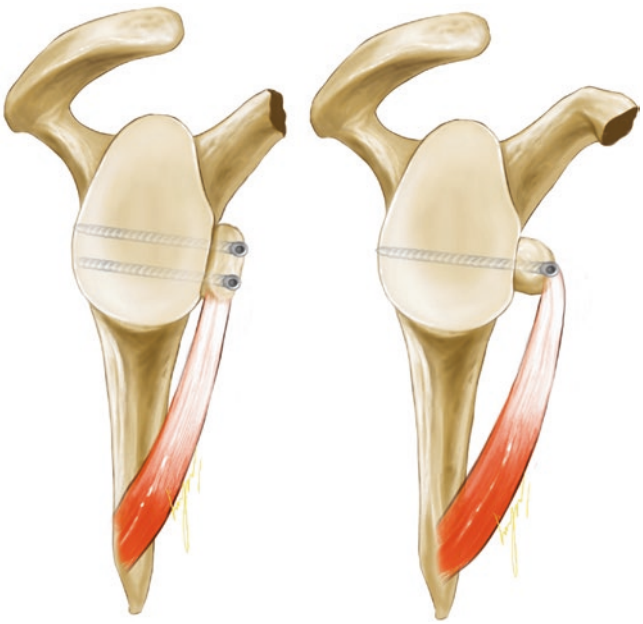

Fig. 27.2 Latarjet-Bristow surgery for repair of bony Bankart lesion

block was implanted onto the defect area via anterior approach under arthroscopy. Then, the grafted bone block was flattened and aligned with the articular surface followed by temporary fixation with 2-mm-diameter Kirschner wires. Two allograft bone pins with suture thread were inserted along the drilling holes to transfix the defect. Subsequently, suture thread was inserted to stitch the bone block to the surrounding soft tissue. Finally, the skin incision was sutured followed by postoperative imaging examination (Figs. 27.14, 27.15, 27.16, and 27.17). A sling or abduction brace was used for postoperative immobilization, and function training was performed as per the rehabilitation protocol.

27.2 Critical Points

1. The bone block is taken inner 1/3 to 1/3 of the scapula, to avoid the injury of the acromion and the acromion of the suprascapular artery.
2. Soft tissue release: Tissue relaxation around the glenoid is one of the important factors for a successful operation.
3. The glenoid bone bed should be freshened to ensure good healing of the bone block, which is conducive to the bone healing of the grafted bone block and the glenoid bone.

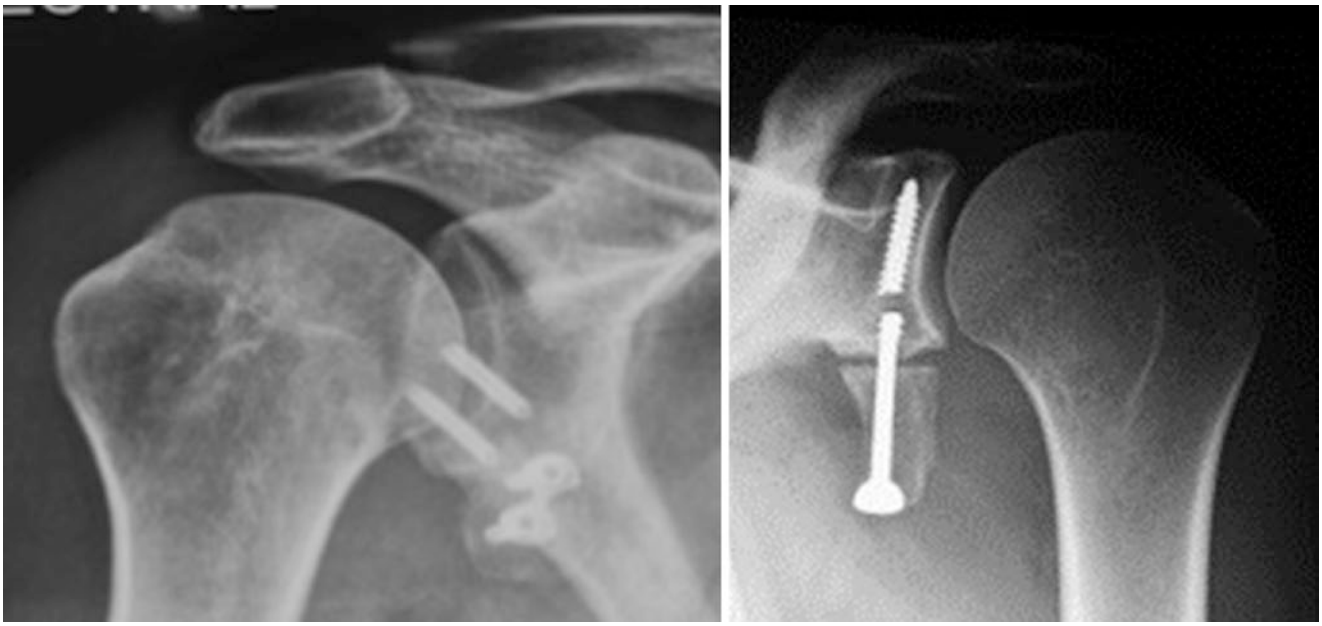

Fig. 27.3 Screw breakage and bone resorption after Latarjet-Bristow surgery

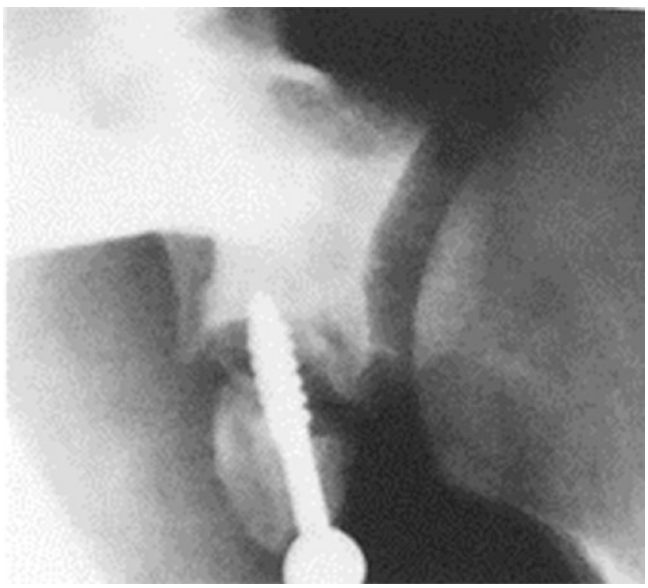

Fig. 27.4 Screw breakage and bone nonunion after Latarjet-Bristow surgery

Fig. 27.5 Screw displacement due to infected bone resorption

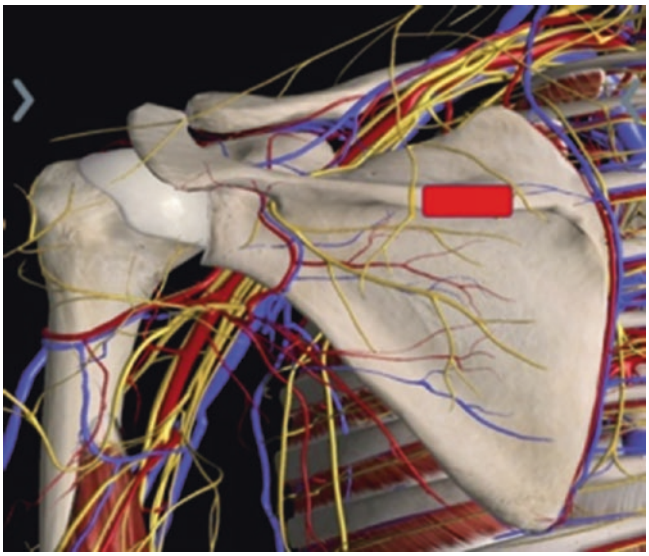

Fig. 27.6 Anatomical observation around the scapula

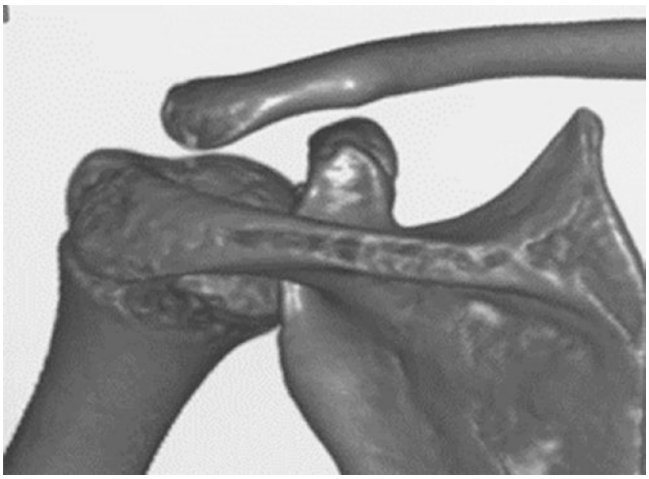

Fig. 27.7 Three-dimensional CT reconstruction of the scapula

Fig. 27.8 Marking important bony landmarks of the shoulder joint before operation

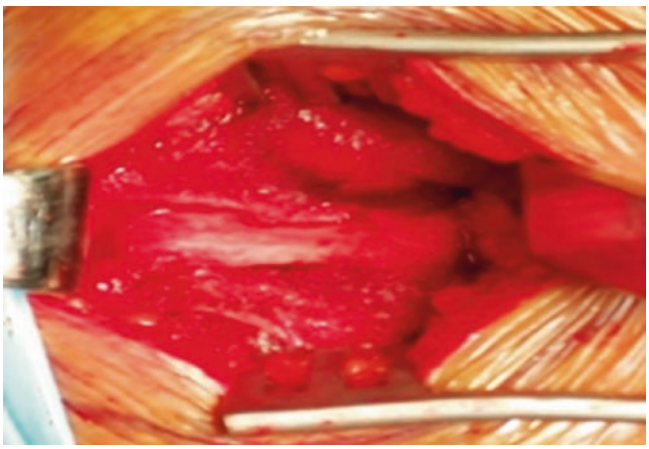

Fig. 27.9 Exposure of the scapular spine by peeling off the skin and surrounding soft tissue along the scapula

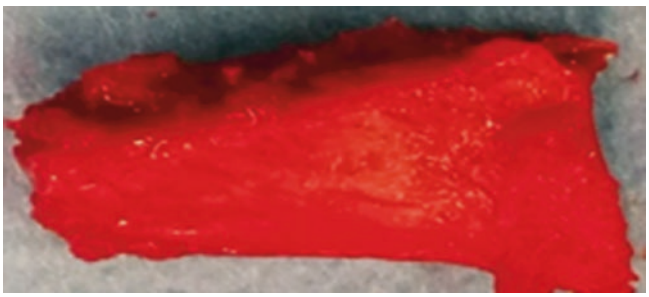

Fig. 27.10 Bone block removed of the scapular

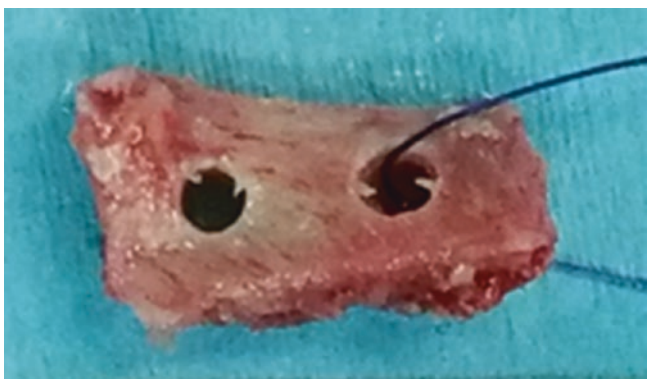

Fig. 27.11 Trimming and drilling holes of the bone block

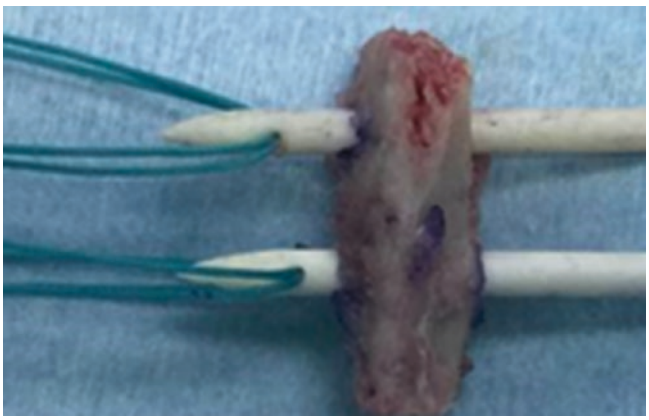

Fig. 27.12 Allograft bone spins with a diameter of 3.3 mm inserted into the bone holes

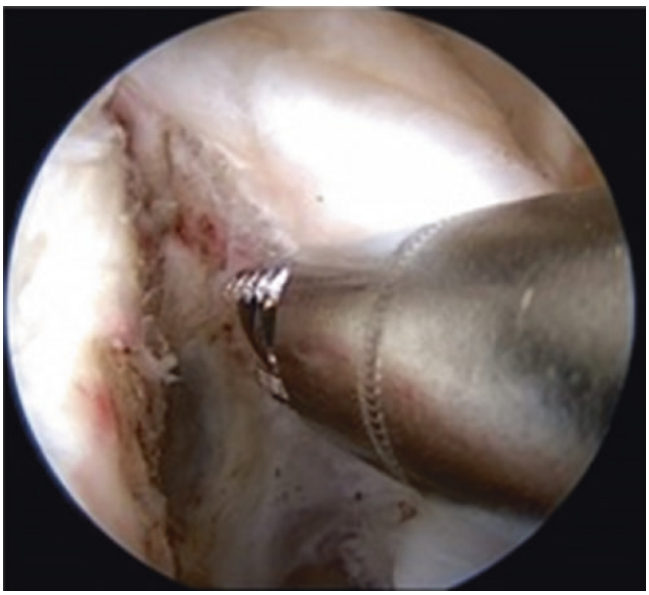

Fig. 27.13 The bone bed of the scapular spine was detected, cleaned, and freshened

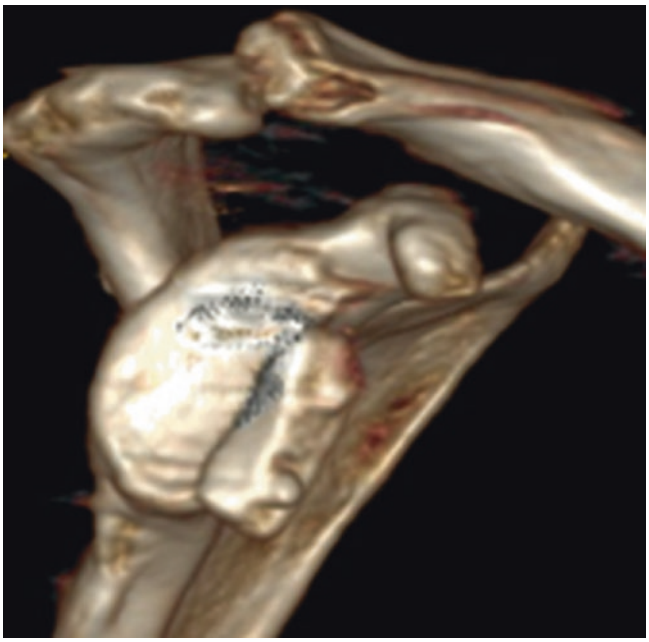

Fig. 27.14 Three-dimensional CT reconstruction of the glenoid shows that the grafted bone block is firmly fixed

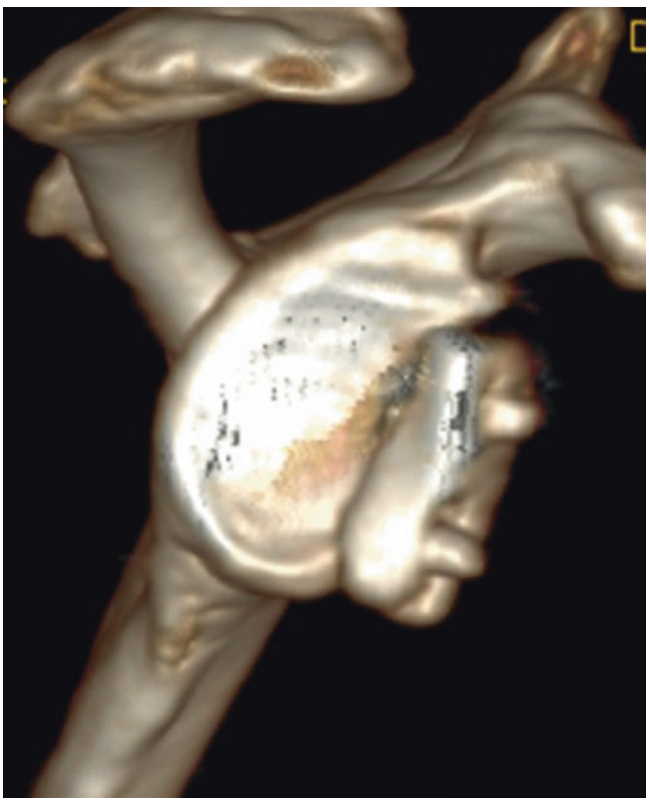

Fig. 27.15 Two-dimensional CT reconstruction at 2 months after surgery shows that the grafted bone block and the scapula are well positioned in the recipient area

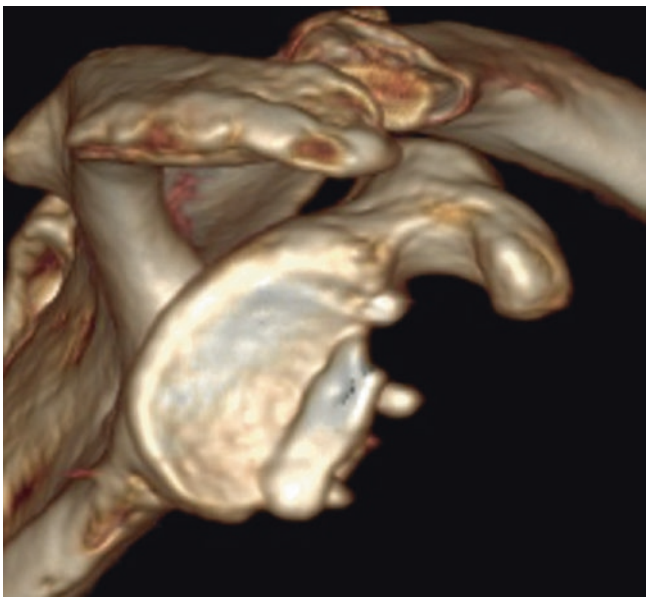

Fig. 27.16 Three-dimensional CT reconstruction at 5 months after surgery shows fusion of bone pins and grafted bone block with the scapula in the recipient area

Fig. 27.17 CT scan and three-dimensional CT reconstruction at 14 months after surgery show that the grafted bone block has been completely fused with the scapula of the recipient area, and the glenoid is completely restored

References

1. Yamamoto N, Muraki T, Sperling JW, et al. Stabilizing mechanism in bone-grafting of a large glenoid defect. J Bone Joint Surg Am. 2010;92(11):2059–66.
2. Boileau P, Thelu CE, Mercier N, et al. Arthroscopic Bristow-Latarjet combined with bankart repair restores shoulder stability in patients with glenoid bone loss. Clin Orthop Relat Res. 2014;472(8):2413–24.
3. Frank RM, Gregory B, O'Brien M, et al. Ninety-day complications following the Latarjet procedure. J Shoulder Elb Surg. 2019;28(1):88–94.
4. Ming LU, Yu-jie LIU, Xue-zhen SHEN, et al. Bone block from scapular spine transversely fixed with bone allograft pin for repairing bony Bankart lesion. Orthopedic J China. 2018;26(14):1333–7.

28 Arthroscopic Superior Capsular Reconstruction Using "Sandwich" Complex Patch Graft for Irreparable Rotator Cuff Tears

Shao-hua Ding and Yu-jie Liu

28.1 Introduction

In 2013, Japanese scholar, Teruhisa Mihata originally described superior capsular reconstruction (SCR) for the treatment of 24 patients with irreparable posterosuperior rotator cuff tears. Recently, contemporary SCR technique has been a hot topic in repairing massive rotator cuff tears.

SCR technique is regarded as a procedure to restore the superior stability of the shoulder by fixing the medial side of the graft at the superior glenoid and lateral side of the graft at the rotator cuff footprint with resulting outcomes of force couple recovery and function improvement. It was reported that ASES score was improved from the preoperative 23.5 to the postoperative 92.5 [1]. SCR technique provides a new treatment selection for patients with massive rotator cuff tears [2].

The graft selection for SCR technique is very important. Ideal patch materials require dual abilities of healing with the receiving area and sufficient mechanical strength. Currently, the most commonly used patch materials were dermis allografts and fascia lata. The mechanical strength of dermal material is good, but the healing rate is 45% [3]. The fascia lata graft has high healing rate of 83.3% [4], while the mechanical strength is poor, and the graft is prone to elongation and absorption [5] (Figs. 28.1, 28.2, and 28.3).

In order to prevent graft elongation, loose, and re-tear due to fascia lata "patch creep" and to increase graft strength, we created a "sandwich" patch graft with polyethylene terephthalate (PET) scaffold interspaced between two-folded layers of fascia lata autograft and used it for massive rotator cuff repair. The main advantage of the "sandwich" patch graft is that during the creep replacement and healing period, PET provides mechanical support for the patch remodeling and effectively prevents fascia lata autograft from creep, elongation, and re-tear resulting in improved strength and healing rate of the graft with good clinical outcomes [5].

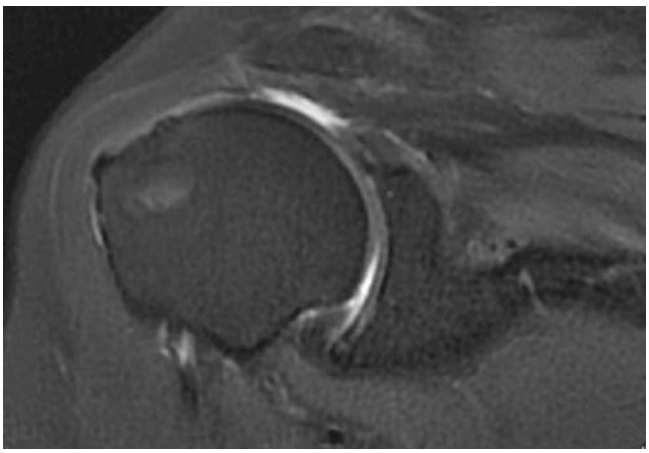

Fig. 28.1 Preoperative MRI revealed a massive rotator cuff tear

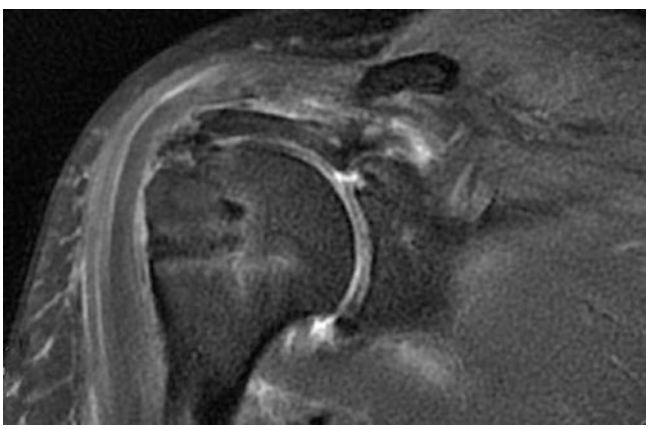

Fig. 28.2 Postoperative MRI immediately showed the fascia lata patch graft after SCR procedure

S.-h. Ding
Department of Orthopedics, Medical Center of Ningbo, Lihuili Hospital, Ningbo, China

Y.-j. Liu (✉)
Department of Orthopedics, Chinese PLA General Hospital, Beijing, China

Y.-j. Liu et al. (eds.), *Advanced Application of Arthroscopy*, https://doi.org/10.1007/978-981-15-4684-6_28

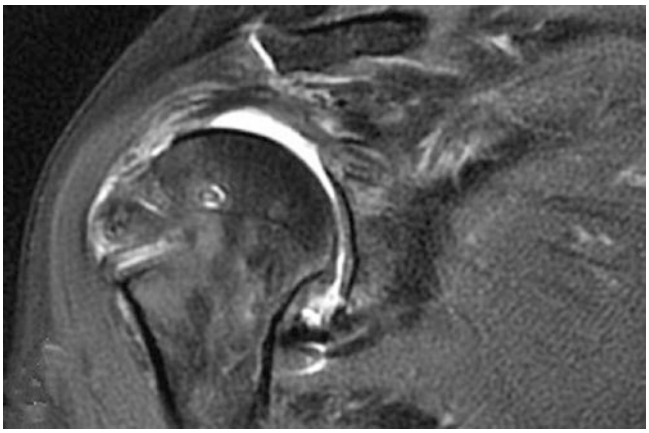

Fig. 28.3 Postoperative MRI at 18 months showed that fascia lata patch graft is thinning and loose with humeral head superior shifting

Fig. 28.4 X-radiograph at anteroposterior view showed mild superior shifting of the humeral head, Hamada II

28.2 Preoperative Evaluation

Preoperative evaluations were performed to assess the bone quality of glenohumeral joint and rotator cuff injuries by using radiographs in the planes of the anteroposterior view and scapular Y view (Fig. 28.4) and MRI (Figs. 28.5 and 28.6).

28.3 Shoulder Arthroscopy Examination

1. Anesthesia and Patient Positioning
   Under general anesthesia, patients are placed in lateral decubitus position with the upper limb 20°anteflexion and 45° abduction. The shoulder joint and ipsilateral thigh are sterilized, and the ipsilateral thigh is prepared for the fascia lata harvesting.
2. Arthroscopic Debridement and Acromioplasty
   After diagnostic arthroscopy, arthroscopic shoulder debridement is performed, and then the subacromial bony spurs are removed to achieve subacromial decompression with coracoid ligament protected (Fig. 28.7). The dimension of the defect of torn rotator cuff is measured under arthroscopy for the fascia lata harvesting (Fig. 28.8).

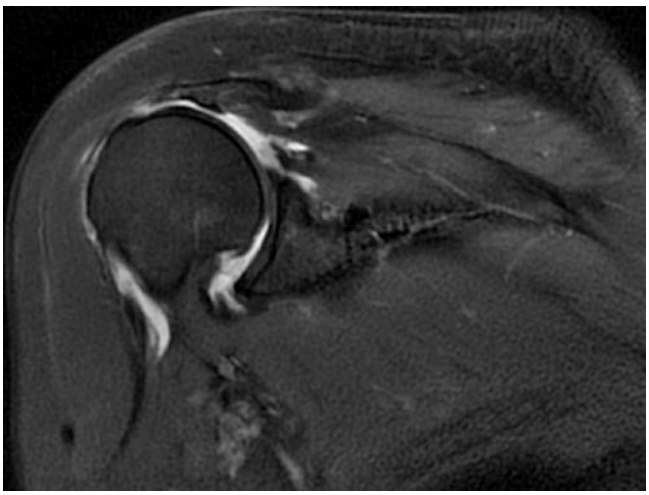

Fig. 28.5 Oblique coronal MRI revealed supraspinatus tendon retraction to glenoid plane

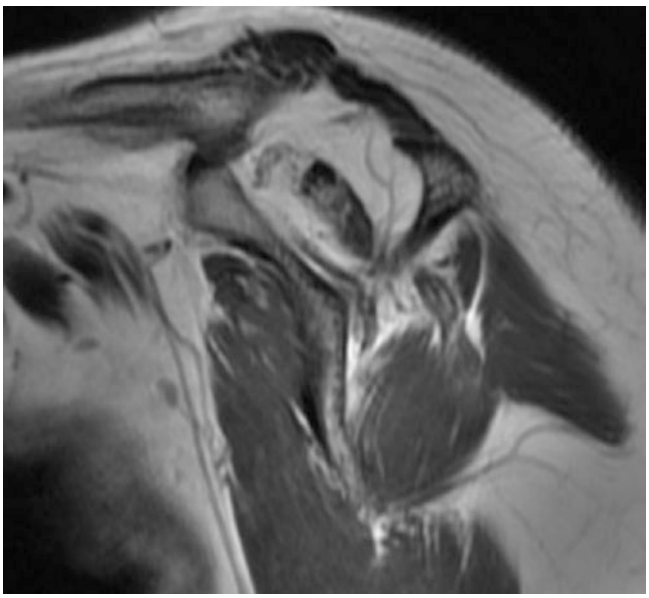

Fig. 28.6 MRI. T1-weighted oblique sagittal MRI revealed supraspinatus muscle and infraspinatus muscle atrophy with grade IV fatty degeneration of Goutallier classification

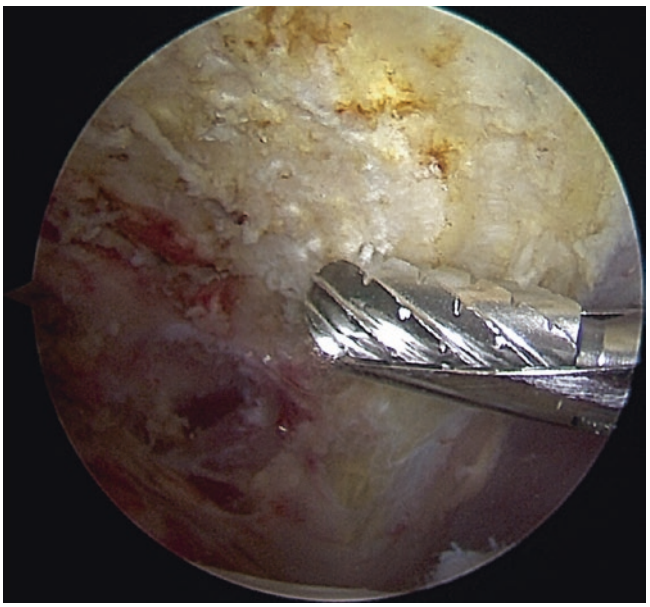

Fig. 28.7 Subacromial decompression by removing subacromial bony spurs

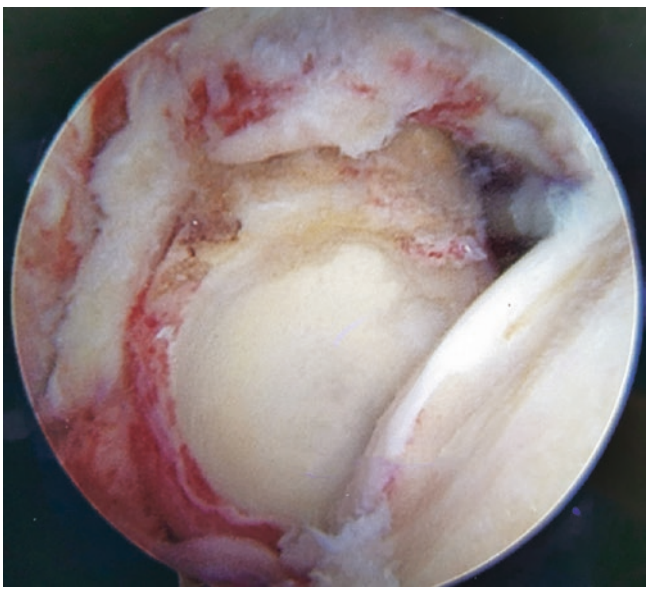

Fig. 28.8 Massive rotator cuff tears

28.4 Sandwich Patch Preparation

1. A fascia lata is harvested at the ipsilateral thigh, and its size is made by the dimension measurements of the defect of torn rotator cuff (Figs. 28.9 and 28.10).
2. The PET is shaped to produce an artificial scaffold graft as the same width and size as the fascia lata graft (Fig. 28.11) and then interspaced between twofolded layers of fascia lata autograft (Figs. 28.12 and 28.13).

Fig. 28.9 Harvesting fascia lata at ipsilateral thigh

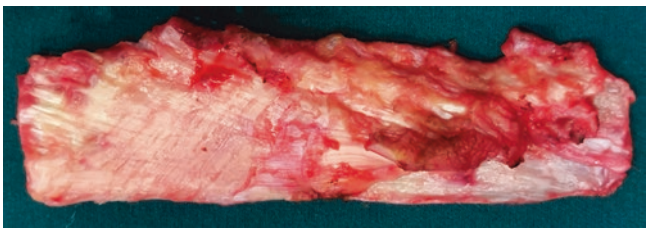

Fig. 28.10 Fat and muscle of fascia lata are removed

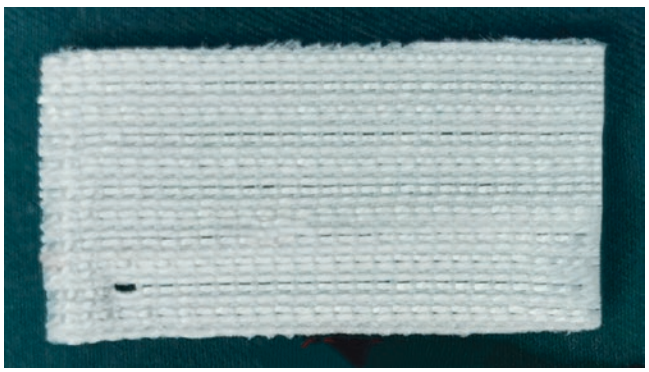

Fig. 28.11 PET graft

Fig. 28.12 Shape the PET to the same width and length as the fascia lata

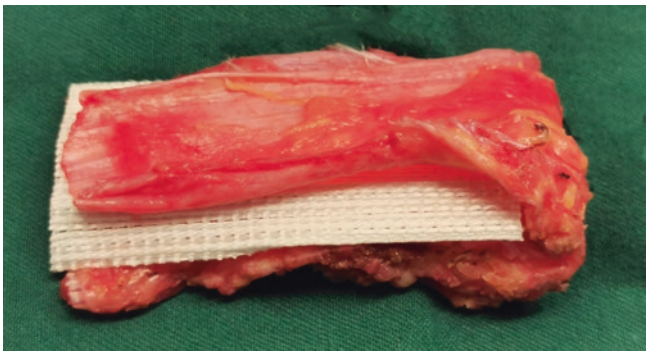

Fig. 28.13 Interspace the PET between twofolded layers of fascia lata to create a "sandwich" patch graft

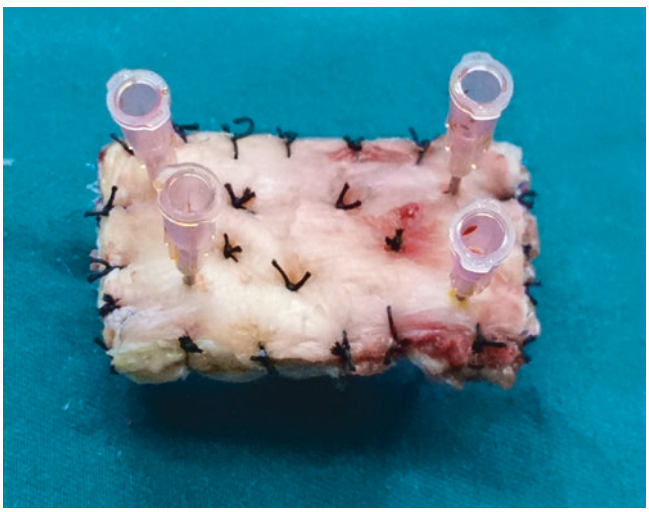

Fig. 28.14 "Sandwich" patch graft with edges stitched

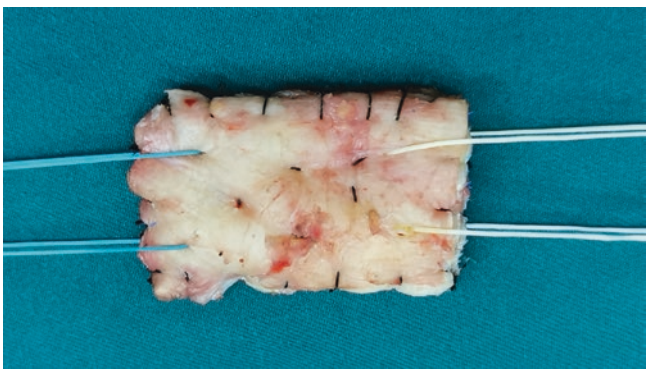

Fig. 28.15 Two different color pulling strings are shuttled at each corner

3. Every corner of the "sandwich" patch was fixed in the sterile plate using no.16 injector needles, and every edge and center of the patch is stitched by nonabsorbable suture (Fig. 28.14).
4. "Sandwich" patch graft is completed, and its thickness is 6–8 mm (Figs. 28.15 and 28.16). Each side of the patch graft is shuttled with two fiber wire sutures (different colors) as pulling strings to introduce the graft into the shoulder joint.

Fig. 28.16 Patch graft thickness measurement

28.5 Key Points for "Sandwich" SCR Technique

1. Subscapularis tendon tear should be repaired if the SCR technique is considered to perform. If the subscapularis tendon can't be repaired with the tear extending to lower third of the tendon, SCR should be quitted, and alternative techniques such as pectoralis major transposition technique should be considered (Fig. 28.17 and 28.18).
2. If the tear involves the infraspinatus tendon and teres minor tendon, teres minor tendon must be repaired. If it can't be achieved, SCR should also be used instead of other effective techniques such as latissimus dorsi or trapezius tendon transfer (Figs. 28.19 and 28.20).
3. Bone Bed Preparation and Suture Anchor Placement
   The superior glenoid bone bed and the greater tuberosity footprint area should be cleaned and freshened (Figs. 28.21, 28.22, and 28.23).
4. "Sandwich" Patch Graft Insertion and Fixation
   The sharp part of a 10.0-mL injector cannula is cutoff, and a longitudinal notch is made in the cannula for easy introduction of the patch into the subacromial space of the

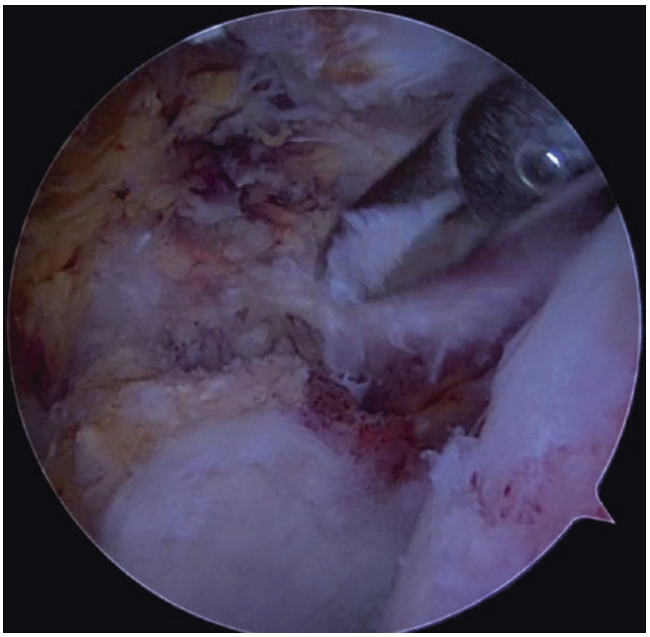

Fig. 28.17 Subscapularis tendon partial tear

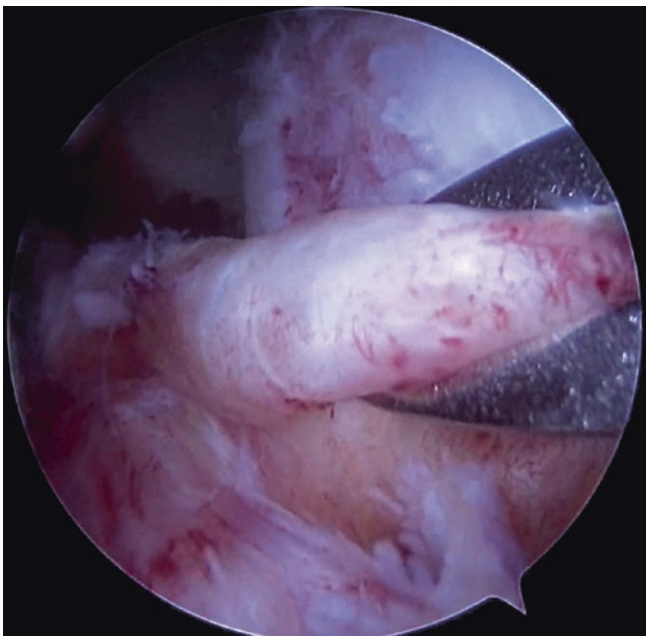

Fig. 28.19 Infraspinatus tendon tear with teres minor tendon tear

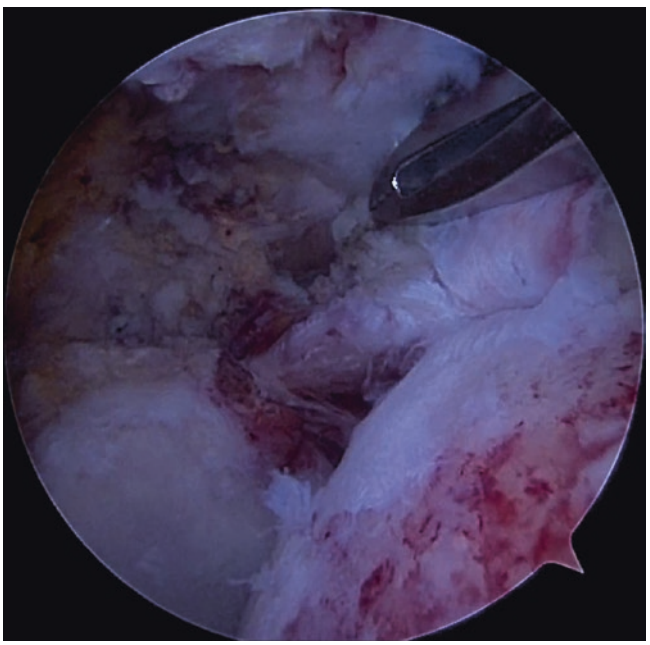

Fig. 28.18 Subscapularis tendon tear is repaired

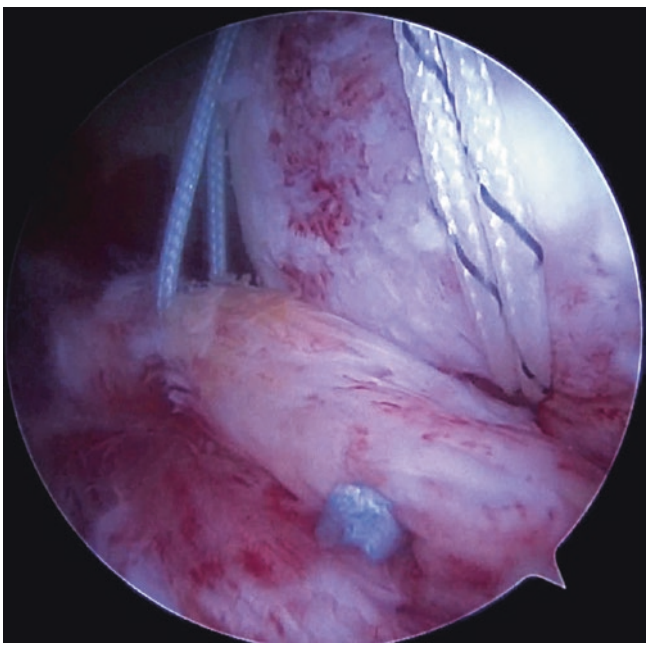

Fig. 28.20 Repaired infraspinatus tendon and teres minor tendon by single-row suture technique

shoulder through the anterolateral portal (Fig. 28.24). The glenoid anchor sutures are pulled out in order anteroposteriorly and passed through the medial part of the sandwich patch. A PDS suture is used to pull the two medial-corner pulling strings of the patch out of the joint from the anterior portal and posterior portal. Then the patch graft is introduced into the subacromial space along the direction of the glenoid anchor suture through the cannula with the straining of the pulling strings which keep the patch from unfurling (Fig. 28.25). When the patch graft is cling to the glenoid and humeral head, suture knots are performed to fix the graft (Fig. 28.26). A double-pulley technique with the SpeedBridge technique is used to fix the patch laterally (Fig. 28.27). A side-to-side suture is added between the graft and the remaining infraspinatus (Fig. 28.28). Finally, arthroscopic evaluation is performed to inspect the patch graft after the SCR (Fig. 28.29).

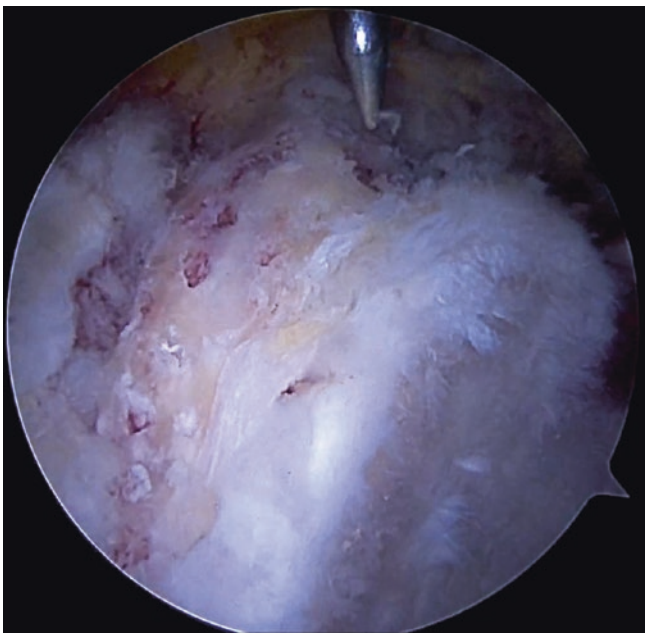

Fig. 28.21 Glenoid bone bed is cleaned and given microfracture for bone marrow exudate to enhance graft-to-bone healing

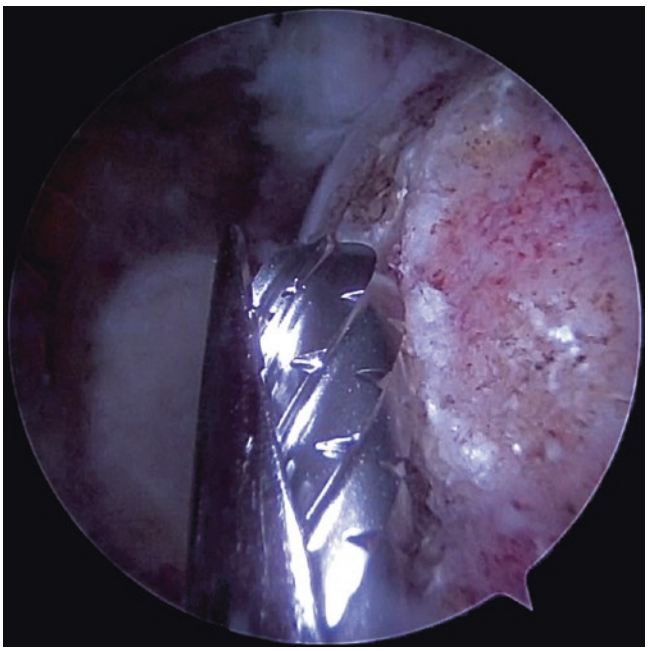

Fig. 28.22 Remove the osteophytes and freshen the greater tuberosity footprint area by arthroscopic shaver

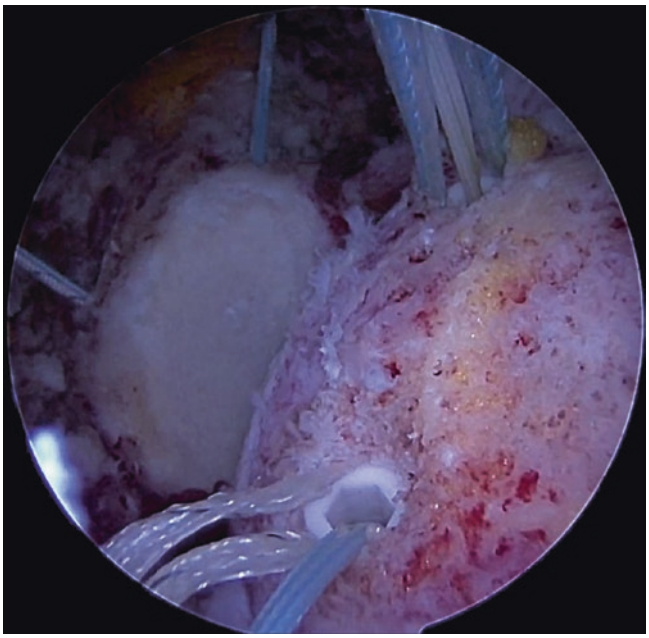

Fig. 28.23 After glenoid anchor and humeral head anchor placement, the strands of anchor sutures are pulled out though the anterior portal and posterior portal to avoid interference for the patch delivery

Fig. 28.24 The patch graft is introduced into the subacromial space along the cannula through the anterolateral portal

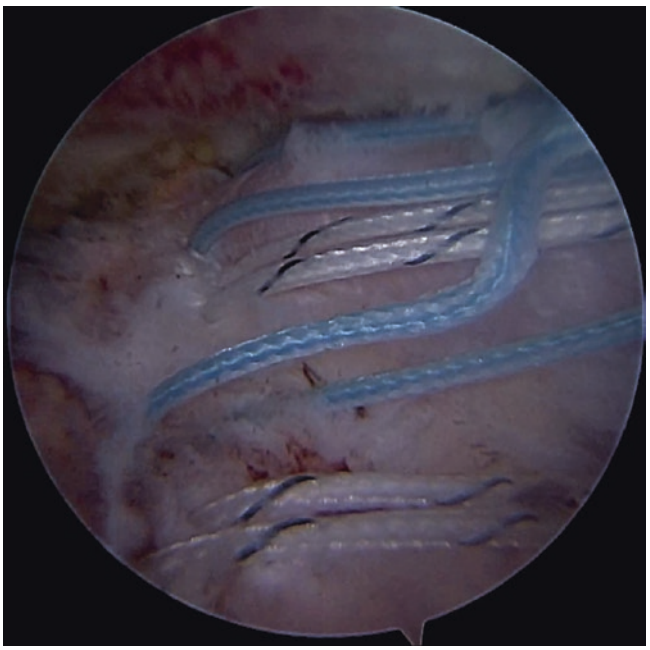

Fig. 28.25 After the patch graft is introduced, the pulling strings are strained to make the graft cling to the glenoid and humeral head

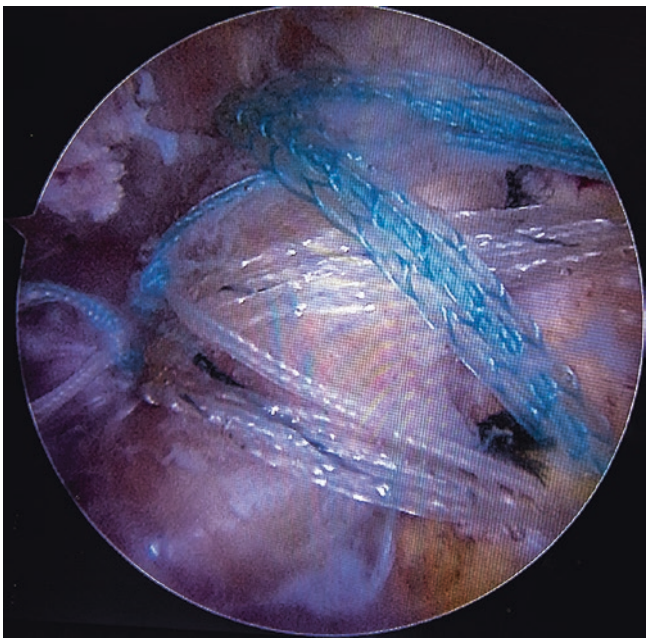

Fig. 28.27 A double-pulley technique with the SpeedBridge technique is used to fix the patch laterally

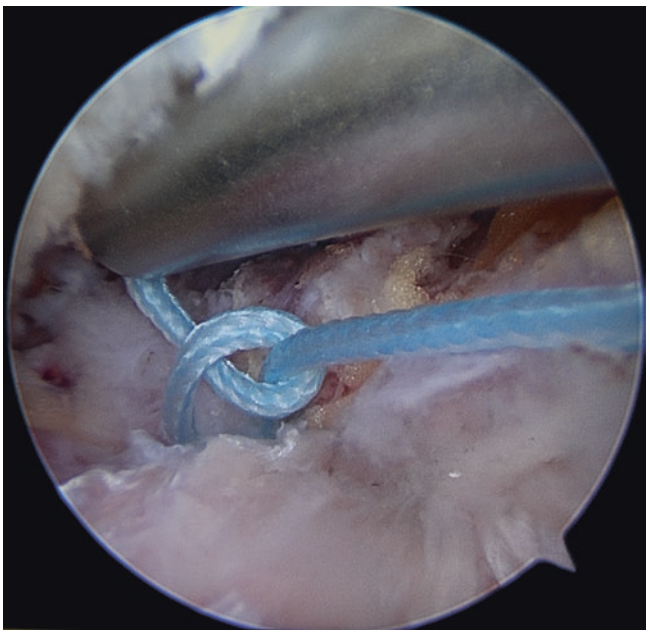

Fig. 28.26 Suture knots are preformed to fix the graft

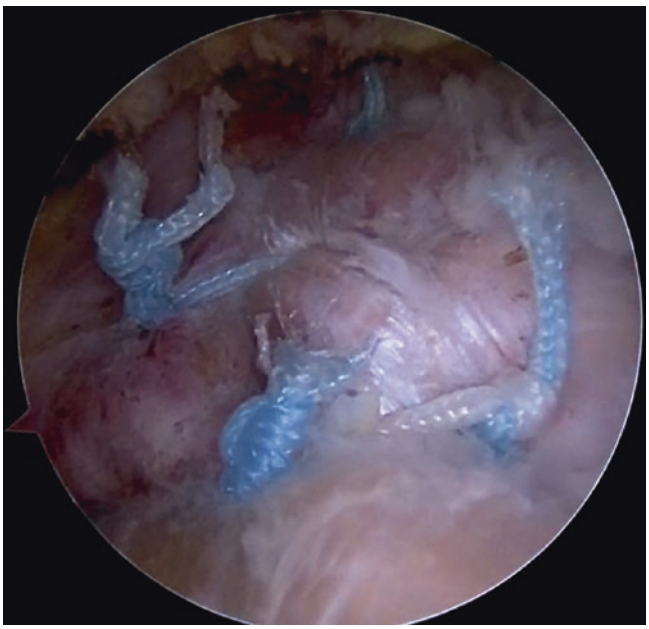

Fig. 28.28 A side-to-side suture is added between the graft and the remaining infraspinatus

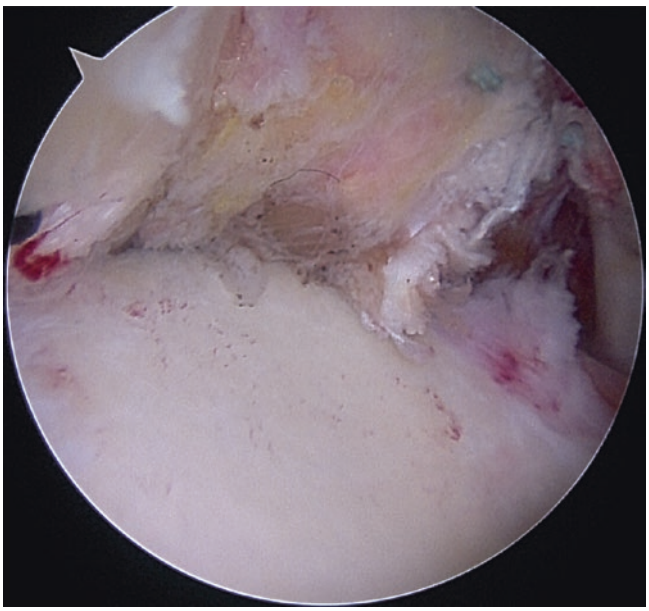

Fig. 28.29 Reconstructed superior capsular by using "sandwich" patch graft

Fig. 28.30 Postoperative X-ray showed increased AHD

28.6 Postoperative Rehabilitation and Radiological Evaluation

After the SCR surgery, x-plain film showed declined humeral head and increased AHD; MRI showed sandwich patch graft with PET material inside (Figs. 28.30, 28.31, 28.32, 28.33, 28.34, and 28.35).

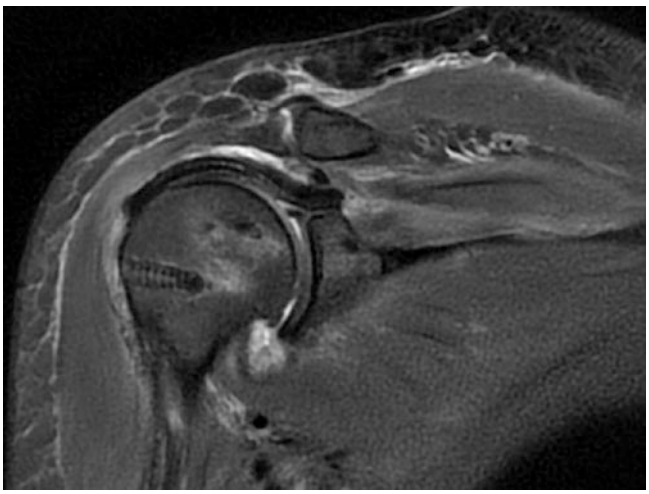

Fig. 28.31 MRI showed sandwich patch graft with PET material inside

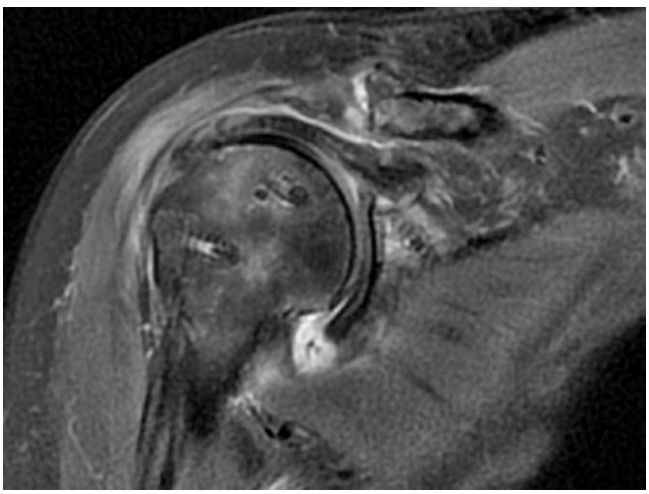

Fig. 28.32 Graft healing condition evaluation by postoperative MRT at 7 weeks

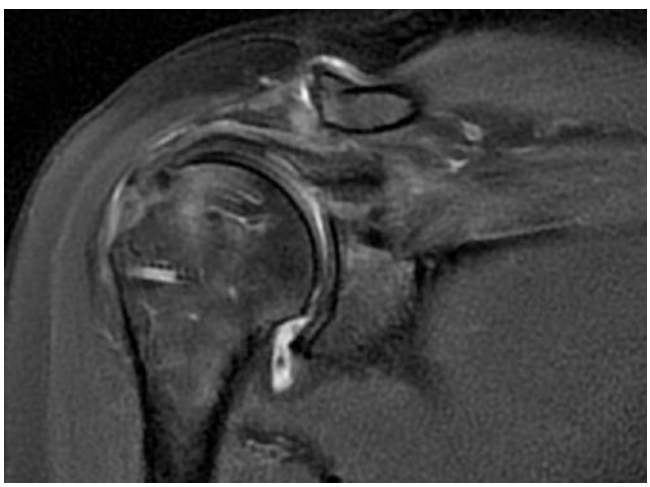

Fig. 28.33 Postoperative MRI at 6 months

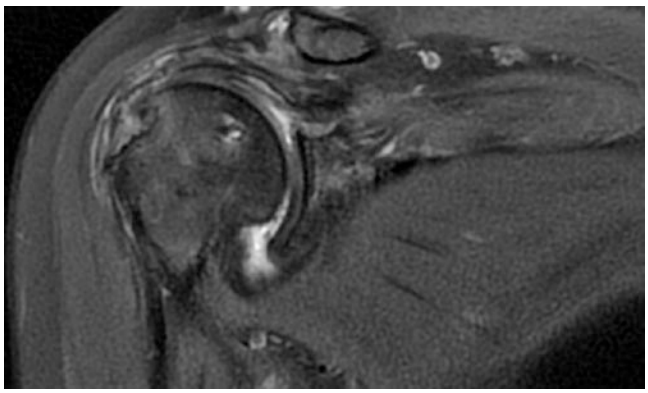

Fig. 28.34 Postoperative MRI at 12 months showed sandwich patch graft has healed well

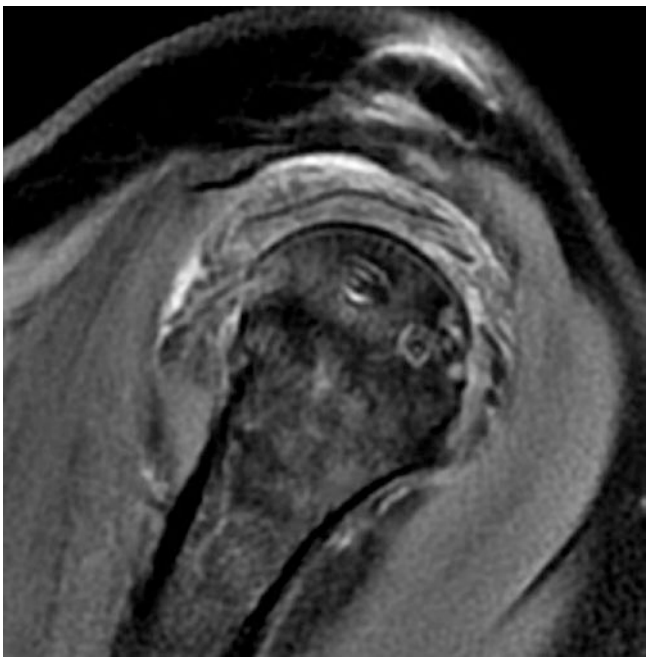

Fig. 28.35 Postoperative oblique-sagittal MRI at 12 months. The arrow indicates the PET material

Fig. 28.36 Abduction pillow used after surgery (use the image provided separately)

28.7 Postoperative Rehabilitation

Use of an abduction pillow for 6 weeks after SCR is recommended (Fig. 28.36). Limited passive forward flexion exercises with non-weight bearing are allowed to prevent shoulder joint adhesion during the immobilization period. Active exercises are initiated after 6 weeks; active motion exercises and muscle strength training are expanded gradually from 4 months postoperatively and are not limited at 12 months (Fig. 28.37).

Fig. 28.37 Postoperative physical examination-evaluation at 12 months. No pain; normal range of motion; grade 5 – abduction of muscle strength. (Use the image provided separately)

References

1. Mihata T, Lee TQ, Watanabe C. Clinical Results of Arthroscopic Superior Capsule Reconstruction for Irreparable Rotator Cuff Tears. Arthroscopy. 2013;29(3):459–70.
2. Hartzler RU, Burkhart SS. Superior Capsular Reconstruction. Orthopedics. 2017 Oct;40(5):271–80.
3. Patrick J, Denard MD, Paul C, Brady MD, et al. Preliminary Results of Arthroscopic Superior Capsule Reconstruction with Dermal Allograft. Arthroscopy: The Journal of Arthroscopic and Related Surgery. 2018, January;34(1):93–9.
4. Mihata T, Lee TQ, Watanabe C, et al. Clinical results of arthroscopic superior capsule reconstruction for irreparable rotator cuff tears. Arthroscopy. 2013;29:459–70.
5. Shaohua Ding BM, Yunshen Ge MD, et al. Arthroscopic Superior Capsular Reconstruction Using "Sandwich" Patch Technique for Irreparable Rotator Cuff Tears. Arthroscopy Techniques. 2019;8(9):e1–7.

29 Clearance and Radial Head Resection of Elbow Joint of Rheumatoid Arthritis Under Arthroscopy

Yu-jie Liu and Chun-bao Li

Rheumatoid arthritis is a chronic autoimmune disease, and the major pathological changes are as follows: in the early stage, it occurs inflammatory hyperplasia and hypertrophy of synovial membrane, and then pannus would infiltrate into articular cartilage that features joint pains and arthroncus and ultimately lead to joint deformity, limited movement, and dysfunction in the later stage.

The disease mainly affects the small and medium joints of the limbs, and the large joints as well, among which the elbow is one of the most commonly affected joints. The elbow joint consists of three joints, namely, the humeroulnar joint, the humeroradial joint, and the proximal radioulnar joint (Fig. 29.1). It can do forward bend and back stretch movement and participate in the forearm pronation and supination movement.

As synovial tissue impinges on cartilage, the X-ray shows osteoporosis, narrowing of joint space, and deformation of radial head in severe cases (Fig. 29.2). It features elbow swelling, pain, limited flexion, and rotation of brachioradial and superior ulnar radial joints.

Arthroscopy can reveal synovial hyperplasia (Fig. 29.3) and irregular, worm- eaten destruction of articular cartilage [1] (Fig. 29.4). Due to severe lesion erosion of cartilage and deformity of elbow joint, which affects its flexion-extension and rotation, elbow joint needs to be cleaned, and radial head resection should be performed if necessary to resolve dysfunction of flexion-extension and rotation.

The anatomical structure of elbow joint is complex with abundant vessels and nerves around it. The traditional incision operation are difficult to guarantee with great trauma, many interferences to the local anatomical structure, slow postoperative recovery, and easiness to joint stiffness, while arthroscopic surgery has the advantages of small incision, low recurrence rate, little effects on the anatomical structure of elbow joint and its surroundings, and quick recovery.

Y.-j. Liu (✉) · C.-b. Li
Department of Orthopedics, Chinese PLA General Hospital, Beijing, China

29.1 Posture and Anesthesia

Preoperative markers are used to mark the bone anatomy, vascular and nerve positions around the elbow joint, and surgical approaches (Fig. 29.5). Surgery may be performed in the supine, tummy, or lateral position according to the situation and the surgeon's habits (Fig. 29.6).

Anesthesia can be performed with interscalenus sulcus nerve block anesthesia or general anesthesia, as well as intra-articular local anesthesia, all of which can achieve the operation needs of anesthesia purposes. Sensory and motor functions can be observed at any time during local anesthesia.

A wide-angle arthroscope with a diameter of 30° and 2.7 mm, a plasma knife, and a manual planer are used, with a television monitor placed on the opposite side of the affected limb. The perfusion liquid is up to 1.5 meters high from the surgical bed, and in 0.1% epinephrine, 1.0 ml is added to 3000 ml normal saline. Pressure pump is used when necessary, and the pressure is maintained at 40 ~ 60 mmHg.

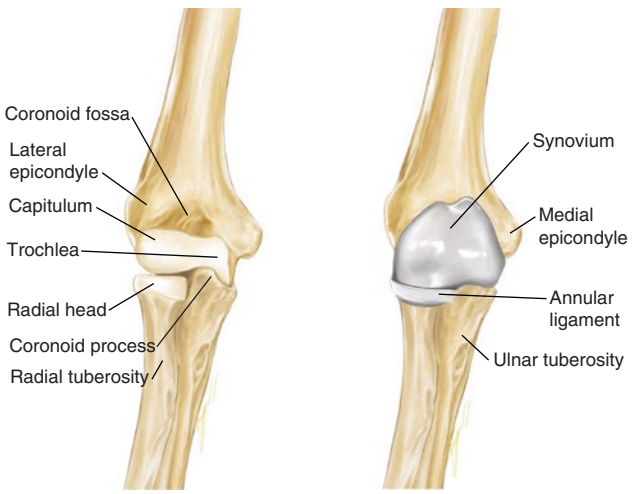

Fig. 29.1 Gross anatomy of elbow joint

Y.-j. Liu et al. (eds.), *Advanced Application of Arthroscopy*, https://doi.org/10.1007/978-981-15-4684-6_29

Fig. 29.2 X-ray shows osteoporosis of elbow joint, narrowing of joint, and deformation of the radial head space

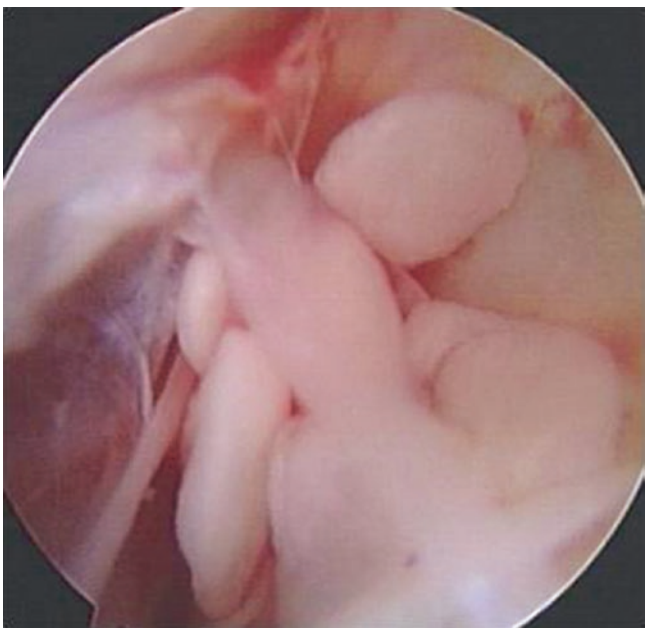

Fig. 29.3 Arthroscopy shows synovial hyperplasia of the elbow joint

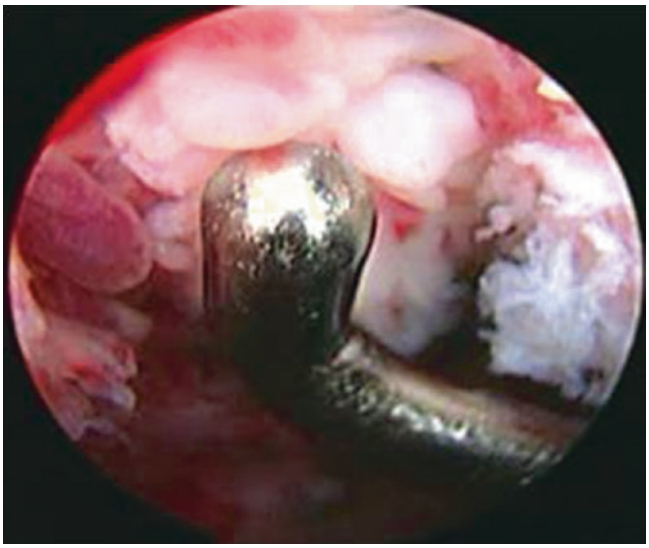

Fig. 29.4 shows irregular, worm-eaten destruction of articular cartilage

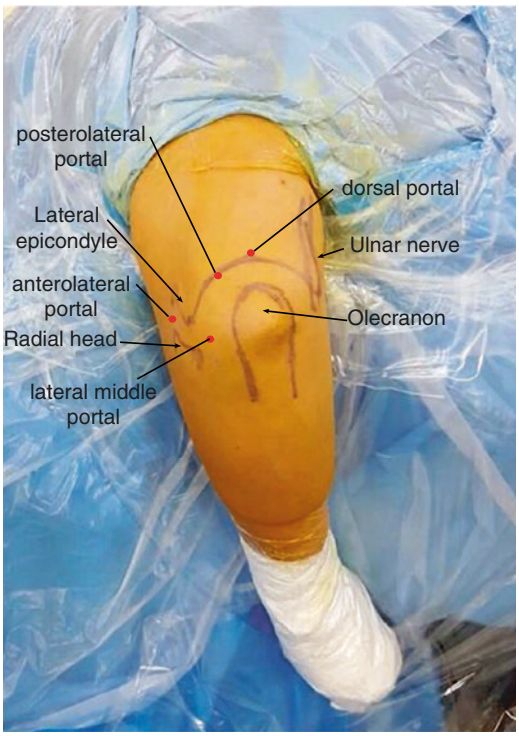

Fig. 29.5 Shows the bone markers, vascular and nerve locations around the elbow and the surgical approach (**a**, medial side view; **b**, lateral side view)

Fig. 29.6 Lateral position for elbow arthroscopic surgery

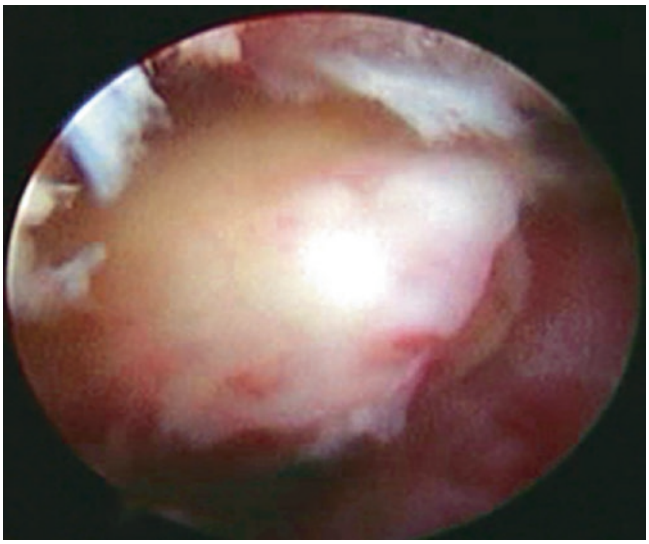

Fig. 29.7 Hyperplasia and deformation of the radial head and cartilage defect

29.2 Surgical Procedures

Prior to arthroscopy, epinephrine in saline or local anesthetic 25 to 30 ml can be injected from the anterolateral approach to dilate the elbow capsule. A sharp knife is used to cut through the skin for 3 mm, and then the arthroscopic puncture cannula is inserted into the joint. From the anterolateral approach to elbow, check the ulna coronary, crest, and the medial coronoid process nest, pulley, and joint capsule. The conditions of radial head and brachioradial joint are observed under arthroscopy, and the conditions of the superior ulnar and radial joint are observed before and after forearm rotation (Fig. 29.7). Check and clean the synovial membrane of elbow joint (Fig. 29.8).

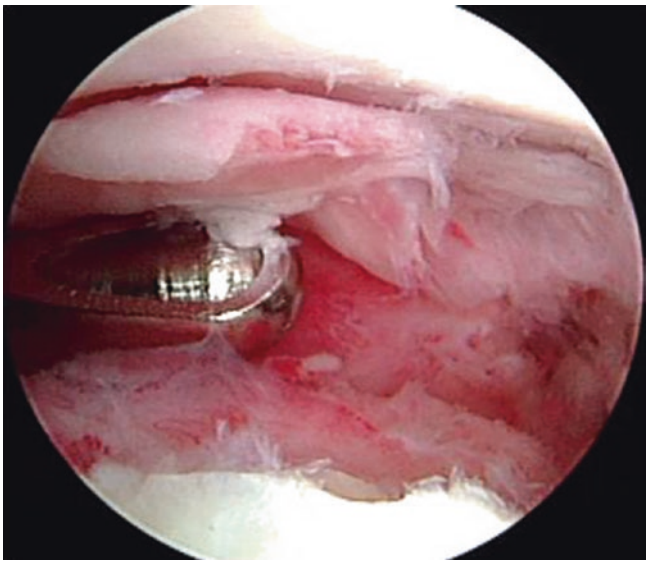

Fig. 29.8 The clearance of synovial tissue in the elbow joint cavity

Based on the findings of the major factors affecting the rotation of the elbow joint, determine the scope for the resection of the small head of the radius. Cylindrical grinding drill is used to cut the radial head about 5 mm from the anterolateral side of the elbow joint (Fig. 29.9), and the residual end of the radial head is trimmed and smooth until flexion, extension, and rotation are not limited, and the annular ligament of the radial head is retained. Postoperative elbow joint movement is examined, including the examinations of sensation and movement of median nerve, ulnar nerve, and radial nerve, and postoperative X-ray (anteroposterior and lateral view) of the elbow joint should be taken (Fig. 29.10). Regular review of elbow function is needed (Fig. 29.11).

29.3 Critical Points

1. The surgeon should be familiar with the vascular and nerve distribution around the elbow joint to avoid intraoperative injury.
2. For rheumatoid patients being with severe osteoporosis, the operation should be gentle, to avoid fracture caused by rough actions.
3. After clearing the synovial lesion with hypertrophy, hemostasis should be fully stopped, and debris in the joint cavity should be washed to prevent the residual.
4. The range of the grinding of the small head of the radius should meet the condition that the flexion and extension of the elbow joint and rotation are not limited.
5. Pay attention to protect the annular ligament during the operation.
6. Patients should continue the medical treatment of anti-rheumatology to control the progress of rheumatology.

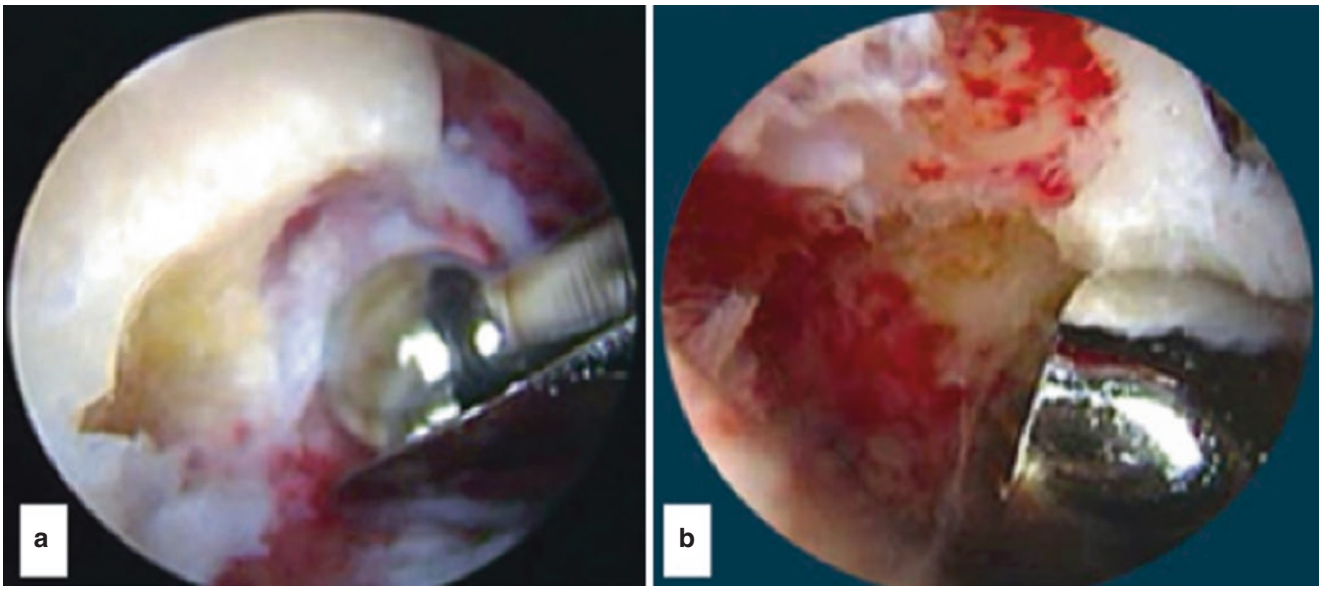

Fig. 29.9 Anterior lateral cutting of the elbow about 5 mm (**a**, before; **b**, after cutting)

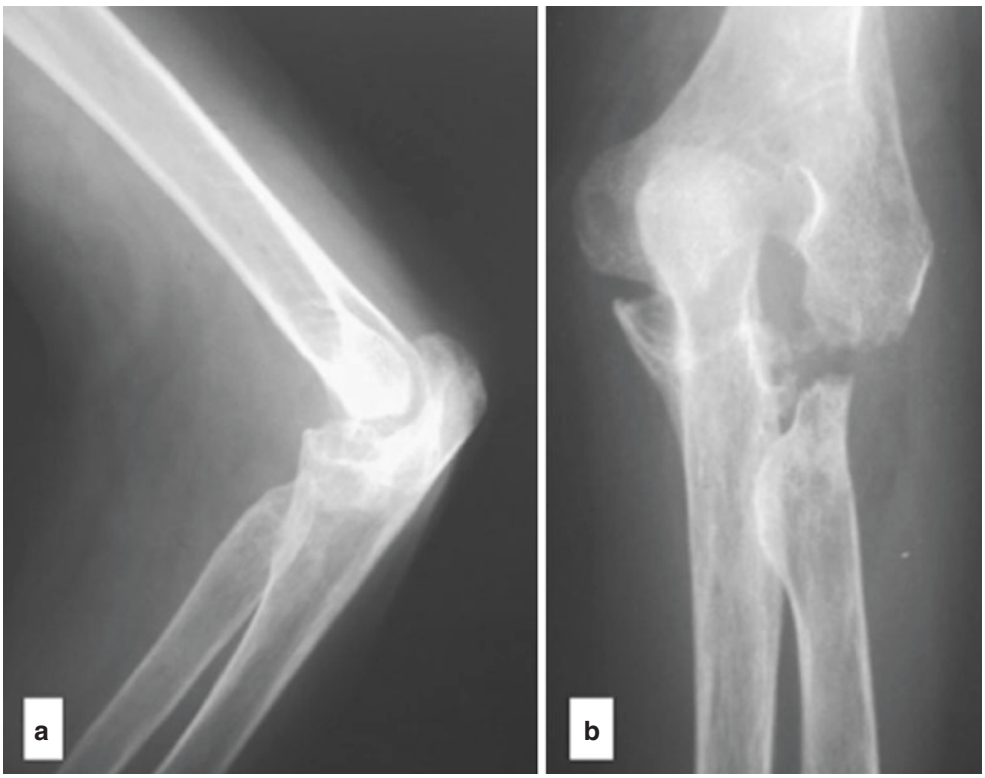

Fig. 29.10 Postoperative X-ray (anteroposterior and lateral view) of the elbow joint (**a**, lateral view; **b**, AP view)

Fig. 29.11 Function after radial head resection 12 years ago for elbow arthritis

Reference

1. Smith J, Field LD. Elbow arthroscopy made simple: indications and techniques. Arthroscopy. 2019 Jul;35(7):1952–3. https://doi.org/10.1016/j.arthro.2019.05.014.

Ankle Arthrodesis Under Arthroscopy

30

Yu-jie Liu and Chun-bao Li

Kashin-Beck disease, severe traumatic osteoarthritis, degenerative osteoarthritis, and flatfoot with talonavicular arthritis often cause pain and dysfunction due to cartilage damage in ankle joint. Conventional open ankle arthrodesis was often chosen in patients with failure of conservative treatment. With the development of minimally invasive technology, ankle arthrodesis under arthroscopy shows many advantages when compared with traditional open surgery: less surgical trauma, clearer operative vision, no observational blind corner, less tissue invasion around the ankle, no loss of bone mass, and no interfere with local blood supply, which is conducive to the ankle joint fusion [1–2].

30.1 Indications and Contraindications

Ankle arthrodesis under arthroscopy is employed in severe ankle osteoarthritis, severe talus fracture with arch collapse (Fig. 30.1), ankle comminuted fracture (Fig. 30.2), Kashin-Beck disease (Fig. 30.3), rheumatoid arthritis, talonavicular arthritis (Fig. 30.4), ankle traumatic osteoarthritis with severe scar tissue around the ankle (Fig. 30.5), and terrible skin condition not suitable for open surgery. Arthroscopic bone graft fusion is required in talus ischemic necrosis with arch collapse and severe bone defect. Lower limb alignment correction rather than mere arthrodesis is necessary, in ankles with serious varus, serious valgus, or anteroposterior angulation more than 15°.

30.2 Preoperative Preparation

Epidural or nerve block anesthesia is used, and patient is on the supine position in operation. Before operation, the ankle joint bony landmarks, including blood vessels, nerves, ankle mortises, and arthroscopic anterior internal and anterior external portals, are marked. The pneumatic tourniquet is used in the surgery and drape with sterile sheet after routine disinfection in the operation area.

30.3 Operation Procedures

The anterior external and anterior internal approach is adopted. A 3 mm incision is made by sharp knife on the skin, and then the blunt puncture and cannula are inserted into the joint cavity. The 2.7 mm or 4.0 mm arthroscopy is inserted, and the ankle joint is examined in sequence.

30.3.1 Tibiotalar Arthrodesis

In order to expand the intra-articular operative vision, a planer is used to clean the hypertrophic synovium and scar tissue, the cartilage collapse is next checked (Fig. 30.6), and different cleaning tools are selected according to the pathological changes of the lesions.

1. Talar Cartilage Removal
   The cartilage on talus dome is removed with blades of different angles under arthroscopy (Fig. 30.7), so as to expand the operative vision. An arc-shaped blade is needed to remove the cartilage on posterior malleolus, which is difficult to clean as the mound-shape talus. Then an arc-shaped bone file is used to grind the subchondral bone to bleeding (Fig. 30.8).
2. Cartilage Removal of Distal Tibia and Ankle Mortise
   The cartilages on distal tibia and lateral and medial malleoli were removed by shovel. Generally, the remaining cartilage is removed by curette instead of power drill to avoid bone loss.
3. Subchondral Bone Microfracture
   Microfracture procedure with each of drilling point 2 mm interval is performed on the subchondral bone of

Y.-j. Liu (✉) · C.-b. Li
Department of Orthopedics, Chinese PLA General Hospital, Beijing, China

Y.-j. Liu et al. (eds.), *Advanced Application of Arthroscopy*, https://doi.org/10.1007/978-981-15-4684-6_30

Fig. 30.1 Severe talus fracture with arch collapse

Fig. 30.2 Comminuted fracture of distal tibia

Fig. 30.3 Narrow joint space and severe wear of articular cartilage in Kashin-Beck disease

talus, distal tibia, and lateral and medial malleoli by microfracture cone, so that the bone marrow blood is infiltrated into the ankle joint space (Fig. 30.9) to improve local blood supply and promote arthrodesis.

4. Cross Kirschner Wire Prefixation
   At 3–4 cm above the horizontal line of ankle joint, two crossing Kirschner wires are drilled through the skin. Under arthroscopic monitoring, the two Kirschner wires penetrate the tibia subchondral bone in different before

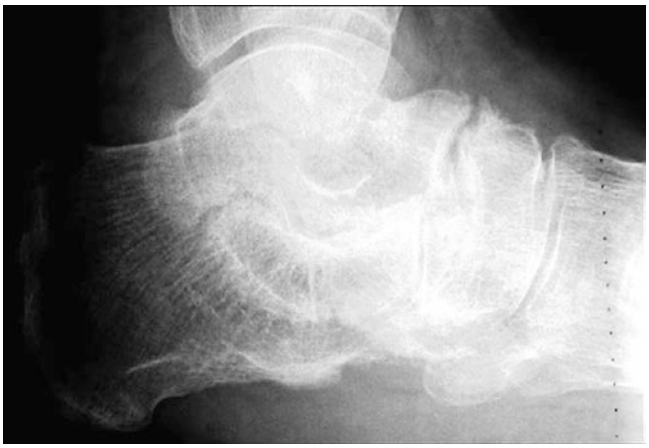

Fig. 30.4 Osteoproliferation of taloclavicular arthritis in flatfoot X-ray

Fig. 30.5 Cicatrization of skin damage in ankle talus fracture

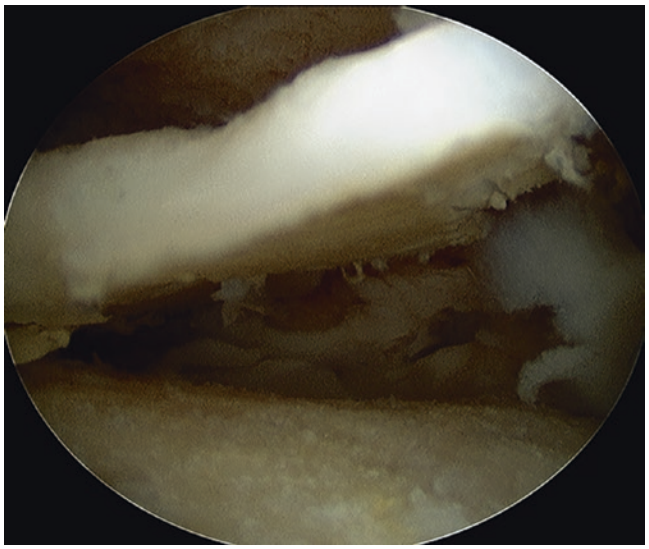

Fig. 30.6 The cartilage is collapsed in tibiotalar joint

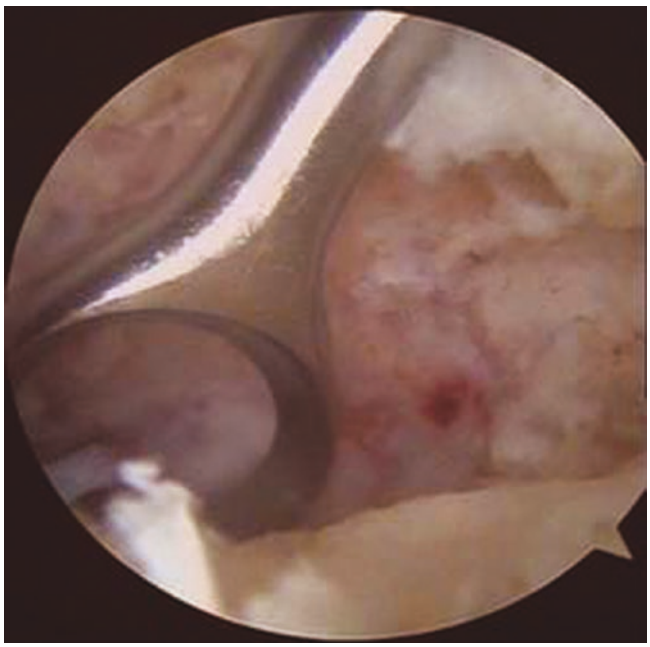

Fig. 30.7 The cartilage on talus dome is removed under arthroscopy

and after planes, and the ankle position and angle are adjusted to make the calcaneus valgus 5° (Fig. 30.10). The Kirschner wires are drilled into the talus (Fig. 30.11), then the ankle position and angle are examined by X-ray, and the implanted screw length is also measured. If there is bone defect, autogenous or allogeneic freeze-dried shattered cancellous bone grains can be implanted through cannula to fill the bone defect cavity (Fig. 30.12).

Two 6.6 mm hollow screws were screwed along the Kirschner wires to make sure the tibia and talus tight compression and crossed fixation. X-ray confirms the screw length, fixation angle, and bone grafting (Fig. 30.13). After the operation, brace is used to protect the ankle, and this allows weight-bearing walking. Patients will be followed up at regular intervals until solid bone fusion.

30.3.2 Taloclavicular Arthrodesis

Taloclavicular arthrodesis is required in flatfoot osteoarthritis due to longitudinal arch collapse or osteoarthritis with traumatic taloclavicular dislocation.

A thick needle is inserted into the taloclavicular joint, and the normal saline containing adrenaline is injected after fluoroscopy. Arthroscopy is inserted to found the peeled-off articular cartilage and the exposed subchondral bone (Fig. 30.14), planer or radiofrequency is used to clean the synovium and cartilage in taloclavicular joint (Fig. 30.15), and next the cartilage on the joint surface is planed or scraped (Fig. 30.16) and then polished. The autogenous cancellous bone is implanted into the taloclavicular joint. In order to restore the longitudinal arch of the foot, the "V" shape bone graft should be implanted and fixed with screws or inserter (Fig. 30.17). After operation, the joint is fixed in the functional position by plaster.

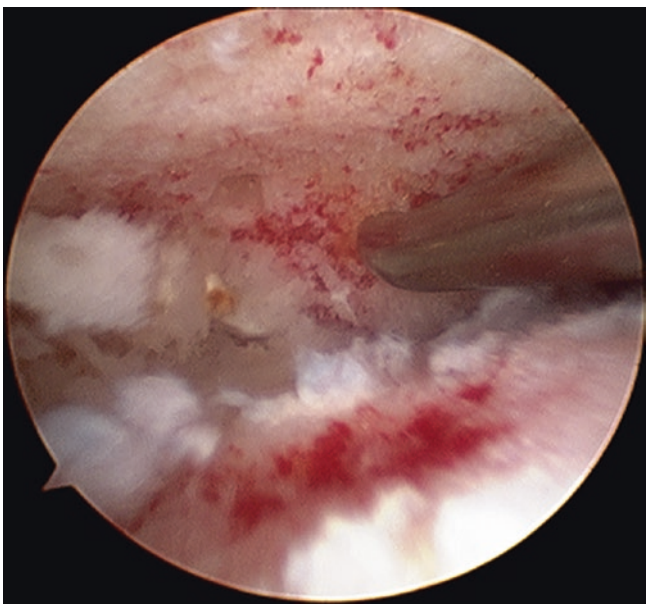

Fig. 30.8 The arc-shaped bone file is used to grind the subchondral bone to bleeding

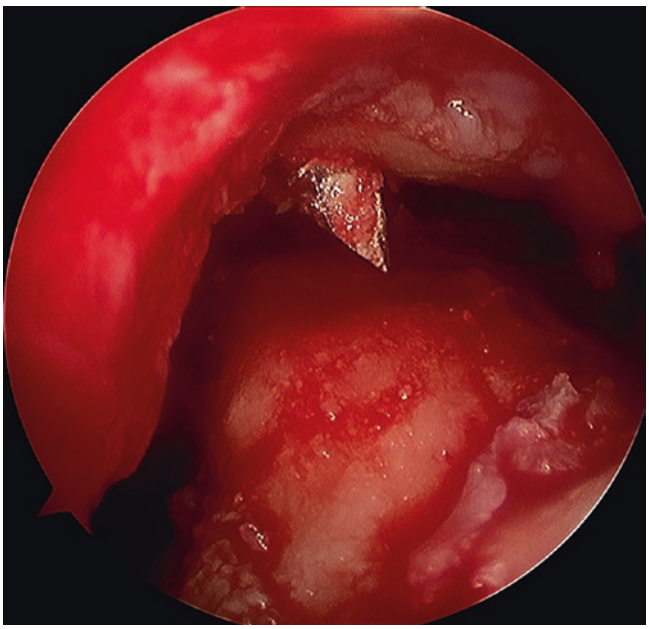

Fig. 30.10 Drilling the cross Kirschner wires through the tibiotalar joint under arthroscopy

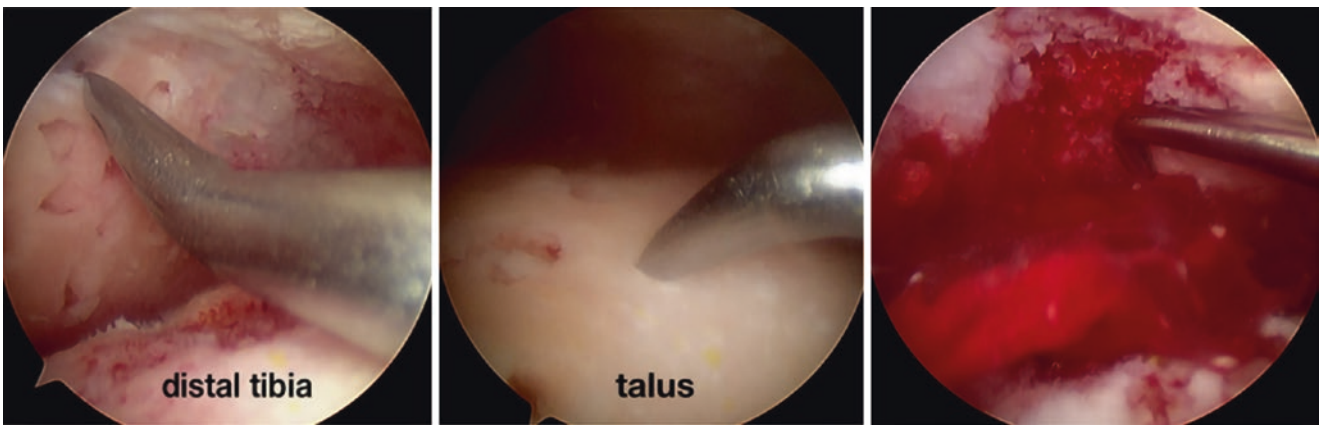

Fig. 30.9 Microfracture is performed on the subchondral bone of talus, distal tibia, and lateral and medial malleoli to make the bone marrow blood infiltrated into the ankle joint space

Fig. 30.11 Two crossing Kirschner wires are drilled through tibia subchondral bone into the talus

Fig. 30.12 Autogenous or allogeneic freeze-dried shattered cancellous bone grains are implanted through cannula to fill the bone defect cavity

30.4 Critical Points

1. The skin and soft tissue around ankle are thin, so the planer blade should not face to the subcutaneous tissue when cleaning the synovium, to avoid the injury of dorsal artery and nerve.
2. Complete removal of articular cartilage, microfracture of astragaloscaphoid bone, and enough graft bone are important for arthrodesis.
3. The hollow screws should not penetrate the cartilage of subtalar joint to avoid osteoarthritis.
4. The ankle should keep in neutral position with calcaneus valgus 5° when compression screw is fixed. Fluoroscopy should be used to confirm if necessary.

Fig. 30.13 X-ray confirms two 6.6 mm hollow screws were properly fixed, including the screw length, fixation angle, and bone grafting

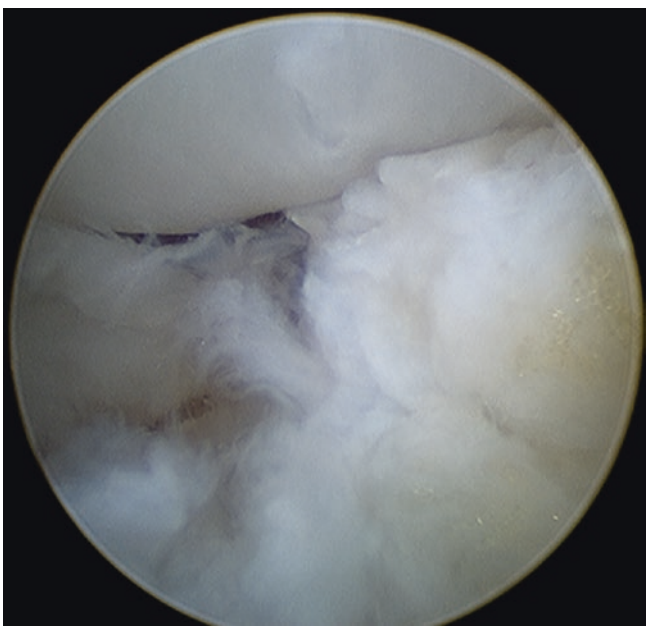

Fig. 30.14 The peeled-off articular cartilage and the exposed subchondral bone of the taloclavicular joint

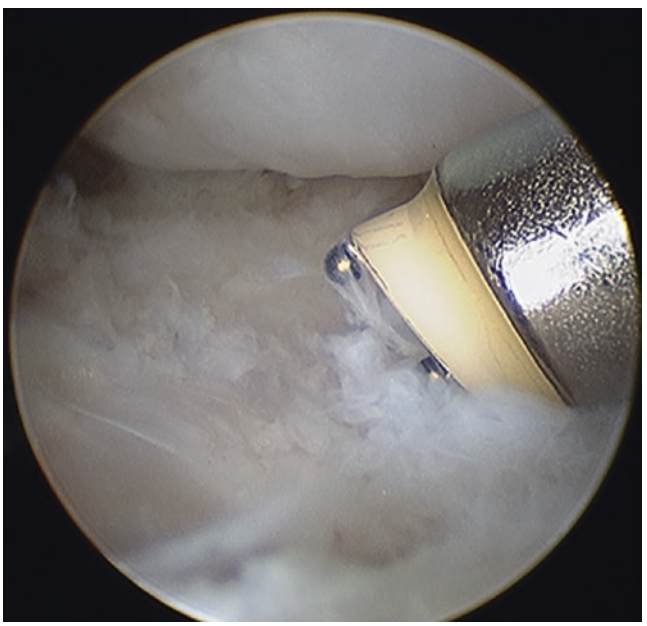

Fig. 30.15 Planer or radiofrequency is used to clean the synovium and cartilage in taloclavicular joint

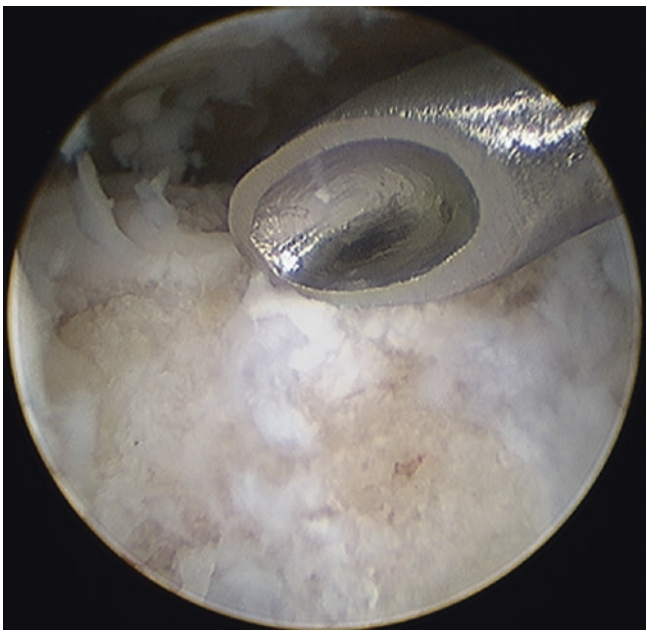

Fig. 30.16 The cartilage on the joint surface is planed or scraped

Fig. 30.17 Two hollow screws were properly fixed in the taloclavicular joint

References

1. Liu YJ, Chen JY, et al. Arthroscopic assisted foot and ankle joint arthrodesis. Chinese Truma Mag. 2005;05:333–5.
2. Rippstein P, Kumar B, Müller M. Ankle arthrodesis using the arthroscopic technique. Oper Orthop Traumatol. 2005;17(4–5): 442–56.

Debridement of Early Hip Joint Lesions in Ankylosing Spondylitis

31

Chun-bao Li and Yu-jie Liu

Ankylosing spondylitis (AS) mostly occurs in adolescent patients, mainly involving the spine, sacroiliac joint, and hip joint. If the early treatment is not in time, further progression of the disease can lead to stiffness or rigidity of the hip joint. The disability rate is high, and total hip arthroplasty (THA) is eventually performed in the end stage. How to stop the progression of the disease and avoid hip arthroplasty is an important issue that has not been resolved today.

31.1 Clinical Features

In the early stage of the disease, there were no obvious abnormal changes in the spine and hip joints. Due to the development of spine and hip joint diseases, the spine and hip pain gradually worsened, and the patient could not lie flat but on the side with hip flexion and adduction deformity (Fig. 31.1). In severe cases, hump, hip flexion, and adduction deformity occur. In the early stage, the X-ray shows mild stenosis of joint space in spine and hip space. MRI shows hip joint effusion (Fig. 31.2) and joint space narrowing (Fig. 31.3) gradually.

Physical examination revealed hip flexion and adduction deformity. Figure-"4" test is positive. Flexion and extension were limited, and in flexion, adduction, and internal rotation test, Thomas sign is positive. In severe cases, hip rigidity eventually occurs, and the patients' daily life and self-care ability are completely lost. Eventually, total hip replacement is required (Fig. 31.4).

C.-b. Li · Y.-j. Liu (✉)
Department of Orthopedics, Chinese PLA General Hospital, Beijing, China

31.2 Hip Arthroscopy Minimally Invasive Technology for the Treatment of Early Hip Joint Lesion in Ankylosing Spondylitis [1, 2]

In order to prevent the further progression of AS hip joint disease causing serious dysfunction and avoid THA, the early arthroscopic debridement of abnormal synovitis is recommended. This procedure is performed after hip joint massage is release under general anesthesia to restore the normal range of motion of hip joint. The medical treatment and rehabilitation training were recommended after it. Those could effectively control the course of the disease, reduce the disability rate of AS, and improve the function of the hip joint according to the follow-up research.

31.2.1 Anesthesia and Preoperative Preparation

After general anesthesia in supine position, both hip joints were performed gently manipulations in the directions of flexion and extension (Fig. 31.5), adduction, abduction, and internal and external rotation in order to release the hip joint. Move the patient to the surgical traction table and fix the bilateral ankle joints on the traction frame (Fig. 31.6). Fix the sponge pad of the perineal column of the traction bed to avoid traction and perineal injury. Mark the bone anatomy, neurovascular structure, and surgical portal around the hip joint with a marker pen (Fig. 31.6). After the surgical area is routinely sterilized and draped is completed, traction of the affected lower extremity is performed, the traction weight is 10 kg, X-ray shows that the joint space is distracted to 8–10 mm (Fig. 31.7), and hip arthroscopy can be performed.

After the hip joint adhesion was released by manipulations, there is bleeding in the joint that affects the surgical field of vision. A saline containing epinephrine can be injected into the joint before arthroscopic insertion. After the arthroscopy was inserted, it was repeatedly rinsed with

Y.-j. Liu et al. (eds.), *Advanced Application of Arthroscopy*, https://doi.org/10.1007/978-981-15-4684-6_31

Fig. 31.1 Hip flexion and adduction deformity of AS patient

Fig. 31.2 The X-ray shows mild stenosis of hip joint space in the early stage

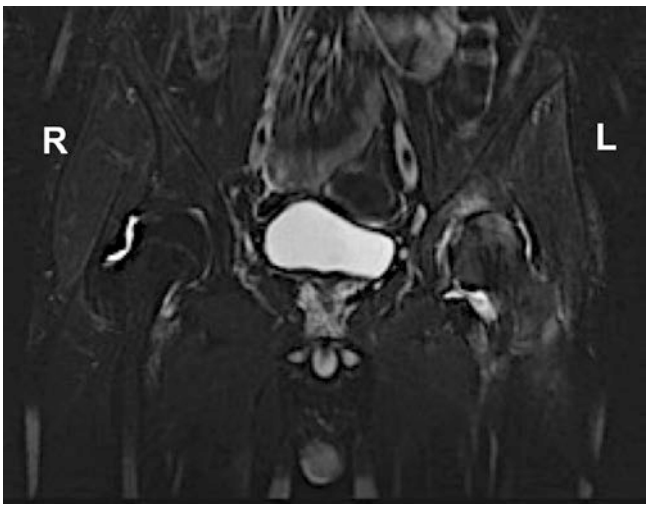

Fig. 31.3 MRI shows hip joint effusion in the early stage

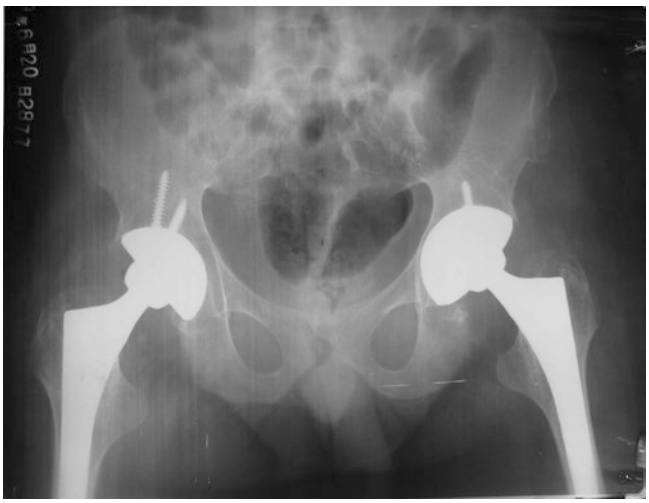

Fig. 31.4 The joint received total hip replacement at the end edge

saline, and the perfusion liquid was 3000 ml + 0.1% epinephrine 1 ml, which was 150 cm higher than the operating table.

31.2.2 Hip Arthroscopy Portal

- Anterior lateral portal (AL): Take the anterior superior iliac spine and the top of the greater trochanter to make a connection. The midpoint of the connection is the anterolateral portal (Fig. 31.8). The anterolateral portal is the most commonly used portal for arthroscopy. The only important anatomical structure of the anterolateral portal is the superior gluteal nerve. After this nerve exits the sciatic fossa, it travels laterally from back to front and passes through the deep surface of the gluteal medius.
- Anterior portal (AP): Make a straight line distally from the anterior superior iliac spine and then make a horizontal line from the upper edge of the greater trochanter. This portal is not commonly used (Fig. 31.8).
- Mid-anterior auxiliary portal (MAP): The connection of the anterior lateral portal and anterior portal is the bottom edge, and an equilateral triangle is formed distally. The apex of the distal end of the triangle is the mid-anterior auxiliary portal (Fig. 31.8). It can be shifted 1–2 cm medially according to the patient's height and muscle conditions. A portal is established between the tensor fascia lata and the sartorius muscle space to reduce muscle tissue damage and facilitate postoperative rehabilitation. This portal is the most commonly used operational portal.

Fig. 31.5 The bilateral hip joints were performed manipulations gently under general anesthesia

Fig. 31.6 The bilateral ankle joints were fixed on the traction frame. The bone anatomy, neurovascular structure, and surgical portal around the hip joint were marked

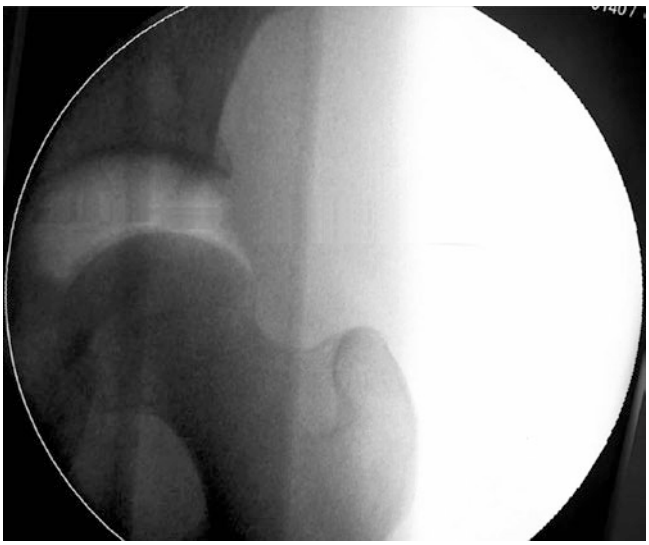

Fig. 31.7 After distraction, the joint space is distracted to 8–10 mm

- Arthroscopic Portal Establishment

Firstly, establish the anterolateral portal of the hip joint. Under the X-ray perspective, the puncture needle is 45 degrees from the proximal side and 30 degrees from the midline. The puncture needle penetrates the lateral hip joint capsule. After confirming the insertion into the hip joint by X-ray fluoroscopy, insert the guide wire into the puncture needle, pull out the puncture needle to retain the guide wire, and insert a hollow core guide rod with a diameter of 5 mm along the guide wire into the joint cavity. Arthroscopic puncture cannula is introduced into the articular cavity along the guide rod, and a mid-anterior auxiliary portal is established under arthroscopic monitor.

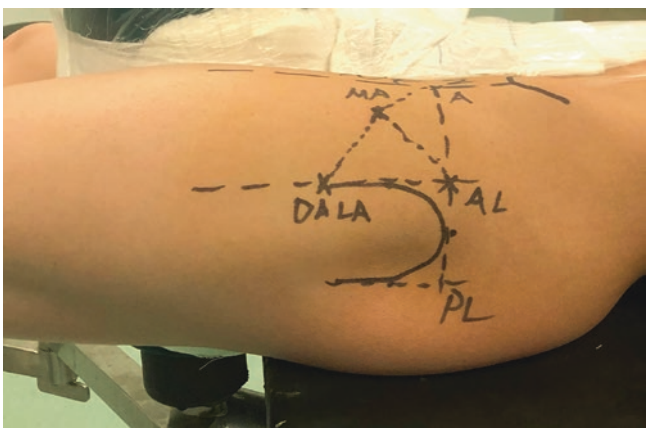

Fig. 31.8 The commonly used portals of hip arthroscopy

31.2.3 Debridement Under Hip Arthroscopy (Fig. 31.9)

Due to different degrees of lesion, the arthroscopy observations are not consistent. It can be seen in different hyperplasia and hypertrophy of synovial tissue and congestion and edema in the joint (Fig. 31.9a). Synovial hyperplasia usually occurs at articular capsule and round ligament fossa. Some synovium crawls to the surface of cartilage (Fig. 31.9b). The cartilage and subchondral bone are exfoliated to different degrees (Fig. 31.9c).

Use a motorized shaver or radiofrequency to clean the hypertrophic synovium (Fig. 31.9d) and exfoliated cartilage in the hip joint. Generally, the unstable cartilage can be cleaned up to the normal edge, which is the stable part. After debridement, remove the lower limb traction, make the

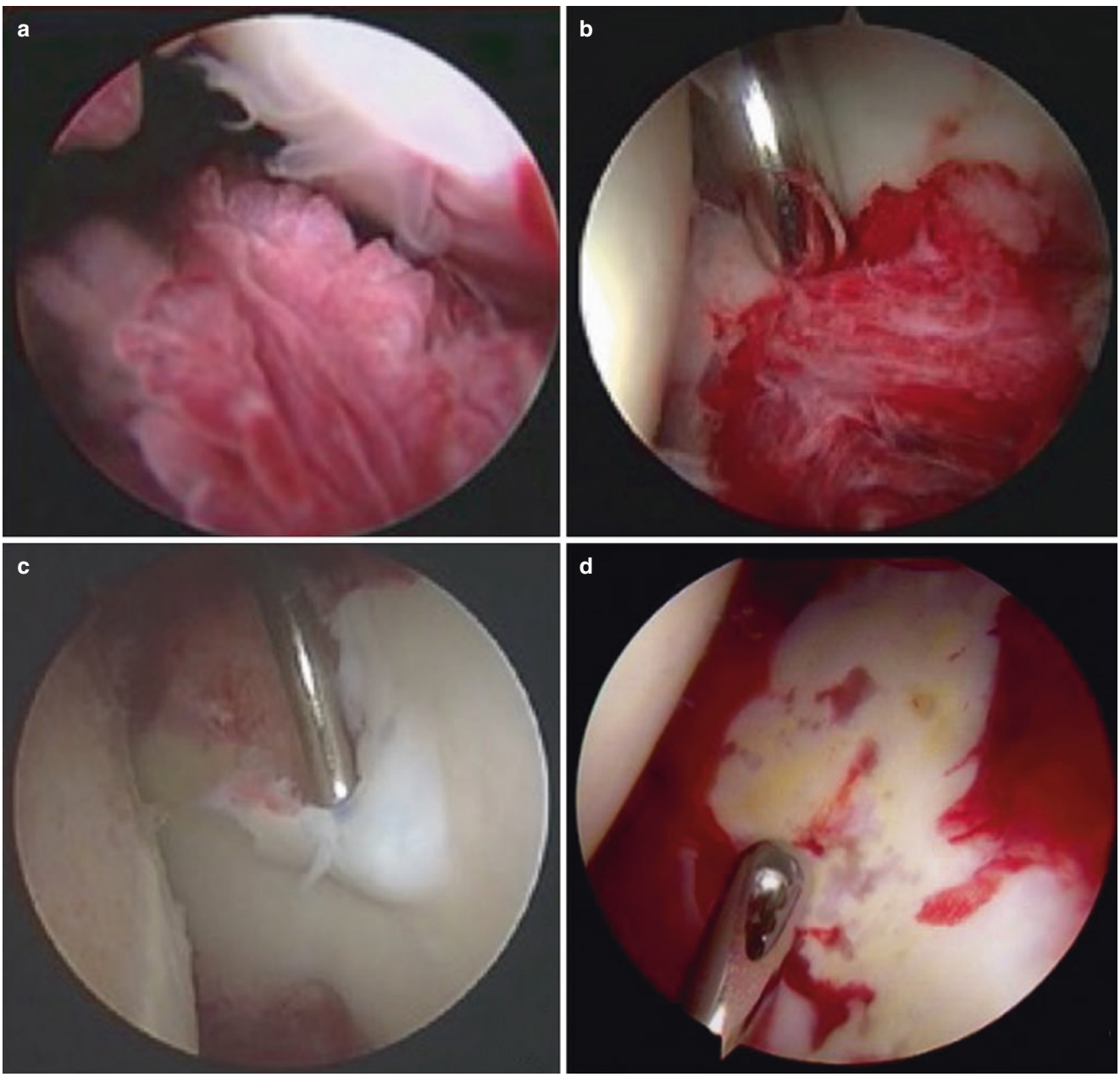

Fig. 31.9 The arthroscopic appearance of the pathological changes of synovitis and cartilage and hip joint and its treatment (**a**) the hyperplasia of synovial of hip joint; (**b**) Cutting the synovium with a planer; (**c**) the cartilage was collapsed from the subchondral bone of acetabulum; (**d**) the degeneration of cartilage and exposure of subchondral bone of acetabulum

femoral head part into the acetabular, and flex the hip 30–45 °to relax the joint capsule. Finally complete the synovial tissue clearance in peripheric room.

31.3 Postoperative Rehabilitation and Medical Treatment

It is necessary to continue systematic comprehensive medical treatment and functional rehabilitation training in painless state after hip arthroscopy.

The treatments are mainly for patients with hip flexion, adduction, and contracture deformities. After operation, patients lie in the prone position, pad their thighs, thorax, and abdomen, and load 15–20 kg sandbags on the hips to fully relax the quadriceps and iliopsoas. Make the pubis symphysis and the front of the hip joint and the thigh completely close to the bed, gradually straighten the hip joint, and gradually correct hip flexion and adduction deformity. Strengthen hip abduction training after surgery to restore gluteal muscle function. The purpose of using the hip joint continuous passive function exerciser (Fig. 31.10) is to help restore hip joint mobility and help cartilage nutrition and repair.

Fig. 31.10 The continuous passive function exerciser (CPM) is used to help restore hip joint mobility and help cartilage nutrition and repair

31.4 Critical Points

1. Patients often have joint adhesions and contractures of muscle and soft tissues around the joints. Hip massage must be performed under general anesthesia.
2. AS patients are thin and weak and have osteoporosis usually. Massage should be performed gently, avoid violence, and prevent fractures.
3. Attention must be payed to the diameter and flexibility of the perineal column during traction. Carefully attention should be performed to avoid excessive traction, which is likely to cause perineal nerve, foot and ankle skin pressure injuries, and neurovascular structure or soft tissue injury.
4. For patients with significant spinal involvement, cardiopulmonary function should be sufficiently assessed.

References

1. Li CB, Qi W, et al. Midterm clinical outcome for ankylosing spondylitis patients with early hip-involved diseases treated with arthroscopic technique. Zhongguo Gu Shang. 2017 Mar 25;30(3):236–40.
2. Zhou M, Wang Y, et al. Outcome of arthroscopic debridement and synovium resection for hip lesion in patients with ankylosing spondylitis. J Chinese PLA Postgrad Med Sch. 2011;32(02):138–40.